



## City Research Online

### City, University of London Institutional Repository

---

**Citation:** Beranova, E. (2007). Post stroke depression. (Unpublished Doctoral thesis, City, University of London)

This is the accepted version of the paper.

This version of the publication may differ from the final published version.

---

**Permanent repository link:** <https://openaccess.city.ac.uk/id/eprint/30273/>

**Link to published version:**

**Copyright:** City Research Online aims to make research outputs of City, University of London available to a wider audience. Copyright and Moral Rights remain with the author(s) and/or copyright holders. URLs from City Research Online may be freely distributed and linked to.

**Reuse:** Copies of full items can be used for personal research or study, educational, or not-for-profit purposes without prior permission or charge. Provided that the authors, title and full bibliographic details are credited, a hyperlink and/or URL is given for the original metadata page and the content is not changed in any way.

**PHOTOPOLYMERISATION USING  
ORGANOMETALLIC INITIATORS**

**BY**

**RICHARD BOWSER**

*A thesis submitted for the degree of Doctor of  
Philosophy at The City University for work  
carried out in the Chemistry Department.*

**April 1993**

## CONTENTS

	<u>Page</u>
Chapter 1. Introduction	1
1.1 Introduction to photochemistry	2
1.1.1 Principles of photochemistry	2
1.1.2 Properties of light	2
1.1.3 Molecular energy levels	4
1.1.4 Absorption of light	5
1.1.5 The absorption spectrum	6
1.1.6 Reactions of excited states	9
1.1.7 Electron transfer quenching	12
1.1.8 Heavy atom quenching	13
1.1.9 Quenching by molecular oxygen	14
1.1.10 Electronic energy transfer	14
1.2 Structure, bonding, and excited states of coordination compounds	16
1.2.1 Metal orbitals	17
1.2.2 A complex with $d^3$ configuration	18
1.2.3 A complex with $d^4$ configuration	19
1.2.4 Ligand orbitals	20
1.2.5 Combination of metal and ligand orbitals	21
1.3 Characterisation of excited states	23
1.4 Free radical initiation of polymerisation	23
1.4.1 Photoinitiation	23
1.4.2 Types of photoinitiators	24
1.4.3 Properties of the photoinitiator	26
1.4.4 Kinetics of free radical polymerisation	26
1.4.5 Oxygen inhibition of free radical polymerisation	29
1.5 Cationic initiation of polymerisation	31
1.5.1 Introduction to cationic polymerisation	31
1.5.2 Kinetics of cationic polymerisation	39
1.6 Industrial applications of photopolymerisation	41
1.6.1 Light sources	44
1.7 Experimental test procedures	45
1.7.1 UV curing	46
1.7.2 Real-time infrared (RTIR) spectroscopy	50
1.7.3 Photo-DSC	54
1.7.4 EPR spectroscopy	59
1.8 References	66

	<u>Page</u>
Chapter 2.      Photopolymerisation initiated by allyl, benzyl and associated silanes and stannanes	72
2.1    The synthesis of silanes and stannanes	73
2.1.1      Via Grignard reaction	73
2.1.2      Via Barbier reaction	75
2.1.3      Via reductive silylation	76
2.1.4      Via Wurtz coupling	78
2.2    Physical and chemical properties of silanes and stannanes	79
2.2.1 $p\pi-d\pi$ bonding	79
2.2.2 $\sigma-\pi$ hyperconjugation	80
2.3    Photochemistry of benzylsilanes and stannanes	84
2.3.1      Photochemistry of benzylstannanes	84
2.3.2      Photochemistry of benzylsilanes	85
2.4    Electron paramagnetic resonance (EPR) spectroscopy results	86
2.4.1      EPR results of benzylsilanes	87
2.4.2      EPR results of benzylstannanes	87
2.4.3      EPR results of allyl & cinnamyl stannanes	89
2.4.4      Structure & stability of radical cations	90
2.5    UV curing results	92
2.5.1      UV curing results of benzylsilanes	92
2.5.2      UV curing results of benzylstannanes	102
2.5.2.1    Photo-DSC of benzyltri- <i>n</i> -butylstannane	104
2.5.3      UV curing results of naphthyllic compounds (and higher)	107
2.5.4      UV curing results of allylsilanes	108
2.5.5      UV curing results of allylstannanes	109
2.5.6      UV curing results of cinnamyl and styryl silanes and stannanes	111
2.5.7      Photoinduced electron transfer reactions	113
2.5.8      UV curing: sensitisation using DCA	115
2.5.9      UV curing of benzylsilanes with DCA	117
2.5.10     UV curing of benzylstannanes with DCA	118
2.5.11     UV curing of naphthylsilanes with DCA	119
2.5.12     UV curing of allylsilanes with DCA	120
2.5.13     UV curing of allylstannanes with DCA	121
2.5.14     Sensitisation of polymerisation with aromatic ketones	122

	<u>Page</u>	
2.5.15	UV curing results of benzylsilanes and stannanes with benzanthrone	125
2.5.16	UV curing results of allylsilanes and stannanes with benzanthrone	127
2.5.17	UV curing results of naphthylsilanes and stannanes with benzanthrone	128
2.5.18	UV curing using 4,4'-dimethylbenzil (DMB) as a sensitiser	129
2.5.19	UV curing results using thiopyrylium salts as sensitisers	132
2.6	Real-time infrared spectroscopy (RTIR) results	137
2.6.1	Introduction	137
2.6.2	RTIR results of benzylsilanes	138
2.6.3	RTIR results of benzylic silanes	139
2.6.4	RTIR results of benzylstannanes	140
2.6.5	RTIR results of naphthyl (and higher) silanes and stannanes	142
2.6.6	RTIR results of allylsilanes & stannanes	144
2.6.7	RTIR results of benzylsilanes with DCA	145
2.6.8	RTIR results of benzyl and naphthylstannanes with DCA	148
2.6.9	RTIR results of an allylstannane with DCA	152
2.6.10	RTIR results using 4,4'-dimethylbenzil (DMB) as a sensitiser	152
2.6.11	Introduction	152
2.6.12	RTIR results of benzylsilanes with DMB	155
2.6.13	RTIR results of benzylic silanes with DMB	156
2.6.14	RTIR results of benzylstannanes with DMB	158
2.6.15	RTIR results of naphthylsilanes and stannanes with DMB	159
2.6.16	RTIR results of allylsilanes and stannanes with DMB	160
2.7	Experimental section	163
2.8	References	206
Chapter 3.	Photoinitiation of free radical polymerisation using organometallic amines of silicon and tin	216
3.1	Introduction	217
3.2	Previous synthetic routes	217
3.2.1	Synthetic routes used	218

	<u>Page</u>
3.3 Applications of alkylaminosilanes and stannanes	220
3.4 Electron paramagnetic resonance (EPR) spectroscopy results	222
3.5 UV curing results	225
3.5.1 UV curing results of Et <sub>2</sub> NCH <sub>2</sub> SiMe <sub>3</sub>	225
3.5.2 UV curing results of dimethylaminoalkylsilanes	226
3.5.3 UV curing results of dimethylaminoalkylsilanes and stannanes	228
3.5.4 Sensitisation of polymerisation using benzanthrone	230
3.5.5 UV curing results of dimethylaminoalkylsilanes and stannanes with benzanthrone	232
3.6 Real-time infrared (RTIR) spectroscopy results	233
3.6.1 RTIR results of dimethylaminoalkylsilanes and stannanes	233
3.6.2 RTIR results of dimethylaminoalkylsilanes and stannanes with benzanthrone	236
3.7 Experimental section	241
3.8 References	252
Chapter 4. Photoinitiation of free radical and cationic polymerisation using iron-arene complexes	255
4.1 Introduction	256
4.2 Photochemistry of iron-arene complexes	259
4.3 Photoimaging using iron-arene complexes	262
4.4 UV curing results for iron-arene complexes in cationic polymerisation	264
4.5 UV curing results for iron-arene complexes in free radical polymerisation	269
4.5.1 UV curing results for iron-arene complexes with N-methyldiethanolamine in free radical polymerisation	272

	<u>Page</u>
4.6 Real-time infrared (RTIR) spectroscopy results for iron-arene complexes	275
4.6.1 Introduction	275
4.6.2 RTIR results of iron-arene complexes in free radical polymerisation	275
4.6.3 UV curing results for cationic polymerisation using an iron-arene salt sensitised with a diphenyliodonium salt	277
4.7 Photo-differential scanning calorimetry (Photo-DSC) results of iron-arene complexes	281
4.7.1 Photo-DSC results of iron-arene complexes in cationic polymerisation	281
4.7.2 Photo-DSC results of iron-arene complexes in free radical polymerisation	284
4.8 Experimental section	290
4.9 References	297
 Appendix	 A1
5.1 Introduction	A2
5.2 Cobaloximes	A2
5.3 Porphyrins	A5
5.4 Experimental section	A7
5.5 Table 5.1: The oxidation and ionisation potentials for a number of silanes and stannanes	A12
5.6 Figure 5.1: UV spectra	A14
5.7 References	A17

## LIST OF TABLES

<u>Table 1.1</u>	The timescales of excited state processes
<u>Table 2.1</u>	The Grignard synthesis of silanes and stannanes
<u>Table 2.2</u>	The Barbier synthesis of silanes and stannanes
<u>Table 2.3</u>	Preparation of silanes via reductive silylation
<u>Table 2.4</u>	UV curing results of benzylsilanes incorporated at 5% w/w in TMPTA
<u>Table 2.5</u>	UV curing results of benzylic silanes incorporated at 5% w/w in TMPTA
<u>Table 2.6</u>	Sensitisation of diphenyliodonium hexafluorophosphate for use in cationic photopolymerisation using 'thioxanthone' with all compounds incorporated at 1% w/w in 3,4-epoxycyclohexylmethyl-3',4'-epoxycyclohexane carboxylate
<u>Table 2.7</u>	Evidence for a dual cure system in the photopolymerisation of a 50:50 acrylate:epoxy resin mixture using diphenyliodonium hexafluorophosphate and 9-trimethylsilylthioxanthene
<u>Table 2.8</u>	UV curing results of benzylstannanes incorporated at 5% w/w in TMPTA
<u>Table 2.9</u>	The rate and the degree of conversion values at different light intensities for the photopolymerisation of TMPTA using benzyltri-n-butylstannane as determined by photo-DSC
<u>Table 2.10</u>	UV curing results of naphthyl (and higher) compounds incorporated at 5% w/w in TMPTA
<u>Table 2.11</u>	UV curing results of allylsilanes incorporated at 5% w/w in TMPTA
<u>Table 2.12</u>	UV curing results of allylstannanes incorporated at 5% w/w in TMPTA
<u>Table 2.13</u>	UV curing results of cinnamyl and styryl compounds
<u>Table 2.14</u>	UV curing of TMPTA with benzylsilanes (1% w/w) sensitised using DCA (0.25% w/w)

<u>Table 2.15</u>	UV curing of TMPTA with benzylstannanes (1% w/w) sensitised using DCA (0.25% w/w)
<u>Table 2.16</u>	UV curing of TMPTA with naphthylsilanes (1% w/w) sensitised by DCA (0.25% w/w)
<u>Table 2.17</u>	UV curing of TMPTA with allylsilanes (1% w/w) sensitised by DCA (0.25% w/w)
<u>Table 2.18</u>	UV curing of TMPTA with allylstannanes (1% w/w) sensitised by DCA (0.25% w/w)
<u>Table 2.19</u>	UV curing of TMPTA with benzylsilanes and stannanes (both 5% w/w) sensitised by benzanthrone (1% w/w)
<u>Table 2.20</u>	UV curing of TMPTA with allylsilanes and stannanes (both at 5% w/w) sensitised by benzanthrone (1% w/w)
<u>Table 2.21</u>	UV curing of TMPTA with naphthylsilanes and stannanes (both at 5% w/w) sensitised by benzanthrone (1% w/w)
<u>Table 2.22</u>	UV curing results for the sensitisation of polymerisation of TMPTA using 4,4'-dimethylbenzil (1% w/w) with silanes (1% w/w) and stannanes (5% w/w)
<u>Table 2.23</u>	UV curing results of 2,4,6-triphenylthiopyrylium tetrafluoroborate (0.25%) with benzylic silanes and stannane (all at 1% w/w) in the presence of TMPTA
<u>Table 2.24</u>	UV curing results of 2,4,6-triphenylthiopyrylium tetrafluoroborate (0.25% w/w) with allylic stannanes and silane (all at 1% w/w) in the presence of TMPTA
<u>Table 2.25</u>	UV curing results of 4-n-butoxyphenyl-2,6-bis(4-methoxyphenyl)thiopyrylium tetrafluoroborate (1% w/w) with benzylic and allylic silanes and stannanes (all 5% w/w)
<u>Table 2.26</u>	RTIR results of the photopolymerisation of TMPTA using benzylsilanes
<u>Table 2.27</u>	RTIR results of the photopolymerisation of TMPTA using benzylic silanes
<u>Table 2.28</u>	RTIR results of the photopolymerisation of TMPTA using benzylstannanes
<u>Table 2.29</u>	RTIR results of the photopolymerisation of TMPTA using naphthyl (and higher) silanes and stannanes

<u>Table 2.30</u>	RTIR results of the photopolymerisation of TMPTA using allylic silanes and stannanes
<u>Table 2.31</u>	RTIR spectroscopy results for the photopolymerisation of TMPTA using benzylsilanes sensitised by DCA
<u>Table 2.32</u>	RTIR spectroscopy results for the photopolymerisation of TMPTA using benzylic stannanes sensitised by DCA
<u>Table 2.33</u>	The effect of sensitisation on the $R_{p(max)}$ value of photopolymerisation of TMPTA using DCA with benzylsilanes and stannanes
<u>Table 2.34</u>	The effect of sensitisation on the degree of conversion value of photopolymerisation of TMPTA using DCA with benzylsilanes and stannanes
<u>Table 2.35</u>	RTIR spectroscopy results for the photopolymerisation of TMPTA using an allylstannane sensitised by DCA
<u>Table 2.36</u>	RTIR spectroscopy results for the photopolymerisation of TMPTA using benzylsilanes sensitised by DMB
<u>Table 2.37</u>	RTIR spectroscopy results for the photopolymerisation of TMPTA using benzylic silanes sensitised by DMB
<u>Table 2.38</u>	RTIR spectroscopy results for the photopolymerisation of TMPTA using benzylstannanes sensitised by DMB
<u>Table 2.39</u>	RTIR spectroscopy results for the photopolymerisation of TMPTA using naphthyllic silanes and stannanes sensitised by DMB
<u>Table 2.40</u>	RTIR spectroscopy results for the photopolymerisation of TMPTA using allylic silanes and stannanes sensitised by DMB
<u>Table 3.1</u>	The reaction times and yields of the synthesis of a number of dimethylaminoalkylsilanes and stannanes using ultrasound
<u>Table 3.2</u>	UV curing results of the polymerisation of TMPTA using $Et_2NCH_2SiMe_3$ in the presence and absence of sensitisers
<u>Table 3.3</u>	UV curing results of dimethylaminoalkylsilanes in the presence and absence of sensitisers

<u>Table 3.4</u>	UV curing results for a number of dimethylaminoalkyl- silanes and stannanes (1% w/w) in TMPTA
<u>Table 3.5</u>	Sensitisation of polymerisation of TMPTA using dimethylaminoalkyl- silanes and stannanes (1% w/w) with benzanthrone (1% w/w)
<u>Table 3.6</u>	RTIR spectroscopy results for the photopolymerisation of TMPTA using organometallic amines
<u>Table 3.7</u>	RTIR spectroscopy results for the photopolymerisation of TMPTA using organometallic amines sensitised using benzanthrone
<u>Table 4.1</u>	UV curing results for the cationic polymerisation of 3,4-epoxycyclohexylmethyl-3',4'-epoxycyclohexane carboxylate using iron-arene photoinitiators
<u>Table 4.2</u>	UV curing results for the free radical polymerisation of TPGDA initiated by iron-arene complexes
<u>Table 4.3</u>	UV curing results for the free radical polymerisation of TMPTA initiated by iron-arene complexes
<u>Table 4.4</u>	UV curing results for the free radical polymerisation of TPGDA initiated by iron-arene complexes (1% w/w) in the presence of N-methyldiethanolamine (5 %w/w)
<u>Table 4.5</u>	RTIR spectroscopy results of the free radical polymerisation of TMPTA initiated by iron-arene complexes
<u>Table 4.6</u>	Cationic polymerisation of an epoxide using diphenyliodonium hexafluorophosphate sensitised with an iron arene salt
<u>Table 5.1</u>	The oxidation and ionisation potentials for a number of silanes and stannanes

#### LIST OF FIGURES

<u>Figure 1.1</u>	The electromagnetic spectrum
<u>Figure 1.2</u>	Photochemically produced excited states
<u>Figure 1.3</u>	Jablonski diagram

<u>Figure 1.4</u>	The configuration of the d-orbitals in an octahedral complex
<u>Figure 1.5</u>	The energy levels of the orbitals of pyridine
<u>Figure 1.6</u>	Electronic transitions in transition metal complexes
<u>Figure 1.7</u>	The four different irradiation conditions
<u>Figure 1.8</u>	The UV Colordry apparatus
<u>Figure 1.9</u>	The RTIR spectroscopy apparatus
<u>Figure 1.10</u>	The RTIR spectroscopy results
<u>Figure 1.11</u>	Photo-DSC apparatus
<u>Figure 1.12</u>	An exothermic polymerisation trace
<u>Figure 1.13</u>	Schematic diagram of an EPR spectrometer
<u>Figure 2.1</u>	$p_{\pi}$ - $d_{\pi}$ bonding versus $\sigma$ - $\pi$ hyperconjugation in allylic and benzylic silanes and stannanes
<u>Figure 2.2</u>	The limiting conformations of the C=C double bond with respect to the metal- $\text{CH}_2$ in an allylic system
<u>Figure 2.3</u>	Photo-DSC results of the polymerisation of TMPTA initiated by benzyltri- <i>n</i> -butylstannane at two different light intensities
<u>Figure 3.1</u>	A plot of the degree of conversion versus time obtained from the RTIR spectroscopy results of the curing of TMPTA for an organometallic amine in the presence and absence of a sensitiser (benzanthrone)
<u>Figure 4.1</u>	The Photo-DSC results for the cationic polymerisation of an epoxide initiated by an iron-arene complex
<u>Figure 4.2</u>	The Photo-DSC results for the free radical polymerisation of TMPTA, in air and under nitrogen, initiated by an iron-arene complex
<u>Figure 4.3</u>	The Photo-DSC results for the free radical polymerisation of TMPTA initiated by an iron-arene complex (on it's own in air [b] and nitrogen [d], and in the presence of $\text{PhCH}_2\text{SnBu}_3$ in air [c])

## LIST OF SCHEMES

- Scheme 1.1 The fate of excited states
- Scheme 1.2 Oxygen inhibition of polymerisation
- Scheme 1.3 Cationic polymerisation of an epoxide
- Scheme 1.4 Photolysis of diaryliodonium salts
- Scheme 1.5 Photolysis of triarylsulphonium salts
- Scheme 1.6 The polymerisation of epoxides using iron-arene salts
- Scheme 1.7 The production of a negative-working lithoplate
- Scheme 1.8 The radiolytic processes of  $\text{CFCl}_3$
- Scheme 2.1 Cinnamylation of the polymer chain (PC)
- Scheme 2.2 [2 + 2] cycloaddition of cinnamyl groups
- Scheme 3.1 The proposed fragmentation of  $[\text{Me}_2\text{N}(\text{CH}_2)_3\text{SnBu}_3]^{++}$  at 77K from epr spectroscopic evidence
- Scheme 4.1 Photochemistry of iron-arene complexes
- Scheme 4.2 Mechanism of cationic polymerisation of epoxides using iron-arene salts
- Scheme 4.3 A general mechanism for the polymerisation of epoxides using iron-arene salts
- Scheme 4.4 The nucleophilic character of sulphur in the cationic polymerisation of an epoxide
- Scheme 4.5 The role of oxygen in the sensitisation of diphenyliodonium hexafluorophosphate in cationic polymerisation using  $\eta^6$ -thioxanthene- $\eta^5$ -cyclopentadienyliron hexafluorophosphate
- Scheme 4.6 Proposed reaction scheme for the photopolymerisation of TMPTA in air using  $\eta^6$ -fluorene- $\eta^5$ -cyclopentadienyliron hexafluorophosphate (1% w/w) with benzyltri-*n*-butylstannane (1% w/w)

## KEY TO SYMBOLS & ABBREVIATIONS

CIDNP:	chemically induced dynamic nuclear polarisation
Cp:	cyclopentadienyl
CT:	charge transfer
Conv:	conversion
Decalin:	decahydronaphthalene
DCA:	9,10-dicyanoanthracene
DMB:	4,4'-dimethylbenzil
DSC:	differential scanning calorimetry
EPR:	electron paramagnetic resonance
exciplex:	excited complex
EXPT:	experiment
HOMO:	highest occupied molecular orbital
IPA:	isopropanol
ISC:	intersystem crossing
LUMO:	lowest unoccupied molecular orbital
PE:	photoelectron
RTIR:	real-time infrared
THF:	tetrahydrofuran
TMPTA:	trimethylolpropane triacrylate
TPGDA:	tripropylene glycol diacrylate
% w/w:	percentage weight for weight

## ACKNOWLEDGEMENTS

I would like to thank my supervisor, Professor R S Davidson, for his tuition, advice and encouragement throughout the course of this work. I also wish to thank Dr John Coyle for his assistance and discussions prior to undertaking these studies.

I thank my colleagues and the technical staff who made my time in the laboratories so enjoyable. Thanks to fellow members of Lab 307, Dr Patricia Moran, Dr Stephen Collins, Dr David Chappell, Dr Eleanor Cockburn, & Dr Sandra Lewis, those from 'across the way' in Lab 305, Dr Phil Duncanson, Paul Crick, Nergis Arsu, Niaz Khan, & Audrey O'Donnell, and those Inorganic chaps from the 'other side', Mark Gray, Dr Andy Thomas, & Martin Stimpson. Special thanks to Dr Patricia Moran - for sharing her expertise in organic synthesis, Dr Phil Duncanson - for his general advice and discussions, Jeff Abrahams - for his comments and technical assistance, & Dr Alan Osborne - for useful discussions and suggestions. I would also like to thank Grant Bradley for setting up the RTIR spectroscopy apparatus. I wish to thank Dr Chris Rhodes and his group at Queen Mary & Westfield College for providing several EPR spectra and for the subsequent illuminating discussions. I thank the staff at the CSIC Polymer Institute in Madrid for their technical assistance, particularly on the Photo-DSC.

I am grateful to the SERC and Cookson Group plc and IPC for the provision of funding for the whole of this work. Thanks also to the European Photochemistry Association and to IPC for providing financial assistance for my work in Madrid. I would also like to thank the Royal Society of Chemistry and Cookson Group plc for assistance with expenses towards attending conferences.

I am indebted to my wife, Coz, for her constant source of support and encouragement throughout the course of this work.

## Statement

The experimental work in this thesis has been carried out by the author in the laboratories of the Department of Chemistry at the City University, between November 1988 and October 1991, as well as a short period of this time spent working at the CSIC Polymer Institute in Madrid in June 1991. This work has not been presented for any other degree.

I grant powers of discretion to the University Librarian to allow this thesis to be copied in whole or in part without further reference to me. This permission covers only single copies made for study purposes, subject to normal conditions of acknowledgement.



Richard Bowser

Date 28th April 1993

Some of this work has been previously published, as follows:

Photopolymerisation using Organometallic Initiators, *14th IUPAC Symposium on Photochemistry, Photochemistry Abstracts*, 132-133, 1992

SOME NEW DEVELOPMENTS IN RADIATION CURING, *J.Chem.Soc.*, 1992 (in press)

THE USE OF ULTRASOUND IN ORGANIC SYNTHESIS, '*Current Trends in Sonochemistry*', *Royal Society of Chemistry*, Ed. G.J.Price, 50-58, 1992

STRUCTURES AND FRAGMENTATIONS OF ORGANOSILICON AND ORGANOTIN RADICAL CATIONS, *J.Chem.Soc., Perkin Trans. 2*, 1469-1474, 1992

CLEAVAGE OF ONE ELECTRON BONDS IN ORGANOSILICON AND ORGANOTIN RADICAL CATIONS, *J.Organomet.Chem.* 436, C5-C8, 1992

## ABSTRACT

A number of organometallic compounds have been synthesised and evaluated for use as photoinitiators for polymerisation based on the cleavage of metal-carbon (M-C) bonds.

Numerous allyl, benzyl, and naphthyl silanes and stannanes have been prepared. Both the homolytic M-C cleavage and the cleavage of the radical cations of the organometals (produced via electron transfer to a suitable acceptor such as 9,10-dicyanoanthracene) have been investigated as a means of initiating free radical polymerisation. In certain instances both free radical and cationic polymerisation occurred together, using the same initiating system, giving rise to a dual cure system.

A number of silicon and tin amines were synthesised using a novel 'one-pot' route which reduced the reaction time and the need for several steps. The amines were shown to be effective at initiating free radical polymerisation when used with a suitable aromatic ketone sensitiser.

Electron paramagnetic resonance spectra of the radical cations of the above compounds were recorded in order to gain an insight into the behaviour of the cleavage of the radical cations when used to initiate polymerisation via an electron transfer mechanism. The results indicated that C-Sn cleavage in the radical cations occurred more readily than for C-Si bonds.

A number of iron-arene salts were synthesised and evaluated for use as photoinitiators in both cationic and free radical polymerisation. Thus it was shown that a dual-cure system was possible when using these initiators. Evidence was also presented showing that oxygen had a beneficial effect on both cationic and free radical polymerisation.

Some cobaloximes and some porphyrins were synthesised in an attempt to produce alkyl free radicals via M-C bond homolytic cleavage on irradiation. Initial work with cobaloximes indicated some promise but time did not permit further advances in this area.

The evaluation of photopolymerisation on all the above compounds was carried out using the following techniques:

- (i) A commercial UV cure apparatus for thin film polymerisation.
- (ii) Real-Time Infrared (RTIR) Spectroscopy which gave the rate of polymerisation and the degree of monomer consumption.
- (iii) Photo-Differential Scanning Calorimetry (Photo-DSC) which gave similar parameters as RTIR spectroscopy as well as an assessment of the post-cure which developed after irradiation had ceased (especially important for cationic polymerisation).

*Dedicated to my parents,  
Marjorie and Jack  
and to my wife, Coz,  
for all their help and support.*

# **Chapter 1.**

## **INTRODUCTION**

## 1.1 Introduction to Photochemistry

In the following section the basic principles of photochemistry are explained as an introduction to the subject. The behaviour of an electronically excited molecule with a very short lifetime has a number of features that differ from those of ground state chemical species. Firstly, only very fast reactions can take place, and secondly, excited molecules may have sufficient energy to cause bond cleavage.

### 1.1.1 Principles of Photochemistry

It was in the nineteenth century that Grotthus and Draper stated that only light absorbed by the system can cause a chemical change in it which became known as the first law of photochemistry. A later observation by Stark and Einstein was that the rate of chemical change in a given molecular system was proportional to the light intensity. Thus a second law of photochemical equivalence was suggested in which one quantum of light is absorbed for each molecule which reacts.

### 1.1.2 Properties of light

Photochemical action is the result of absorption of light, visible or ultraviolet (UV) for example, by molecular systems.

The duality of light is an important feature in photochemistry. On the one hand the colour of light is determined by its wavelength as a fundamental property, whilst in other cases it is the energy of a particle of light, a photon, that is important. The two are related by the fundamental expression in equation 1.1 below.

$$E = hc/\lambda \qquad 1.1$$

where, E = energy per photon, h = Planck's constant, c = velocity of light, and  $\lambda$  = wavelength of light.

Part of the electromagnetic spectrum is shown below in figure 1.1 to illustrate the relationship between the wavelength and the energy of light.

Figure 1.1 The electromagnetic spectrum

Far UV	Ultraviolet	Visible		Near IR	IR	Far IR
150nm	200	400	800	1000		
			0.8 $\mu$	1	2.5	15
						250

The UV region of the spectrum extends from 200-400 nanometres (nm) and the visible part of the spectrum extends from 400-700 nm. Light can be polychromatic, having a distribution of wavelengths, or monochromatic with its distribution limited to one wavelength or, more realistically, a narrow range of wavelengths.

### 1.1.3 Molecular energy levels

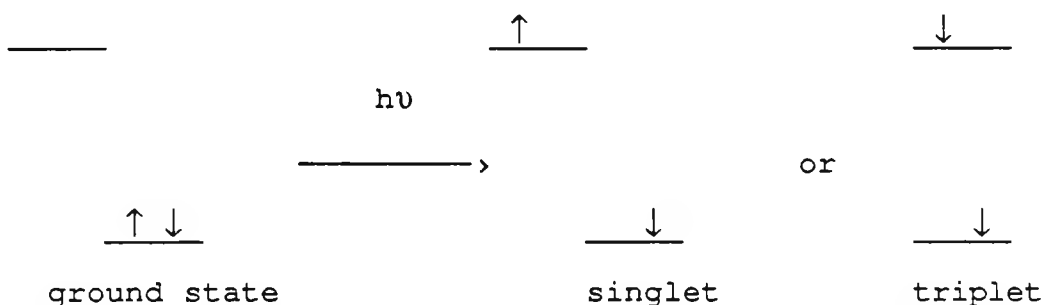
The theoretical model, known as quantum theory, in which a molecule can take up or lose energy was formulated by de Broglie, Schrodinger, and Heisenberg, around 1926. The particular distribution of electrons in a molecule is characterised by a wave function, the square of which, in a given point in space, gives the probability of finding an electron at that point. Each particular electronic distribution has a specific energy and the molecule is only allowed to have these particular electronic energies, and no other energies are allowed.

As well as electronic energy, the molecule can contain translational, rotational, and vibrational energy. It can be shown by quantum theory that the molecule can only contain prescribed amounts of these energies. The particular prescription depends upon the molecular characteristics, such as atomic weight of constituent atoms, bond length, and strength of bonds.

Absorption of light in the photochemically interesting wavelength region of the visible and UV is attributed to changes in the electronic state of the molecule. The change accompanying absorption of a photon redistributes the electrons around the nuclei of the molecule. In molecular orbital terms an electron from an occupied lower energy orbital is promoted to a higher unoccupied orbital.

The redistribution may give rise for example to singlet excited states with no change in spin of the promoted electron, or to triplet excited states which involves an inversion of spin of the promoted electron. Both situations are represented below in figure 1.2.

Figure 1.2 Photochemically produced excited states



#### 1.1.4 Absorption of light

Of fundamental importance is the Lambert-Beer law of absorption in which absorbance,  $A$ , of a material with light path length,  $l$ , is related to the concentration,  $c$ , of absorbent by equation 1.2 below.

$$A = \log(I_0/I_t) = \epsilon cl \quad 1.2$$

where  $I_0$  = incident light intensity,  $I_t$  = transmitted light intensity, and  $\epsilon$  = molar extinction coefficient.

The molar extinction coefficient,  $\epsilon$ , is a fundamental property of the molecule. Its value is characteristic of

the wavelength of absorbance and is normally quoted as such. The Lambert-Beer law cannot be obeyed if the incident light is polychromatic over a range in which  $\epsilon$  is not constant. Further if there are equilibria in the system so that the concentration of the absorbing species is not proportional to the stoichiometric concentration, again the law will not be obeyed. The total absorbance, if there are two absorbing species present, is just the sum of the absorbances of the individual components. The fraction of light,  $f_1$ , absorbed by one of the species is given by equation 1.3 below.

$$f_1 = \epsilon_1 c_1 / (\epsilon_1 c_1 + \epsilon_2 c_2) \quad 1.3$$

Where  $\epsilon_1$  and  $\epsilon_2$  are the molar extinction coefficients for species 1 and 2 respectively, and  $c_1$  and  $c_2$  are the respective concentration of species 1 and 2. This holds providing the above conditions for the validity of the Lambert-Beer law are met.

#### 1.1.5 The absorption spectrum

Absorption of light in the visible and UV regions results in formation of electronically excited states of the absorbing species. Each excited state has a unique energy relative to that of the ground state. Extinction coefficients of bands in the spectra of molecules are related to the nature of transition. The most commonly encountered transitions in organic compounds are  $n \rightarrow \pi^*$ ,  $\pi \rightarrow \pi^*$ ,  $n \rightarrow \sigma^*$ ,

and  $\sigma \rightarrow \sigma^*$  which are listed in order of increasing energy. Thus light of the highest energy (in the far UV) is necessary for  $\sigma \rightarrow \sigma^*$  excitation, while  $n \rightarrow \pi^*$  promotions are caused by ordinary UV light.

For organometallic compounds the situation is often more complicated due to the involvement of d orbitals in bonding which means that other transitions such as  $d \rightarrow d$ , or  $d \rightarrow \pi^*$  can occur (See section 1.2.5).

When a transition is fully allowed by the principles of quantum mechanics, the extinction coefficient at the band centre is large. If the transition is forbidden then the extinction coefficient at the band centre will be relatively small.

The integrated extinction coefficient for one band in the spectrum is directly related to the transitional probability connecting the upper and lower states. The reciprocal of the transitional probability is the lifetime that the upper state would have with respect to spontaneous emission of a photon and reverting to the ground state in the absence of all other possible processes. Although the relationship is not exact an approximation for the radiative constant,  $k$ , can be used to give an estimation of the natural or intrinsic lifetime of the excited state,  $\tau$ , using equation 1.4 below.

$$k = 1/\tau = 3 \times 10^{-9} \epsilon_{\max} \bar{\nu}^2 \Delta\bar{\nu} \quad 1.4$$

where  $\epsilon_{\max}$  = extinction coefficient at centre of band,  $\bar{\nu}$  = wavenumber at centre of band, and  $\Delta\bar{\nu}$  = width of band at half peak height.

This represents a simplified view where the natural lifetime represents only the maximum possible lifetime for an excited state. In reality other processes can contribute to make the lifetime appreciably shorter. This is usually found to be the case.

This effectively means that a range in the lifetime of photophysical processes is observed as illustrated by the documented timescales for a number of different photophysical processes given in table 1.1 (Calvert and Pitts, 1966; Turro, 1978).

Table 1.1 The timescales of excited state processes

STEP	PROCESS	TIMESCALE (s)
1. Excitation	$S_0 + h\nu \rightarrow S_1$	$10^{-15}$
2. Internal conversion	$S_1 \rightarrow S_1 + \Delta$	$10^{-11}$ - $10^{-14}$
3. Fluorescent emission	$S_1 \rightarrow S_0 + h\nu_f$	$10^{-6}$ - $10^{-11}$
4. Intersystem crossing	$S_1 \rightarrow T + \Delta$	$10^{-8}$ - $10^{-11}$
5. Internal conversion	$T_1 \rightarrow T_1 + \Delta$	$10^{-11}$ - $10^{-14}$
6. Phosphorescent emission	$T_1 \rightarrow S_0 + h\nu_p$	$10^2$ - $10^{-3}$

The processes that affect the fate of excited molecules will be discussed in the next section.

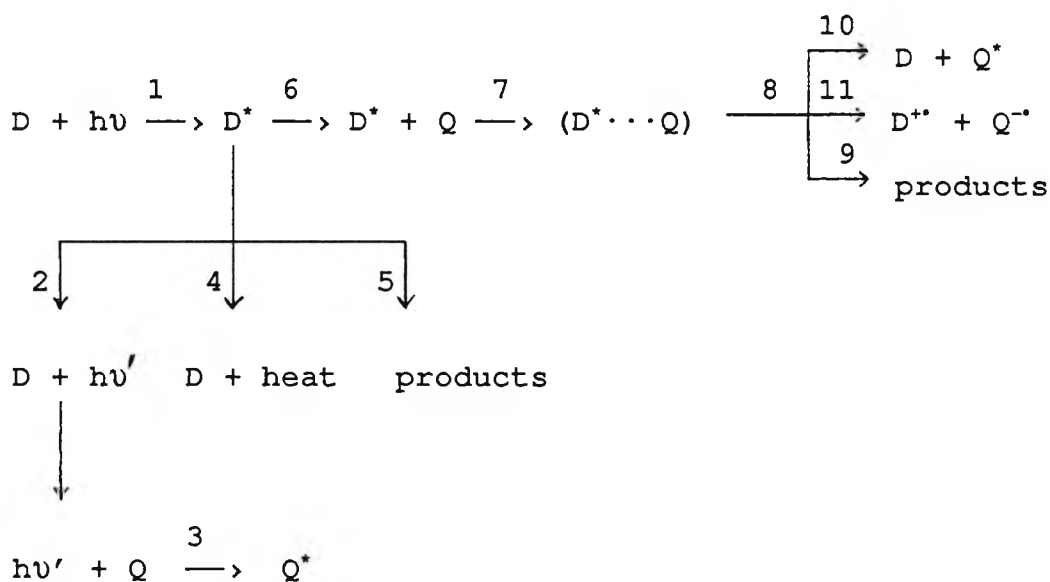
### 1.1.6 Reactions of excited states

There are a number of possible pathways available to an electronically excited state,  $D^*$ , obtained when a molecule,  $D$ , absorbs a photon of suitable energy according to equation 1.5 below.



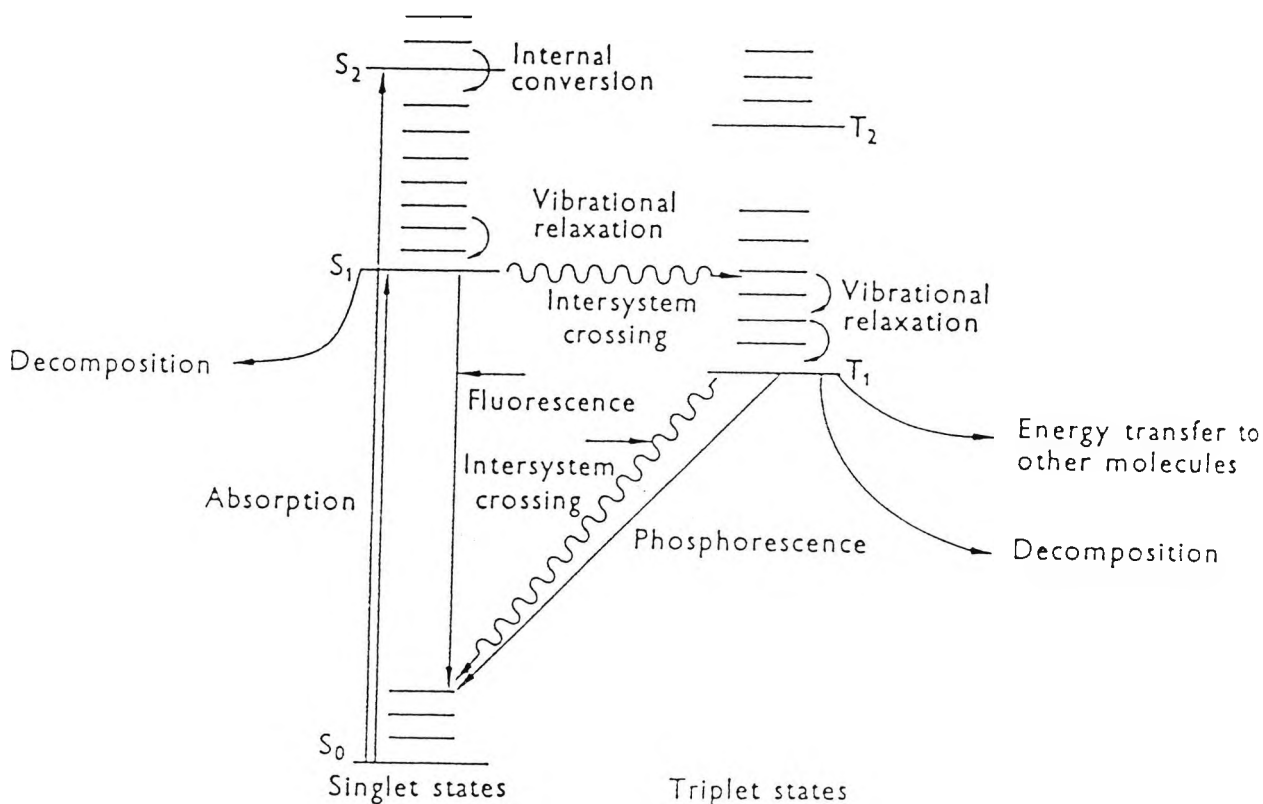
There are a number of possible processes available to the new chemical species,  $D^*$ , which are illustrated in scheme 1.1 below.

Scheme 1.1 The fate of excited states



A brief explanation of the various pathways depicted in scheme 1.1 can be given when used in conjunction with a Jablonski diagram, shown in figure 1.3.

Figure 1.3 Jablonski diagram



The nomenclature used in figure 1.3, whilst normally reserved for organic compounds, may be similar for some organometallic complexes though others have different multiplicity levels. The important feature of all systems is that the excited states have spin multiplicities that can be different or the same as the ground state. Using scheme 1.1 and figure 1.3 the various reaction pathways may be described as follows.

1. A ground state molecule D absorbs a photon of light which promotes it to an excited state  $D^*$ .
2. A radiative, or emissive, transition giving rise to either fluorescence, with no change in spin multiplicity (eg.  $S_1 \rightarrow S_0$ ), or phosphorescence involving a change in multiplicity (eg.  $T_1 \rightarrow S_0$ )
3. Radiative energy transfer
4. A non-radiative relaxation process terminating at the ground state.
5. Excitation may give rise to intramolecular processes leading to reaction including unimolecular cleavage (eg.  $D^* \rightarrow R_1^* + R_2^*$ )
6. The excited molecule,  $D^*$ , may come into contact with a ground state molecule, Q.
7. The interaction of excited molecule,  $D^*$ , and ground state molecule, Q, requires close approach before an encounter can take place. The rate of this diffusion controlled process is found to be dependent on factors such as the viscosity of the medium, the dielectric constant of the medium, and the encounter distance, and may be calculated by means of the Debye equation.

8. Once an encounter complex is formed a number of so called quenching processes are possible for the bimolecular excited state complex.
9. This involves quenching of excited states by "chemical" rather than "physical" processes for example by ligand substitution.
10. Non-radiative energy transfer.
11. Electron transfer quenching.

#### 1.1.7 Electron transfer quenching

Electron transfer involves the complete transfer of an electron from an electron donor (D) to an electron acceptor (A). Commonly a ground state donor molecule donates an electron to a previously excited singlet state of an acceptor molecule. This process occurs in an encounter complex as shown in scheme 1.1 (equation 7). The resultant single electron transfer (SET) in scheme 1.1 (equation 11) is not the only pathway and competes with other deactivation routes. The likelihood of an electron transfer mechanism occurring in a given situation was shown by Rehm and Weller (Rehm and Weller, 1970) to be related to the free energy of the electron transfer process in an expression that they derived shown in equation 1.6 below.

$$\Delta G^{\circ} = E_{\text{ox}} - E_{\text{red}} - e^2/\epsilon' a - \Delta E_{00} \quad 1.6$$

$\Delta G_0$  = free energy of electron transfer

$E_{\text{ox}}$  = oxidation potential of the donor

$E_{\text{red}}$  = reduction potential of the acceptor

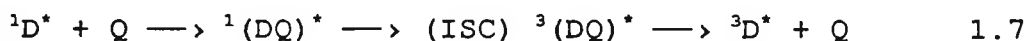
$e^2/\epsilon' a$  = coulombic interaction energy between the two radical ions of charge  $e$  at the encounter distance  $a$  in the solvent of dielectric constant  $\epsilon'$

$\Delta E_{00}$  = the electronic excitation energy of the fluorescer

The rate of quenching,  $k_q$ , can be calculated from spectroscopic and electrochemical data and is shown to be equal to the rate of diffusion,  $k_{\text{diff}}$ , ( $10^{-10}$  mol/l/s) when  $\Delta G^{\circ}$  is more exothermic than 20-40 kJ/mol (or 5-10 kcal/mol).

#### 1.1.8 Heavy atom quenching

Molecular fluorescence is quenched by the presence of species containing heavy atoms and it appears that this is due to the formation of a singlet exciplex, which because of the heavy atom effect, undergoes enhanced intersystem crossing to the triplet exciplex followed by dissociation shown in equation 1.7.



Evidence in support of this mechanism has been provided (Medinger and Wilkinson, 1965) showing the quenching of the fluorescence of several aromatic hydrocarbons by xenon and

various bromine and iodine-containing compounds. It is also known that organometallic compounds can effect the above process (Vander Donckt and Vogels, 1971).

#### 1.1.9 Quenching by Molecular Oxygen

The quenching of the excited states of many organic molecules is known to be diffusion controlled (Birks, 1970). The process may occur via either the singlet or triplet states of the excited molecule. For a singlet state the process depends on enhanced intersystem crossing (ISC) and results in an excited triplet state as shown below in equation 1.8.



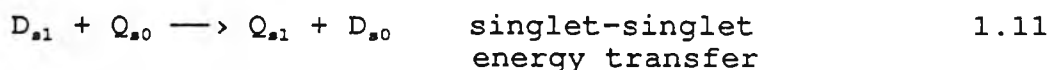
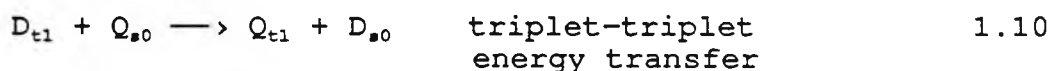
Quenching of the triplet state may occur via ISC or triplet energy transfer with the same end result of loss of energy to reach the ground state as shown below in equation 1.9.



#### 1.1.10 Electronic energy transfer

A molecule in an excited state may transfer its excess energy to another molecule in the environment. The excited molecule (termed D for donor) transfers its energy to a ground state molecule (termed Q for quencher) which itself

becomes excited as shown in scheme 1.1 (equation 10). The likelihood of an energy transfer is related to the relative energies of the donor and the quencher and is most efficient when the excited donor has a higher energy than the excited quencher. The excess energy appears as kinetic energy of D and Q\*. It is also important that the total electron spin does not change after the energy transfer. This is in accordance with the Wigner spin-conservation rule which is actually a special case of the law of conservation of momentum. In the two most important types of energy transfer, both of which obey the Wigner rule, a triplet excited state generates another triplet (Equation 1.10) and a singlet excited state generates another singlet (Equation 1.11) as shown below.



In general singlet-singlet transfer can take place over relatively long distances (40Å) whereas triplet-triplet transfer normally requires a collision between molecules which requires a closer approach (7Å). In most cases quenching processes operate via a collisional mechanism which depends upon both the distance separating D and Q and the rate of diffusion of a given excited state of D\*. Thus during a given lifetime of the excited state a collision with a quencher molecule Q must take place for the process of energy transfer to occur.

From diffusion theory it has been shown that in a non-viscous medium a molecule diffuses  $15\text{\AA}$  in  $10^{-9}\text{s}$  and  $15,000\text{\AA}$  in  $10^{-3}\text{s}$  whereas in a polymer-like viscous medium the same molecule moves  $0.1\text{\AA}$  in  $10^{-9}\text{s}$  and  $50\text{\AA}$  in  $10^{-3}\text{s}$  (Birks, 1973). Energy transfer in polymer-like viscous media may occur under conditions where diffusion is limited. In this case a different model exists which assumes that an effective quenching sphere exists about  $D^*$  and if a quencher molecule,  $Q$ , is within the sphere then  $D^*$  is deactivated with unit efficiency. It is only for concentrated solutions that there is a high probability that  $D^*$  will on average have a molecule of  $Q$  nearby.

## 1.2 Structure, bonding, and excited states of coordination compounds

The existence of coordination compounds in solution opens up a rich field of photochemistry since, after absorption of light, these substances can react or participate in energy transfer or reach excited states where they rapidly equilibrate and become new species with sets of thermodynamic properties entirely different from those characteristics of the ground state.

Since the low-lying electronic states of complexes dominate the photochemistry of inorganic systems, attention is focused on the different types of configuration and energy levels in complexes.

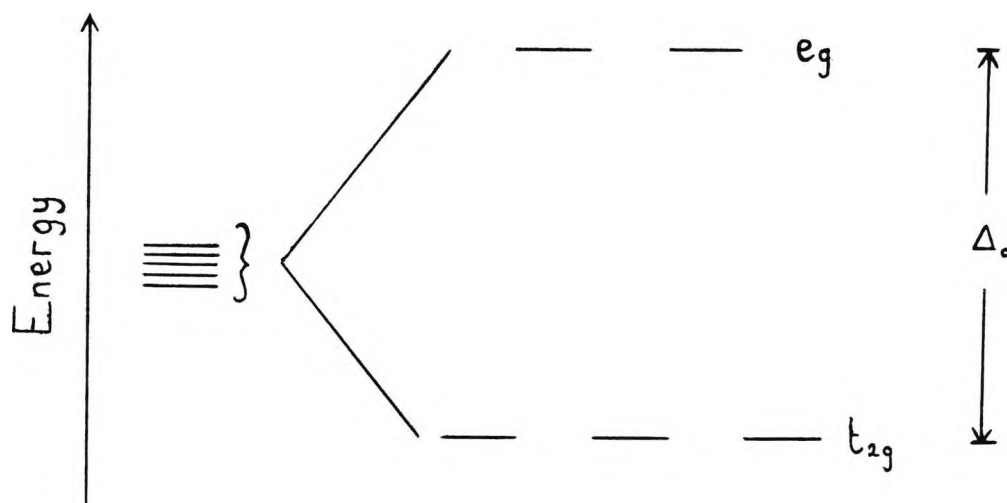
A useful model is to divide the electrons of a complex into two separate sets, one localised on the metal ion and a second set located on the ligand system. After considering the details of each set of electrons separately, one can combine the two to arrive at a electronic model for the complex. New features such as the charge transfer transitions not present in the constituent parts, arise in this composite model. In the following section the metal and ligand orbitals will be looked at separately and the combined picture will be described.

#### 1.2.1 Metal orbitals

A large number of coordination complexes can be assumed to possess octahedral symmetry. Consider the metal orbitals of an octahedral complex. The five degenerate d-orbitals are split into two sets ( $t_{2g}$  and  $e_g$ ) as shown below in figure 1.4.

Figure 1.4

The configuration of the d-orbitals in an octahedral complex



$\Delta_o$  = crystal field splitting parameter.

Ligand field theory can be used to explain the electronic distribution of the metal ion and thus predict the most probable excited state transitions. To illustrate some principles of this theory consider the following examples:

### 1.2.2 A complex with $d^3$ configuration

Detailed theory predicts that the ground state configuration will be  $(t_{2g})_3$ . This corresponds to the lowest energy configuration in which each electron occupies a different, but degenerate, orbital and all the spins are parallel. Pairing two of the spins produces states of higher energy. Excitation of a  $(t_{2g})_3$  system can occur in two different ways.

An electron may be promoted to an empty  $e_g$  orbital ( $t_{2g} \rightarrow e_g$ ). This orbital promotion involves the crystal field-splitting parameter and thus energy required for this transition is a sensitive function of the factors involved in determining  $\Delta_o$ . In the second mode of excitation the excited electron remains in the  $t_{2g}$  orbital but its spin is reversed. Pairing energy,  $P$ , must be added but  $\Delta_o$  is not involved in the excitation process and thus the resultant electron redistribution is virtually independent of the excited state.

### 1.2.3 A complex with $d^4$ configuration

For a complex with 4 d-electrons the ground state configuration may exist as  $(t_{2g})_4$  with two electrons paired in one of the  $t_{2g}$  orbitals or as  $(t_{2g})_3(e_g)_1$  with all electrons in single orbitals and of the same spin. The crucial factor in determining which state predominates is the relative energies of  $\Delta_o$  and  $P$ .

If  $\Delta_o > P$   $(t_{2g})_4$  predominates (also known as low spin configuration)

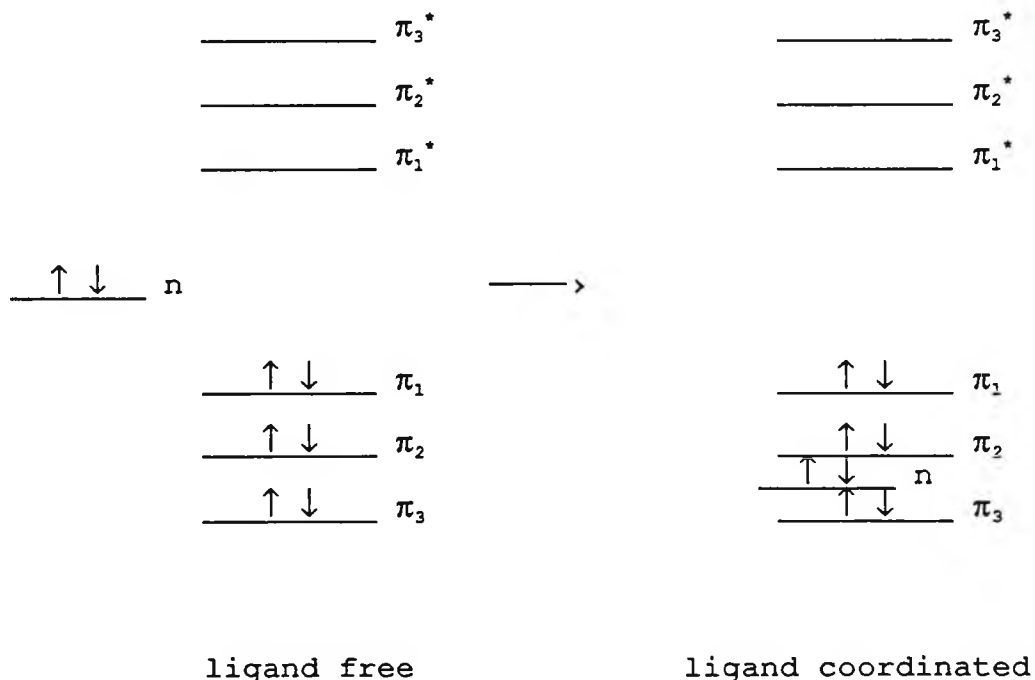
If  $\Delta_o < P$   $(t_{2g})_3(e_g)_1$  predominates (known as high spin configuration)

For complexes where  $\Delta_o \sim P$  an equilibrium between the two different types of ground state may occur.

### 1.2.4 Ligand orbitals

For many ligands the excitation energies of the valence electrons can be comparable to those of the metal electrons described above. Many ligands contain non-bonding electrons, (n), which can be promoted into anti-bonding orbitals, for example ( $\pi^*$ ) orbitals on an aromatic ring. In this case the lowest energy transition of the free ligand is of  $n \rightarrow \pi^*$  character. Complexation often involves the coordination of non-bonding electrons to the metal which lowers the energy of the non-bonding electrons with respect to the ligand electrons and thus the lowest energy transition will be  $\pi \rightarrow \pi^*$ . This situation may be depicted for pyridine, a common ligand, in figure 1.5.

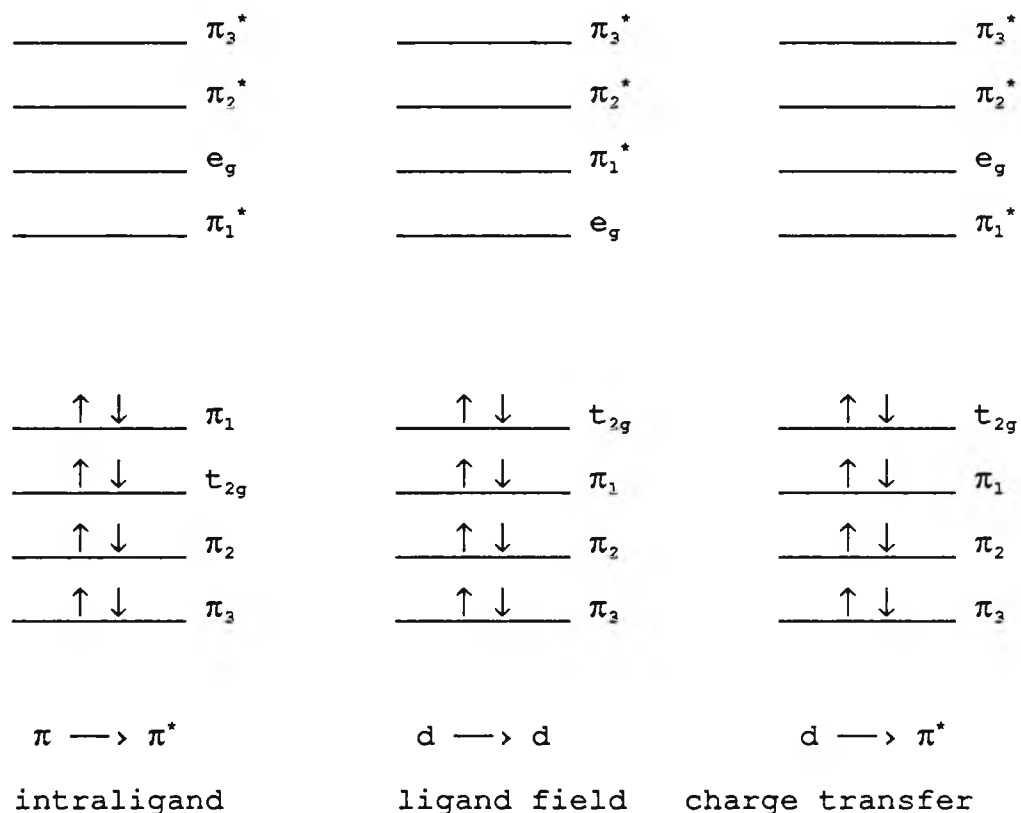
Figure 1.5 The energy levels of the orbitals of pyridine



### 1.2.5 Combination of metal and ligand orbitals

There are a number of different transitions that may occur upon excitation to the lowest (usually) excited state. Some examples of the combination of metal and ligand orbitals for low spin  $d^6$  complexes are given below in figure 1.6 to illustrate the different types of transitions that may occur.

Figure 1.6 Electronic transitions in transition metal complexes



A very elegant study (Crosby et al, 1970) for Iridium III ( $d^6$ ) has shown that it is possible to "tune" the lowest excited state type by altering the ligand. Thus for the same metal ion a  $d \longrightarrow d$ , a  $d \longrightarrow \pi^*$ , or a  $\pi \longrightarrow \pi^*$  emission from complexes with slightly different ligands was obtained. This has obvious implications for designing molecules utilising excited state chemistry.

### 1.3 Characterisation of excited states

The existence of the different types of excited states may be inferred from both absorption and emission spectroscopy. In absorption spectroscopy characteristics of absorption bands give rise to predictions of the transitions involved based on previous results from assigned transitions. Thus from a study of the spectra of a series of closely related complexes of a given metal ion, one can often deduce the configurations and multiplicities of the excited states. The emission spectrum can be a source for deducing the nature of the excited species. Similarly to absorption spectroscopy there are characteristic features of the spectrum which can infer a particular type of excited state.

### 1.4 Free radical initiation of polymerisation

#### 1.4.1 Photoinitiation

The initiation of photopolymerisation requires the presence of a photoinitiating system, PI. The first step involves irradiation of the system to produce an excited state species, PI\*, shown in equation 1.12 below.



The excited state species,  $PI^*$ , as mentioned previously (section 1.1.6) can undergo a number of physical and chemical transformations. The interesting pathway with regard to free radical polymerisation is that pathway that results in a free radical species,  $I^*$ , shown below in equation 1.13.



Presuming that the radical species,  $I^*$ , has suitable reactivity towards a polymerisable substrate such as a monomer,  $M$ , then the radical,  $I^*$ , can go on to initiate polymerisation as depicted in equation 1.14 below.



#### 1.4.2 Types of photoinitiators

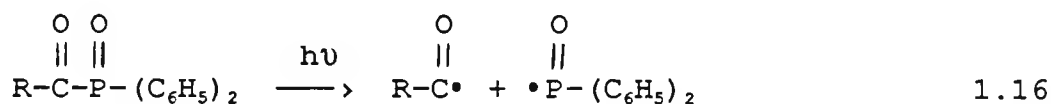
There are numerous reports on the many different types of photoinitiators for free radical polymerisation. In general terms the plethora of initiators may be broadly classified by the mechanism by which they operate. In order to illustrate the principles involved a brief outline of the methods of initiation is presented.

Photoinitiators for free radical polymerisation fall into three main categories, which are:

1. Photoinitiation by homolytic fission from the excited state of the molecule (equation 1.15).



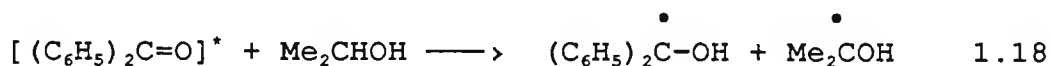
An example of this type of photoinitiator are the acylphosphine oxides (equation 1.16) [Baxter et al, 1987].



2. Photoinitiation by hydrogen abstraction from a donor molecule (equation 1.17).



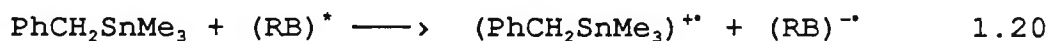
This mechanism is typified by aromatic ketones with various H donors such as alcohols, ethers, and amines. One of the best documented reactions of this type is the photoreduction of benzophenone by isopropanol (equation 1.18).



3. Photoinitiation by electron transfer between a donor, D, and an acceptor, A, as shown below in equation 1.19.



The photoreduction of rose bengal (RB) by benzylstannanes is an example of this type of reaction (equation 1.20) [Eaton, 1979].



#### 1.4.3 Properties of the photoinitiator

The ideal requirements for a good photoinitiator include:

1. High extinction coefficient at the desired absorption wavelength/s.
2. Efficient generation of radicals that are capable of attacking the olefinic double-bond of vinyl monomers.
3. Adequate solubility in the resin system.
4. High storage stability in the dark, and good thermal stability.
5. Do not impart yellowing or unpleasant odours to the cured material.
6. Should be non-toxic itself, as should be any products arising from it.

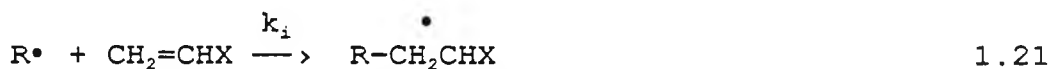
#### 1.4.4 Kinetics of free radical polymerisation

Free radical polymerisation involves three major processes which are:

1. Initiation (equation 1.21)
2. Propagation (equation 1.22)
3. Termination (equations 1.23, 1.24)

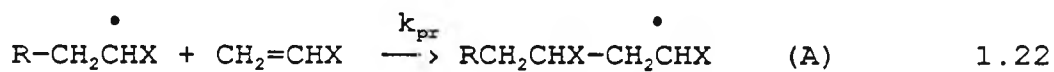
These steps can be represented by following the reaction of a radical,  $R^\bullet$ , with a vinylic monomer  $CH_2=CHX$  ( $X$ =substituent group eg. when  $X=Ph$ , monomer=styrene), by a series of equations.

### 1. Initiation



$k_i$  = rate constant for initiation

### 2. Propagation



$k_{pr}$  = rate constant for propagation

### 3. Termination

(i) by combination



$k_{tc}$  = rate constant for termination by combination

(ii) by disproportionation

eg.



$k_{td}$  = rate constant for termination by disproportionation

It is often difficult to distinguish between  $k_{tc}$  and  $k_{td}$  and an overall rate constant for termination,  $k_t$ , may be determined where;

$$k_t = k_{tc} + k_{td} \quad 1.25$$

Free radical polymerisation is a typical chain reaction in which the polymer chain grows rapidly by successive additions of monomer units during the short interval between initiation and termination of the chain. The actual lifetime of a growing chain radical is of the order of a few seconds, which is sufficient time for successive addition of thousands of monomer units. As is usual for chain reactions the values of the individual rate constants are not readily accessible but the overall characteristics of the reaction can be deduced by using a 'steady-state' assumption that the rate of initiation is equal to the rate of termination. This leads to a number of rate equations for the various stages in polymerisation which can be verified experimentally.

$$\text{Rate of initiation, } R_i = \frac{d[M\bullet]}{dt} = 2k_i[I] \quad 1.26$$

(assuming two radicals produced from one initiator molecule)

$$\text{Rate of propagation, } R_{pr} = -\frac{d[M]}{dt} = k_p [M^\bullet] [M] \quad 1.27$$

$$\text{Rate of termination, } R_t = -\frac{d[M^\bullet]}{dt} = 2k_t [M^\bullet]^2 \quad 1.28$$

Under steady state conditions,  $R_i = R_t$  so that

$$[M^\bullet] = (k_i/k_t)^{1/2} [I]^{1/2} \quad 1.29$$

$$\text{Rate of polymerisation, } R_p = k_p (k_i/k_t)^{1/2} [M] [I]^{1/2} \quad 1.30$$

where,

[M] = monomer concentration

[M<sup>•</sup>] = concentration of propagating radical

[I] = initiator concentration

#### 1.4.5 Oxygen inhibition of free radical polymerisation

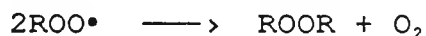
Photoinitiated polymerisation conducted in air is more complicated. The initiator species and the growing polymer chain may be deactivated by reaction with molecular oxygen (a diradical), as shown in scheme 1.2 below.

#### Scheme 1.2 Oxygen inhibition of polymerisation

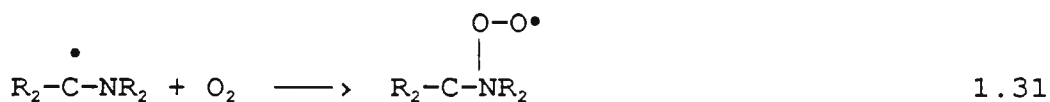
##### Propagation



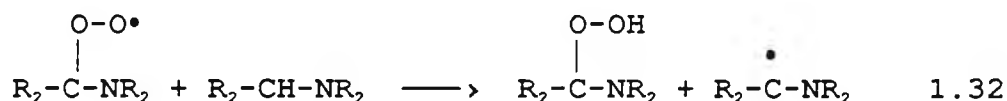
##### Termination



The addition of oxygen to the radical is extremely fast and is probably diffusion controlled in many cases (rate constant =  $10^9 \text{ l mol}^{-1} \text{ s}^{-1}$ , Ingold, 1969). The length of the induction period before polymerisation starts is directly proportional to the number of inhibitor molecules initially present. These undesirable reactions with oxygen occur primarily at the air interface where the concentration of oxygen is the greatest. The result is that an induction period is observed giving a reduction in both the rate of polymerisation and the degree of conversion. A number of different strategies have been used to reduce oxygen inhibition of radical polymerisation. The photopolymerisation can be conducted in vacuo or in an inert atmosphere such as nitrogen. This is difficult to achieve, in practical terms, for the UV coatings industry and so a number of other strategies have been investigated. These include increasing the light intensity (Rubin, 1974), incorporating paraffin waxes in the coating formulation which migrate to the surface on irradiation (Bolon and Webb, 1978), and the use of additives such as *t*-amines in the formulations. It has been shown that the *t*-amines can perform a dual role of both oxygen quenchers and as the initiating species (Bartholomew and Davidson, 1971a; Bartholomew and Davidson, 1971b; Bartholomew *et al*, 1971). The radicals derived from the  $\alpha$ -aminoalkyl groups *t*-amines via hydrogen abstraction can react with oxygen present to form peroxy radicals.



The peroxy radical can then react with another molecule of *t*-amine.

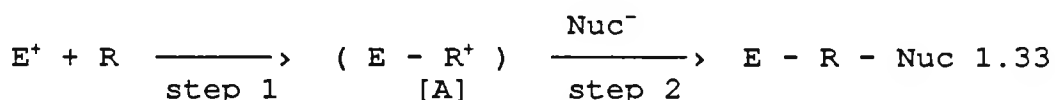


Thus the oxygen inhibition effect is reduced and the added bonus of an initiating  $\alpha$ -aminoalkyl radical is produced in the process.

## 1.5 Cationic initiation of polymerisation

### 1.5.1 Introduction to cationic polymerisation

Cationic polymerisation may be regarded as a special case of electrophilic addition.



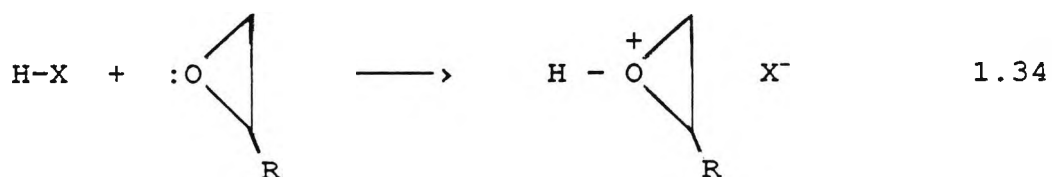
Product [A] shows a positively charged species which must be prevented from collapsing through reaction with a nucleophile [Nuc<sup>-</sup>] (step 2) for long enough to allow a large number of successive monomer additions. It is therefore important that prospective photoinitiators must be designed with non-nucleophilic character of any anions present. In other words there must be propagation of the growing chains giving rise to high reaction rates due to the lack of chain terminating side reactions. Thus low viscosity monomers can

be polymerised as easily as high viscosity monomers. In addition, cations do not react with oxygen, and therefore cationic polymerisation can be carried out effectively in air. This is in marked contrast to free radical polymerisation where oxygen inhibition of polymerisation is an important factor. It has been reported that in certain instances oxygen enhances the rate of cationic polymerisation (Tsuroska and Tanaka, 1988). This is thought to be due to the formation of hydroperoxides which are known to be efficient hydrogen donors and thus will accelerate the production of initiating species. The properties of materials based on photoinitiated cationic polymerisation are generally superior to those obtained from free radical polymerisation. This is particularly so with regard to electrical resistance, stability to heat and chemicals, adhesion, and mechanical strength (Curtis et al, 1986; Green and Stark, 1981; Lohse and Zweifel, 1986). In contrast to free radical systems, only a relatively small number of alkenes and heterocyclic molecules are susceptible to cationic polymerisation. Generally alkenes need adjacent electron-donating groups, such as alkoxy in the case of vinyl ethers, and of the heterocyclic monomers, epoxides are the most common. Epoxides are Lewis bases and their ring opening by cationic species is easy. The polymerisation of an epoxide by a cationic pathway is depicted below in scheme 1.3.

### Scheme 1.3 Cationic polymerisation of an epoxide

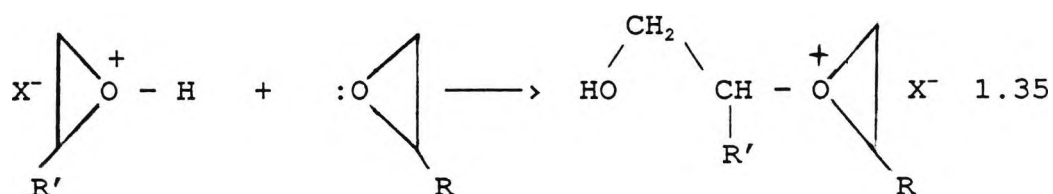
#### 1. Initiation

Initiation involves the nucleophilic attack of the lone pair on the oxygen of the epoxide towards the initiating species.



#### 2. Propagation

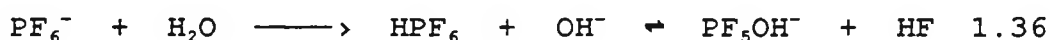
Propagation continues via nucleophilic attack by the monomer on the tertiary oxonium ions until either termination or chain transfer of the polymer chain occurs.



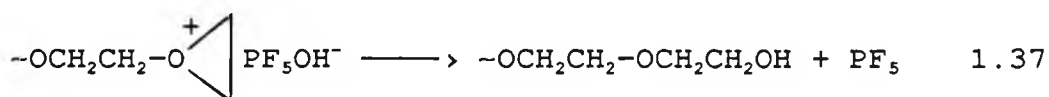
#### 3. Termination

In a very pure system termination reactions are scarce which emphasises the 'living nature' of cationic polymerisation. As this is difficult to achieve there are often trace impurities in the system which can cause termination. Thus

termination of the growing cationic chain end may be via reaction with nucleophilic or basic impurities or corresponding reactive sites of the polymers. One such impurity is water which may have an adverse effect on the polymerisation as follows.



This produces a counterion that is more nucleophilic than the  $\text{PF}_6^-$  counterion and can attack the growing polymer chain.



If as in scheme 1.3 the monomer contains only one epoxide group, photopolymerisation produces a linear polymer. In most commercial systems efficient crosslinking is required to produce mechanically strong and chemically resistant three dimensional macromolecular structures. It is for this reason that bis(epoxides) and poly(epoxides) are commonly used (NB cycloaliphatic epoxies show higher reactivities than glycidyl ethers and glycidyl esters see J.V.Crivello in UV Curing, Science and Technology, (S.P.Pappas, ed) Stamford, Technology Marketing Corp., p23, 1978). Cationic polymerisation, unlike radical polymerisation, involves living polymers, and so polymerisation continues after the light source has been removed. Thus it is possible to observe post-curing in these systems. In one instance 60% of polymerisation was shown to be due to post cure (Decker

and Moussa, 1988). Typical catalysts for cationic polymerisation include aprotic acids (Lewis acids and Friedel-Crafts halides), protonic species (Brönsted acids), and stable carbenium-ion salts. All these are strong electron acceptors. Many of them, particularly the Lewis acids, require a co-catalyst, usually a Lewis base or other proton donor, to initiate polymerisation.

Cationic polymerisation was discovered in 1839 by Deville using tin IV chloride as a catalyst for polymerisation of styrene (Deville, 1839). Since then a number of reports of cationic polymerisation catalysts have been documented. Cationic photoinitiation has received considerable attention over the last 20 years. Prior to this there was a dearth of suitable photoinitiators. The first efficient catalysts for photopolymerisation of epoxides were aromatic diazonium salts with anions of low nucleophilicity (Schlesinger, 1974a; Schlesinger, 1974b). The spectral response of the diazonium salts can be varied throughout the UV-visible region of the spectrum by altering the substituents on the aromatic ring (Schlesinger, 1974a). On irradiation these salts generate Lewis acids which can initiate the polymerisation. The disadvantages of using diazonium salts are the liberation of nitrogen gas on irradiation, which limits the practical usefulness due to formation of bubbles in the polymers, and their limited thermal stability, preventing long term storage of formulated systems.

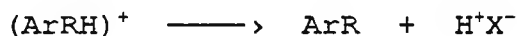
These problems were largely overcome with the discovery of photoactive onium salts and in particular the diaryliodonium salts (Crivello and Lam, 1977; Crivello and Lam, 1979c), and the triarylsulphonium salts (Crivello and Lam, 1979a; Crivello and Lam, 1980a; Crivello and Lam, 1980b), both with anions of low nucleophilicity. On irradiation the onium salts generate Brønsted acids, as shown in schemes 1.4 and 1.5 below, which are very effective catalysts for the polymerisation of epoxides.

Scheme 1.4 Photolysis of diaryliodonium salts

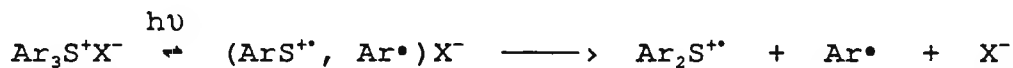
Major



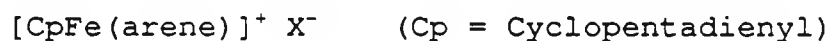
Minor



Scheme 1.5 Photolysis of triarylsulphonium salts

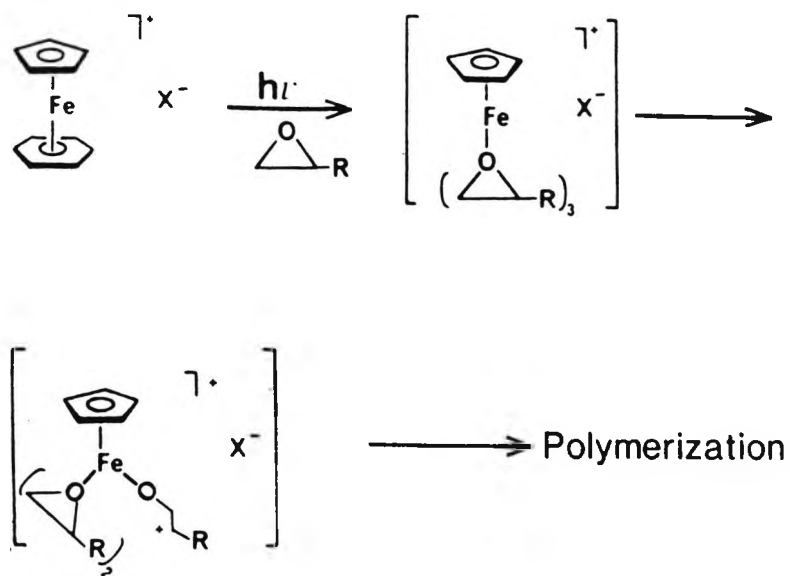


Onium salt photoinitiators have strong absorption bands in the deep UV region, but their sensitivity can be extended to longer wavelengths by use of suitable sensitizers (Crivello and Lam, 1978; Crivello and Lam, 1979b). Also triarylsulphonium salt photoinitiators with extended conjugation systems and thus improved spectral sensitivity have been reported (Crivello and Lam, 1979a; Crivello and Lam, 1980b). Recently Meier and Zweifel have reported that iron arene salts with anions of low nucleophilicity can be used as efficient photoinitiators for the cationic polymerisation of epoxides (Lohse and Zweifel, 1986; Meier and Zweifel, 1985a; Meier and Zweifel, 1986a; Meier and Zweifel, 1986b). Various types of such complexes described by the following general formula are listed in the literature (Schumann, 1984).



Upon irradiation the iron arene complexes lose the uncharged arene ligand and thereby yield a Lewis acid. It is postulated that this Lewis acid reacts with an epoxy monomer to give a complex with three epoxide ligands coordinated to the iron moiety (Klingert et al, 1988). Ring opening polymerisation could then start within the ligand sphere of the iron cation leading to poly(ethers) as shown below in scheme 1.6.

Scheme 1.6 The polymerisation of epoxides using iron-arene salts



Iron arene photoinitiators have good light absorption properties in the UV region of the spectrum. The absorption characteristics can be modified over a wide range by altering the arene ligands. The photolysis has also been sensitised with anthracene derivatives (Meier and Zweifel, 1985b). The oxidation state of the iron in these photoinitiators is +2 before and after exposure to irradiation. Oxidation of the iron complex to the +3 oxidation state leads to a Lewis acid with increased activity for epoxide polymerisation. Thus in the presence of an oxidant, such as cumene hydroperoxide, polymerisation occurs at an enhanced rate compared to the rate obtained in the absence of oxidant (Lohse and Zweifel, 1986). The absorption spectrum of the iron arene complex changes on exposure to irradiation.

As photolysis proceeds the arene fragment is depleted and thus the optical density in the near UV and visible part of the spectrum decreases with time. This effectively means that the system is photobleachable and thus permits light penetration into thick layers as photolysis proceeds. DSC experiments show that the iron arene photoinitiators are generally less reactive than Brönsted acids obtained from sulphonium salts and therefore heat treatment is required after irradiation to effect polymerisation.

### 1.5.2 Kinetics of cationic polymerisation

The steps involved in cationic polymerisation are similar to those in free radical polymerisation and are:

1. Initiation (Equations 1.38, 1.39)
2. Propagation (Equation 1.40)
3. Termination (Equation 1.41)
4. Transfer (Equation 1.42)



where,

A = catalyst, RH = co-catalyst, M = monomer, K = rate constant for formation of initiator,  $k_i$  = rate constant for initiation,  $k_p$  = rate constant for propagation,  $k_t$  = rate constant for termination,  $k_{tr}$  = rate constant for transfer  
This gives rise to a series of rate equations that may be derived from the above expressions.

$$\text{Rate of initiation, } R_i = K k_i [A] [RH] [M] \quad 1.43$$

In strong contrast to free radical polymerisation the termination is first order, thus;

$$\text{Rate of termination, } R_t = k_t [M^*] \quad 1.44$$

Using the steady state assumption that  $R_i = R_t$ ,

$$[M^*] = \frac{K k_i}{k_t} [A] [RH] [M] \quad 1.45$$

and the overall polymerisation rate,

$$R_p = k_p [M] [M^*] \quad 1.46$$

$$= K \frac{k_i k_p}{k_t} [A] [RH] [M]^2 \quad 1.47$$

The degree of polymerisation,  $x_n$ , can be calculated.

If termination predominates over transfer then,

$$x_n = \frac{k_p}{k_t} [M] \quad 1.48$$

Or if transfer predominates then,

$$x_n = \frac{k_p}{k_{tr}} \quad 1.49$$

The ease of polymerisation of a given cyclic monomer depends on the reactivity of the functional group in the ring, the size of the ring, and the catalyst used.

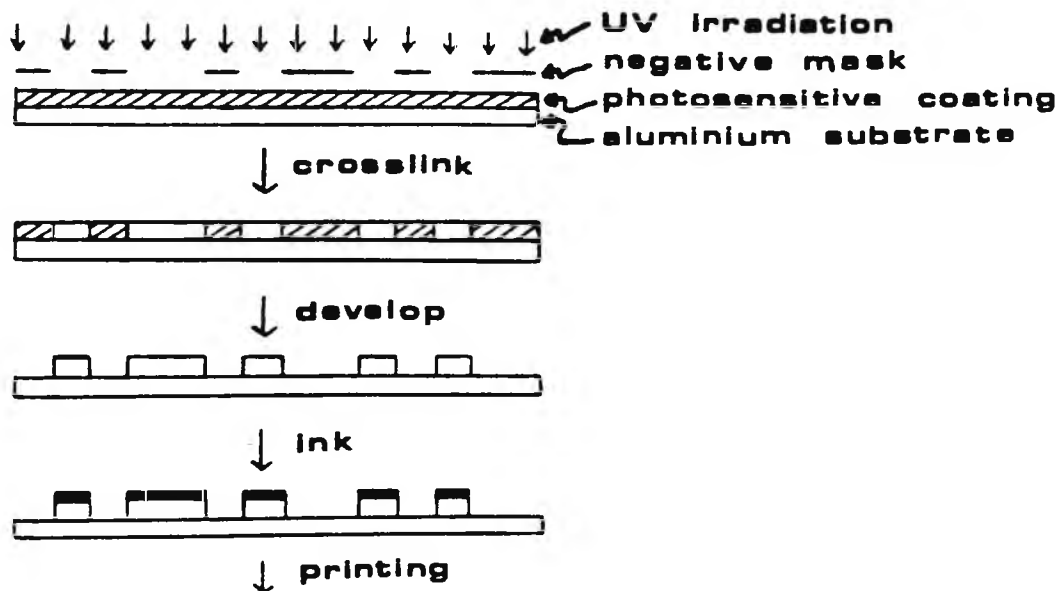
### 1.6 Industrial applications of photopolymerisation

The spirit of enquiry was typified by the ancient Egyptians who wrapped mummies in light-sensitive linen cloths, whose light sensitivity was facilitated by dipping them in a mixture of lavender oil and Syrian asphalt. This procedure was developed thousands of years later in 1822 by Niepce who coated a glass plate with Syrian asphalt and removed the unexposed (and therefore uncrosslinked) part of the coating by washing with turpentine, to yield an early type of lithographic plate for producing prints (Jackel, 1989).

Nowadays photopolymerisation is the basis of an important commercial process with wide ranging applications such as photoimaging (Thompson et al, 1983), and UV curing (Pappas, 1978; Roffey, 1982; Pappas, 1984). Photopolymerisation utilises electromagnetic radiation as the energy source for polymerisation of functional monomers, multifunctional monomers (or oligomers), and pre-polymers used in combination with a photoinitiating system. The polymerisation process effects a modification in the chemical structure of the resin system which in turn alters

the physical properties. This usually results in solvent discrimination between the crosslinked and uncrosslinked areas. There are two main types of photopolymer systems widely employed commercially. Firstly, there are those that crosslink on irradiation forming a three dimensional network which results in a decrease in solubility of the exposed areas, termed negative working systems. Secondly, there are those that are originally macromolecular structures, which on irradiation decrease in molecular weight resulting in an increase in solubility of the exposed areas, termed positive working systems. It is only the former, negative working systems, that will be discussed here. Selective areas can be exposed to UV light through a photographic negative and then these areas alone will become crosslinked and thus insoluble. This is the principle used in the lithographic printing industry to create printing plates. An example of a negative working lithoplate is shown below in scheme 1.7.

Scheme 1.7 The production of a negative-working lithoplate



The main advantages of UV curing over conventional means of effecting polymerisation, such as heating or mixing, are that rapid network formation occurs in a short time period. Generally irradiation times of a few seconds are sufficient and in some cases a few hundredths of a second are adequate. Less energy is required and many systems do not require a solvent to be present.

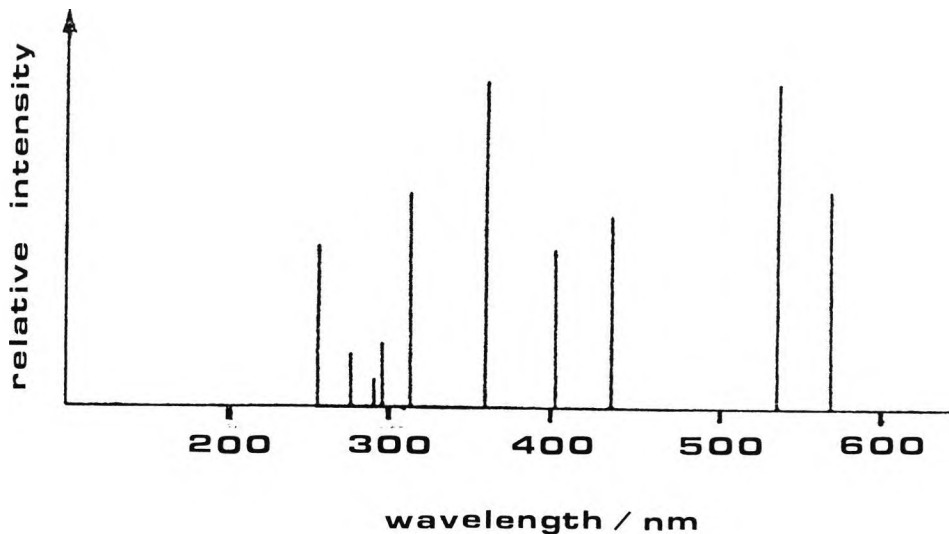
The properties of the coatings such as hardness, flexibility, abrasion resistance, and solvent resistance are determined by the composition of the resin system. The design of the resin system has been the subject of many reports (Roffey, 1982; Pappas, 1984). Commonly free radical photoinitiated polymerisation of acrylate resins has been extensively used commercially. Photoinduced cationic polymerisation can also be used in photoresist and printed circuit technologies (McGinnis, 1979). In general cationic polymerisation has received less attention than radical polymerisation due to the lack of suitable photoinitiators available. The rate of cationic polymerisation is relatively slow when compared to radical polymerisation and it is often the case that the rate of the polymerisation dictates the material used in the commercially orientated marketplace.

Important parameters in photoimaging applications include resolution, sensitivity, and reproducibility.

Resolution may be described as the limit of discrimination between image (crosslinked) and non-imaged (uncrosslinked) areas of the printed typescript. Lithographic sensitivity may be expressed in terms of the dose requirement required to produce a crosslinked network and is generally of the order of tenths to tens of  $\text{mJ}/\text{cm}^2$  for commercial systems.

### 1.6.1 Light sources

Many types of light sources can be used in photopolymerisation (McGinnis, 1978). The light source that is normally used in commercial UV curing is the medium pressure mercury-arc lamp which has its main outputs at 313, 365, 404, and 436nm shown below.



There are also a number of lasers available that can be used in the UV region such as the rare gas halide excimer lasers and in the visible region such as the He-Cd source at 441.6nm and the Ar source at 488nm.

### 1.7 Experimental test procedures

In order to assess the efficiency of photoinitiators in photoinitiated polymerisations, experimental methods are required that enable the rates of polymerisation to be measured under reproducible conditions. A number of different techniques have been developed utilising methods based on differential scanning calorimetry (Tryson and Shultz, 1979; Moore, 1980), dilatometry (Cundall et al, 1987), laser nephelometry (Decker and Fizet, 1980), infrared spectroscopy (Lee and Doorakian, 1977), real-time infrared spectroscopy (Decker and Moussa, 1988), NMR (Barret, 1979), and Fourier Transform infrared spectroscopy (Small et al, 1984).

Of the above methods real-time infrared (RTIR) spectroscopy, and differential scanning calorimetry (DSC), another real-time method, have been used to follow photopolymerisation reactions. UV curing, an important technique in the industrial sector, has also been used to assess the properties of photoinitiators in thin films.

Electron paramagnetic resonance (EPR) spectroscopy has been used to investigate the properties of several radical cations with particular regard to their fragmentation pathways. All four of these experimental techniques are described in the next section.

#### 1.7.1 UV Curing

A number of the prepared compounds have been investigated for use as a component in a photoinitiating system. The photoinitiating systems tested have been comprised of either one component or two components. The photoinitiating system was then mixed with a polymerisable monomer. All of the prepared compounds under test were loaded at various percentage levels (usually at 1-5% weight/weight {w/w} in the monomer), along with the other component of the photoinitiating system if incorporated. This combined mixture was then subjected to light irradiation and the polymerisation was monitored. The monomers under test fall into two categories ; those polymerisable by a radical initiator eg. acrylates, and those polymerisable by a cationic initiator eg. epoxides. The extent of polymerisation both with and without a photoinitiating system present was tested for all formulations. A comparison of the two results then yields useful information on the efficiency of the photoinitiating system present. The choice of monomer is determined by the type of initiating species produced upon irradiation. There are

often proposed mechanisms of initiation given in the literature for given types of compounds which are helpful for choosing monomer type, but occasionally the mechanism is not fully understood and a more investigative approach must prevail.

The formulation of each system was carried out in such a way that as little UV light as possible was able to interact with the initiating/monomer system. The formulation was then coated onto GNT paper substrate using a manually operated R-K Meyer bar coater (No. 3; thickness 25 $\mu$ ). A number of operations were then carried out on the coating to give four different test conditions. These are outlined below and represented in figure 1.7 below.

#### 1. Touching quartz

A piece of quartz is placed directly in contact with the film. This allows the full output of the lamp to irradiate the coating, and since the quartz is touching the film the diffusion of oxygen into the film is minimised (especially important in radical polymerisation).

#### 2. Touching glass

A piece of glass is placed in direct contact with the film. This allows the output of the lamp beyond approximately 310nm to irradiate the coating, since the glass is touching the film the oxygen inhibition effect is minimised as above.

### 3. In air

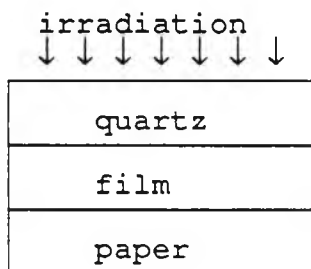
The film is irradiated directly from the light source in the presence of air.

### 4. Glass filter

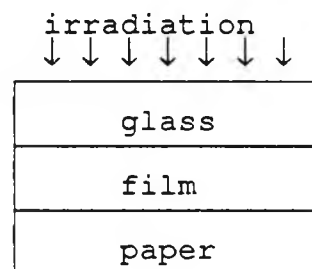
A glass filter is placed above the film, but not touching it, to act as a filter of light with wavelength below 310nm. Thus the film is irradiated in air but without the full spectral output of the lamp.

Figure 1.7 The four different irradiation conditions

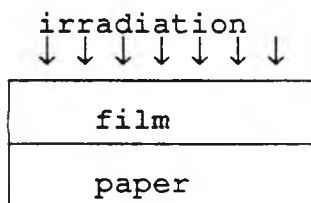
#### 1. Touching quartz



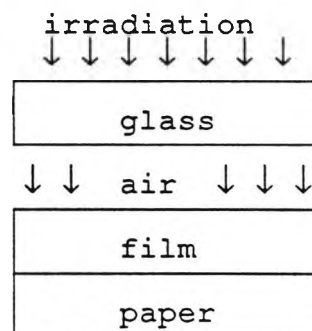
#### 2. Touching glass



#### 3. In air

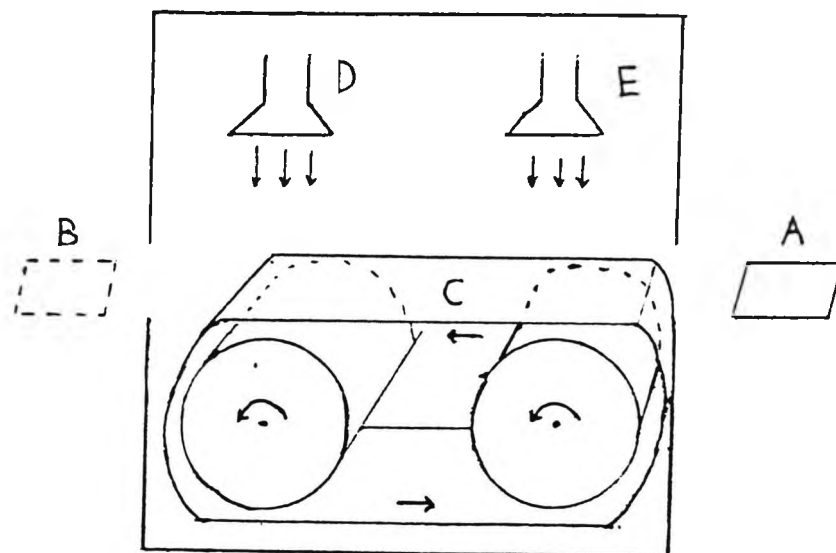


#### 4. Glass filter



The coated substrate is then mounted onto a steel plate and secured . The steel plate is then placed onto a moving belt and irradiated with UV light, using a Colordry twin lamp UV unit (see figure 1.8), operating at various moving belt speeds, and utilising either one lamp or two.

Figure 1.8 The UV Colordry apparatus



The number of passes is recorded for the coated layer to become tack-free. The term tack-free represents the point where the liquid film becomes solid due to the crosslinked network formed during polymerisation. One pass is represented as the movement of the substrate from position A to position B on moving belt C beneath irradiation from lamp(s) D or/and E.

### 1.7.2 Real-time infrared (RTIR) spectroscopy

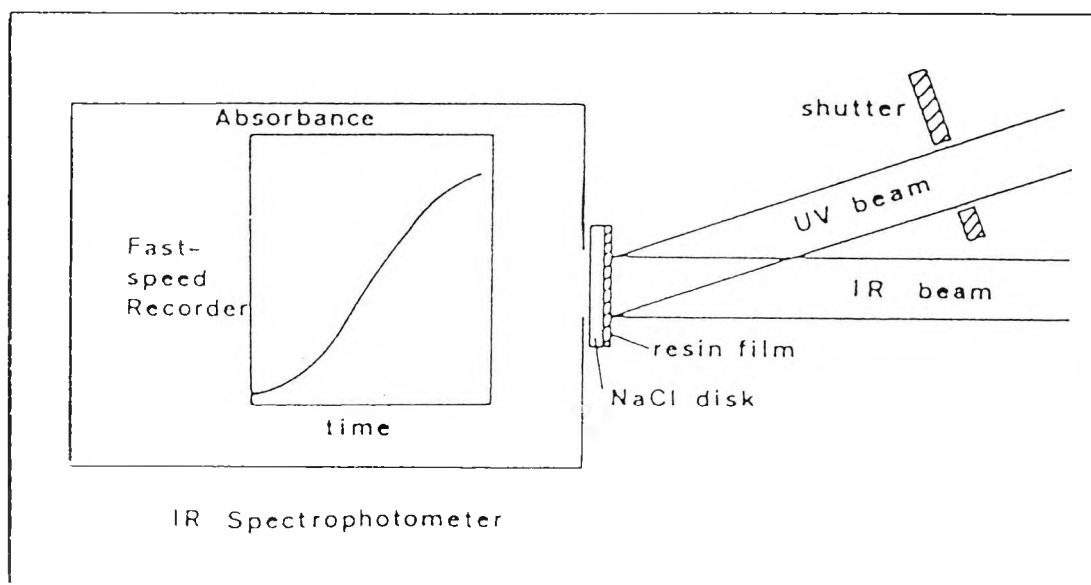
RTIR spectroscopy has been used to monitor polymerisations in real-time, quantitatively and in situ, that take place in less than a second. The technique has been used to study the effect on the polymerisation rate of the photoinitiator efficiency, the monomer reactivity, the light intensity, the film thickness, oxygen inhibition, and the postcure that develops after the end of the irradiation (Decker and Moussa, 1988). The technique has been used to monitor UV and laser induced photopolymerisations of both acrylic (Decker and Moussa, 1990a) and epoxy (Decker and Moussa, 1990b) monomers.

#### Experimental details

RTIR spectroscopy was used to follow quantitatively the photopolymerisation in situ by monitoring the disappearance of the infrared absorption characteristic of the polymerisable monomer under test.

The experimental set-up shown in figure 1.9 was devised so that the sample was exposed to the UV beam and the analysing IR beam at the same time.

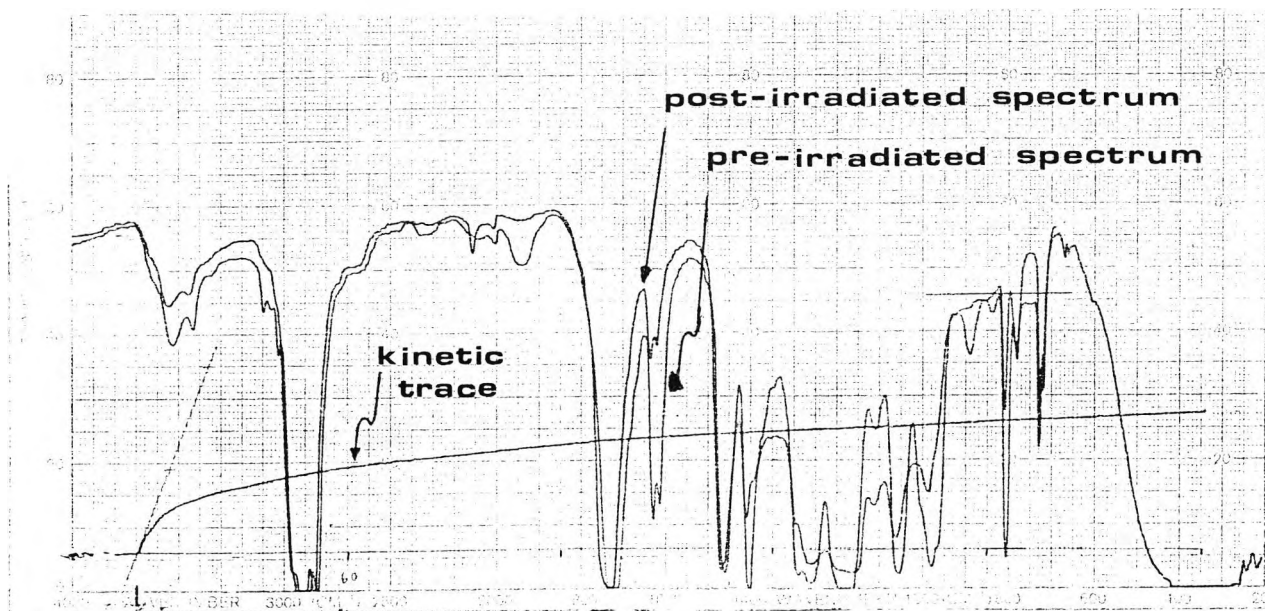
Figure 1.9 The RTIR spectroscopy apparatus



The sample formulation, which consisted of photoinitiating system and monomer, was applied onto a NaCl salt disc using R-K Meyer bar coater No. 3 (thickness 25 microns) and a polyethylene cover slip (for UV see appendix: Figure 5.1) was placed in direct contact with the film. The coated disc was then placed into an infrared spectrometer and a pre-irradiation infrared spectrum was recorded. Then the

spectrometer was programmed to operate in the time-drive mode and thus the infrared wavelength was fixed. For acrylates this corresponds to the strong C=C stretching vibration at  $810\text{cm}^{-1}$ . The detection of the infrared signal was made by operating the spectrometer in the absorbance mode. The sample was then exposed to the radiation of a medium pressure mercury lamp and at the same time the disappearance of the  $810\text{cm}^{-1}$  signal was monitored as a kinetic trace of polymerisation. The irradiation and the kinetic trace were stopped together, unless postcure detection was desired, and the spectrometer was reverted back to the normal working mode. Finally a post-irradiated spectrum was recorded. The pre-irradiated spectrum, kinetic trace, and the post-irradiated spectrum were all recorded on the same axes as shown in figure 1.10.

Figure 1.10 The RTIR spectroscopy results



The degree of conversion is directly related to the decrease of the IR absorbance, and can be calculated (for acrylates) using equation 1.50.

$$\text{Degree of conversion} = \frac{(A_{810})_t}{(A_{810})_0} \times 100\% \quad \text{Equation 1.50}$$

where  $(A_{810})_0$  and  $(A_{810})_t$  are the respective absorbances at  $810\text{cm}^{-1}$  of the sample before and after UV exposure during time  $t$ . Since the degree of conversion can be readily calculated it follows that the degree of residual unsaturation in the photopolymerised coating can be calculated by using the relationship in equation 1.51.

$$\text{Degree of residual unsaturation} = \frac{(A_{810})_0 - (A_{810})_t}{(A_{810})_0} \times 100\% \quad \text{Equation 1.51}$$

From figure 1.10 the rate of polymerisation can be deduced using equation 1.52.

$$R_p = [M]_0 \frac{(A_{810})_{t_1} - (A_{810})_{t_2}}{(A_{810})_0 [t_2 - t_1]} \quad \text{Equation 1.52}$$

where  $[M]_0$  is the original concentration of acrylate double bonds and  $(A_{810})_0$ ,  $(A_{810})_{t_1}$  and  $(A_{810})_{t_2}$  are the respective absorbances at  $810\text{cm}^{-1}$  at times  $t=0$ ,  $t_1$  and  $t_2$  (where  $t_2 > t_1$ ). Thus the rate of polymerisation can be deduced for a particular period of the reaction.

### 1.7.3 Photo-differential scanning calorimetry (Photo-DSC)

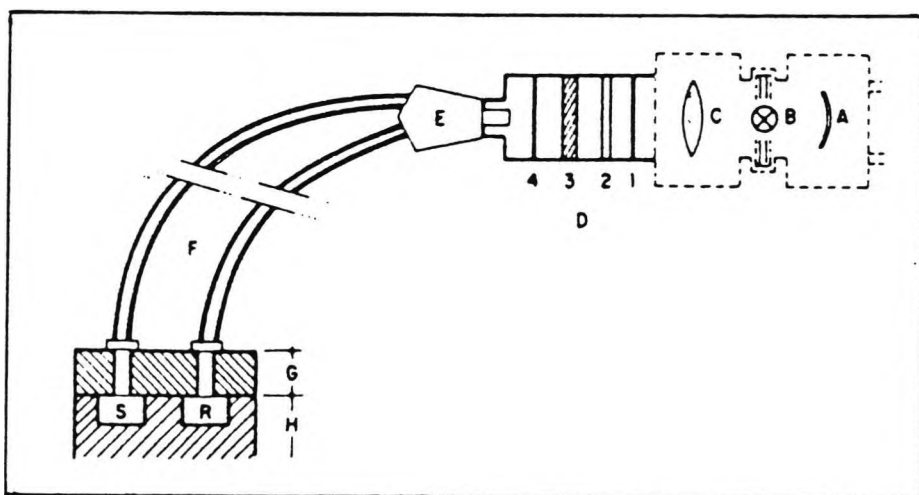
A differential scanning calorimeter can be used to measure the rate of heat produced and the total amount of heat from a chemical reaction. During polymerisation, which is exothermic, this can be related to the rate of conversion of monomer to polymer and to the total amount of monomer polymerised. A conventional commercial differential scanning calorimeter can easily be modified to study photoinitiated polymerisations (Moore et al, 1975). A number of reports appeared in the 1970's that utilised photo-DSC to study acrylate photopolymerisation (Moore et al, 1975; Wight and Hicks, 1978; Tryson and Shultz, 1979), and epoxide photopolymerisation (Crivello & Lam, 1977; Shultz and Stang, 1976). More recently the kinetics of photopolymerisation of epoxides has been studied (Shultz and Stang, 1987) and the technique has been used to study the bulk photopolymerisation of lauryl acrylate (Sastre et al, 1988).

#### Experimental details

The photo-DSC experiments were carried out in the laboratories of the CSIC Polymer Institute in Madrid using a modified Perkin-Elmer DSC-4 calorimeter which has been described previously (Sastre et al, 1989). A schematic representation of the experimental set up is shown below in

figure 1.11.

Figure 1.11 Photo-DSC apparatus



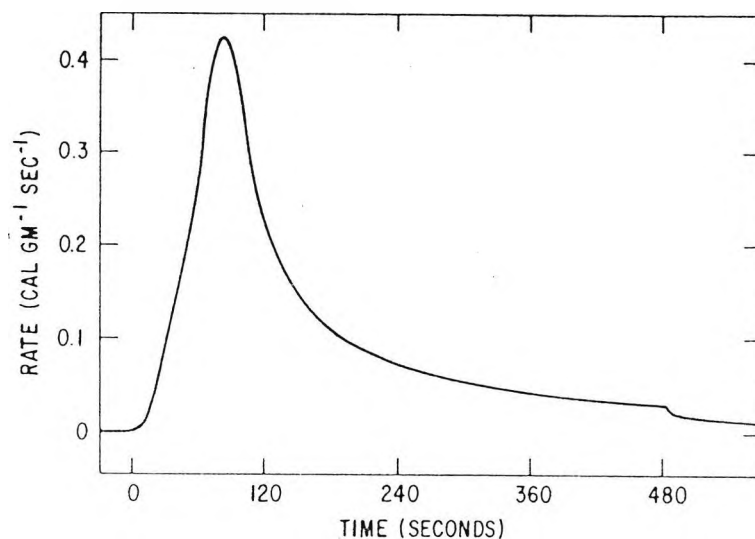
Schematic diagram of modified DSC-4: A, aluminium mirror; B, light source; C, focusing optics; D, aluminium cylinder cavity (1, neutral density filter; 2, solid IR filter; 3, interference filter; 4, shutter); E, fibre optics connector; F, two-branch flexible light-guide fibres; G, DSC swing away cover; H, DSC head; S, sample holder; R, reference holder.

The optics were aligned such that sample and reference cells were irradiated with the same light intensity. All experiments were performed using the calorimeter in the isothermal mode of operation. This means that any temperature difference between sample and reference pans is automatically set to zero by electrical compensation. The energy needed for this compensation corresponds directly to

the absorbed or released heat by the substance tested and is displayed as the measured signal. A purge gas, usually nitrogen, can be introduced into the system. The sample size was kept constant to reduce the possible side effects on the polymerisation rates. Filters could be incorporated in the path of the light source to give irradiation of a fixed wavelength band. A 365nm band pass filter was used in this context for all experiments performed. Prior to irradiation the samples were allowed to equilibrate to the operating temperature of 40°C for 5 minutes. This was also the case when a purge gas was used (eg. nitrogen) to equilibrate the samples to both the temperature and the inert atmosphere. The DSC-4 experimental run was allowed to begin for 1 minute without irradiation. This was to allow the DSC-4 to equilibrate and to check that a suitable flat baseline was recorded for later mathematical calculations. After 1 minute, irradiation from the Hg lamp was started by means of a shutter and the exothermic trace was recorded. After a suitable period of irradiation (generally around 5 minutes) the irradiation was stopped leaving the DSC-4 in the operating mode. This allowed the detection of any polymerisation occurring in the dark and meant that the trace eventually returned to the original baseline position. This was important for later calculations in which the integration of the appropriate area under the polymerisation exotherm was required to give a representative value for the rate of polymerisation. The rate of heat released by the sample ( $dH/dt$  in mcal/sec) was plotted versus the elapsed

time of the reaction. A typical exothermic trace due to polymerisation is shown in figure 1.12.

Figure 1.12 An exothermic polymerisation trace



The data acquired was analysed using the appropriate software programme on the data station. Analysis of the isothermal polymerisation follows the procedure previously documented (Barrett, 1967).

The total area, (A), of the exotherm curve corresponds to the total heat of polymerisation of the sample as shown in equation 1.53.

$$\Delta H_{\text{polym}} = A$$

1.53

and the degree of conversion can be represented by equation 1.54.

$$\text{Degree of conversion} = \frac{\text{area under exotherm/cal/g}}{\text{heat for 100\% reaction/cal/g}} \times 100\%$$

Equation 1.54

The area under the exotherm can be integrated at different time intervals to give a profile of the polymerisation as it proceeds. This is achieved using cursor lines in the appropriate software. The heat for 100% reaction of TMPTA has been calculated to be 195 cal/g (Tryson and Shultz, 1979).

The rate of polymerisation,  $R_p$ , is given by equation 1.55.

$$R_p = \frac{\text{Degree of conversion} \times [M]}{\text{time}} \quad \text{Equation 1.55}$$

[M] = monomer concentration /  $\text{moll}^{-1}$

Time = time of experimental run / s

Thus the rate of polymerisation can be determined at any point during reaction by integration of the exothermic curves using the necessary software programme. Therefore the efficiencies of different initiating systems can easily be evaluated using this technique.

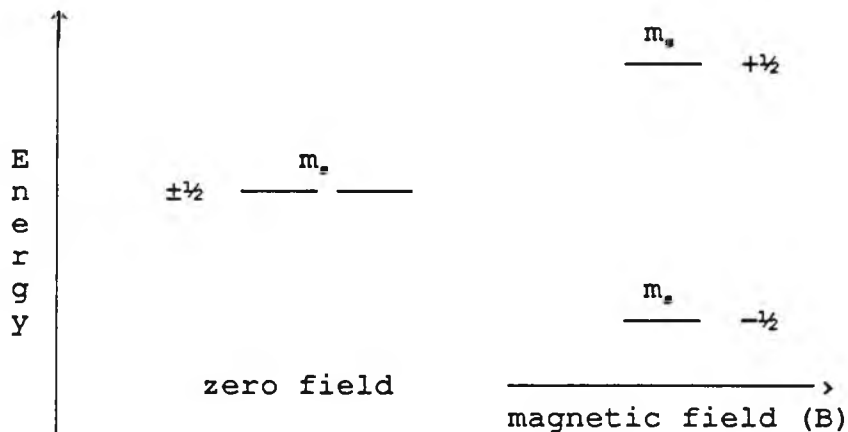
#### 1.7.4 Electron Paramagnetic Resonance (EPR) Spectroscopy

##### Introduction

The first successful EPR experiment was performed by a Russian physicist (Zavoisky, 1945) in the same year that early reports of the related technique nuclear magnetic resonance spectroscopy (NMR) appeared. The EPR method was developed further by chemists when it became apparent that free radicals could be detected and studied using this technique.

##### Principles of EPR

The basic EPR experiment involves the irradiation of a sample containing unpaired electrons with microwave radiation in the presence of an external magnetic field (B). In the absence of a magnetic field there are two possible spin states that may be exhibited by an unpaired electron denoted by spin quantum numbers  $m_s = +\frac{1}{2}$  and  $m_s = -\frac{1}{2}$ . These two spin states have the same energy and are equally populated. On the application of a magnetic field this is no longer the case and there is a net lowering of the energy of the spin state  $m_s = -\frac{1}{2}$  and a corresponding increase for that of the  $m_s = +\frac{1}{2}$  spin state as depicted below.



In practise it is convenient to use a microwave source of fixed frequency and to vary the magnetic field (B) until the condition for resonance is achieved. The energy level splitting ( $\Delta E$ ) between the  $m_s = +\frac{1}{2}$  and  $m_s = -\frac{1}{2}$  states is a function of B and is given by equation 1.56.

$$\Delta E = h\nu = g\mu_B B \qquad 1.56$$

where,

$g$  =  $g$  factor (which is dimensionless, compare to chemical shift in NMR)

$\mu_B$  = Bohr magneton

$B$  = magnetic field

Since the  $m_s = -\frac{1}{2}$  state now has a lower energy it is more greatly populated than the  $m_s = +\frac{1}{2}$  state and their relative populations may be expressed using the Maxwell-Boltzmann law.

$$N_{m_s = +\frac{1}{2}} / N_{m_s = -\frac{1}{2}} = \exp(\Delta E/kT)$$

Equation 1.57

where the symbol (N) represents the number of unpaired electrons in each state shown and k is the Boltzmann constant. The EPR spectrometer measures the net absorption of energy created in the 'upward' transition from the  $m_s = -\frac{1}{2}$  state to the  $m_s = +\frac{1}{2}$  state. Thus by sweeping the field (B) at constant frequency ( $\nu$ ) the field ( $B_0$ ) required for resonance may be measured directly at the maximum of the absorption peak with a suitable field probe.

### The g factor

The so called g-factor depends on the orientation of the radical with respect to the magnetic field B. Assuming there are no external factors affecting the spin of the unpaired electron then this 'free electron' would have a g value of 2.0023. This is not the usual case and generally the local field at the electron depends to some extent on its environment (as is the case for nuclei in NMR spectroscopy so that chemical shifts are observed) and its value may be of diagnostic value. Shifts in the g factor value may be positive or negative compared to the free electron value. The source of the variation is due to the differences in spin-orbit coupling, which can create a secondary field, which couples with the magnetic moment of the electron due to its intrinsic spin.

## Hyperfine splitting

This is analogous to nuclear spin-spin coupling in NMR spectroscopy and is an important feature of EPR spectroscopy. It can reveal the nature of the magnetic nuclei that are present in a particular paramagnetic species and is, therefore, of diagnostic value.

For example in the case of the hydrogen atom ( $H^\bullet$ ) the associated proton may take either the  $m_I = +\frac{1}{2}$  or  $-\frac{1}{2}$  state with respect to the electron. Thus the magnetism due to the intrinsic proton spin may either augment ( $+\frac{1}{2}$ ) or detract ( $-\frac{1}{2}$ ) from the applied magnetic field giving rise to four possible spin states of the electron, all of different energies.

In more complex systems quantum mechanical restrictions give rise to the general rule that if a group of (n) equivalent nuclei with spin (I) are coupled to the unpaired electron  $2nI + 1$  spectral lines will be observed arising from the same number of transitions.

## Intensities

As is the case for NMR spectroscopy the net intensities of the lines in any multiplet, arising from the coupling of the odd electron with a set of n equivalent nuclei, are given by the coefficient of the Binomial expansion represented by Pascal's Triangle. Therefore, the four lines in the EPR spectrum of  $CH_3^\bullet$  are in the ratio 1:3:3:1.

## EPR spectra of radical cations

The best method of generating these species is by the use of halocarbon solvents with "freons" being most commonly used (Symons, 1984). The procedure is to prepare a dilute (0.1-1.0 w/w%) solution of the substrate in a solvent such as  $\text{CFCl}_3$ , freeze to 77K and then expose the frozen material to  $\gamma$  radiation. Taking the example of  $\text{CFCl}_3$ , the relevant radiolytic processes may be summarised as follows in scheme 1.8.

### Scheme 1.8 The radiolytic processes of $\text{CFCl}_3$

1.  $\text{CFCl}_3 \longrightarrow \text{CFCl}_3^{+\bullet} + e^-$
2.  $\text{CFCl}_3 + e^- \longrightarrow [\text{CFCl}_3^{\cdot-}] \longrightarrow \text{CFCl}_2^\bullet + \text{Cl}^-$
3.  $\text{CFCl}_3^{+\bullet} + \text{CFCl}_3 \longrightarrow \text{CFCl}_3 + \text{CFCl}_3^{+\bullet}$
4.  $\text{CFCl}_3^{+\bullet} + \text{S} \longrightarrow \text{CFCl}_3 + \text{S}^{+\bullet}$

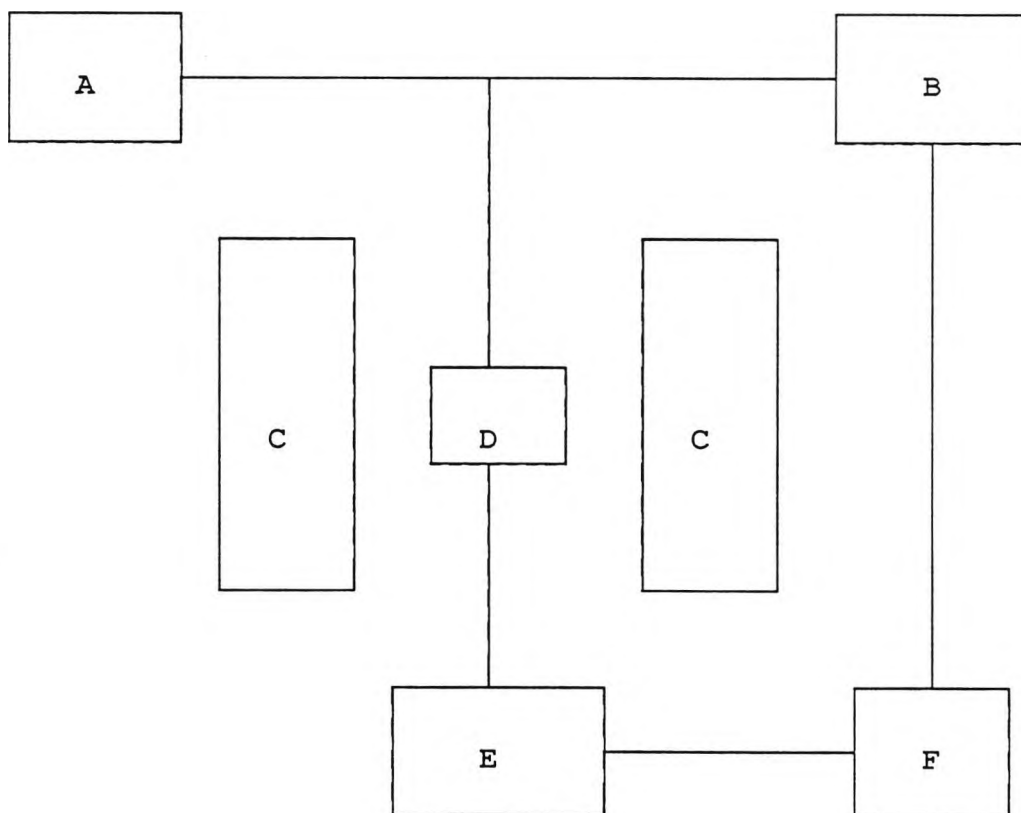
The advantage of this method is that the radiolytically produced electrons are efficiently scavenged (step 2) and are converted to product radicals with very broad EPR signals so that only the sharper features of the substrate (S) radical cations  $\text{S}^{+\bullet}$ , as produced in step 4, are normally

observed. Providing the substrate has a lower ionisation potential than the "freon" solvent (around 12eV) this is an appropriate method to study the behaviour of the radical cation.

### Instrumentation

Full details of the design of EPR spectrometer systems can be found in textbooks on the subject (Poole, 1967; Wilmshurst, 1967). A simplified overview of the essential components used is given in the block diagram in figure 1.13.

Figure 1.13 Schematic diagram of an EPR spectrometer



A = microwave bridge, B = detector crystal, C = electromagnet, D = cavity, E = modulation input, F = phase sensitive detector, G = signal output

Within the microwave bridge is contained the klystron (or Gunn diode) which supplies the microwaves which are transmitted to the resonant cavity and the detector by means of waveguides. A strong magnetic field is applied to the cavity, which contains the paramagnetic sample, by a strong electromagnet. Since the microwave source is of fixed frequency, the magnetic field is 'swept' so as to achieve the condition of resonance.

## 1.8 References

- Barrett, K.E.J., (1967). *J.Appl.Poly.Sci.*, **11**, 1617
- Barret, J.L., (1979). *J.Rad.Curing*, **6** (4), 20
- Bartholomew, R.F., and Davidson, R.S., (1971b). *J.Chem.Soc. (C)*, 2342
- Bartholomew, R.F., and Davidson, R.S., (1971a). *J.Chem.Soc. (C)*, 2347
- Bartholomew, R.F., Davidson, R.S., and Howell, M.J., (1971). *J.Chem.Soc. (C)*, 2804
- Baxter, J.E., Davidson, R.S., and Hageman, H.J., (1987). *Makromol.Chem.,Rapid Commun.*, **8**, 311
- Birks, J.B., (1970). "Photophysics of Aromatic Molecules", Wiley-Interscience, London
- Birks, J.B., (1973). "Organic Molecular Photophysics", Vol. 1, 403 (ed. Birks, J.B.), Wiley, New York
- Bolon, D.A., and Webb, K.K., (1978). *J.Appl.Polymer.Sci.*, **22**, 2543
- Calvert, J.G., and Pitts, J.N., (1966). *Photochemistry*,

Wiley, New York

Crivello, J.V., and Lam, J.H.W., (1977). *Macromolecules*,  
10, 1307

Crivello, J.V., and Lam, J.H.W., (1978). *J.Polym.Sci.,*  
*Polym.Chem.Edn.*, 16, 2441

Crivello, J.V., and Lam, J.H.W., (1979a). *J.Polym.Sci.,*  
*Polym.Chem.Edn.*, 17, 977

Crivello, J.V., and Lam, J.H.W., (1979b). *J.Polym.Sci.,*  
*Polym.Chem.Edn.*, 17, 1059

Crivello, J.V., and Lam, J.H.W., (1979c). *J.Polym.Sci.,*  
*Polym.Chem.Edn.*, 17, 3845

Crivello, J.V., and Lam, J.H.W., (1980a). *J.Polym.Sci.,*  
*Polym.Chem.Edn.*, 18, 2677

Crivello, J.V., and Lam, J.H.W., (1980b). *J.Polym.Sci.,*  
*Polym.Chem.Edn.*, 18, 2697

Crosby, G.A., Watts, R.J., and Carstens, D.H.W., (1970).  
*Science*, 170, 1195

Cundall, R.B., Dandiker, Y.M., Davies, A.K., and Salim,  
M.S., (1987). *Polymers Paint Colour Journal*, 177 (4188),

Curtis, H., Irving, E., and Johnson, B.F.G., (1986).  
*Chem.Brit.*, 327

Decker, C., and Fizet, M., (1980). *Makromol.Chem., Rapid Commun.*, 1, 637

Decker, C., and Moussa, K., (1988). *Makromol.Chem.*, 189, 2381

Decker, C., and Moussa, K., (1990a). *ACS Symp.Ser.*, 417, 438

Decker, C., and Moussa, K., (1990b). *J.Polym.Sci., Polym.Chem.*, 28, 3429

Deville, (1839). *Ann.Chim.*, 75, 66

Eaton, D.F., (1979). *Photogr.Sci.Eng.*, 23, 150

Green, G.E., and Stark, B.P., (1981). *Chem.Brit.*, 17, 228

Ingold, K.U., *Acc.Chem.Res* 2,1

Jackel, K.P., (1989). *Prog.Org.Coatings*, 16, 355

Klingert, B., Riediker, M., and Roloff, A., (1988).  
*Comments Inorg.Chem.*, 7 (3), 109

Lee, G.A., and Doorakian, G.A., (1977). *J.Radiat. Curing*, 4,2

Lohse, F., and Zweifel, H., (1986). *Adv.Polym.Sci.*, 78, 61

McGinnis, V.D., (1978). "Light Sources; in UV Curing Science and Technology" (Pappas, S.P., [ed.]), Technology Marketing Corporation, Stamford, Connecticut 1978 pp96-132

McGinnis, V.D., (1979). *Photogr.Sci.Eng.*, **23**, 124

Medinger, T., and Wilkinson, F., (1965). *Trans.Faraday Soc.*, **61**, 620

Meier, K., and Zweifel, H., (1985a). *Polym.Preprints*, **26**, 347

Meier, K., and Zweifel, H., (1985b). *Eur.Pat.Appl.No.*, 0'152'377 to Ciba-Geigy

Meier, K., and Zweifel, H., (1986a). *J.Rad.Curing*, **26** (October)

Meier, K., and Zweifel, H., (1986b). *J.Imaging Sci.*, **30**, 174

Moore, J.E., Schroeter, S.H., & Shultz, A.R., (1975) *Org.Coat.Plast.Prep.*, **35**, 239

Moore, J.E., (1980). "UV Curing, Science and Technology", Ed. by S.P.Pappas, Technol.Market.Corp., Norwalk, Conn., USA, 133-159

Pappas, S.P., (ed.), (1978). 'UV Curing: Science and Technology', Vol. 1, Stamford Technology Marketing, Norwalk, CT

Pappas, S.P., (ed.), (1984). 'UV Curing: Science and Technology', Vol. 2, Stamford Technology Marketing, Norwalk, CT

Poole, C.P., (1967). "Electron Spin Resonance: A Comprehensive Treatise on Experimental Techniques", Wiley-Interscience, New York

Rehm, D., and Weller, A., (1970). *Isr.J.Chem.*, **8**, 259

Roffey, C.G., (1982). 'Polymerisation of Surface Coatings', Wiley-Interscience, New York

Rubin, H., (1974). *J.Paint Technol.*, **46**, 74

Sastre, R., Conde, M., and Mateo, J.L., (1988). *J.Photochem.Photobiol.,A:Chem.*, **44**, 111

Sastre, R., Conde, M., Catalina, F., and Mateo, J.L., (1989). *Rev.Plast.Mod.*, **393**, 375

Schlesinger, S.I., (1974a). *Photograph.Sci.Eng.*, **14**, 513

Schlesinger, S.I., (1974b). *Photograph.Sci.Eng.*, **18**, 387

Schumann, H., (1984). *Chemiker Zeitung*, **108**, 345

Shultz, A.R., and Stang, L.D., (1976). Paper presented at 7th Northeast Regional Meeting ACS, Albany, NY, August 8.

Shultz, A.R., and Stang, L.D., (1987). "Crosslinked Epoxies", Walter de Gruyter & Co., Berlin, 93-115

Small, R.D., Ors, J.A., and Royce, B.S., (1984). ACS Symp.Ser., 242, 325

Symons, M.C.R., (1984). Chem.Soc.Rev., 13, 393

Thompson, L.F., Willson, C.G., and Bowden, M.J., (eds.), (1983). 'Introduction to Microlithography', ACS Symp.Ser., No. 219, ACS Washington, D.C.

Turro, N.J., (1978). "Modern Molecular Photochemistry", Benjamin/Cummings, Menlo Park, California

Tryson, G.R., and Shultz, A.R., (1979). J.Polym.Sci., Polym.Phys.Ed., 17 (12), 2059

Tsuroska, M., and Tanaka, M., (1988). Proceed.Conf.Radiation Curing Tokyo, 403

Vander Donckt, E., and Vogels, C., (1971). Spectrochim.Acta., 27A, 2157

Wight, F.R., & Hicks, G.W., (1978). Polym.Eng.Sci., 18, 378

Wilmshurst, T.H., (1967). "Electron Spin Resonance Spectrometers", Adam Hilger, London

Zavoisky, E., (1945). J.Phys.USSR, 9, 211

## **Chapter 2.**

# **PHOTOPOLYMERISATION INITIATED USING ALLYL, BENZYL AND ASSOCIATED SILANES AND STANNANES**

## 2.1 The synthesis of silanes and stannanes

### Preparation

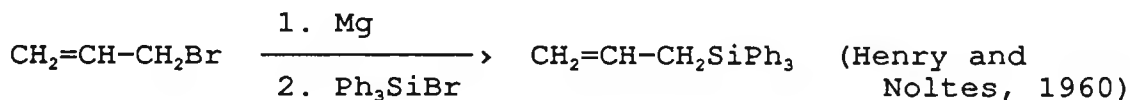
An introduction to synthetic routes that have been used in this work is presented. For a more comprehensive treatise on the many different synthetic methods the reader is referred to a number of excellent articles that have been published (Chan and Fleming, 1979; Colvin, 1981; Wilkinson et al, 1982; Sarkar, 1990a; Sarkar, 1990b).

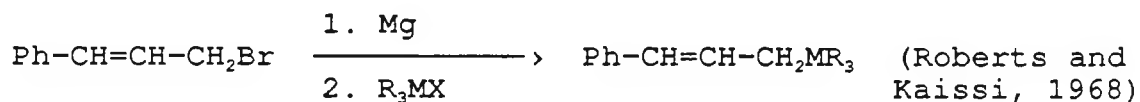
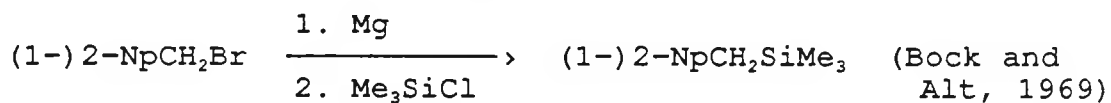
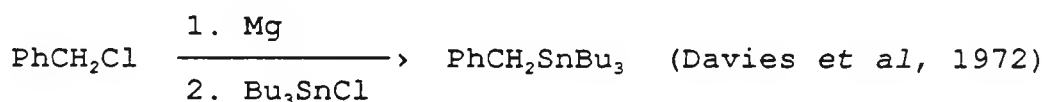
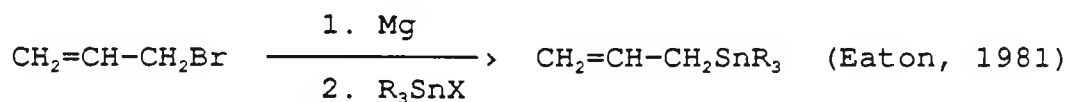
#### 2.1.1 Via Grignard reaction

This is undoubtedly the simplest and most direct route and it is applicable to a variety of substrates. In 1912 an early example of this reaction was the preparation of benzyltrimethylsilane (Bygden, 1912).



A more general reaction of great versatility involves the reaction of the trisubstituted metal halide with the Grignard reagent of the organic halide as demonstrated in the following examples:





A number of compounds have been successfully synthesised in this work using the Grignard route. A summary of the reaction times and yields is given in table 2.1.

Table 2.1 The Grignard synthesis of silanes and stannanes

Compound	Reaction time (h)	Yield (%)	Solvent	Reaction temp/°C
4-Me-C <sub>6</sub> H <sub>4</sub> CH <sub>2</sub> SiMe <sub>3</sub>	5	48	Et <sub>2</sub> O	38
PhCH <sub>2</sub> SnMe <sub>3</sub>	5	63	THF	68
CH <sub>2</sub> =CHCH <sub>2</sub> SiPh <sub>3</sub>	16	74	THF	20
CH <sub>2</sub> =CHCH <sub>2</sub> SnBu <sub>3</sub>	16	56	Et <sub>2</sub> O	38

The main problem of this method is that regioselectivity cannot always be controlled, especially in the case of substituted allylic derivatives, and separation of a required isomer can be tedious.

### 2.1.2 Via Barbier reaction

One possible way to overcome the problem of regioselectivity is to use the related Barbier synthesis using a modified procedure. Using this route the allylic halide is added to a mixture of the trialkylmetal halide and magnesium. This procedure was used to good effect with external irradiation of ultrasound to give an extremely facile and stereoselective preparation of a number of allylstannanes (Naruta *et al*, 1986). This method also has the advantage of converting the allyl halides to the corresponding allylstannanes minimising the formation of Wurtz-type coupling products so often encountered in the course of preparation of allylic Grignard reagents. This procedure was adopted and further extended to synthesise a number of silanes and stannanes in good yield (Bowser and Davidson, 1992). The preparations involved relatively short reaction times and gave great stereoselectivity of products as given in table 2.2.

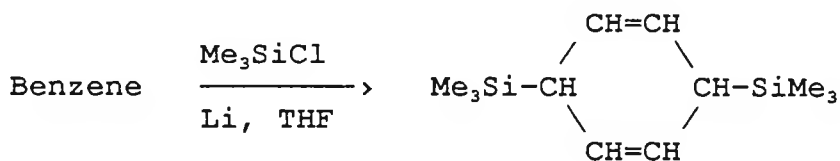
**Table 2.2** The Barbier synthesis of silanes and stannanes

Compound	Reaction time (h)	Yield (%)
4-MeO-C <sub>6</sub> H <sub>4</sub> CH <sub>2</sub> SiMe <sub>3</sub>	3.5	98
PhCH <sub>2</sub> SnBu <sub>3</sub>	1	86
4-Me-C <sub>6</sub> H <sub>4</sub> CH <sub>2</sub> SnBu <sub>3</sub>	1	45
4-MeO-C <sub>6</sub> H <sub>4</sub> CH <sub>2</sub> SnBu <sub>3</sub>	3.5	100
1-NpCH <sub>2</sub> SiMe <sub>3</sub>	10	62
2-NpCH <sub>2</sub> SiMe <sub>3</sub>	10	88
1-NpCH <sub>2</sub> SnBu <sub>3</sub>	5	63
2-NpCH <sub>2</sub> SnBu <sub>3</sub>	5	78
2-NpCH <sub>2</sub> SnMe <sub>3</sub>	2	46
*MeCH=CHCH <sub>2</sub> SnBu <sub>3</sub>	2	69
CH <sub>2</sub> =CMeCH <sub>2</sub> SnBu <sub>3</sub>	2	62
Me <sub>2</sub> C=CHCH <sub>2</sub> SnBu <sub>3</sub>	2	77
*Ph-CH=CHCH <sub>2</sub> SnBu <sub>3</sub>	2	44

\* = trans - isomer

### 2.1.3 Via reductive silylation

Reductive silylations of both dienes and aromatic systems using chlorosilane/metal reagents to yield allylic silanes have been studied (Calas and Dunogués, 1976).

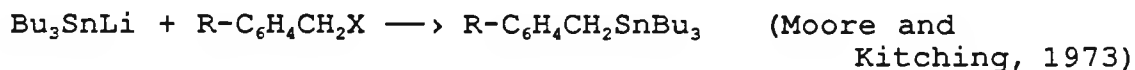


Another useful method was discovered in which the reductive

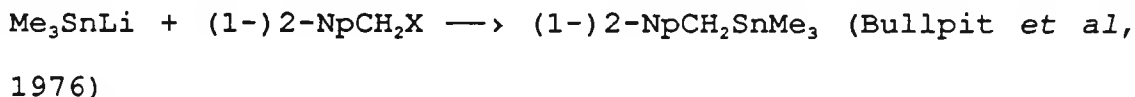


#### 2.1.4 Via Wurtz coupling

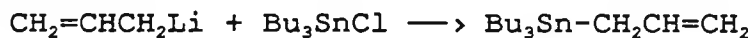
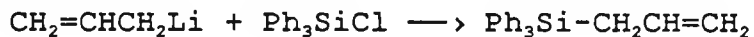
This involves the coupling reaction of a halide with a lithium reagent. Usually a preformed lithiated trisubstituted silane or stannane such as  $\text{Ph}_3\text{SiLi}$  (George et al, 1960),  $\text{Me}_3\text{SnLi}$ ,  $\text{Bu}_3\text{SnLi}$ ,  $\text{Ph}_3\text{SnLi}$  (Tamborski et al, 1963; Still, 1976) or  $\text{Me}_3\text{SiLi}$  (Hudrlik et al, 1984) is reacted with the allylic or benzylic halide as shown below.



R = 4- (H, Me, MeO)



In a similar vein it has also been reported that the lithiated organic moiety will couple with the trisubstituted metal halide (Seyferth and Weiner, 1961).



A Wurtz coupling reaction was used to synthesise hexamethyldisilane in good yield.

## 2.2 Physical and Chemical properties of Silanes and Stannanes

Photoelectron (PE) spectroscopic studies have shown that group 4A organometallics, particularly those containing a metal-carbon bond  $\beta$  to a neighbouring  $\pi$  system, are exceedingly electron rich (Hosomi and Traylor, 1975). Both the ionisation potentials and the oxidation potentials of these compounds are in the range of typical conventional donors effective in charge transfer schemes. The first ionisation potentials and the oxidation potentials for a number of group 4A organometallics are given in table 5.1 (see Appendix). The general trend in the data in table 5.1 is that the ease of ionisation/oxidation is in the order of naphthyl > benzyl > allyl and also Sn > Si. Substituents can also have a marked effect on the ionisation/oxidation potentials. From the data in table 5.1 it appears that the  $R_3M-C$  ( $M=Si, Sn$ ) unit offers a strong stabilising, electron donating effect to an adjacent electron deficient centre. The mechanism of this electron donation has been the subject of contention for a number of years. The two main theories involved in explaining the effects of the  $R_3M-C$  group involve either  $p_\pi-d_\pi$  bonding or  $\sigma-\pi$  hyperconjugation outlined below.

### 2.2.1 $p_\pi-d_\pi$ bonding

$p_\pi-d_\pi$  bonding, also known as neighbouring group participation, is an example of a non-vertical stabilisation

process. This essentially means that the substituent changes its geometry or its distance from the stabilised species as the transition state is approached.

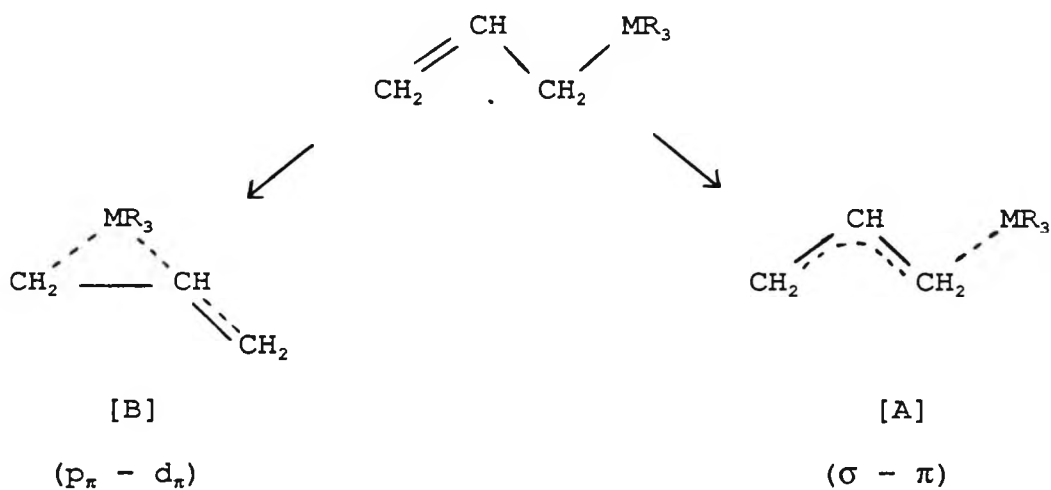
### 2.2.2 $\sigma$ - $\pi$ hyperconjugation

$\sigma$ - $\pi$  hyperconjugation is an example of a vertical stabilisation process. This means that the substituent does not change its geometry or its distance from the stabilised species, as the transition state is approached.

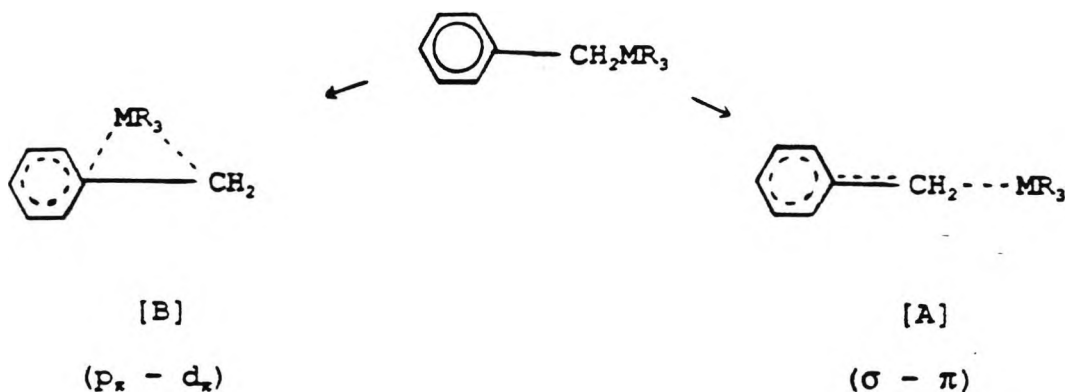
Both these situations may be represented below in figure 2.1.

Figure 2.1  $p_\pi$ - $d_\pi$  bonding versus  $\sigma$ - $\pi$  hyperconjugation in allylic and benzylic silanes and stannanes

Allylic compounds:



Benzylic compounds:



(where M = Si, Sn)

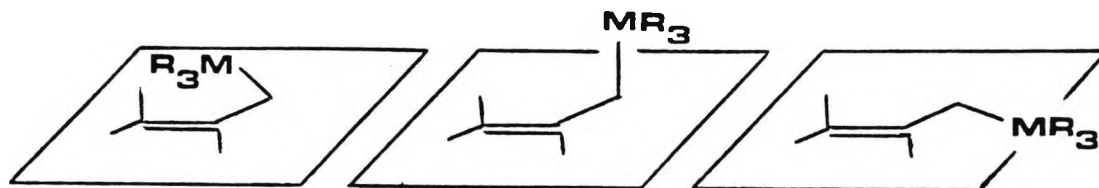
Such vertical  $\sigma$ - $\pi$  hyperconjugation (A) is preferred over the alternative of neighbouring group participation (B) to account for a number of anomalous features in the physical and chemical properties of allylic, benzylic, and related silanes and stannanes. Several Russian authors used this  $\sigma$ - $\pi$  hyperconjugation rationale to interpret the reactivity and spectral behaviour of allyl and benzylsilanes (Petrov et al, 1956; Egorov et al, 1961; Leites, 1963). Around the same time Eaborn suggested the possibility of C-Si  $\sigma$ - $\pi$  hyperconjugation in benzyltrimethylsilane (Eaborn, 1956). It was not until the early 1970s that the  $\sigma$ - $\pi$  hyperconjugation theory was further substantiated. A number of papers from the laboratories of Bock (Pitt and Bock, 1972; Bock et al, 1972;) and Schweig (Weidner and Schweig, 1972a; Weidner and Schweig, 1972b; Schweig et al, 1973a; Schweig et al, 1973b) appeared on the photoelectron spectroscopy of allylic and benzylic organometallic systems.

In these papers the usefulness of  $\sigma$ - $\pi$  hyperconjugation for the interpretation of photoelectron spectra was clearly demonstrated. Other evidence was provided by charge-transfer (CT) spectra (Hanstein et al, 1970a; Hanstein et al, 1970b), particularly with tetracyanoethylene.

In addition to the quantitative interpretation of CT and PE spectra, the hyperconjugation concept has been supported by numerous qualitative arguments based on steric considerations. Thus it has been suggested that  $\sigma$ - $\pi$  hyperconjugation requires coplanarity of the C-M bond and the axis of the electron deficient  $\pi$  orbital (Nesmeyanov and Kritskaya, 1958; Traylor and Ware, 1967). The  $\sigma$ - $\pi$  hyperconjugation effect should be maximised when the  $R_3M$   $\sigma$  bond is parallel to the  $\pi$  orbitals of the C=C double bond (Bach and Scherr, 1973). In other words the extent of the  $\sigma$ - $\pi$  hyperconjugation is dependent on the dihedral angle ( $\theta$ ) between the C-M bond and the  $\pi$  system, being at a maximum when  $\theta$  is at zero (Hanstein et al, 1970b; Pitt, 1970). This conformational requirement has also been invoked from EPR studies of tin-containing radicals (Lyons and Symons, 1971). Trying to assess the relative amounts of  $\sigma$ - $\pi$  hyperconjugation versus  $p_\pi$ - $d_\pi$  bonding in allylic, benzylic, and related organometallics requires an understanding of the relative populations of the ground state conformers. The limiting conformations for an allylic compound, as an example, are shown below in figure 2.2.

Figure 2.2

The limiting conformations of the C=C double bond with respect to the metal-CH<sub>2</sub> in an allylic system.



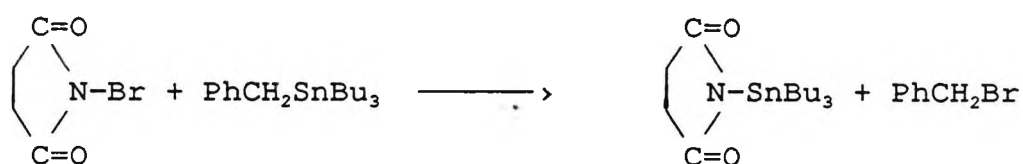
Thus the overall picture may be a combination of several effects, creating the so called  $\beta$ -effect, whilst the most important of these appears to be the  $\sigma$ - $\pi$  hyperconjugation. It is also possible that this  $\sigma$ - $\pi$  hyperconjugation may play a significant role in the weakening of the M-C bond and thus promote the cleavage processes which are often encountered in the reactions of  $\beta$ -functionalised organosilanes and stannanes. In allylic, benzylic and related silanes and stannanes the highest occupied molecular orbital (HOMO) is raised due to the  $\sigma$ - $\pi$  hyperconjugation effect, resulting in a lower ionisation potential of these compounds when compared to the analogous carbon derivative (see table 5.1: Appendix). It is these properties that are thought to be important in the proposed electron transfer reactions of these compounds which are discussed later (see section 2.5.7).

### 2.3 Photochemistry of benzylsilanes and stannanes

It is well known that various benzylic substituted compounds undergo homolytic cleavage upon irradiation (Slocum *et al*, 1981; Hilinski *et al*, 1984; Johnston and Scaiano, 1985). Previous evidence, outlined below, has also been presented that indicates benzylsilanes and benzylstannanes undergo homolytic cleavage reactions to form benzylic and metal centred radicals.

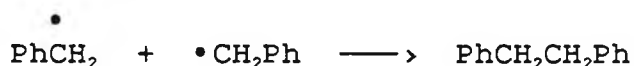
#### 2.3.1 Photochemistry of benzylstannanes

It was proposed in the early 1970's that benzyltri-*n*-butylstannane reacted with N-bromosuccinimide by a free radical chain mechanism involving bimolecular homolytic substitution by the succinimyl radical at the tin centre (Davies *et al*, 1970; Davies *et al*, 1972) shown below.

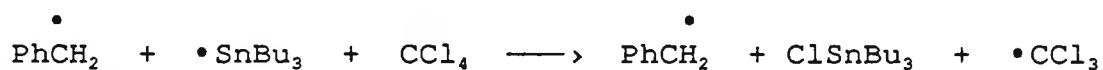


A later study (Soundararajan and Platz, 1987) suggested that photolysis of benzyl and naphthylstannanes leads to homolytic cleavage via the excited singlet state to form the corresponding benzyl (or naphthyl) radical and the tri-*n*-butyltin radical. Evidence was invoked from the photolysis

products of a number of benzylic stannanes in different solvents. The photolysis products in benzene were rationalised by homolytic fission followed by radical recombination shown below for benzyltri-*n*-butylstannane.

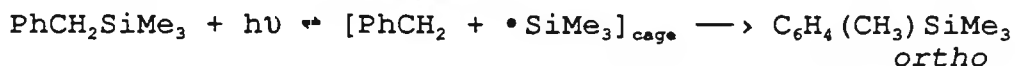


In carbon tetrachloride the developing  $\overset{\bullet}{\text{SnBu}_3}$  radical rapidly abstracts Cl from the solvent to form  $\text{Bu}_3\text{SnCl}$  and a new radical pair product which eventually form stable products as depicted below for benzyltri-*n*-butylstannane.



### 2.3.2 Photochemistry of benzylsilanes

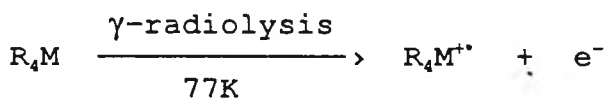
Benzyltrimethylsilane has been described as photochemically inert (Valkovich et al, 1974) but a later study, the first to investigate the intrinsic photochemistry of the benzylsilane chromophore, was reported to give homolysis of the benzylic carbon-silicon bond shown below (Kira et al, 1985).



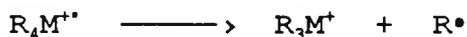
Benzyltrimethylsilane was isomerised to o-tolyltrimethylsilane in 2% yield. It is not clear as to whether the photolysis quantum yield is high and a major process occurs as an in-cage recombination, or that the quantum yield of photolysis is low, explaining the low yield of product.

#### 2.4 Electron Paramagnetic Resonance (EPR) spectroscopy results

EPR spectroscopy has been used to study radical cations derived from organosilicon and organotin compounds, as isolated in solid trichlorofluoromethane matrices at low temperatures. The primary radical cations were formed by  $\gamma$ -radiolysis of the neutral parents in solid  $\text{CFCl}_3$  matrices at 77K as shown below.



In previous photochemical studies of simple silanes and stannanes ( $\text{R}_4\text{M}$ ), in the presence of electron acceptors, the initially formed  $\text{R}_4\text{M}^{+\cdot}$  radical cations were proposed to fragment as follows:



Direct evidence for this reaction has been obtained for tetraalkyltin radical cations (Boschi *et al*, 1973; Evans *et al*, 1979), from which radicals R<sup>•</sup> may be detected by EPR spectroscopy even under cryogenic conditions. In view of the above, it seemed worthwhile to study a range of silanes and stannanes by EPR spectroscopy to determine any relationship between the structure and relative ease of fragmentation of their radical cations.

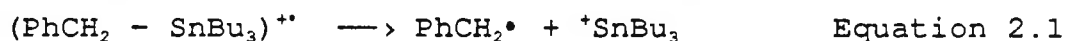
#### 2.4.1 EPR results of benzylsilanes

EPR spectra of the radical cations of benzyltrimethylsilane and its 4-methyl and 4-methoxy derivatives were recorded at 77K and showed that most of the spin density resided on the aromatic ring and a small amount is located in the silicon to benzylic carbon bond (Butcher *et al*, 1992). On warming the matrix (160K) no direct evidence could be obtained for the formation of benzylic radicals. This observation is in agreement with earlier work claiming that nucleophilic attack at silicon is required to cause fragmentation (Ohga and Mariano, 1982; Dinnocenzo *et al*, 1989; Sirimanne *et al*, 1991).

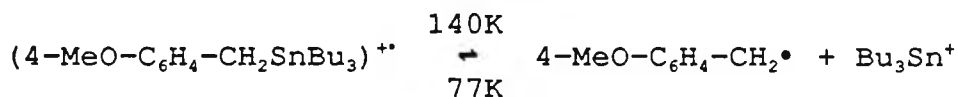
#### 2.4.2 EPR results of benzylstannanes

EPR spectra of the radical cations of benzyltri-*n*-butylstannane and the 4-methoxy analogue were recorded at 77K (Butcher *et al*, 1992). The spectrum of [PhCH<sub>2</sub>SnBu<sub>3</sub>]<sup>•+</sup> at

77K shows an intense feature which is associated with the presence of *n*-butyl radicals. This spectrum was compared to that of the radical cation of tetra-*n*-butyltin which was also recorded at 77K. The differences in the spectra reflects some delocalisation of the positive hole from the electron-depleted benzylic C-Sn bond onto the aromatic group. On warming to 155K the spectrum of  $[\text{PhCH}_2\text{SnBu}_3]^{+\bullet}$  showed an overall loss of this signal and new features appeared which can readily be assigned to free benzyl radicals. This is in accordance with the structural view of an electron-depleted C-Sn bond which fragments as shown in equation 2.1.



In the case of the 4-methoxy analogue the radical cation remained intact at 77K. On warming to 140K features assigned to the benzylic radical grew with a similar reduction in the signal associated with the primary intact radical cations. Recooling to 77K resulted in the regeneration of the original radical cation signal with minimal loss in intensity. Thus the fragmentation of the 4-methoxy analogue and its subsequent recombination was shown to be a thermally reversible process as shown below.

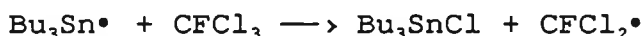
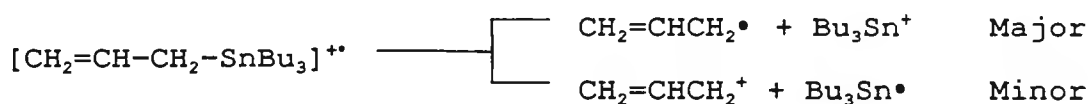


The requirement of a lower temperature for fragmentation for

$(4\text{-MeO-C}_6\text{H}_4\text{-CH}_2\text{SnBu}_3)^{+\bullet}$  (140K) compared to  $[\text{PhCH}_2\text{SnBu}_3]^{+\bullet}$  (155K) shows that the activation energy for benzylic C-Sn bond cleavage of the radical cation is lowered by 4-MeO substitution.

### 2.4.3 EPR results of allyl and cinnamyl stannanes

The EPR spectra of the radical cations of allyl and cinnamyl tri-*n*-butylstannane have been recorded at 77K (Butcher, et al, 1992). On warming the allyltri-*n*-butylstannane radical cation to 120K features were observed belonging to free allyl radicals. This shows that the activation energy for C-Sn bond cleavage for the organotin radical cations is reduced for the allyl derivative (120K) when compared to the benzyl analogues (140K and 155K). A simple explanation for this result is a product development argument based on the greater stability of an allyl radical compared to a benzyl radical (Vedeneyev et al, 1966). There was also evidence (observation of the fluorodichloromethyl radical,  $\text{CFCl}_2\bullet$ ) that fragmentation of the allyltri-*n*-butylstannane radical cation can occur in two ways.



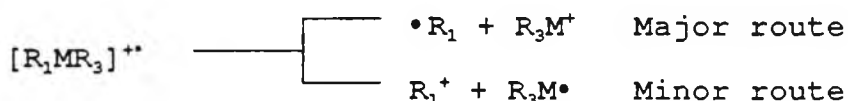
The spectrum of  $[\text{PhCH}=\text{CHCH}_2\text{SnBu}_3]^{+\bullet}$  showed evidence that

fragmentation occurred at 77K to yield the cinnamyl radical and the  $\text{Bu}_3\text{Sn}^+$  species, as observed in the major route for the allylstannane radical cation. Again the fragmentation at the lower temperature is probably due to the greater stability of the carbon-centred radicals produced in the cinnamyl case (77K) when compared to the allyl derivative (120K).

#### 2.4.4 Structure and stability of radical cations

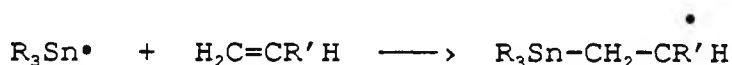
There is a definite depletion of electron density from the C-Sn(Si) bonds on ionisation in all the compounds studied. It was observed that the ease of fragmentation in the radical cations does not follow the order of electron depletion but instead appears to relate to the stabilisation of the developing radical/cation fragments, giving rise to a transition state effect.

An important observation in the context of the UV curing results is the cleavage of the allylstannane via two different pathways. It would seem that radical cations of the type  $[\text{R}_1\text{MR}_3]^{\bullet+}$  have two possible fragmentation routes.



This confirms an earlier report on the fragmentation of radical cations of benzyltrialkylstannanes which suggested that fragmentation occurred by dual modes as above (Eaton, 1980a). Eaton suggested that to increase the favourability

of the minor pathway electron-donating substituents should be incorporated on the aromatic ring. This was to help stabilise the formation of the benzylic cation intermediate and thus increase the ratio of minor route:major route. The major pathway is of no benefit to the curing process whereas the minor pathway is of significance since trialkyltin radicals are known to react with alkenes via a free radical chain mechanism (Neumann *et al*, 1961; Davies, 1977).



From the EPR studies it is not known if the thermal energy which is available to the radical cations at room temperature is able to increase the favourability of the minor pathway to give metal-centred radicals. Fragmentation of benzylsilane radical cations was not observed under the conditions used which suggests that (C-Si)<sup>••</sup> bond cleavage occurs less readily than (C-Sn)<sup>••</sup> bond cleavage. Thus it is the tin compounds that are anticipated to be the more responsive under ionising conditions in developing photoresists.

## 2.5 UV Curing results

### 2.5.1 UV curing results of benzylsilanes

A number of benzylsilanes were tested at 5% w/w in the presence of a free radical polymerisable monomer, (TMPTA), using the UV Colordry apparatus described earlier (see section 1.7.1). This was in order to assess the free radical initiating properties of the compounds under test. The results are presented below in table 2.4.

Table 2.4

UV curing results of benzylsilanes incorporated at 5% w/w in TMPTA

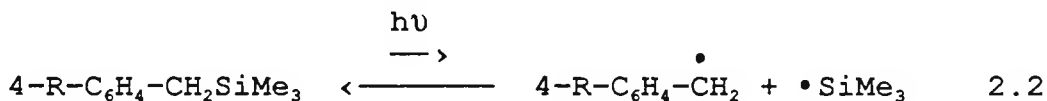
E X P T	INITIATOR	NUMBER OF PASSES			
		Touching Quartz	Touching Glass	In Air	Glass Filter
1	$\text{PhCH}_2\text{SiMe}_3$	4	28	*	*
2	$4\text{-Me-C}_6\text{H}_4\text{CH}_2\text{SiMe}_3$	4	*	*	*
3	$4\text{-MeO-C}_6\text{H}_4\text{CH}_2\text{SiMe}_3$	3	24	*	*
4	$4\text{-Ph-C}_6\text{H}_4\text{CH}_2\text{SiMe}_3$	2	11	*	*
5	TMPTA	6	40	*	*

Belt speed = 10 ft/min for all experiments

\* = polymerisation not detected after 30 passes

## Touching quartz and touching glass

The results indicate that the benzylsilanes will initiate free radical polymerisation as evidenced by the reduced number of passes required to reach tack free cure when compared to the monomer, TMPTA, on its own (EXPT 5). The mechanism of polymerisation is proposed to be via homolytic cleavage of the C-Si benzylic bond followed by attack by a free radical on the monomer to initiate polymerisation. It appears that the cleavage of the C-Si benzylic bond is not efficient even when using the full spectral output of the lamp and also reducing the effect of oxygen inhibition in the touching quartz experiments. This indicates that either the quantum yield of photolysis is low or the in-cage recombination of photolysis products is high and can be represented by equation 2.2 below.



The improved response of the biphenyl derivative (EXPT 4) in the touching glass experiment can be attributed to the improved absorption properties of this compound in the region beyond the glass filter (>310nm). Consequently further syntheses of substituted benzylic silanes with improved absorption properties were carried out in the hope that better photoinitiating properties would accrue. The results of the UV curing of these compounds are given below

in table 2.5 along with that of benzyltrimethylsilane for comparison.

Table 2.5 UV curing results of benzylic silanes incorporated at 5% w/w in TMPTA

E X P T	INITIATOR	NUMBER OF PASSES			
		Touching Quartz	Touching Glass	In Air	Glass Filter
1	PhCH <sub>2</sub> SiMe <sub>3</sub>	4	28	*	*
2	Ph <sub>2</sub> CHSiMe <sub>3</sub>	3	9	*	*
3	9-trimethylsilyl- fluorene	2	5	30	*
4	9-trimethylsilyl- thioxanthene	2	4	10	16
5	TMPTA	6	40	*	*

Belt speed = 10 ft/min for all experiments

\* = polymerisation not detected after 30 passes

#### Touching glass

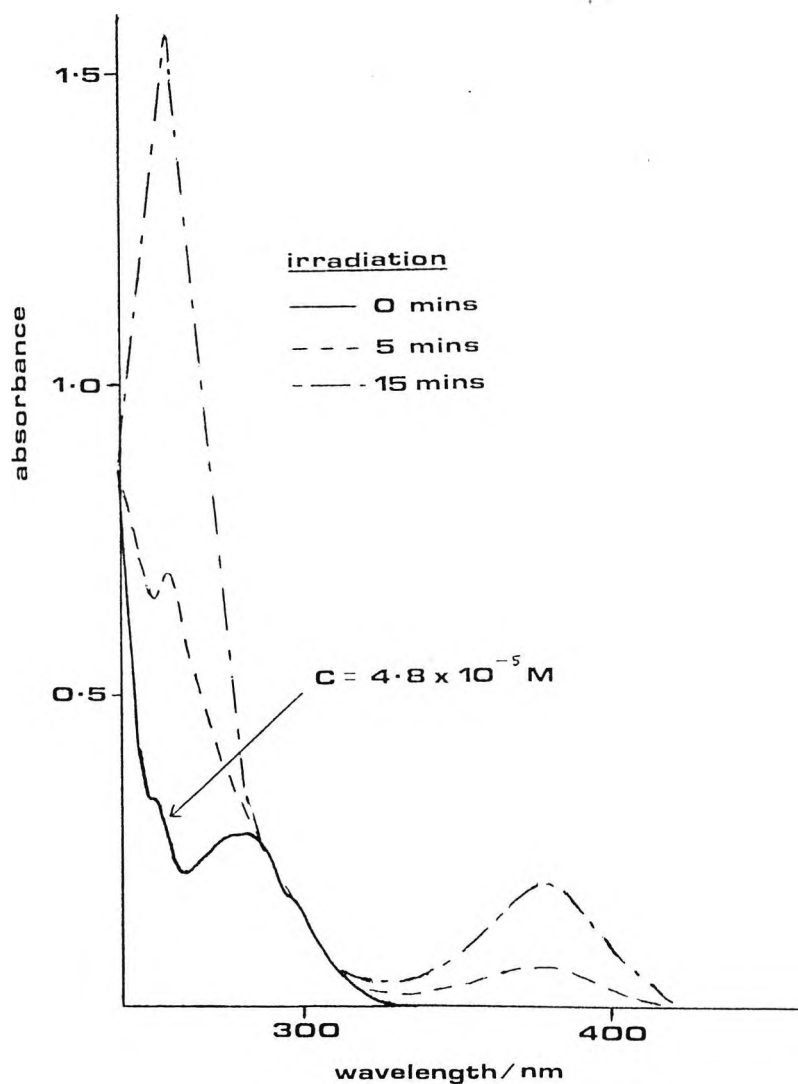
It is noticeable that the more substituted benzylic silanes (EXPT's 2, 3, and 4) cure at a greater rate than benzylsilane (EXPT 1) which is linked to their greater absorption in the wavelength region beyond the glass filter range (>310nm).

#### In air

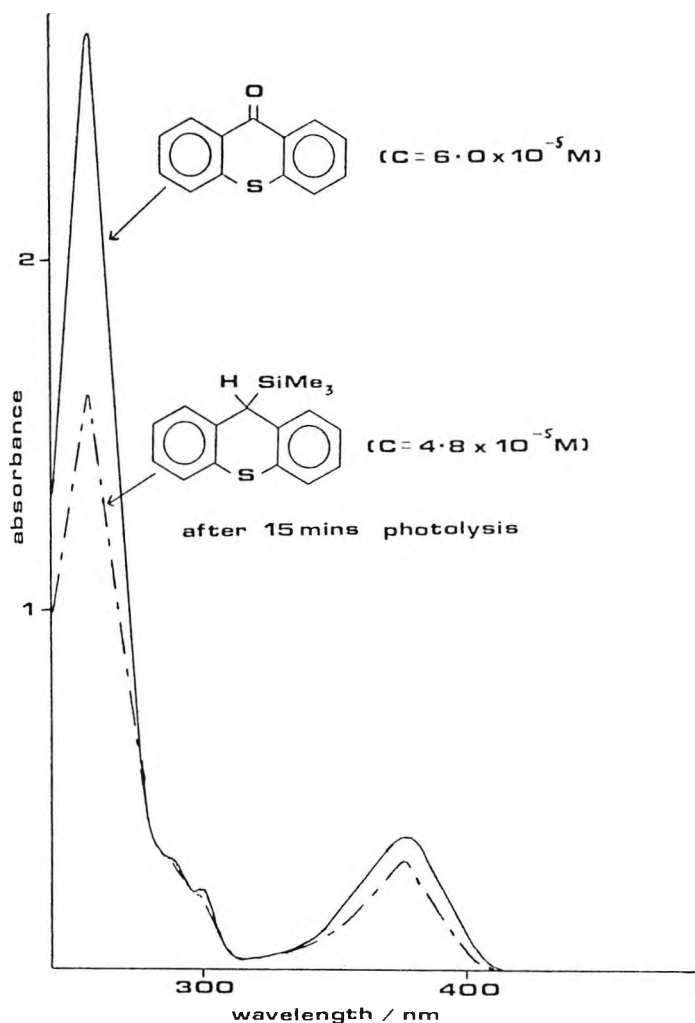
In EXPT's 3 and 4 cure is observed in air. A further

observation made was that with both the fluorene derivative (EXPT 3) and the thioxanthene derivative (EXPT 4) the thin films changed from colourless to yellow on irradiation. This feature was more prominent for the thioxanthene derivative.

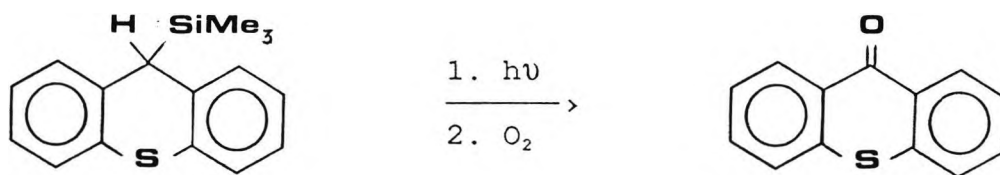
Further insight into this reaction was gained from following the photolysis of the thioxanthene derivative in methanolic solution using UV spectroscopy. The results are presented below.



It is proposed that on photolysis the benzylic C-Si bond is converted to the carbonyl group, C=O, thus giving rise to the yellow coloured compound of thioxanthone. This becomes apparent when the UV spectra of thioxanthone is compared with the corresponding photolysis product of the thioxanthene derivative as shown below.



The above result may be rationalised by the following mechanism:



This reaction reduces the effect of oxygen inhibition of polymerisation and explains why polymerisation is observed in air for the thioxanthene derivative (EXPT 4). A similar effect occurs for the fluorene derivative, albeit to a lesser extent than the thioxanthene derivative, and this explains the polymerisation observed in air for this compound (Table 2.5; EXPT 3).

#### Glass cover

Polymerisation was observed under a glass cover slide for the thioxanthene derivative (EXPT 4) indicating that the conversion of this compound to thioxanthone is a particularly efficient process. In order to verify the proposed mechanism a further UV curing experiment was performed. It is known that thioxanthone sensitises diphenyliodonium salts in cationic polymerisation (Gatechair and Pappas, 1983). It was decided to test the thioxanthene derivative in conjunction with diphenyliodonium hexafluorophosphate in the presence of a cationically polymerisable monomer, 3,4-epoxycyclohexylmethyl-3',4'-epoxycyclohexane carboxylate, to determine whether sensitisation of polymerisation, via thioxanthone, occurred (EXPT 3; Table 2.6). The results presented in table 2.6 can be compared to the experiment where thioxanthone was used as the sensitiser (EXPT 2).

Table 2.6 Sensitisation of diphenyliodonium hexafluorophosphate for use in cationic photopolymerisation using 'thioxanthone' with all compounds incorporated at 1% w/w in 3,4-epoxycyclohexylmethyl-3',4'-epoxycyclohexane carboxylate

EXPT	INITIATING SYSTEM	BELT SPEED/ ft/min	NUMBER OF PASSES	
			In Air	Glass Filter
1	$\text{Ph}_2\text{I}^+\text{PF}_6^-$	10	7	*
2	$\text{Ph}_2\text{I}^+\text{PF}_6^-$ + thioxanthone	10	1	1
3	" + "	230	5	8
4	$\text{Ph}_2\text{I}^+\text{PF}_6^-$ + 9-trimethylsilylthioxanthene	10	1	6
5	" + "	230	5	17

\* = polymerisation not detected after 30 passes

The first point to make is that sensitisation using thioxanthone with diphenyliodonium hexafluorophosphate occurs (EXPT's 2 and 3) compared to the iodonium salt used on its own (EXPT 1). The second more interesting point is that sensitisation occurs when the thioxanthene derivative is used with the iodonium salt (EXPT's 4 and 5) when compared to the iodonium salt on its own (EXPT 1). The most striking feature of the results is that the number of passes required to reach cure in air in EXPT 3 is identical to that

in EXPT 5. This indicates that the conversion of the thioxanthene derivative to thioxanthone is an efficient process when the full output of the lamp is used (in air). When a glass filter is used (>310nm) with the thioxanthene derivative sensitisation is still achieved (EXPT 5; 17 passes) but to a lesser extent than the corresponding value when thioxanthone was used (EXPT 3; 8 passes).

Another experiment was performed to ascertain if the combination of the thioxanthene derivative and the diphenyliodonium salt could be used to effect both free radical and cationic polymerisation simultaneously to give a dual cure system. A formulation of the thioxanthene derivative and the iodonium salt was incorporated into a 50:50 (w/w) mixture of two monomers, one polymerisable by a free radical pathway (TMPTA), and one polymerisable by a cationic pathway (3,4-epoxycyclohexylmethyl-3',4'-epoxycyclohexane carboxylate). The results are given below in table 2.7.

Table 2.7 Evidence for a dual cure system in the photopolymerisation of a 50:50 acrylate:epoxy resin mixture using diphenyliodonium hexafluorophosphate and 9-trimethylsilylthioxanthene

E X P T	INITIATING SYSTEM	R E S I N	NUMBER OF PASSES			
			Touching Quartz	Touching Glass	In Air	Glass Filter
1	9-Me <sub>3</sub> Si-thioxan thene (TMS-TX) <sup>+</sup>	A	2	4	10	16
2	Ph <sub>2</sub> I <sup>+</sup> PF <sub>6</sub> <sup>-</sup>	A	4	*	4	*
3	Ph <sub>2</sub> I <sup>+</sup> PF <sub>6</sub> <sup>-</sup>	E	-	-	7	*
4	TMS-TX + Ph <sub>2</sub> I <sup>+</sup> PF <sub>6</sub> <sup>-</sup>	AE	1	1	2	4
5	"	"	2 <sup>a</sup>	5 <sup>a</sup>	8 <sup>a</sup>	18 <sup>a</sup>
6	TMS-TX + Ph <sub>2</sub> I <sup>+</sup> PF <sub>6</sub> <sup>-</sup>	E	-	-	1	6
7	"	"	-	-	5 <sup>a</sup>	17 <sup>a</sup>

a = belt speed 230 ft/min

Belt speed = 10 ft/min for all other experiments

A = acrylate resin = TMPTA

E = epoxy resin = 3,4-epoxycyclohexylmethyl-3',4'-  
epoxycyclohexane carboxylate

AE = 50:50 mixture (w/w) of resins A and E above

- = difficult to evaluate

\* = 5% w/w in TMPTA, for all other instances the  
initiator/sensitiser is incorporated at 1% w/w in the resin

The curing of an epoxide when touching quartz and glass is difficult to follow since the cured epoxide adheres to the touching quartz and glass slides during the early stages of polymerisation. This makes the detection of tack-free polymerisation difficult and reproducible results are not possible.

When the 50:50 resin system is used in the sensitised polymerisation (EXPT's 4 and 5) the assessment of the touching quartz and touching glass results becomes much easier due to the better film-forming properties of this resin system compared to the epoxide on its own (EXPT's 6 and 7). It is also envisaged that the improvement in the rate of polymerisation of the dual system when touching quartz and touching glass (EXPT's 4 and 5) compared to the epoxide (EXPT's 6 and 7) is due to the incorporation of the acrylate, TMPTA. This dual cure system (EXPT's 4 and 5) does not show an improvement, however, in comparison to the situation where only the epoxy resin is present when in air and with a glass cover (EXPT's 6 and 7). This is probably due to the effect of oxygen inhibition on the free radical polymerisation in the dual cure system. It has been estimated that this oxygen inhibition effect occurs significantly in dual cure systems which incorporate > 40% of the free radical polymerisable monomers (Ketley and Tsao, 1979).

## 2.5.2 UV curing results of benzylstannanes

A number of benzylstannanes were tested (5% w/w) in the presence of a monomer, TMPTA, using the UV Colordry apparatus described earlier (see section 1.7.1). This was in order to assess the free radical initiating properties of the compounds under test. The results are presented below in table 2.8. For comparison the result for benzyltrimethylsilane is also included (EXPT 1).

Table 2.8 UV curing results of benzylstannanes incorporated at 5% w/w in TMPTA

EXPT	INITIATOR	NUMBER OF PASSES			
		Touching Quartz	Touching Glass	In Air	Glass Filter
1	PhCH <sub>2</sub> SiMe <sub>3</sub>	4	28	*	*
2	PhCH <sub>2</sub> SnMe <sub>3</sub>	2	9	*	*
3	PhCH <sub>2</sub> SnBu <sub>3</sub>	1	3	*	*
4	PhCH <sub>2</sub> SnBu <sub>3</sub>	2 <sup>a</sup>	-	-	-
5	4-Me-C <sub>6</sub> H <sub>4</sub> CH <sub>2</sub> SnBu <sub>3</sub>	1	3	25	*
6	4-Me-C <sub>6</sub> H <sub>4</sub> CH <sub>2</sub> SnBu <sub>3</sub>	2 <sup>b</sup>	10 <sup>b</sup>	-	-
7	4-MeO-C <sub>6</sub> H <sub>4</sub> CH <sub>2</sub> SnBu <sub>3</sub>	1	1	*	*
8	4-MeO-C <sub>6</sub> H <sub>4</sub> CH <sub>2</sub> SnBu <sub>3</sub>	1 <sup>b</sup>	4 <sup>b</sup>	-	-
9	TMPTA	6	40	*	*

\* = polymerisation not detected after 30 passes

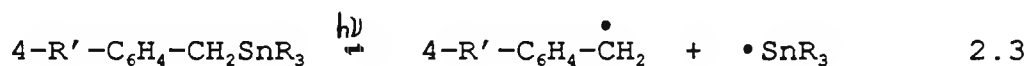
- = experiment not performed

a = belt speed 80 ft/min

b = belt speed 230 ft/min

Belt speed = 10 ft/min for all other experiments

The results show that a much lower number of passes is required to achieve a tack free coating for the benzylstannanes when compared to the benzylsilane (EXPT 1). This indicates that the homolysis of the benzylic C-Sn bond occurs more readily than that of the benzylic C-Si bond and may be represented by equation 2.3.



[R = Me, n-Bu; R' = H, Me, MeO]

A comparison can be made between benzyltrimethylsilane (EXPT 1) and benzyltrimethylstannane (EXPT 2) as to the effect of the different metals on the number of passes required to achieve cure. In both the touching quartz and the touching glass experiments benzyltrimethylstannane requires fewer passes than benzyltrimethylsilane indicating a greater extent of reaction of the tin species. This could be due to a greater degree of homolysis or attributed to an enhanced reactivity of the metal centred radical produced.

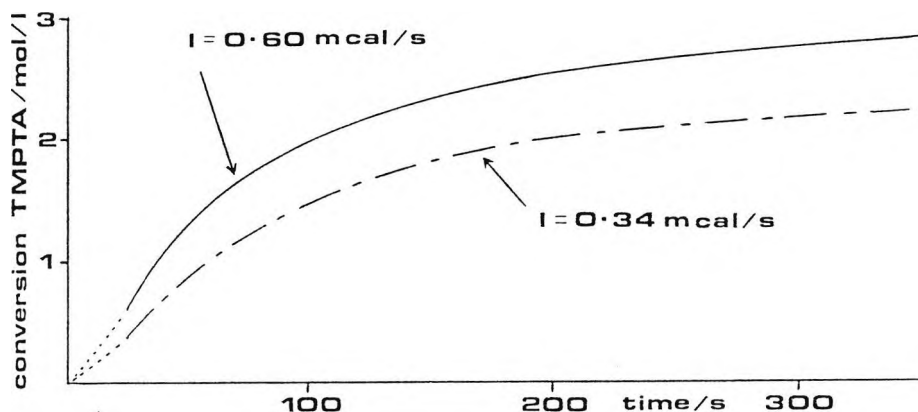
A similar comparison can be made between the results of benzyltri-n-butylstannane (EXPT's 3 and 4) and benzyltrimethylstannane (EXPT 2) to determine the effect of

the R group on changing from SnMe<sub>3</sub> to SnBu<sub>3</sub>. In the touching quartz and touching glass experiments benzyltri-*n*-butylstannane (EXPT's 3 and 4) requires a fewer number of passes to achieve cure than benzyltrimethylstannane (EXPT 2). This probably reflects the relative ease with which the C-Sn bond in the stannanes will undergo homolytic fission, with particular emphasis on the greater degree of stabilisation achieved via hyperconjugation when R = Bu than when R = Me.

#### 2.5.2.1 Photo-DSC of benzyltri-*n*-butylstannane

A photo-DSC experiment was performed on a sample of benzyltri-*n*-butylstannane (7.5% w/w) in TMPTA. The amount of stannane incorporated was calculated to give 'total absorption' of the available light. The intensity of the light was then reduced to determine the effect of this on the polymerisation as followed by photo-DSC. The resultant polymerisation curves are shown in figure 2.3.

Figure 2.3 Photo-DSC results of the polymerisation of TMPTA initiated by benzyltri-*n*-butylstannane at two different light intensities



The effect of reducing the light intensity is to reduce both the maximum rate of polymerisation,  $R_{p(max)}$ , and the degree of polymerisation after one minute illustrated in table 2.9.

Table 2.9 The rate and the degree of conversion values at different light intensities for the photopolymerisation of TMPTA using benzyltri-*n*-butylstannane as determined by photo-DSC

EXPT	Light intensity/ mcal/s	$R_{p(max)}$ / mol/l/s	Degree of conversion after 1 minute/ %
1	0.60	0.040	13.0
2	0.34	0.020	9.1

The values of  $R_{p(max)}$  and the degree of conversion are low because the intensity of the light has been much reduced with the use of a neutral density filter in combination with

a narrow band-width filter centred on 365nm. The reduction in the  $R_p$  value can be predicted from the two curves, using equation 1.30 (see section 1.4.4), assuming total absorption of light by the initiator. For example consider the situation at 300 seconds;

$I_1 = 0.60$  mcal/s, conversion of  $[\text{TMPTA}]_1 = 2.80$  mol/l

$I_2 = 0.34$  mcal/s, conversion of  $[\text{TMPTA}]_2 = 2.18$  mol/l

The overall rate of polymerisation,  $R_p$ , is proportional to the light intensity,  $I_o$ , by the equation;

$R_p \propto \sqrt{I_o}$  From the two experiments it follows that,

$$\frac{\sqrt{I_1}}{\sqrt{I_2}} = \frac{[\text{TMPTA}]_1}{[\text{TMPTA}]_2}$$

From the experimental values measured for the light intensity,

$$\frac{\sqrt{I_1}}{\sqrt{I_2}} = \frac{\sqrt{0.60}}{\sqrt{0.34}} = 1.33$$

and from the calculated values of the degree of conversion,

$$\frac{[\text{TMPTA}]_1}{[\text{TMPTA}]_2} = \frac{2.80}{2.18} = 1.28$$

The two results are within reasonable experimental error and confirm the predictions that can be made when using the theoretical equations.

### 2.5.3 UV curing results of naphthyl compounds (and higher)

A number of naphthylsilanes and stannanes were synthesised in order to increase the conjugation and extend the wavelength range for direct irradiation compared to the corresponding benzylic derivatives. Taking this idea further a pyrene derivative, which is a pale yellow colour, was synthesised and tested. The results are presented below in table 2.10.

Table 2.10 UV curing results of naphthyl (and higher) compounds incorporated at 5% w/w in TMPTA

E X P T	INITIATOR	NUMBER OF PASSES			
		Touching Quartz	Touching Glass	In Air	Glass Filter
1	1-NpCH <sub>2</sub> SiMe <sub>3</sub>	4	7	30	*
2	2-NpCH <sub>2</sub> SiMe <sub>3</sub>	3	5	*	*
3	1-NpCH <sub>2</sub> SnBu <sub>3</sub>	1	1	(*)	*
4	"	1 <sup>a</sup>	1 <sup>a</sup>	-	-
5	2-NpCH <sub>2</sub> SnBu <sub>3</sub>	1	1	(*)	*
6	"	1 <sup>a</sup>	1 <sup>a</sup>	-	-
7	2-NpCH <sub>2</sub> SnMe <sub>3</sub>	1	2	*	*
8	1-pyreneCH <sub>2</sub> SiMe <sub>3</sub>	1	4	*	*
9	TMPTA	6	40	*	*

\* = curing not detected after 30 passes

(\*) = curing observed but not tack-free after 30 passes

- = experiment not performed

a = belt speed 230 ft/min

Belt speed = 10 ft/min for all other experiments

The results again bear out the relationship that the rate of polymerisation is in the order:  $\text{NpCH}_2\text{SnBu}_3 > \text{NpCH}_2\text{SnMe}_3 > \text{NpCH}_2\text{SiMe}_3$

which is in agreement with the previous results (see section 2.5.2).

The pyrene derivative (EXPT 8) shows an improvement in rate of cure when compared to the naphthylsilanes (EXPT's 1 and 2), which is probably due to, the enhanced absorption properties of the pyrene moiety.

#### 2.5.4 UV curing results of allylsilanes

A number of allylsilanes were tested (5% w/w) in the presence of a monomer, TMPTA, using the UV Colordry apparatus described earlier (see section 1.7.1). This was in order to assess the free radical-initiating properties of the compounds under test. The results are presented below in table 2.11.

Table 2.11

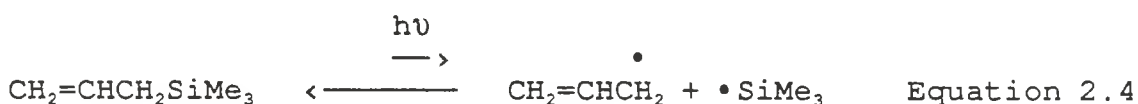
UV curing results of allylsilanes  
incorporated at 5% w/w in TMPTA

E X P T	INITIATOR	NUMBER OF PASSES			
		Touching Quartz	Touching Glass	In Air	Glass Filter
1	CH <sub>2</sub> =CHCH <sub>2</sub> SiMe <sub>3</sub>	3	20	*	*
2	Me <sub>2</sub> C=CHCH <sub>2</sub> SiMe <sub>3</sub>	3	13	*	*
3	CH <sub>2</sub> =CHCH <sub>2</sub> SiPh <sub>3</sub>	6	*	*	*
4	TMPTA	6	40	*	*

\* = no curing observed after 30 passes

Belt speed = 10 ft/min for all experiments

The results indicate that the allylsilanes will initiate radical polymerisation by homolytic cleavage. The situation is similar to benzylsilanes where the equilibrium in equation 2.4 lies well to the left.



### 2.5.5 UV curing results of allylstannanes

A number of allylstannanes were tested (5% w/w) in the presence of a monomer, TMPTA, using the UV Colordry apparatus described earlier (see section 1.7.1). This was in order to assess the free radical-initiating properties of the compounds under test. The results are presented below in table 2.12. For comparison the result of

allyltrimethylsilane is included (EXPT 1, table 2.12).

Table 2.12 UV curing results of allylstannanes incorporated at 5% w/w in TMPTA

EXPT	INITIATOR	NUMBER OF PASSES			
		Touching Quartz	Touching Glass	In Air	Glass Filter
1	$\text{CH}_2=\text{CHCH}_2\text{SiMe}_3$	3	20	*	*
2	$\text{CH}_2=\text{CHCH}_2\text{SnBu}_3$	2	14	*	*
3	$\text{CH}_2=\text{C}(\text{Me})\text{CH}_2\text{SnBu}_3$	2	13	*	*
4	$\text{MeCH}=\text{CHCH}_2\text{SnBu}_3$	2	11	*	*
5	$\text{Me}_2\text{C}=\text{CHCH}_2\text{SnBu}_3$	1	6	*	*
6	TMPTA	6	40	*	*

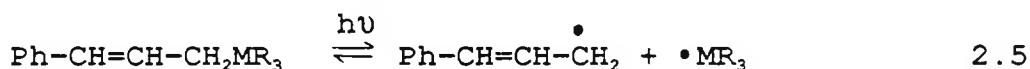
\* = no polymerisation detected after 30 passes

Belt speed = 10 ft/min for all experiments

The allylstannanes are more reactive than the allylsilanes in initiating photopolymerisation, which is probably due to the weaker bond strength, and thus easier homolytic cleavage, of the C-Sn bond when compared to the C-Si bond. In the case of the tri-*n*-butylstannanes (EXPT's 2 to 5) it is the more substituted allylstannane that shows greater reactivity towards photopolymerisation. This can be explained in terms of the stability of the allylic radical produced upon homolytic cleavage.

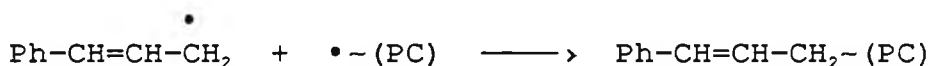


uncharacteristic for the majority of the allylic, benzylic, and naphthyllic silanes and stannanes previously tested. It is believed that the curing in air is related to the function of the cinnamyl radical formed on photolysis (equation 2.5).



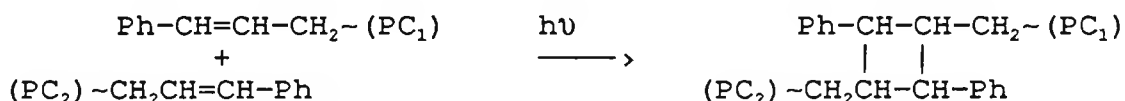
The cinnamyl radical can react with a growing polymer chain radical to give the cinnamyl functionality attached to the polymer backbone as in scheme 2.1.

Scheme 2.1 Cinnamylation of the polymer chain (PC)



If the cinnamyl group attached encounters another cinnamyl functionality attached to a different polymer backbone then it is possible that a reaction between the two cinnamyl groups via a [2+2] cycloaddition process may occur as in scheme 2.2.

Scheme 2.2 [2 + 2] cycloaddition of cinnamyl groups



Cycloaddition polymerisation, in contrast to free radical polymerisation, is a non-radical process and does not exhibit a marked oxygen inhibition effect on the rate of polymerisation. This could explain why the cinnamylstannane (EXPT 1) gave curing in air in contrast to the analogous allyl and benzyl stannanes which showed no evidence of curing in air.

This prompted the synthesis of the styrylsilane to see if a similar effect was possible. It was shown that polymerisation was not detected for the styrylsilane in air (EXPT 2) although for a more appropriate comparison the styrylstannane is required.

#### 2.5.7 Photoinduced electron transfer reactions

There has been a lot of interest in the electron transfer reactions of allylic and benzylic silanes and stannanes. This can be attributed to the low oxidation potentials of these compounds which render them effective electron donors (see table 5.1: Appendix). Early work indicated that benzyltri-*n*-butylstannane could be used as an activator in the dye sensitised free radical polymerisation of vinylic monomers (Eaton, 1979). This was proposed to be via a mechanism similar to that of the dye/amine reaction proposed earlier (Davidson and Trethewey, 1975). The same author reported on the one electron transfer reaction of benzyltrialkylstannanes with tetracyanoethylene (Eaton,

1980a). The radical cation formed was shown to fragment by dual modes in which the partition ratio depended on the substituent on the aromatic ring of the benzylstannane.

Other evidence was presented for electron transfer reactions of allylic and benzylic silanes and stannanes via the product studies of the photoreactions with a number of cyanoaromatic compounds. These include 9,10-dicyanoanthracene (Eaton, 1980b; Eaton, 1981; Mizuno et al, 1985b), p-dicyanobenzene (Mizuno et al, 1985a; Mizuno et al, 1988c), and 1,4-dicyanonaphthalene (Mizuno et al, 1988a; Sulpizio et al, 1989). Other electron acceptors that have been used include the aryldicyanoethylenes (Mizuno et al, 1987; Mizuno et al, 1988b).

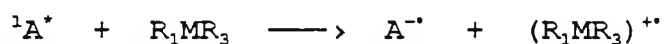
The photoaddition of allyl- and benzylsilanes to iminium salts via electron transfer has been extensively studied by Mariano and co-workers (Ohga and Mariano, 1982; Chen et al, 1983; Lan et al, 1984; Lan et al, 1987; Tu and Mariano, 1987).

Evidence has also been reported for electron transfer photoadditions of allylstannanes to pyrrolinium perchlorates (Borg and Mariano, 1986) and another report on the photoallylation of quinones via photoinduced electron transfer using allylstannanes (Maruyama et al, 1986). The proposed mechanism of photoinduced electron transfer from an allylstannane to a quinone was later confirmed by the same workers using CIDNP studies (Maruyama and Imahori, 1989). The photoinduced electron transfer addition reaction of trimethylallylstannane to benzophenone has also been

described (Takuwa et al, 1987) whereas in a later report by the same group the photoreaction of benzophenone with trimethylallylsilane no electron transfer products were reported (Takuwa et al, 1989). Later work showed that other carbonyl derivatives, including a variety of diketones, such as benzil derivatives and acenaphthenequinone, could be used to sensitise the photoinduced electron transfer reactions with allyl, benzyl, and cinnamylstannanes (Takuwa et al, 1990).

#### 2.5.8 UV Curing: sensitisation using DCA

As was mentioned earlier (see section 2.5.7) cyanoaromatics have been used effectively as sensitisers in photoreactions involving electron transfer in the presence of allylic and benzylic silanes and stannanes. A schematic representation of the proposed mechanism via the photoinduced single electron transfer pathway is given below:

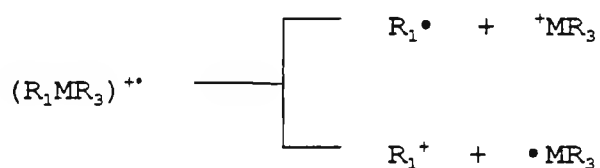


$R_1$  = allyl, benzyl, naphthyl

R = Me, n-Bu, Ph

M = Si, Sn

The radical cation so produced in the above scheme may fragment via two different routes:



The interesting route from the UV curing point of view is the one that produces the metal-centred radical which is capable of initiating polymerisation. This hypothesis was tested experimentally by irradiating a formulation of the sensitiser, DCA, and the organometallic donor in the presence of a free radical polymerisable monomer, TMPTA. The UV spectra of the sensitiser, DCA, and a number of representative silanes and stannanes are shown in the Appendix (Figure 5.1). The results of the testing carried out using the UV Colordry apparatus (see section 1.7.1) are presented below.

2.5.9 UV curing results of benzylsilanes with DCA

Table 2.14 UV curing of TMPTA with benzylsilanes (1% w/w) sensitised using DCA (0.25% w/w)

E X P T	INITIATING SYSTEM	BELT SPEED ft/min	NUMBER OF PASSES			
			Touching Quartz	Touching Glass	In Air	Glass Filter
1	PhCH <sub>2</sub> SiMe <sub>3</sub> + DCA	10	1	1	*	*
2	"	80	2	3	-	-
3	PhCH <sub>2</sub> SiMe <sub>3</sub>	10	6	20	*	*
4	4-PhC <sub>6</sub> H <sub>4</sub> CH <sub>2</sub> -SiMe <sub>3</sub> +DCA	10	1	2	30	*
5	"	80	2	4	-	-
6	4-PhC <sub>6</sub> H <sub>4</sub> CH <sub>2</sub> -SiMe <sub>3</sub>	10	3	6	*	*
7	Ph <sub>2</sub> CHSiMe <sub>3</sub> + DCA	10	1	1	*	*
8	"	230	2	5	-	-
9	Ph <sub>2</sub> CHSiMe <sub>3</sub>	10	3	9	*	*
10	DCA	10	6	15	*	*

\* = polymerisation not detected after 30 passes

- = experiment not performed

Sensitisation in the presence of DCA occurs for all the benzylsilanes tested when touching quartz and touching glass

as evidenced by the reduced number of passes required to achieve tack-free cure. This is proposed to be via an electron transfer mechanism with the ground state benzylsilane donating an electron to the excited singlet state of the sensitiser. This results in the formation of  $\text{Me}_3\text{Si}\cdot$  radicals which enhance the rate of polymerisation.

#### 2.5.10 UV curing results of benzylstannanes with DCA

Table 2.15 UV curing of TMPTA with benzylstannanes (1% w/w) sensitised using DCA (0.25% w/w)

EXPT	INITIATING SYSTEM	BELT SPEED ft/min	NUMBER OF PASSES			
			Touching Quartz	Touching Glass	In Air	Glass Filter
1	$\text{PhCH}_2\text{SnBu}_3$ + DCA	10	1	2	*	*
2	"	80	2	4	-	-
3	$\text{PhCH}_2\text{SnBu}_3$	10	1	3	*	*
4	"	80	2	-	-	-
5	$4\text{-MeC}_6\text{H}_4\text{CH}_2$ $\text{-SnBu}_3$ DCA	10	1	1	*	*
6	"	80	1	3	-	-
7	$4\text{-MeC}_6\text{H}_4\text{CH}_2$ $\text{-SnBu}_3$	10	1	3	*	*
8	"	80	2	-	-	-
9	DCA	10	6	15	*	*

\* = polymerisation not detected after 30 passes

- = experiment not performed

The effect of sensitisation is much reduced for the benzylstannanes (table 2.15) when compared to the benzylsilanes (table 2.14). This is undoubtedly due in part to the greater lability of the C-Sn (benzylic) bond to homolytic cleavage via photolysis compared to that of the C-Si (benzylic) bond. This homolytic process for the benzylstannanes probably dominates in the touching quartz experiments since the whole Hg lamp spectrum is available. There is a small effect of sensitisation in the touching glass experiments due to the filter effect of the glass cut off. Another feature of note is that the energy of the light corresponding to the UV spectrum of these compounds is greater than the bond strength.

#### 2.5.11 UV curing results of naphthylsilanes with DCA

Table 2.16 UV curing of TMPTA with naphthylsilanes (1% w/w) sensitised by DCA (0.25% w/w)

E X P T	INITIATING SYSTEM	NUMBER OF PASSES			
		Touching Quartz*	Touching Glass	In Air	Glass Filter
1	1-NpCH <sub>2</sub> SiMe <sub>3</sub> + DCA	2	4	*	*
2	1-NpCH <sub>2</sub> SiMe <sub>3</sub>	4	7	*	*
3	2-NpCH <sub>2</sub> SiMe <sub>3</sub> + DCA	2	4	*	*
4	2-NpCH <sub>2</sub> SiMe <sub>3</sub>	3	6	*	*
5	DCA	6	15	*	*

Belt speed = 10 ft/min for all experiments

\* = polymerisation not detected after 30 passes

There is a small effect of sensitisation and this is probably due to competitive absorption of the sensitiser and the naphthylsilanes. Thus sensitisation is not as effective as in the case of the benzylic compounds.

#### 2.5.12 UV curing results of allylsilanes with DCA

Table 2.17 UV curing of TMPTA with allylsilanes (1% w/w) sensitised by DCA (0.25% w/w)

E X P T	INITIATING SYSTEM	NUMBER OF PASSES			
		Touching Quartz	Touching Glass	In Air	Glass Filter
1	$\text{CH}_2=\text{CHCH}_2\text{SiMe}_3$ + DCA	5	9	*	*
2	$\text{CH}_2=\text{CHCH}_2\text{SiMe}_3$	4	14	*	*
3	$\text{CH}_2=\text{CHCH}_2\text{SiPh}_3$ + DCA	6	13	*	*
4	$\text{CH}_2=\text{CHCH}_2\text{SiPh}_3$	6	18	*	*
5	DCA	6	15	*	*
6	TMPTA	6	40	*	*

Belt speed = 10 ft/min for all experiments

\* = polymerisation not detected after 30 passes

The sensitisation of the allylsilanes using DCA (Table 2.17)

is much reduced when compared to the sensitisation of benzylsilanes by DCA (Table 2.14). This is thought to be due to the higher oxidation potentials of the allylsilanes when compared to the benzylsilanes (see Table 5.1: Appendix) which render them less useful, on energetic grounds, in electron transfer schemes.

### 2.5.13 UV curing results of allylstannanes with DCA

Table 2.18 UV curing of TMPTA with allylstannanes (1% w/w) sensitised by DCA (0.25% w/w)

E X P T	INITIATING SYSTEM	NUMBER OF PASSES			
		Touching Quartz	Touching Glass	In Air	Glass Filter
1	$\text{CH}_2=\text{CHCH}_2\text{SnBu}_3$ + DCA	2	5	*	*
2	$\text{CH}_2=\text{CHCH}_2\text{SnBu}_3$	3	11	*	*
3	$\text{CH}_2=\text{C}(\text{Me})\text{CH}_2\text{SnBu}_3$ + DCA	2	4	*	*
4	$\text{CH}_2=\text{C}(\text{Me})\text{CH}_2\text{SnBu}_3$	3	8	*	*
5	$\text{Me}_2\text{C}=\text{CHCH}_2\text{SnBu}_3$ + DCA	1	1	*	*
6	"	2 <sup>a</sup>	4 <sup>a</sup>	*	*
7	$\text{Me}_2\text{C}=\text{CHCH}_2\text{SnBu}_3$	1	5	*	*
8	DCA	6	15	*	*

a = belt speed 80 ft/min

Belt speed = 10 ft/min for all other experiments

\* = polymerisation not detected after 30 passes

The sensitisation of the allylstannanes using DCA (Table 2.18) appears to be related to the relative oxidation potentials of the prospective electron donors (see Table 5.1: Appendix). Thus it is the allylstannane that is expected to have the lowest oxidation potential, which shows the greatest effect of sensitisation (EXPT 5).

#### 2.5.14 Sensitisation of polymerisation with aromatic ketones

A number of aromatic ketone triplet photosensitisers exist, with the classical example being benzophenone. The related cyclic aromatic ketones xanthone and thioxanthone and 1,2-diketones such as benzil, as well as both 1,4- and 1,2-quinones, behave in a similar manner. All these compounds can be used as triplet sensitisers and will abstract hydrogen from a suitable H-donor through an encounter complex. One reaction of this type that has received considerable attention is the photoreduction of aromatic ketones with *t*-amines possessing  $\alpha$ -hydrogen atoms (Cohen et al, 1973; Davidson, 1975; Davidson, 1983). It was shown by several workers that an electron transfer mechanism was operative with the transfer occurring from the nitrogen lone-pair to the carbonyl oxygen in the excited complex (exciplex). The exciplex can proceed to a ketyl radical and

an  $\alpha$ -amino alkyl radical, which can then go on and initiate radical polymerisation. The rates of polymerisation of various monomers using *t*-amine/ketone combinations have been determined (see Hageman, 1985 and references within). The major factor in determining the efficiency of the photoreduction was shown to be the ionisation potential of the amine. It was shown that there exists a rough correlation between the ionisation potential of the amine and the rate of quenching of the excited carbonyl for amines with an ionisation potential of  $< 9\text{eV}$  (Turro, 1978).

Since the prepared silanes and stannanes have low oxidation potentials there is the possibility that these compounds undergo electron transfer reactions with ketones. It was decided to test this hypothesis and see whether these organometallics would form such exciplexes with aromatic carbonyl compounds which would lead to an increase in the rate of polymerisation. Early reports in the literature indicated that these organometallics would undergo photoinduced electron transfer reactions with suitable aromatic carbonyl sensitisers. The first report in this area was the photoreaction of quinones with allylstannanes to give allylated quinones (Maruyama *et al*, 1986). Formation of these products indicated the involvement of an electron transfer process. Later work by the same group reported on the photoallylation of benzophenone and benzaldehyde derivatives by allylic stannanes and these reactions were proposed as occurring via an electron

transfer mechanism (Takuwa et al, 1987).

Interestingly no photoinduced electron transfer reaction occurred with benzophenone when allyltrimethylsilane was used instead of allyltributylstannane. According to a later report the reason for this behaviour is understandable on the basis of the free energy of the electron transfer process between the allylsilane and the photoexcited triplet of benzophenone which was estimated to be positive (Takuwa et al, 1989). Further work was documented of the photoreaction of allyl and benzyl stannanes with a quinone and the values for the free energy of this reaction were calculated to be negative which is indicative of the feasibility of an electron transfer pathway (Maruyama and Imahori, 1989). The photoreaction of allylic stannanes with triplet carbonyl sensitizers was extended to include benzil derivatives and acenaphthenequinone (Takuwa et al, 1990). The free energy changes from the Rehm-Weller equation for the reaction of allyltrimethylstannane ( $E_{ox} = 1.06V$ ) and 3-methyl-2-butenyltrimethylstannane ( $E_{ox} = 0.68V$ ) with benzil were calculated to be  $-5.5$  and  $-17.5$  kcal mol<sup>-1</sup> respectively. The same workers also looked at the conjugate addition of allylic groups, including allylic and cinnamyl stannanes, to a variety of  $\alpha,\beta$ -unsaturated ketones via an electron transfer pathway (Takuwa et al, 1991). An elegant experiment from this work illustrated the importance of the reduction potential of the sensitizer in electron transfer schemes. Irradiation of 1,3-diphenyl-2-propen-1-one ( $E_{red} = -$

1.45V) with allyltrimethylstannane gave only [2 + 2] cycloaddition products without the formation of any allylated products. On the other hand, chalcones having a cyano group on the phenyl ring yielded allylated products presumably via an electron transfer mechanism which is rendered possible due to their lower reduction potentials.

2.5.15 UV curing results of benzylsilanes and stannanes with benzanthrone

The aromatic ketone sensitiser looked at was benzanthrone which showed good absorption characteristics in the UV region. UV spectra of benzanthrone and a number of representative silanes and stannanes are given in the Appendix.

Table 2.19 UV curing of TMPTA with benzylsilanes and stannanes (both 5% w/w) sensitised by benzanthrone (1% w/w)

E X P T	INITIATING SYSTEM	NUMBER OF PASSES			
		Touching Quartz	Touching Glass	In Air	Glass Filter
1	PhCH <sub>2</sub> SiMe <sub>3</sub> + Benzanthrone	4	8	21	*
2	PhCH <sub>2</sub> SiMe <sub>3</sub>	4	28	*	*
3	4-PhC <sub>6</sub> H <sub>4</sub> CH <sub>2</sub> SiMe <sub>3</sub> + Benzanthrone	4	7	15	*
4	4-PhC <sub>6</sub> H <sub>4</sub> CH <sub>2</sub> SiMe <sub>3</sub>	2	11	*	*
5	Ph <sub>2</sub> CHSiMe <sub>3</sub> + Benzanthrone	3	7	21	*
6	Ph <sub>2</sub> CHSiMe <sub>3</sub>	3	9	*	*
7	PhCH <sub>2</sub> SnBu <sub>3</sub> + Benzanthrone	2	6	18	*
8	PhCH <sub>2</sub> SnBu <sub>3</sub>	1	3	*	*
9	Benzanthrone	4	10	25	*

Belt speed = 10 ft/min for all experiments

\* = polymerisation not detected after 30 passes

There is some evidence of an improvement in the cure rate when using benzanthrone with the benzylsilanes and the stannane. This could be due to sensitisation of polymerisation when using benzanthrone, or via a combination of different initiation pathways from the sensitiser and the silane/stannane. Further experiments are required to elucidate the mechanism of initiation.

UV curing results of allylsilanes and stannanes  
with benzanthrone

Table 2.20 UV curing of TMPTA with allylsilanes and stannanes (both at 5% w/w) sensitised by benzanthrone (1% w/w)

E X P T	INITIATING SYSTEM	NUMBER OF PASSES			
		Touching Quartz	Touching Glass	In Air	Glass Filter
1	CH <sub>2</sub> =CHCH <sub>2</sub> SiMe <sub>3</sub> + Benzanthrone	4	10	25	*
2	CH <sub>2</sub> =CHCH <sub>2</sub> SiMe <sub>3</sub>	3	20	*	*
3	CH <sub>2</sub> =CHCH <sub>2</sub> SiPh <sub>3</sub> + Benzanthrone	6	12	25	*
4	CH <sub>2</sub> =CHCH <sub>2</sub> SiPh <sub>3</sub>	6	*	*	*
5	CH <sub>2</sub> =CHCH <sub>2</sub> SnBu <sub>3</sub> + Benzanthrone	8	11	<b>20</b>	*
6	CH <sub>2</sub> =CHCH <sub>2</sub> SnBu <sub>3</sub>	2	14	*	*
7	Benzanthrone	4	10	25	*

Belt speed = 10 ft/min for all experiments

\* = polymerisation not detected after 30 passes

There appears to be little benefit of using benzanthrone to 'sensitise' the polymerisation of TMPTA using the allylic derivatives. Thus the allylic compounds (Table 20) are not sensitised by benzanthrone to the same extent as the benzylic compounds (Table 19). This suggests that there is some exciplex formation between benzanthrone and the

organometal which will be favoured by lower oxidation potentials of the organometal. In general the benzylic compounds have lower oxidation potentials than the allylic compounds which supports this argument and the allylstannane (EXPT 5; table 20), which has the lowest oxidation potential of the allylic compounds tested, shows a small improvement in cure rate in air.

2.5.17 UV curing results of naphthylsilanes and stannanes with benzanthrone

Table 2.21 UV curing of TMPTA with naphthylsilanes and stannanes (both at 5% w/w) sensitised by benzanthrone (1% w/w)

E X P T	INITIATING SYSTEM	NUMBER OF PASSES			
		Touching Quartz	Touching Glass	In Air	Glass Filter
1	1-NpCH <sub>2</sub> SiMe <sub>3</sub> + Benzanthrone	5	8	<b>15</b>	*
2	1-NpCH <sub>2</sub> SiMe <sub>3</sub>	4	7	30	*
3	1-NpCH <sub>2</sub> SnBu <sub>3</sub> + Benzanthrone	1	1	<b>11</b>	<b>30</b>
4	"	2 <sup>a</sup>	2 <sup>a</sup>	-	-
5	1-NpCH <sub>2</sub> SnBu <sub>3</sub>	1	1	30	*
6	"	2 <sup>a</sup>	2 <sup>a</sup>	-	-
7	Benzanthrone	4	10	25	*

a = belt speed 80 ft/min

Belt speed = 10 ft/min for all other experiments

\* = polymerisation not detected after 30 passes

- = experiment not performed

The results for the naphthylic compounds indicate that there may be sensitisation taking place when benzanthrone is used. This effect with the naphthylic compounds could be due to the lower oxidation potentials of these derivatives. This would explain why there is little effect of sensitisation when using the benzylic (Table 2.19) and allylic (Table 2.20) derivatives, which have higher oxidation potentials than the naphthylic derivatives (see Table 5.1: Appendix). The 'sensitisation' with the naphthylic derivatives, could also be due to the combined separate initiating properties of benzanthrone and the naphthylic derivative.

#### 2.5.18 UV curing results using 4,4'-dimethylbenzil (DMB) as a sensitiser

The first report on the photochemical reactions of a number of allylstannanes and benzyltrimethylstannane with benzil derivatives appeared recently (Takuwa et al, 1990). Irradiation (400-480nm) of the benzil derivatives in the presence of the respective stannane gave the allylated or benzylated product. The reaction was proposed to proceed via a photoinduced electron transfer mechanism.

It was decided to test a number of silanes and stannanes prepared in view of this mechanistic conjecture since

radicals produced could effect polymerisation. The silane or stannane was incorporated along with the sensitiser, 4,4'-dimethylbenzil, in the monomer, TMPTA, and tested using the UV Colordry apparatus described earlier (see section 1.7.1). The UV spectra of 4,4'-dimethylbenzil and a number of representative silanes and stannanes are given in the Appendix. The UV curing results are given in table 2.22 below.

Table 2.22 UV curing results for the sensitisation of polymerisation of TMPTA using 4,4'-dimethylbenzil (1% w/w) with silanes (1% w/w) and stannanes (5% w/w)

E X P T	INITIATOR	NUMBER OF PASSES			
		Touching Quartz	Touching Glass	In Air	Glass Filter
1	$\text{Me}_2\text{C}=\text{CHCH}_2\text{SnBu}_3$ + DMB	1	1	5	10
2	$\text{Me}_2\text{C}=\text{CHCH}_2\text{SnBu}_3$	1	6	*	*
3	$4\text{-MeC}_6\text{H}_4\text{CH}_2\text{SnBu}_3$ + DMB	1	1	4	9
4	$4\text{-MeC}_6\text{H}_4\text{CH}_2\text{SnBu}_3$	1	3	*	*
5	DMB + $\text{CH}_2=\text{CHCH}_2\text{SiPh}_3$	2 <sup>a</sup>	4 <sup>a</sup>	-	-
6	DMB + $\text{Me}_3\text{Si-SiMe}_3$	1 <sup>a</sup>	3 <sup>a</sup>	-	-
7	DMB	1	1	17	*
8	"	3 <sup>a</sup>	6 <sup>a</sup>	-	-

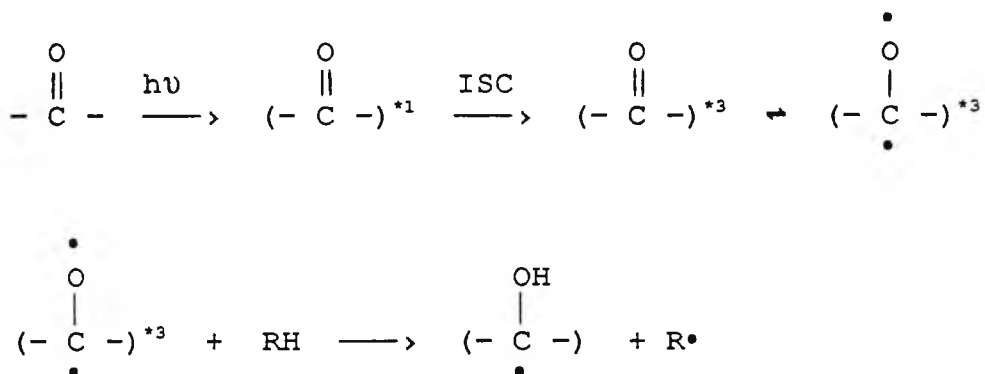
\* = polymerisation not detected after 30 passes

a = belt speed 230 ft/min

Belt speed = 10 ft/min for all other experiments

- = experiment not performed

These preliminary results, especially when using the stannanes, looked promising since curing in air (both in air and with glass cover) was observed. One important point to note is that 4,4'-dimethylbenzil will effect polymerisation when it is used on it's own (EXPT's 7 and 8). This type of aromatic ketone will act as a photoinitiator by an intermolecular hydrogen abstraction from donor molecules by the following illustrative mechanism:



It is thought that the donor RH could originate from either the monomer or from the activated CH<sub>3</sub> group on the benzil derivative.

It was also noticed that on irradiation the films in EXPT's 1 and 3 (when the stannanes were used) underwent a colour change from light yellow to a much darker yellow/orange. This is discussed further in the RTIR results where testing

of a wide range of silanes and stannanes was carried out (see section 2.6.10).

#### 2.5.19 UV curing results using thiopyrylium salts as sensitisers

The photocuring of epoxides using thiopyrylium salts with anions derived from Lewis acids has been described (Ketley and Tsao, 1979) and patented (US 4,139,655). In all cases the UV cure rates of the epoxides were shown to be considerably lower for the thiopyrylium salts than for sulphonium salts under comparable conditions. In a different role 2,4,6-triphenylpyrylium salts were used as electron acceptors in photoinduced charge transfer schemes with pinacolic donors (Sankararaman and Kochi, 1989). The pyrylium salts were found to rival more conventional singlet sensitisers such as the cyanoarenes. In the light of this work it appeared that the pyrylium/thiopyrylium salts could be effective as sensitisers for free radical photopolymerisation when used in conjunction with suitable electron donors such as allyl and benzyl silanes and stannanes. This led to the testing of this idea using formulations of a thiopyrylium salt with an organometallic donor in the presence of a radically polymerisable monomer, TMPTA. The results of the tests using the UV Colordry apparatus (see section 1.7.1) are given below in tables 2.23, 2.24, and 2.25.

Table 2.23 UV curing results of 2,4,6-triphenylthiopyrylium tetrafluoroborate (thiopyrylium A) (0.25%) with benzylic silanes and stannane (all at 1% w/w) in the presence of TMPTA

E X P E R I M E N T	INITIATING SYSTEM	NUMBER OF PASSES			
		Touching Quartz	Touching Glass	In Air	Glass Filter
1	PhCH <sub>2</sub> SiMe <sub>3</sub> + Thiopyrylium A	2	3	*	*
2	PhCH <sub>2</sub> SiMe <sub>3</sub>	4	28	*	*
3	4-PhC <sub>6</sub> H <sub>4</sub> CH <sub>2</sub> SiMe <sub>3</sub> + Thiopyrylium A	2	3	*	*
4	4-PhC <sub>6</sub> H <sub>4</sub> CH <sub>2</sub> SiMe <sub>3</sub>	3	6	*	*
5	PhCH <sub>2</sub> SnBu <sub>3</sub> + Thiopyrylium A	1	3	*	*
6	PhCH <sub>2</sub> SnBu <sub>3</sub>	4	20	*	*
7	Thiopyrylium A	7	23	*	*

Belt speed = 10 ft/min for all experiments

\* = polymerisation not detected after 30 passes

It is noticeable that sensitisation of polymerisation occurs in all the touching quartz and touching glass examples of results of 2,4,6-triphenylthiopyrylium tetrafluoroborate with benzylic silanes and stannane. Sensitisation is more evident in the touching glass experiments. This is probably

because in the case of the touching glass experiments the thiopyrylium salt absorbs virtually all of the available light since the benzylic organometals do not absorb to any great extent beyond the glass cut-off point (>310nm).

Table 2.24 UV curing results of 2,4,6-triphenylthiopyrylium tetrafluoroborate (thiopyrylium A) (0.25% w/w) with allylic stannanes and silane (all at 1% w/w) in the presence of TMPTA

E X P T	INITIATING SYSTEM	NUMBER OF PASSES			
		Touching Quartz	Touching Glass	In Air	Glass Filter
1	CH <sub>2</sub> =CHCH <sub>2</sub> SiPh <sub>3</sub> Thiopyrylium A	6	<b>10</b>	*	*
2	CH <sub>2</sub> =CHCH <sub>2</sub> SiPh <sub>3</sub>	6	18	*	*
3	CH <sub>2</sub> =CHCH <sub>2</sub> SnBu <sub>3</sub> + Thiopyrylium A	3	<b>6</b>	*	*
4	CH <sub>2</sub> =CHCH <sub>2</sub> SnBu <sub>3</sub>	2	14	*	*
5	Me <sub>2</sub> C=CHCH <sub>2</sub> SnBu <sub>3</sub> + Thiopyrylium A	2	<b>5</b>	*	*
6	Me <sub>2</sub> C=CHCH <sub>2</sub> SnBu <sub>3</sub>	2	7	*	*
7	Thiopyrylium A	7	23	*	*

Belt speed = 10 ft/min for all experiments

\* = polymerisation not detected after 30 passes

It is apparent that the allylic organometallic compounds

(Table 2.24) are not sensitised to the same extent as the benzylic compounds (table 2.23) when using the same thiopyrylium salt. This may be due to the fact that in general the allylic compounds have higher ionisation potentials (see Table 5.1: Appendix) than benzylic compounds and are consequently less able to undergo electron transfer reactions. In order to discover the general applicability of this sensitised photopolymerisation another thiopyrylium salt was used in conjunction with a variety of allylic and benzylic organometallic compounds of silicon and tin. The results are presented below.

Table 2.25 UV curing results of 4-*n*-butoxyphenyl-2,6-bis(4-methoxyphenyl)thiopyrylium tetrafluoroborate (1% w/w) with benzylic and allylic silanes and stannanes (all 5% w/w)

E X P T	INITIATOR	NUMBER OF PASSES			
		Touching Quartz	Touching Glass	In Air	Glass Filter
1	PhCH <sub>2</sub> SiMe <sub>3</sub> + Thiopyrylium B	1	3	*	*
2	PhCH <sub>2</sub> SiMe <sub>3</sub>	4	28	*	*
3	4-PhC <sub>6</sub> H <sub>4</sub> CH <sub>2</sub> SiMe <sub>3</sub> + Thiopyrylium B	1	2	29	*
4	4-PhC <sub>6</sub> H <sub>4</sub> CH <sub>2</sub> SiMe <sub>3</sub>	2	11	*	*
5	PhCH <sub>2</sub> SnBu <sub>3</sub> + Thiopyrylium B	1	4	*	*
6	PhCH <sub>2</sub> SnBu <sub>3</sub>	1	5	*	*

Table 2.25 continued

7	4-MeC <sub>6</sub> H <sub>4</sub> CH <sub>2</sub> SnBu <sub>3</sub> + Thiopyrylium B	1	3	*	*
8	4-MeC <sub>6</sub> H <sub>4</sub> CH <sub>2</sub> SnBu <sub>3</sub>	1	3	*	*
9	CH <sub>2</sub> =CHCH <sub>2</sub> SnBu <sub>3</sub> + Thiopyrylium B	<b>1</b>	<b>2</b>	*	*
10	CH <sub>2</sub> =CHCH <sub>2</sub> SnBu <sub>3</sub>	2	14	*	*
11	Thiopyrylium B	3	6	*	*

Belt speed = 10 ft/min for all experiments

\* = polymerisation not detected after 30 passes

Sensitisation of polymerisation is seen in the case of the benzylic silanes (EXPT'S 1 and 3) and the allylstannane (EXPT 9) but little effect is observed with the benzylic stannanes (EXPT'S 5 and 7). This could be due to the competition in the case of the benzylstannane of sensitisation by the thiopyrylium salt with homolytic cleavage of the C-Sn bond. This would be dependent on the relevant absorption properties in the desired wavelength range of the benzylstannane and the thiopyrylium salt.

At the same time another group was working in the same area and an article was published concerned with the photoalkylation of a pyrylium salt with group 14 donors via electron transfer (Kyushin et al, 1990). The electron donors used included allylstannanes and benzylstannanes. It was concluded from the published work that the radical

cation of the group 14 organometallic compound releases the group which is the most stable as a radical in the following order;

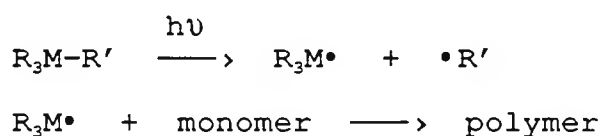


## 2.6 Real-time infrared spectroscopy (RTIR) results

### 2.6.1 Introduction

The maximum rate of polymerisation,  $R_{p(\text{max})}$ , and the degree of conversion have been evaluated at various time intervals utilising the technique of RTIR spectroscopy, which has been described previously (see section 1.7.2). The results of the initiator under test may then be compared to the situation where a sensitiser has been incorporated into the formulation. The efficiency of the sensitisation can be inferred from the comparison of the rates of polymerisation in the situations with and without the use of a sensitiser.

The RTIR results of the initiators used on their own gives an indication of the ease of cleavage of the M-C bond since the proposed mechanism of initiation is via homolytic cleavage of the M-C bond.



It is also worth noting that a number of the initiators tested using the RTIR spectroscopy apparatus did not show any signs of polymerisation which is believed to be due to the lack of absorption of the light source since a cover slip of polyethylene was used in all the experiments which absorbed in the UV region (see Figure 5.1: Appendix). A number of the compounds tested absorb in the same region as the cover-slip and hence the observed kinetic trace showed no evidence of polymerisation. For these compounds in particular the UV curing results obtained using the UV Colordry apparatus are useful since an indication of the effectiveness of these compounds in initiation can be deduced and compared to the remainder of the initiators.

### 2.6.2 RTIR results of benzylsilanes

Table 2.26 RTIR results of the photopolymerisation of TMPTA using benzylsilanes

E X P T	INITIATOR	UV/ $\lambda_{\max}$ ( $\epsilon$ )	% initiator		$R_p$ (max) / mol/l/s	% Conv/ at 1 min
			w/w	mol		
1	PhCH <sub>2</sub> SiMe <sub>3</sub>	274 (750)	1.6	2.9	-	-
2	4-MeC <sub>6</sub> H <sub>4</sub> CH <sub>2</sub> - SiMe <sub>3</sub>	273 (650)	5.0	8.3	-	-
3	4-MeOC <sub>6</sub> H <sub>4</sub> CH <sub>2</sub> - SiMe <sub>3</sub>	283 (1850)	5.0	7.6	0.579	43.0
4	4-PhC <sub>6</sub> H <sub>4</sub> CH <sub>2</sub> - SiMe <sub>3</sub>	278 (3500)	1.0	1.2	0.196	16.0

- = no polymerisation detected

The results indicate that under the conditions tested only experiments 3 and 4 show evidence of polymerisation, which is probably related to the greater values of the extinction coefficients and the longer wavelength absorbance of these compounds compared to those in experiments 1 and 2. The results also reflect a similar outcome depicted by the UV curing results shown in table 2.4.

### 2.6.3 RTIR results of benzylic silanes

Table 2.27 RTIR results of the photopolymerisation of TMPTA using benzylic silanes

E X P T	INITIATOR	UV/ $\lambda_{max}$ ( $\epsilon$ )	% initiator		Rp(max) / mol/l/s	% Conv/ at 1 min
			w/w	mol		
1	PhCH <sub>2</sub> SiMe <sub>3</sub>	274 (750)	1.6	2.9	-	-
2	Ph <sub>2</sub> CHSiMe <sub>3</sub>	272 (1400)	1.0	1.2	0.021	5.8
3	9-(SiMe <sub>3</sub> )- fluorene	296 (6500)	1.0	1.2	0.382	28.2
4	9-(SiMe <sub>3</sub> )- thioxanthene	280 (4500)	5.0	5.5	0.224	36.7

- = no polymerisation detected

The first observation is that on going from benzyltrimethylsilane (EXPT 1) to diphenylmethyltrimethylsilane (EXPT 2) there is an approximate two-fold increase in the extinction coefficient when comparing the  $\lambda_{max}$  values of 274nm and 272nm

respectively. This improvement in absorption properties may explain the result of an observed kinetic trace for the diphenylmethyltrimethylsilane (EXPT 2), albeit at a relatively low rate of polymerisation and degree of conversion, compared to the case of benzyltrimethylsilane (EXPT 1) where no polymerisation was detected.

On moving to more conjugated benzylic silanes in experiments 3 and 4 a large increase in the extinction coefficients is realised and this is also illustrated by the increased rate of polymerisation (over 10-fold) and in the degree of conversion when compared to experiment 2.

#### 2.6.4 RTIR results of benzylstannanes

Table 2.28 RTIR results of the photopolymerisation of TMPTA using benzylstannanes

E X P T	INITIATOR	UV/ $\lambda_{\max}$ ( $\epsilon$ )	% initiator		Rp (max) / mol/l/s	% Conv/ at 1 min
			w/w	mol		
1	PhCH <sub>2</sub> SiMe <sub>3</sub>	274 (750)	1.6	2.9	-	-
2	PhCH <sub>2</sub> SnMe <sub>3</sub>	273 (700)	5.0	5.8	0.605	27.7
3	PhCH <sub>2</sub> SnBu <sub>3</sub>	265 (860)	1.2	0.9	0.335	21.7
4	4-MeC <sub>6</sub> H <sub>4</sub> CH <sub>2</sub> - SnBu <sub>3</sub>	279 (850)	1.8	1.4	0.298	19.3
5	4-MeOC <sub>6</sub> H <sub>4</sub> CH <sub>2</sub> - SnBu <sub>3</sub>	281 (2250)	5.0	3.6	1.960	36.9

- = no polymerisation detected

A comparison of the ease of cleavage of the benzylic C-Sn bond compared to the benzylic C-Si bond can be made when comparing the results of benzyltrimethylstannane (EXPT 2) to those of benzyltrimethylsilane (EXPT 1). Both the  $\lambda_{\text{max}}$  values and the extinction coefficients are similar for each of the compounds. The result using benzyltrimethylstannane indicates that light is interacting with the initiator to give cleavage of the C-Sn bond. It must be concluded that light is also being absorbed by benzyltrimethylsilane and that the process of C-Si homolytic cleavage in this case is not an efficient process. When the three Me groups in benzyltrimethylstannane (EXPT 2) are replaced with three n-Bu groups (EXPT 3) initiation is again shown to be more efficient via homolytic cleavage than for benzyltrimethylsilane (EXPT 1). When a 4-MeO substituent is incorporated (EXPT 5) a marked red shift in absorption occurs as well as an increase in the extinction coefficient when compared to the parent compound (EXPT 3). This is reflected in the ability of this compound to initiate polymerisation as depicted by the  $R_{\text{p(max)}}$  value and the degree of conversion.

RTIR results of naphthyl (and higher) silanes  
and stannanes

Table 2.29 RTIR results of the photopolymerisation of TMPTA using naphthyl (and higher) silanes and stannanes

E X P T	INITIATOR	UV/ $\lambda_{\max}$ ( $\epsilon$ )	% initiator		Rp(max)/ mol/l/s	% Conv/ at 1 min
			w/w	mol		
1	1-NpCH <sub>2</sub> SiMe <sub>3</sub>	321 (700)	6.0	8.3	0.195	28.1
2	2-NpCH <sub>2</sub> SiMe <sub>3</sub>	324 (1000)	5.0	6.9	0.187	26.2
3	1-NpCH <sub>2</sub> SnBu <sub>3</sub>	334 (1000)	5.0	3.4	3.78	43.2
4	2-NpCH <sub>2</sub> SnBu <sub>3</sub>	333 (1200)	1.0	0.7	3.91	33.3
5	2-NpCH <sub>2</sub> SnMe <sub>3</sub>	335 (1000)	1.0	1.0	1.60	30.7
6	1-pyreneCH <sub>2</sub> - SiMe <sub>3</sub>	379 (2400) 358 (6200) 347 (17800) 331 (17600)	1.0	1.0	0.202	28.0

The absorption spectra of all of the compounds in table 2.29 show a red shift in absorbance compared to the corresponding benzylic derivatives in tables 2.26, 2.27 and 2.28, as would be expected. Although there is little change in the extinction coefficients when comparing benzyltrimethylsilane (EXPT 1; table 2.26) versus 1- (and 2)naphthylmethyltrimethylsilane (EXPT's 1 and 2 respectively; table 2.29), benzyltrimethylstannane (EXPT 2;

table 2.28) versus 2-naphthylmethyltrimethylstannane (EXPT 5; table 2.29), and benzyltri-*n*-butylstannane (EXPT 3; table 2.28) versus 1-(and 2-)naphthylmethyltri-*n*-butylstannane (EXPT's 3 and 4 respectively; table 2.29), the red shift in the absorption spectra is enough to yield more active initiators in all cases compared here.

It also appears that for the naphthylstannanes the  $(n\text{-Bu})_3\text{Sn}$  group in experiments 3 and 4 has a greater effect on the rate of polymerisation and the degree of conversion than the  $\text{Me}_3\text{Sn}$  group in experiment 5. This suggests that the rate of reaction is in the order  $(n\text{-Bu})_3\text{Sn} > \text{Me}_3\text{Sn}$ , a point which has been observed previously (see section 2.5.2).

When increasing the absorption using the 1-pyrenylmethyltrimethylsilane (EXPT 6) compared to the corresponding naphthylmethyltrimethylsilanes (EXPT 1 and 2) there is little change in either the rate of polymerisation or the degree of conversion. This indicates that there is a limiting factor, namely that C-Si bond scission reaches a maximum rate irrespective of the absorption properties of the molecule. It is concluded that other factors need to be introduced to the molecular structure to induce a greater rate of photopolymerisation utilising the homolytic cleavage of the C-Si bond as a mechanism of initiation.

## 2.6.6 RTIR results of allylic silanes and stannanes

Table 2.30 RTIR results of the photopolymerisation of  
TMPTA using allylic silanes and stannanes

E X P T	INITIATOR	UV/ $\lambda_{\max}$ ( $\epsilon$ )	% initiator		Rp (max) / mol/l/s	% Conv/ at 1 min
			w/w	mol		
1	CH <sub>2</sub> =CHCH <sub>2</sub> - SiMe <sub>3</sub>	271 (100)	5.0	13.0	-	-
2	CH <sub>2</sub> =CHCH <sub>2</sub> - SnBu <sub>3</sub>	240 (5000)	1.5	2.2	0.010	3.8
3	Me <sub>2</sub> C=CHCH <sub>2</sub> - SnBu <sub>3</sub>	270 (50)	1.5	1.9	0.080	9.5
4	Ph-CH=CHCH <sub>2</sub> SnBu <sub>3</sub>	268	5.0	3.6	0.660	35.0

- = polymerisation not detected

The results show that these compounds are relatively ineffective UV initiators in their own right and must be sensitised to be of potential interest. Again it is shown that C-Sn homolytic cleavage is more facile than C-Si homolytic cleavage for the allylic systems tested here.

### RTIR results of a cinnamyllic stannane (EXPT 4; Table 2.30)

This compound does not show a particularly high rate of polymerisation but it does show a relatively high degree of conversion which may be related to the fact that [2 + 2] cycloaddition may be involved.

### 2.6.7 RTIR results of benzylsilanes with DCA

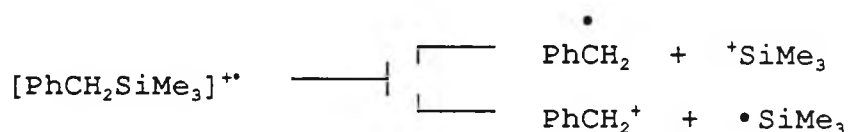
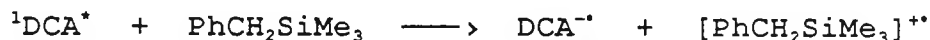
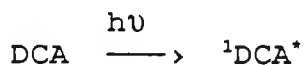
Table 2.31 RTIR spectroscopy results for the photopolymerisation of TMPTA using benzylsilanes sensitised by DCA

EXPT	INITIATING SYSTEM	UV/ $\lambda_{max}$ ( $\epsilon$ )	% initiator		Rp(max) / mol/l/s	% Conv/ at 1 min
			w/w	mol		
1	PhCH <sub>2</sub> SiMe <sub>3</sub> + DCA	274 (750) see expt 9	1.5 0.25	2.7 0.3	0.77	11.1
2	PhCH <sub>2</sub> SiMe <sub>3</sub>	274 (750)	1.6	2.9	-	-
3	Ph <sub>2</sub> CHSiMe <sub>3</sub> + DCA	272 (1400) see expt 9	2.5 0.25	3.0 0.3	1.00	19.6
4	Ph <sub>2</sub> CHSiMe <sub>3</sub>	272 (750)	1.0	1.2	0.02	5.8
5	4-PhC <sub>6</sub> H <sub>4</sub> CH <sub>2</sub> - SiMe <sub>3</sub> + DCA	278 (3500) see expt 9	1.0 0.25	1.2 0.3	0.34	24.0
6	4-PhC <sub>6</sub> H <sub>4</sub> CH <sub>2</sub> - SiMe <sub>3</sub>	278 (3500)	1.0	1.2	0.20	16.0
7	9-(Me <sub>3</sub> Si)-fl- uorene + DCA	296 (6500) see expt 9	1.0 0.25	1.2 0.3	0.11	32.3
8	9-(Me <sub>3</sub> Si)-fl- uorene	296 (6500)	1.0	1.2	0.38	28.2
9	DCA	424 (13000) 376 (11000) 312 (1000)	0.25	0.3	0.003	2.3

- = polymerisation not detected

The results show that there is definite sensitisation occurring for all the benzylic silanes tested when used in conjunction with DCA (apart from the fluorene derivative [EXPT 7] which is a special case and is discussed later). These results fully support the evidence that sensitisation

occurs in the UV curing results for these initiating systems discussed earlier. A most convincing case for sensitisation is obtained when comparing the result where benzyltrimethylsilane is sensitised by DCA (EXPT 1) to those of benzyltrimethylsilane on its own (EXPT 2) and the sensitiser, DCA, on its own (EXPT 9). As has been previously mentioned benzyltrimethylsilane is not an efficient initiator due to both the low homolysis rate on irradiation and the low extinction coefficient for this compound. Thus in the experimental apparatus no polymerisation is observed when benzyltrimethylsilane is used in the absence of any sensitiser (EXPT 2). To act as a standard for comparison, the RTIR spectrum of the sensitiser, DCA, was recorded and it showed a small degree of polymerisation (EXPT 9). When the combination of benzyltrimethylsilane and the sensitiser, DCA, was used (EXPT 1) a large increase in both  $R_{p(max)}$  and the degree of conversion resulted, giving conclusive evidence for sensitisation. The mechanism of sensitisation is believed to occur via photoinduced electron transfer and is outlined below.



Similarly when DCA was used with diphenylmethyltrimethylsilane (EXPT 3) and 1,1'-biphenylmethyltrimethylsilane (EXPT 5) sensitisation is noticed and both  $R_{p(max)}$  and the degree of conversion are increased when compared to the corresponding experiments without the presence of sensitiser (EXPT 4 and EXPT 6 respectively). This analysis is not applicable to the 'sensitisation' of fluorenyltrimethylsilane (EXPT 7). When comparing the  $R_{p(max)}$  for the sensitised case (EXPT 7;  $R_{p(max)} = 0.11$ ) to the value obtained without sensitiser (EXPT 8;  $R_{p(max)} = 0.38$ ) it would appear that DCA has a detrimental effect on the rate of polymerisation. The explanation of this phenomenon lies in an earlier observation regarding the mechanism of initiation of the fluorene derivative in the absence of any sensitiser. It is proposed that fluorenone is formed on photolysis of the fluorenyltrimethylsilane, which consumes oxygen, hence reducing oxygen inhibition of polymerisation, and thus increasing the rate of initiation (usually  $R_{p(max)}$ ). In the presence of the sensitiser, DCA, the two compounds compete for the available light with the net result that less light is absorbed by the fluorenyltrimethylsilane. This reduces the rate of the reaction of the fluorenyltrimethylsilane with oxygen, with a resultant increase in oxygen inhibition, and thus reduces the value of  $R_{p(max)}$  in the 'sensitised' case (EXPT 7) compared to the absence of sensitiser (EXPT 8). In contrast the degree of conversion (at 1 minute) for the sensitised case (EXPT 7; degree of conversion = 32.3) compared to the

degree of conversion (at 1 minute) for the sensitised case (EXPT 7; degree of conversion = 32.3) compared to the absence of sensitiser (EXPT 8; degree of conversion = 28.2) indicates that there is some sensitisation of polymerisation occurring. It seems that this sensitisation has been masked by the competing reaction of the fluorenyltrimethylsilane with oxygen which gives a relatively high  $R_{p(max)}$ .

#### 2.6.8 RTIR results of benzyl and naphthylstannanes with DCA

Table 2.32 RTIR spectroscopy results for the photopolymerisation of TMPTA using benzylic stannanes sensitised by DCA

EXPT	INITIATING SYSTEM	UV/ $\lambda_{max}$ ( $\epsilon$ )	% initiator		$R_p(max)$ / mol/l/s	% Conv / at 1 min
			w/w	mol		
1	PhCH <sub>2</sub> SnBu <sub>3</sub> + DCA	265 (860) see expt 7	1.2 0.25	0.9 0.3	0.80	35.1
2	PhCH <sub>2</sub> SnBu <sub>3</sub>	265 (860)	1.2	0.9	0.34	21.7
3	4-MeC <sub>6</sub> H <sub>4</sub> CH <sub>2</sub> - SnBu <sub>3</sub> + DCA	279 (850) see expt 7	1.2 0.25	0.9 0.3	0.77	31.6
4	4-MeC <sub>6</sub> H <sub>4</sub> CH <sub>2</sub> - SnBu <sub>3</sub>	279 (850)	1.8	1.4	0.30	19.3
5	2-NpCH <sub>2</sub> SnMe <sub>3</sub> + DCA	335 (1000) see expt 7	1.0 0.25	1.0 0.3	1.51	31.9
6	2-NpCH <sub>2</sub> SnMe <sub>3</sub>	335 (1000)	1.0	1.0	1.60	30.7
7	DCA	424 (13000) 376 (10000) 312 (1000)	0.25	0.3	0.003	2.3

photosensitisation of polymerisation occurring when using DCA with benzyltri-*n*-butylstannane (EXPT 1) and the 4-methyl analogue (EXPT 3) when compared to the stannanes in the absence of sensitiser (EXPT 2 and EXPT 4, respectively). In the case of these two benzylstannanes the increase in the  $R_{p(max)}$  value (both gave a 2.5 fold increase) is not as marked as was observed in the benzylsilanes (250 fold increase for benzyltrimethylsilane [EXPT 1 compared to EXPT 9; table 2.31], 50 fold increase for diphenylmethyltrimethylsilane [EXPT 3 compared to EXPT 4; table 2.31]) as shown below in table 2.33.

Table 2.33      The effect of sensitisation on the  $R_{p(max)}$  value of photopolymerisation of TMPTA using DCA with benzylsilanes and stannanes

COMPOUND	$R_{p(max)}/$ mol/l/s		Improvement Ratio A/B
	No DCA (B)	With DCA (A)	
$\text{PhCH}_2\text{SiMe}_3$	0.003	0.77	250
$\text{Ph}_2\text{CHSiMe}_3$	0.02	1.00	50
$\text{PhCH}_2\text{SnBu}_3$	0.34	0.80	2.5
4-MeC <sub>6</sub> H <sub>4</sub> CH <sub>2</sub> SnBu <sub>3</sub>	0.30	0.77	2.5

This contrast in behaviour is due to the fact that the benzylstannanes are effective initiators in the absence of

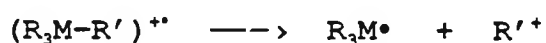
sensitiser whereas the benzylsilanes are relatively poor initiators in the absence of sensitiser. This behaviour reflects the greater tendency of the Sn-C (benzylic) bond to undergo homolytic cleavage compared to the Si-C (benzylic) bond. For the benzylstannanes in the presence of the sensitiser the process of homolytic cleavage will compete with that of sensitisation. The preference of one pathway over the other will depend on both the light available from the source and on the amount of light absorbed from that source.

What is noticeable is that for both the benzylsilanes and the benzylstannanes the effect of introducing the sensitiser, DCA, is to increase the degree of conversion by approximately the same amount as illustrated below.

Table 2.34 The effect of sensitisation on the degree of conversion value of photopolymerisation of TMPTA using DCA with benzylsilanes and stannanes

COMPOUND	% conversion /1 min		Improvement
	No DCA (B)	With DCA (A)	
PhCH <sub>2</sub> SiMe <sub>3</sub>	0.0	11.1	11.1
Ph <sub>2</sub> CHSiMe <sub>3</sub>	5.8	19.6	13.8
PhCH <sub>2</sub> SnBu <sub>3</sub>	21.7	35.1	13.4
4-MeC <sub>6</sub> H <sub>4</sub> CH <sub>2</sub> SnBu <sub>3</sub>	19.3	31.6	12.3

Therefore, there must be further radical species being produced in the presence of DCA that are capable of initiating polymerisation. This suggests that sensitisation takes place and this is proposed to be via an electron transfer mechanism. This also implies that the fragmentation of the radical cation of the organometallic species produced gives rise to initiating radicals, which are likely to be  $R_3M^\bullet$  radicals as depicted below.



In the case of the sensitisation of the 2-naphthylmethyltrimethylstannane (Table 2.32; EXPT 5) there was little evidence to suggest that DCA had any effect on either  $R_{p(\max)}$  or the degree of conversion compared to the situation without sensitiser (Table 2.32; EXPT 6). This is probably due to the competitive absorption of the initiator and the sensitiser in this case.

### 2.6.9 RTIR results of an allylstannane with DCA

Table 2.35 RTIR spectroscopy results for the photopolymerisation of TMPTA using an allylstannane sensitised by DCA

E X P T	INITIATING SYSTEM	UV/ $\lambda_{\max}$ ( $\epsilon$ )	% initiator		Rp (max) / mol/l/s	% Conv/ at 1 min
			w/w	mol		
1	Me <sub>2</sub> C=CHCH <sub>2</sub> - SnBu <sub>3</sub> + DCA	271 (100) see expt 3	1.8 0.25	1.5 0.3	0.08	17.4
2	Me <sub>2</sub> C=CHCH <sub>2</sub> - SnBu <sub>3</sub>	271 (100)	1.5	1.2	0.08	9.5
3	DCA	424 (13000) 376 (11000) 312 (1000)	0.25	0.3	0.003	2.3

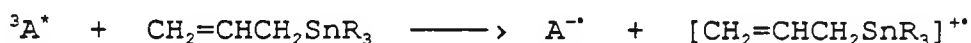
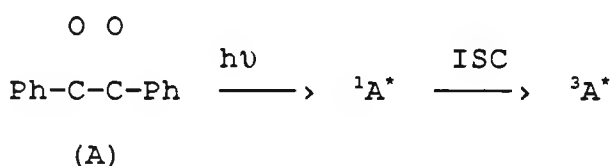
Sensitisation is seen to occur for the allylstannane in table 2.35 with regard to the degree of conversion. There is not a similar effect with other allylsilanes and stannanes which is attributed to the relatively high oxidation potentials of the allylic organometals in general (see Table 5.1; Appendix).

### 2.6.10 RTIR results using 4,4'-dimethylbenzil (DMB) as a sensitiser

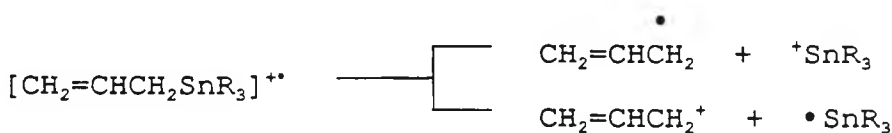
#### 2.6.11 Introduction

It has been reported previously that carbonyl compounds such as benzophenone can be successfully allylated using allylstannanes under photochemical conditions via an

electron transfer mechanism (Takuwa et al, 1987). Later work showed that diphenylethanediones (benzils) afforded  $\alpha$ -allylbenzoins in high yield when photolysed in the presence of allylstannanes which were again proposed to be formed via a one electron transfer pathway (Takuwa et al, 1990). The reaction scheme is shown below.



First the benzil derivative is excited to the singlet state. On intersystem crossing the excited triplet state is arrived at. The ground state allylstannane then interacts with the excited triplet state sensitiser which gives rise to an exciplex. Electron transfer then occurs from the allylstannane to the benzil derivative giving rise to a radical cation in the case of the allylstannane, and a radical anion in the case of the benzil derivative. It is then possible that the radical cation of the allylstannane will fragment. This has been shown to occur by two different pathways.

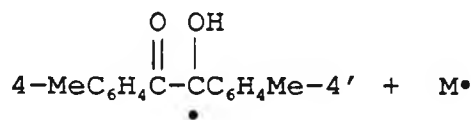
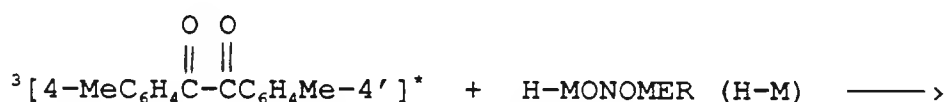


It is known that trialkyltin radicals are effective at initiating free radical polymerisation (Neumann *et al*, 1961; Davies, 1977).

In an attempt to harness the free radical produced in this way a free radical polymerisable monomer, TMPTA, was used as the 'solvent' for photolysis and the ensuing photopolymerisation was followed using the technique of RTIR spectroscopy described earlier (see section 1.7.2).

This reaction scheme has been further extended to include the use of naphthyllic stannanes and silanes in the photopolymerisation of TMPTA.

It is important to mention that the sensitiser used, 4,4'-dimethylbenzil, will initiate photopolymerisation of TMPTA when used on its own without the incorporation of a co-initiator. This is presumably free radical initiation of polymerisation via H-abstraction by the sensitiser from the monomer as shown below.



## 2.6.12 RTIR results of benzylsilanes with DMB

Table 2.36 RTIR spectroscopy results for the photopolymerisation of TMPTA using benzylsilanes sensitised by DMB

E X P T	INITIATING SYSTEM	UV/ $\lambda_{\max}$ ( $\epsilon$ )	mol %	R <sub>p</sub> (max) / mol/l/s	% Conv/ at 1 min
1	PhCH <sub>2</sub> SiMe <sub>3</sub> + DMB	274 (750) see expt 5	8.2 1.2	1.03	36.8
2	PhCH <sub>2</sub> SiMe <sub>3</sub>	274 (750)	2.9	-	-
3	4-MeO-C <sub>6</sub> H <sub>4</sub> CH <sub>2</sub> SiMe <sub>3</sub> + DMB	283 (1850) see expt 5	7.6 1.2	2.08	47.3
4	4-MeO-C <sub>6</sub> H <sub>4</sub> CH <sub>2</sub> SiMe <sub>3</sub>	283 (1850)	7.6	0.58	43.0
5	DMB	269 (29000)	1.2	0.40	32.4

- = no polymerisation detected

It is clear that there is a synergistic effect of the benzylsilanes on the rate of polymerisation in both cases. There is also an improvement in the degree of conversion for both silanes. This is not the case for other benzylic silanes shown below in table 2.37.

### 2.6.13 RTIR results of benzylic silanes with DMB

Table 2.37 RTIR spectroscopy results for the photopolymerisation of TMPTA using benzylic silanes sensitised by DMB

EXPT	INITIATING SYSTEM	UV/ $\lambda_{max}$ ( $\epsilon$ )	mol %	$R_p$ (max) / mol/l/s	% Conv/ at 1 min
1	9-Me <sub>3</sub> Si-fluorene + DMB	296 (6500)	1.2 1.2	0.30	30.2
2	9-Me <sub>3</sub> Si-fluorene	296 (6500)	1.2	0.38	28.2
3	9-Me <sub>3</sub> Si-thioxanthen + DMB	280 (4500)	1.1 1.2	0.04	13.4
4	9-Me <sub>3</sub> Si-thioxanthen	280 (4500)	5.5	0.22	36.7
5	DMB	269 (29000)	1.2	0.40	32.4

It is apparent that both the  $R_{p(max)}$  and the degree of conversion (1 min) are reduced when the fluorene derivative is tested with 4,4'-dimethylbenzil (EXPT 1) when compared to the situation with 4,4'-dimethylbenzil on its own (EXPT 5). There is also a reduction in the  $R_{p(max)}$  value (EXPT 1) when compared to the fluorene derivative on its own (EXPT 2). A similar situation occurs for the combination of the thioxanthene derivative and 4,4-dimethylbenzil (EXPT 3) except that the reduction in both the  $R_{p(max)}$  and the degree of conversion (1 min) is much more evident when compared to the thioxanthene derivative on its own (EXPT 4) and 4,4'-dimethylbenzil on its own (EXPT 5).

One explanation why the  $R_{p(max)}$  and the degree of conversion (1 min) results in the 'sensitised' experiments of the fluorene derivative (EXPT 1) and the thioxanthene derivative (EXPT 3) are not as high as the results of the benzylic silanes in the absence of 'sensitiser' (EXPT's 2 and 4 respectively) could be due to the reaction of these compounds with oxygen discussed earlier (see section 2.5.1). Thus the 'sensitiser' preferentially absorbs the available light which reduces the absorption of light by the benzylic silane. This means that the benzylic silane does not react with oxygen under photolytic conditions to both reduce oxygen inhibition and increase the  $R_{p(max)}$  and the degree of conversion (1 min). In the case of the thioxanthene derivative there could also be triplet quenching of the sensitiser since sulphur compounds can act in this way. This would explain the marked reduction in the  $R_{p(max)}$  and the degree of conversion (1 min) values in EXPT 3.

2.6.14 RTIR results of benzylstannanes with DMB

Table 2.38 RTIR spectroscopy results for the photopolymerisation of TMPTA using benzylstannanes sensitised by DMB

EXPT	INITIATING SYSTEM	UV/ $\lambda_{\max}$ ( $\epsilon$ )	mol %	$R_p(\max)$ / mol/l/s	% Conv/ at 1 min
1	PhCH <sub>2</sub> SnBu <sub>3</sub> + DMB	265 (860) see expt 5	4.0 1.2	1.66	37.2
2	PhCH <sub>2</sub> SnBu <sub>3</sub>	265 (860)	0.9	0.34	21.7
3	4-Me-C <sub>6</sub> H <sub>4</sub> CH <sub>2</sub> SnBu <sub>3</sub> + DMB	279 (850) see expt 5	3.8 1.2	4.54	47.6
4	4-Me-C <sub>6</sub> H <sub>4</sub> CH <sub>2</sub> SnBu <sub>3</sub>	279 (850)	1.4	0.30	19.3
5	DMB	269 (29000)	1.2	0.40	32.4
6	Irgacure 907	-	<b>0.9</b>	6.52	32.4



It is evident that both the benzylstannanes show an improvement in both the  $R_{p(\max)}$  and the degree of conversion (1 min) values in the presence of sensitiser (EXPT's 1 and 3) when compared to the results of the benzylstannanes in the absence of sensitiser (EXPT's 2 and 4 respectively) and the sensitiser on it's own (EXPT 5). In particular the result with 4-Me-C<sub>6</sub>H<sub>4</sub>CH<sub>2</sub>SnBu<sub>3</sub> (EXPT 3) shows a high  $R_{p(\max)}$  value and compares with the measured value of Irgacure 907, a commercial photoinitiator.

2.6.15 RTIR results of naphthylsilanes and stannanes with DMB

Table 2.39 RTIR spectroscopy results for the photopolymerisation of TMPTA using naphthyllic silanes and stannanes sensitised by DMB

EXPT	INITIATING SYSTEM	UV/ $\lambda_{\max}$ ( $\epsilon$ )	mol %	$R_p$ (max) / mol/l/s	% Conv/ at 1 min
1	1-NpCH <sub>2</sub> SiMe <sub>3</sub> + DMB	321 (700) see expt 10	8.5 1.2	0.45	36.8
2	1-NpCH <sub>2</sub> SiMe <sub>3</sub>	321 (700)	10.9	0.20	28.1
3	2-NpCH <sub>2</sub> OSiMe <sub>3</sub> + DMB	see expt 10	1.6 1.2	0.16	25.8
4	2-NpCH <sub>2</sub> SnMe <sub>3</sub> + DMB	335 (1000) see expt 10	1.0 1.2	3.95	34.6
5	2-NpCH <sub>2</sub> SnMe <sub>3</sub>	335 (1000)	1.0	1.60	30.7
6	2-NpCH <sub>2</sub> SnBu <sub>3</sub> + DMB	333 (1200) see expt 10	3.5 1.2	3.99	52.6
7	2-NpCH <sub>2</sub> SnBu <sub>3</sub>	333 (1200)	0.7	3.91	33.3
8	1-NpCH <sub>2</sub> SnBu <sub>3</sub> + DMB	334 (1000) see expt 10	3.5 1.2	3.70	37.9
9	1-NpCH <sub>2</sub> SnBu <sub>3</sub>	334 (1000)	3.5	3.78	43.2
10	DMB	269 (29000)	1.2	0.40	32.4

1-NpCH<sub>2</sub>SiMe<sub>3</sub> shows a small improvement in the  $R_{p(\max)}$  and the degree of conversion (1 min) values when sensitised (EXPT 1), when compared to the situation on its own (EXPT 2) and the sensitiser on its own (EXPT 10). This could be related to the competitive absorption with the sensitiser. The

silyl ether (EXPT 3) does not show any improvement when sensitised (EXPT 3), when compared to the sensitiser on its own (EXPT 10). When 2-NpCH<sub>2</sub>SnMe<sub>3</sub> was tested with the sensitiser (EXPT 4) there is a noticeable increase in the R<sub>p(max)</sub> and the degree of conversion (1 min) values when compared to the stannane on it's own (EXPT 5) and the sensitiser on its own (EXPT 10). The other naphthylstannanes did not show a similar trend, probably due to the higher % levels of these compounds, which means that they compete effectively with the sensitiser for the available light. This means that homolytic cleavage of the stannane will form a part of the overall mechanism of polymerisation as well as the sensitisation process.

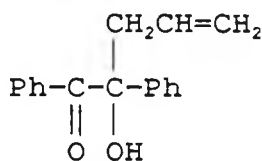
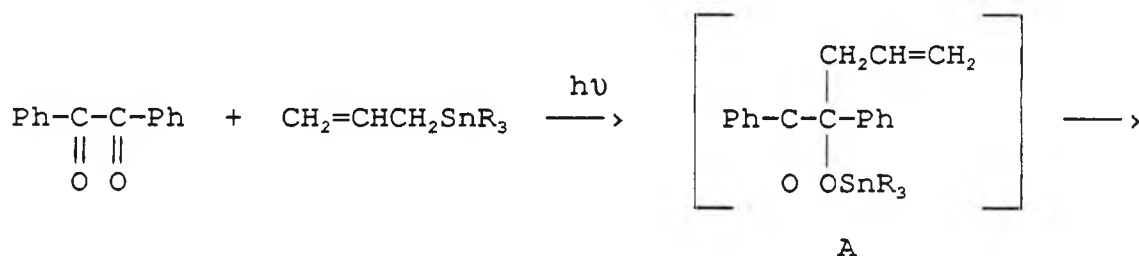
#### 2.6.16 RTIR results of allylsilanes and stannanes with DMB

Table 2.40 RTIR spectroscopy results for the photopolymerisation of TMPTA using allylic silanes and stannanes sensitised by DMB

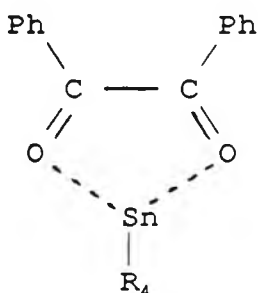
EXPT	INITIATING SYSTEM	UV/ λ <sub>max</sub> (ε)	mol %	R <sub>p</sub> (max) / mol/l/s	% Conv/ at 1 min
1	CH <sub>2</sub> =CHCH <sub>2</sub> SiPh <sub>3</sub> + DMB	see expt 4	1.0 1.2	0.42	30.2
2	Me <sub>2</sub> C=CHCH <sub>2</sub> SnBu <sub>3</sub> + DMB	270 (50) see expt 4	6.3 1.2	0.98	39.0
3	Me <sub>2</sub> C=CHCH <sub>2</sub> SnBu <sub>3</sub>	270 (50)	1.9	0.08	9.5
4	DMB	269 (29000)	1.2	0.40	32.4

The allylstannane shows an improvement in the  $R_{p(max)}$  and the degree of conversion (1 min) values when compared to the stannane on its own (EXPT 3) and the sensitiser on its own (EXPT 4). It appears that the allylsilane has little effect on the polymerisation, which is probably related to its higher oxidation potential than that for the allylstannane, rendering it less effective in an electron transfer mechanism.

One general observation from the results is that the sensitiser has a much greater effect when used with the stannanes than with the silanes. During this work a further report on the photoallylation of benzil with allylstannanes appeared (Takuwa et al, 1991). This gave an insight into the mechanistic details of the photoreaction.



It is proposed that there is a further precursor to species A involving the coordination of the Sn to both the carbonyl groups in a charge transfer complex as depicted below.



This type of complex could be important for symmetrical benzil derivatives with each carbonyl group being equally reactive. This is not the case for the photoreaction of unsymmetrical diketones with allylstannanes where a preferential addition product has been observed (Takuwa et al, 1990).

This could explain the earlier observation during the UV Colordry experiments that films incorporating 4,4-dimethylbenzil and the stannanes gave rise to a colour change on irradiation from light yellow to dark yellow/orange.

The ability of tin to increase its coordination is much greater than for silicon and would explain the apparent difference of behaviour of the silanes and the stannanes with the sensitiser, 4,4'-dimethylbenzil.

## 2.7 Experimental section

All chemicals were purchased from Aldrich and used as received without further purification. Melting points were recorded using a Griffin melting point apparatus and are uncorrected. IR spectra were run on a Perkin-Elmer 983 instrument.  $^1\text{H}$  NMR spectra were recorded using either a Jeol MH 100 instrument or a Jeol PMX 60 spectrometer with TMS as the internal standard. UV/vis absorption spectra were obtained using either a Perkin-Elmer Lambda 5 or a Perkin-Elmer Lambda 16 spectrophotometer. Mass spectra were recorded on either a VG Masslab Biotech Trio-2 instrument or a VG Zab-2F spectrometer. GLC was performed on a Perkin-Elmer Sigma 5 gas chromatograph fitted with a flame ionisation detector. The column (internal diameter 2mm, length 2m) contained liquid phase 5% SE 30. The flow rate of  $\text{N}_2$  was 25mls/min, and the oven temperature was  $100^\circ\text{C}$ . CHN were performed on a Carlo Erba 1106 CHN simultaneous analyser. Photolysis was carried out on solutions in quartz cuvettes (1cm) placed in a circular array of 10x8W lamps having a maximal emission of 300nm. UV curing was performed using a Colordry UV curing unit which housed a medium pressure Hg lamp mounted above a conveyor belt system (lamp 15cm above moving belt; lamp  $80\text{Wcm}^{-1}$  and 23cm in length). Films were coated onto Gateway Natural Tracing (GNT) paper using Meyer bar coater number 3 (thickness  $25\mu$ ). The RTIR spectroscopy apparatus comprised of a Perkin-Elmer 597 spectrophotometer coupled to a Wotan 100W medium

pressure Hg source (Oriel). Kinetic traces were recorded with the spectrophotometer in the time-drive mode. A polyethylene cover slip, in contact with the film under test, was used in all the experiments (for UV see figure 5.1; Appendix). Photo-DSC experiments were run on a modified Perkin-Elmer DSC-4 calorimeter. The two ends of a two-branch UV light conducting fibre were inserted on the cover of the DSC-4 directly above the sample and reference holders. The two-branch flexible UV light guides (50cm long each) ended on a ferrule connector which was plugged into one side of an extended aluminium cylinder. Into this aluminium cylinder were placed a manual shutter to block the incident light on the input end, an interference 365nm filter (International Light NB-365), a solid IR filter (Schott KG-1) and neutral density filters. The extended cylinder assembly was joined to the water-cooling house of a Hanovia Uvitron irradiation system provided with a quartz lens and a 100W high pressure mercury lamp.

## 1. Trimethyl (phenylmethyl) silane

### Method 1

A.

Refluxing and stirring a mixture of benzyl chloride (50.6g; 0.4 mol), trichlorosilane (81.6g; 0.6mol) and tri-*n*-propylamine (57.4g; 0.4mol) at 56-90°C for 20h afforded on work up (ether precipitation of the amine hydrochloride, filtration, and fractionation of the filtrate) 40.0g (40%) of phenylmethyltrichlorosilane with bp 95-96°C/10mm (lit bp 100-102°C/15mm; Benkeser et al, 1969).

B.

A mixture of phenylmethyltrichlorosilane (4.1g; 18mmol) in anhydrous ether (20ml) was added slowly to an ice cooled stirred solution of MeMgBr (20ml; 3M solution in ether; 60mmol) The mixture was stirred at room temperature overnight. The ether was removed and the residue was microdistilled under vacuum to give 1.0g (35%) yield with bp 29°C/0.8mm (lit bp 191.2-191.4/759.5mm; Bygden, 1912)

### Method 2

Trichlorosilane (50g; 0.369mol) was added dropwise under argon with stirring to a mixture of benzaldehyde

(13.1g;0.123mol) and tri-*n*-propylamine (17.6g;0.123mol) in anhydrous ether (100ml). A vigorously exothermic reaction was observed. The mixture was then refluxed for 2h, cooled, and then excess pentane was added until all the amine hydrochloride precipitated. The precipitate was then filtered off. Distillation of the filtrate gave 15.0g (74%) yield of phenylmethyltrichlorosilane with bp 200°C (lit bp 100-102°C/15mm; Benkeser et al, 1969).

B.

MeMgBr (100ml;3M solution in ether;0.30mol) was added dropwise with stirring under argon to phenylmethyltrichlorosilane (15g;0.09mol) in anhydrous ether (100ml). On complete addition the reaction mixture was stirred at room temperature overnight. The reaction mixture was then refluxed for 3h. The reaction was cooled, and quenched with saturated ammonium chloride solution. The mixture was extracted with ether, dried (MgSO<sub>4</sub>), and concentrated. Distillation of the crude product gave 10.0g (32%) yield with bp 188-189°C (lit bp 191.2-191.4°C/759.5mm; Bygden, 1912).

#### Analysis

<sup>1</sup>H NMR:            0.40 (s,9H), 2.20 (s,2H), 6.90-7.50 (m,5H)

IR:                3061 (s), aromatic C-H stretch

2955 (s), aliphatic C-H stretch  
1601 (s), C=C stretch  
1249 (vs), Si-CH<sub>3</sub> stretch  
738 (s), 698 (s), monosubstituted aromatic

UV (EtOH):  $\lambda_{\max}$  274nm ( $\epsilon=750$ )

MS: M<sup>+</sup> 164, 73 (SiMe<sub>3</sub><sup>+</sup>; base peak)

CHN: Calculated for C<sub>10</sub>H<sub>16</sub>Si  
Required C 73.09 H 9.81  
Found C 73.47 H 10.06

## 2. Trimethyl[(4-methylphenyl)methyl]silane

Magnesium turnings (1.95g; 0.08mol) and anhydrous ether (30ml) were placed under argon. The dropping funnel was charged with  $\alpha$ -bromo-p-xylene (10g; 0.055mol) in anhydrous ether (30ml). Stirring was started and a 1-2ml portion of the  $\alpha$ -bromo-p-xylene solution was added into the reaction flask. The resulting temperature rise and cloudiness indicated that the reaction had started. The remainder of the  $\alpha$ -bromo-p-xylene solution was added at such a rate as to maintain a gentle reflux. After complete addition the reaction mixture was refluxed for 1.5h. During reflux the dropping funnel was charged with chlorotrimethylsilane

(6.0g;0.055mol) in anhydrous ether (30ml). After reflux, heating was stopped and the chlorotrimethylsilane solution was added at such a rate as to maintain gentle reflux (36-38°C). After complete addition the reaction mixture was refluxed for 1.5h. The reaction mixture was then quenched with ice-cold saturated ammonium chloride solution to lower the temperature below 35°C. The ether layer was separated, dried (magnesium sulphate), and concentrated. Distillation gave 4.7g (48%) yield of trimethyl[(4-methylphenyl)methyl]silane with bp 212°C (lit bp 211.5°C; Eaborn and Parker, 1955).

#### Analysis

<sup>1</sup>H NMR: relative to SiMe<sub>3</sub>; 0.00 (s,9H), 2.05 (s,2H), 2.30 (s,3H), 7.00 (s,4H)

IR: 3045 (m), aromatic C-H stretching  
2954 (s), aliphatic C-H stretching  
1510 (s), C=C stretching  
1248 (vs), Si-C stretching  
814 (s), 1,4-disubstituted aromatic

MS: M<sup>+</sup> 178, 105 (C<sub>8</sub>H<sub>9</sub><sup>+</sup>), 73 (base peak, SiMe<sub>3</sub><sup>+</sup>)

UV (EtOH): λ<sub>max</sub> = 280nm (ε=600), 273nm (ε=650)

CHN: Calculated for C<sub>11</sub>H<sub>18</sub>Si

Required	C 74.08	H 10.17
Found	C 74.76	H 11.22

### 3. Trimethyl[(4-methoxyphenyl)methyl]silane

4-Methoxybenzyl chloride (5.00g;0.032mol) in anhydrous THF (15ml) was added dropwise at room temperature under argon, with external irradiation of ultrasound, to a mixture of chlorotrimethylsilane (2.93g;0.027mol), magnesium turnings (0.83g;0.034mol) and 1,2-dibromoethane (0.5ml) in anhydrous THF (20ml). After 3.5h irradiation the reaction mixture was quenched with saturated aqueous  $\text{NH}_4\text{Cl}$  solution and then extracted with ether. The combined organic extracts were dried (magnesium sulphate), and concentrated. Bulb to bulb distillation gave 5.2g (98%) yield of trimethyl[(4-methoxyphenyl)methyl]silane with bp 74-75°C/0.1mm (lit bp 238°C; Eaborn and Parker, 1955).

#### Analysis

$^1\text{H}$  NMR: relative to  $\text{SiMe}_3$ ; 0.00 (s,9H), 2.10 (s,2H), 3.90 (s,3H), 6.90-7.20 (m,4H)

IR: 3029, aromatic C-H stretching  
2953, 2896, 2833, aliphatic C-H stretching  
1609, 1580, C=C stretching  
1248, Ar-O stretching

1039, Me-O stretching

830, 1,4-disubstituted benzene

MS:  $M^+$  194, 121 ( $\text{MeO}(\text{C}_6\text{H}_4)\text{CH}_2^+$ ), 73 ( $\text{SiMe}_3^+$ )

UV (EtOH):  $\lambda_{\text{max}} = 283\text{nm}$  ( $\epsilon=1850$ ),  $258\text{nm}$  ( $\epsilon=600$ )

CHN: Calculated for  $\text{C}_{11}\text{H}_{18}\text{OSi}$

Required C 67.98 H 9.34

Found C 68.23 H 9.49

#### 4. (Diphenylmethyl)trimethylsilane

A.

Making sure equipment was dry, trichlorosilane (30.2ml;0.3mol) was added dropwise to a stirred mixture of benzophenone (18.2g,;0.1mol) and tri-*n*-propylamine (19.0ml;0.1mol) at 0°C. After complete addition the reaction mixture was refluxed at 55-75°C for 1 hour. Excess pentane was then added to the cold reaction mixture until complete precipitation of tri-*n*-propylamine hydrochloride occurred. The precipitate was then filtered off and the excess pentane was removed. The crude product was vacuum distilled with bp 109°C/0.5mm (lit bp 141-145°C/2.5mm; Benkeser and Smith, 1969) to give 15.0g (50%) yield of (diphenylmethyl)trichlorosilane with mp 40-42°C (lit mp 48-49°C; Benkeser and Smith, 1969).

B.

A mixture of diphenylmethyltrichlorosilane (2.75g; 9mmol) in anhydrous ether (20ml) was added slowly to an ice cooled stirred solution of MeMgBr (10ml; 3M solution in ether; 30mmol). The mixture was stirred at room temperature overnight. The ether was removed and the residue was microdistilled under vacuum with bp 91°C/0.3mm (lit bp 135°C/4mm; Hauser and Hance, 1951). The product obtained was purified on a silica gel column using cyclohexane as eluent ( $R_f=0.5$ ) to give 0.4g (20%) yield of (diphenylmethyl)trimethylsilane with mp 74-75°C (lit mp 74.5-75.5°C; Hauser and Hance, 1951).

#### Analysis

$^1\text{H NMR}$ : 0.40 (s, 9H), 3.80 (s, 1H), 7.60 (m, 10H)

IR: 3057 (m), aromatic C-H stretch  
2951 (m), aliphatic C-H stretch  
1594 (m), C=C stretch  
1249 (s), Si-CH<sub>3</sub> stretch  
748 (s), 698 (s), monosubstituted aromatic

MS:  $M^+$  240, 73 (base peak; SiMe<sub>3</sub><sup>+</sup>)

UV (EtOH):  $\lambda_{\text{max}} = 272\text{nm}$  ( $\epsilon=1400$ )

5. Trimethyl(1,1'-biphenyl-4-ylmethyl)silane (Hayashi et al, 1981)

A.

NaH (4.4g;60% dispersion in oil;0.11mol) was placed in anhydrous THF (20ml) under argon. A solution of 4-phenylphenol (17g;0.1mol) in anhydrous THF (50ml) was added dropwise with stirring. After complete addition the mixture was stirred for 0.5h. Diethylphosphorchloridate (17.2g;0.1mol) was then added in one portion and stirring was continued overnight. The mixture was diluted with ether (500ml) and washed with NaOH (10%;3x100ml). The combined ethereal extracts were dried (magnesium sulphate), filtered and concentrated to give 15.0g (49%) yield of 1,1'-biphenyl-4-diethylphosphate.

Analysis

<sup>1</sup>H NMR: 1.35 (t, 6H), 4.25 (m, 4H), 7.40 (m, 9H)

B.

1,1'-biphenyl-4-diethylphosphate (5.0g;0.016mol) in anhydrous ether (15ml) was added under argon, to a stirred mixture of Ni(acac)<sub>2</sub> (0.22g;0.0008mol) and trimethylsilylmethylmagnesium chloride (50ml;1M solution in ether;0.05mol). The mixture was then stirred overnight at room temperature and hydrolysed with dilute HCl. The ether

layer was separated, dried (magnesium sulphate), and evaporated to yield a crude brown solid which was purified on a silica gel column with hexane as the eluent ( $R_f=0.55$ ) to give 0.5g (25%) yield, which was recrystallised from MeOH to give colourless crystals with mp 51-52°C.

### Analysis

$^1\text{H NMR}$ : relative to  $\text{SiMe}_3$ ; 0.00 (s, 9H), 2.07 (s, 2H),  
6.90-7.60 (m, 9H)

IR (KBr): 3055 (m), 3032 (m), aromatic C-H stretching  
2955 (m), aliphatic C-H stretching  
1610 (m), 1599 (m), C=C stretching  
1247 (vs), Si-C stretching of  $\text{SiMe}_3$  group

MS:  $M^+$  240, 73 ( $\text{SiMe}_3^+$ ; base peak), 28 ( $\text{Si}^+$ )

UV (EtOH):  $\lambda_{\text{max}} = 278\text{nm}$  ( $\epsilon=3500$ )

CHN: Calculated for  $\text{C}_{16}\text{H}_{20}\text{Si}$   
Required C 79.93 h 8.38  
Found C 80.04 H 8.42

6. (9H-Fluoren-9-yl)trimethylsilane (Bey and Weyenberg,  
1966)

A solution of *n*-BuLi in hexane (0.15mol) was added under argon during 3h at 25-32°C to fluorene (8.31g;0.05mol) in anhydrous THF (125ml). The resulting orange/brown solution was added via a syringe to rapidly stirring trimethylchlorosilane (97.4g;0.90mol) under argon. The temperature was maintained at 10-20°C during the 1h addition. After complete addition the solvent was removed by distillation. The residue was dissolved in chloroform (150ml) and the LiCl filtered off. The filtrate was concentrated on a rotary evaporator. Crystallisation from EtOH (150ml) gave a crude orange product. Further concentration of EtOH gave additional orange/brown product. The crude product was purified on a silica gel column with hexane as the eluent to give a yield of 5.0g (43%) which was recrystallised from methanol to give a crystalline solid with mp 96-97°C (lit mp 97.5°C; Earborn and Shaw, 1955).

#### Analysis

<sup>1</sup>H NMR:                   relative to SiMe<sub>3</sub>; 0.00 (s,9H), 3.80 (s,1H),  
7.00-7.30 (m,8H)

IR:                       3055 (w), aromatic C-H stretch  
2956 (m), aliphatic C-H stretch  
1606 (w), C=C stretching  
1250 (s), Si-C stretching  
740 (s), 1,2-disubstituted aromatic

UV (EtOH):  $\lambda_{\text{max}} = 296\text{nm}$  ( $\epsilon=6500$ )

MS:  $M^+$  238, 222 (base peak,  $C_{15}H_{14}Si^+$ ), 73 ( $SiMe_3^+$ )

## 7. (9H-Thioxanthen-9-yl)trimethylsilane

A.

Trichlorosilane (28.5g;210mmol) was added dropwise under argon, with stirring, to a mixture of thioxanthone (15.0g;70mmol) and tri-*n*-propylamine (10.1g;70mmol) in anhydrous THF (150ml). After complete addition the reaction mixture was refluxed for 4h and cooled. Excess pentane was added to the reaction mixture to precipitate the amine hydrochloride. The mixture was then filtered and the filtrate was rapidly transferred to a distillation flask. The filtrate was first distilled at atmospheric pressure to remove solvent and then under vacuum with the collecting flask immersed in liquid nitrogen to give 15.0g (64%) of the desired (9-trichlorosilyl)thioxanthene with bp 220°C/2mmHg.

B.

Anhydrous THF (50ml) was added to (9-trichlorosilyl)thioxanthene (15.0g;0.045mol) under argon. MeMgBr (50ml;3M solution in ether;0.150mol) was then added dropwise with stirring. On complete addition the reaction mixture was left stirring overnight. The mixture was then

refluxed for 6h, cooled, and quenched with saturated ammonium chloride solution. It was then extracted with ether, dried ( $\text{MgSO}_4$ ), and concentrated. The white solid product was recrystallised from ethanol to give 8.0g (48%) yield of colourless needles with mp 107-108°C.

### Analysis

$^1\text{H}$  NMR: relative to  $\text{SiMe}_3$ ; 0.00 (s, 9H), 3.70 (s, 1H),  
7.70 (m, 8H)

IR (KBr): 3055 (m), aromatic C-H stretch  
2960 (m), aliphatic C-H stretch  
1589 (m), C=C stretch  
1246 (vs), Si-C stretch of  $\text{SiMe}_3$  group  
744 (vs), 1,2-disubstituted aromatic

UV (EtOH):  $\lambda_{\text{max}} = 280\text{nm}$  ( $\epsilon=4500$ )

MS:  $M^+$  270, 197 (base peak;  $\text{C}_{13}\text{H}_9\text{S}^+$ ), 73 ( $\text{SiMe}_3^+$ )

CHN: Calculated for  $\text{C}_{16}\text{H}_{18}\text{SSi}$   
Required C 71.05 H 6.71  
Found C 72.01 H 7.15

### 8. Tri-n-butyl(phenylmethyl) stannane

This compound was prepared by the method described in

experiment 3, using benzyl chloride (5.5ml;0.048mol), chlorotri-*n*-butylstannane (10.8ml;0.040mol), magnesium turnings (1.25g;0.052mol), and 1,2-dibromoethane (0.5ml) with irradiation of ultrasound for 1h. Bulb to bulb distillation gave 13.0g (86%) yield with bp 141°C/0.5mm (lit bp 105°C/0.2mm; Eaton, 1981).

### Analysis

<sup>1</sup>H NMR: 0.50-1.70 (m,27H), 2.24 (s,2H), 6.72-7.32 (m,5H)

IR: 2956 (s), C-H asymmetric stretch of CH<sub>3</sub> group  
2923 (s), C-H asymmetric stretch of CH<sub>2</sub> group  
2871 (s), C-H symmetric stretch of CH<sub>3</sub> group  
2853 (s), C-H symmetric stretch of CH<sub>2</sub> group  
1599 (m), 1489 (m), 1462 (m), C=C stretching  
753 (s), 696 (s), monosubstituted benzene

MS:

M<sup>+</sup> 382, 380, 378; (<sup>120</sup>Sn, <sup>118</sup>Sn, <sup>116</sup>Sn respectively)  
291,289,287; Sn(*n*-butyl)<sub>3</sub><sup>+</sup> (<sup>120</sup>Sn, <sup>118</sup>Sn, <sup>116</sup>Sn respectively)  
235,233,231; SnH(*n*-butyl)<sub>2</sub><sup>+</sup> (<sup>120</sup>Sn, <sup>118</sup>Sn, <sup>116</sup>Sn respectively)  
177,175,173; Sn(*n*-butyl)<sup>+</sup> (<sup>120</sup>Sn, <sup>118</sup>Sn, <sup>116</sup>Sn respectively)  
121,119,117; SnH<sup>+</sup> (<sup>120</sup>Sn, <sup>118</sup>Sn, <sup>116</sup>Sn respectively)  
91; PhCH<sub>2</sub><sup>+</sup>

UV (EtOH): λ<sub>max</sub> = 265nm (ε=860)

<sup>13</sup>C NMR:

5	4	3	2	1	Sn	a	b	c	d
122.8	128.2	127.0	143.7	18.1		9.4	29.2	27.4	13.8

CHN:

Calculated for C<sub>19</sub>H<sub>34</sub>Sn

Required C 59.87 H 8.99

Found C 60.16 H 9.50

### 9. Tri-*n*-butyl[(4-methylphenyl)methyl]stannane

This compound was prepared by the method described in experiment 3, using  $\alpha$ -bromo-*p*-xylene (12.0g;0.065mol), chlorotri-*n*-butylstannane (21.6ml;0.080mol), magnesium turnings (2.50g;0.104mol), and 1,2-dibromoethane (0.5ml) with irradiation of ultrasound for 1h. Bulb to bulb distillation gave 11.5g (45%) yield with bp 144°C/0.3mm (lit bp 101-105°C; Eaton, 1981).

#### Analysis

<sup>1</sup>H NMR: 0.60-1.50 (m,27H), 2.22 (2 singlets,5H),  
6.60-7.00 (m,4H)

IR: 2955 (s), C-H asymmetric stretch of CH<sub>3</sub> group  
2924 (s), C-H asymmetric stretch of CH<sub>2</sub> group  
2871 (s), C-H symmetric stretch of CH<sub>3</sub> group  
2853 (s), C-H symmetric stretch of CH<sub>2</sub> group

1611 (w), 1507 (s), 1461 (s), C=C stretching  
812 (s), 1,4-disubstituted benzene

MS:

M<sup>+</sup> 396, 394, 392 (<sup>120</sup>Sn, <sup>118</sup>Sn, <sup>116</sup>Sn respectively)  
291, 289, 287; Sn(*n*-butyl)<sub>3</sub><sup>+</sup> (<sup>120</sup>Sn, <sup>118</sup>Sn, <sup>116</sup>Sn respectively)  
235, 233, 231; SnH(*n*-butyl)<sub>2</sub><sup>+</sup> (<sup>120</sup>Sn, <sup>118</sup>Sn, <sup>116</sup>Sn respectively)  
177, 175, 173; Sn(*n*-butyl)<sup>+</sup> (<sup>120</sup>Sn, <sup>118</sup>Sn, <sup>116</sup>Sn respectively)  
121, 119, 117; SnH<sup>+</sup> (<sup>120</sup>Sn, <sup>118</sup>Sn, <sup>116</sup>Sn respectively)  
105, [Me(C<sub>6</sub>H<sub>4</sub>)CH<sub>2</sub><sup>+</sup>]

UV (EtOH):  $\lambda_{\text{max}}$  = 279nm ( $\epsilon=850$ ), 264nm ( $\epsilon=935$ )

<sup>13</sup>C NMR:

6	5	4	3	2	1	Sn	a	b	c	d
20.9	132.1	129.0	127.0	140.4	17.6	9.4	29.2	27.4	13.8	

CHN: Calculated for C<sub>20</sub>H<sub>36</sub>Sn  
Required C 60.78 H 9.18  
Found C 60.92 H 9.28

#### 10. Tri-*n*-butyl[(4-methoxyphenyl)methyl]stannane

This compound was prepared by the method described in experiment 3, using 4-methoxybenzyl chloride (5.0g;0.032mol), chlorotri-*n*-butylstannane (8.7g;0.027mol), magnesium turnings (0.83g;0.035mol), and 1,2-dibromoethane (0.5ml) with irradiation of ultrasound for 3.5h. Bulb to

bulb distillation gave 11.0g (100%) yield with bp 44°C/0.02mm (lit bp 125-126°C/0.1mm; Eaton, 1981).

Analysis

<sup>1</sup>H NMR: 0.50-1.60 (m, 27H), 2.24 (s, 2H), 3.68 (s, 3H), 6.53-6.91 (m, 4H)

IR: 2956 (s), C-H asymmetric stretch of CH<sub>3</sub> group  
2925 (s), C-H asymmetric stretch of CH<sub>2</sub> group  
2871 (s), C-H symmetric stretch of CH<sub>3</sub> group  
2854 (s), C-H symmetric stretch of CH<sub>2</sub> group  
1601 (s), C=C stretching  
1247 (s), Ph-O stretch  
1037 (m), Me-O stretch  
830 (m), 1,4-disubstituted benzene

MS:

M<sup>+</sup> 412, 410, 408; (<sup>120</sup>Sn, <sup>118</sup>Sn, <sup>116</sup>Sn respectively)  
291, 289, 287; Sn(*n*-butyl)<sub>3</sub><sup>+</sup> (<sup>120</sup>Sn, <sup>118</sup>Sn, <sup>116</sup>Sn respectively)  
235, 233, 231; SnH(*n*-butyl)<sub>2</sub><sup>+</sup> (<sup>120</sup>Sn, <sup>118</sup>Sn, <sup>116</sup>Sn respectively)  
177, 175, 173; Sn(*n*-butyl)<sup>+</sup> (<sup>120</sup>Sn, <sup>118</sup>Sn, <sup>116</sup>Sn respectively)  
121; MeO(C<sub>6</sub>H<sub>4</sub>)CH<sub>2</sub><sup>+</sup> (base peak)

UV (EtOH): λ<sub>max</sub> = 281nm (ε=2250), 273nm (ε=2260)

CHN: Calculated for C<sub>20</sub>H<sub>36</sub>OSn  
Required C 67.98 H 9.34

### 11. Trimethyl(phenylmethyl)stannane

Chlorotrimethyltin (5.0g; 0.025mol) in anhydrous THF (30ml) was added dropwise with stirring at room temperature under argon to a solution of benzylmagnesium chloride (12.5ml; 2M solution in THF; 0.025mol). On complete addition the mixture was refluxed for 4h, cooled, and quenched with saturated aqueous  $\text{NH}_4\text{Cl}$  solution. The resultant solution was extracted with ether and the combined organic extracts were dried (magnesium sulphate) and concentrated. Bulb to bulb distillation gave 4.0g (63%) yield with bp  $56^\circ\text{C}/1.4\text{mm}$  (lit bp  $89-90^\circ\text{C}/9\text{mm}$ ; Bullpit et al, 1976).

#### Analysis

$^1\text{H}$  NMR: relative to  $\text{SnMe}_3$ ; 0.00 (s, 9H), 2.20 (s, 2H),  
7.00-7.20 (m, 5H)

IR: 3070 (m), 3022 (s), aromatic C-H stretching  
2979 (s), 2915 (s), aliphatic C-H stretching  
1600 (s), C=C stretch  
754 (s), Sn-C stretch of  $\text{SnMe}_3$  group

MS:

$\text{M}^+$  256, 254, 252 ( $^{120}\text{Sn}$ ,  $^{118}\text{Sn}$ ,  $^{116}\text{Sn}$  respectively)

165, 163, 161;  $\text{Sn}(\text{CH}_3)_3^+$  ( $^{120}\text{Sn}$ ,  $^{118}\text{Sn}$ ,  $^{116}\text{Sn}$  respectively)

91, PhCH<sub>2</sub><sup>+</sup>

UV (EtOH):  $\lambda_{\text{max}} = 273\text{nm}$  ( $\epsilon=700$ )

CHN: Calculated for C<sub>10</sub>H<sub>16</sub>Sn  
Required C 47.12 H 6.33  
Found C 47.15 H 6.34

## 12. Trimethyl(1-naphthalenylmethyl)silane

This compound was prepared by the method described in experiment 3, using 1-bromomethylnaphthalene (2.5g;0.011mol), chlorotrimethylsilane (1.0g;0.009mol), magnesium turnings (0.29g;0.012mol), and 1,2-dibromoethane (0.5ml) with irradiation of ultrasound for 10h. Bulb to bulb distillation gave 1.2g (62%) yield with bp 48°C/0.02mm (lit bp 143°C/11mm; Bock and Alt, 1969).

### Analysis

<sup>1</sup>H NMR: relative to SiMe<sub>3</sub>; 0.00 (s,9H), 3.00 (s,2H),  
7.00-7.80 (m,7H)

IR: 3062 (m), aromatic C-H stretch  
2954 (s), aliphatic C-H stretch  
1594 (m), 1508 (m), C=C stretching  
1249 (s), Si-C stretch of SiMe<sub>3</sub> group  
798 (s), 777 (s), C-H deformation for 1-

substituted naphthalene

MS:  $M^+$  214, 141 ( $NpCH_2^+$ ), 73 ( $SiMe_3^+$ ; base peak)

UV (EtOH):  $\lambda_{max}$  = 321nm ( $\epsilon=700$ ), 287nm ( $\epsilon=6000$ )

CHN: Calculated for  $C_{14}H_{18}Si$

Required C 78.44 H 8.46

Found C 78.48 H 8.64

13. Trimethyl(2-naphthalenylmethyl)silane

This compound was prepared by the method described in experiment 3, using 2-bromomethylnaphthalene (2.5g; 0.011mol), chlorotrimethylsilane (1.0g; 0.009mol), magnesium turnings (0.29g; 0.012mol), and 1,2-dibromoethane (0.5ml) with irradiation of ultrasound for 10h. Recrystallisation (EtOH) gave 1.7g (88%) yield with mp 61°C (lit mp 61°C; Bock and Alt, 1969).

Analysis

$^1H$  NMR: relative to  $SiMe_3$ ; 0.00 (s, 9H), 2.30 (s, 2H), 7.10-7.90 (m, 7H)

IR: 3055 (m), aromatic C-H stretch  
2955 (m), 2892 (m), aliphatic C-H stretching  
1625 (m), 1596 (m), 1501 (m), C=C stretching

865 (s), 825 (s), 743 (s), C-H out of plane deformation for 2-substituted naphthalene

MS:  $M^+$  214, 141 ( $NpCH_2^+$ ), 73 ( $SiMe_3^+$ ; base peak)

UV (EtOH):  $\lambda_{max}$  = 324nm ( $\epsilon=1000$ ), 309nm ( $\epsilon=900$ ), 280nm ( $\epsilon=4800$ )

CHN: Calculated for  $C_{14}H_{18}Si$   
Required C 78.44 H 8.46  
Found C 78.69 H 8.82

#### 14. Tri-*n*-butyl(1-naphthalenylmethyl)stannane

This compound was prepared by the method described in experiment 3, using 1-bromomethylnaphthalene (3.5g;0.016mol), chlorotri-*n*-butylstannane (4.23g;0.013mol), magnesium turnings (0.40g;0.017mol), and 1,2-dibromoethane (0.5ml) with irradiation of ultrasound for 5h. Bulb to bulb distillation gave 3.5g (63%) yield with bp 110°C/0.04mm.

#### Analysis

$^1H$  NMR: 0.60-1.90 (m,27H), 2.80 (s,2H), 7.30-8.20 (m,7H)

IR: 3051 (m), aromatic C-H stretch  
2955 (s), C-H asymmetric stretch of  $CH_3$  group

2922 (s), C-H asymmetric stretch of CH<sub>2</sub> group  
2870 (s), C-H symmetric stretch of CH<sub>3</sub> group  
2852 (s), C-H symmetric stretch of CH<sub>2</sub> group  
1596 (m), 1501 (m), 1462 (m), aromatic C=C  
stretching  
791 (s), 774 (s), 1-substituted naphthalene

MS:

M<sup>+</sup> 432 (<sup>120</sup>Sn)

291, 289, 287; Sn(*n*-butyl)<sub>3</sub><sup>+</sup> (<sup>120</sup>Sn, <sup>118</sup>Sn, <sup>116</sup>Sn respectively)

235, 233, 231; SnH(*n*-butyl)<sub>2</sub><sup>+</sup> (<sup>120</sup>Sn, <sup>118</sup>Sn, <sup>116</sup>Sn respectively)

179, 177, 175; SnH<sub>2</sub>(*n*-butyl)<sup>+</sup> (<sup>120</sup>Sn, <sup>118</sup>Sn, <sup>116</sup>Sn respectively)

141 (base peak) NpCH<sub>2</sub><sup>+</sup>

UV (EtOH):  $\lambda_{\text{max}} = 290\text{nm}$  ( $\epsilon = 7500$ )

CHN: Calculated for C<sub>23</sub>H<sub>36</sub>Sn

Required C 64.06 H 8.42

Found C 63.89 H 8.68

### 15. Tri-*n*-butyl(2-naphthalenylmethyl)stannane

This compound was prepared by the method described in experiment 3, using 2-bromomethylnaphthalene (3.1g; 0.014mol), chlorotri-*n*-butylstannane (4.23g; 0.013mol), magnesium turnings (0.40g; 0.017mol), and 1,2-dibromoethane (0.5ml) with irradiation of ultrasound for 5h. Bulb to bulb distillation gave 4.2g (78%) yield, bp 110°C/0.04mm.

## Analysis

$^1\text{H}$  NMR: 0.50-1.70 (m, 27H), 2.40 (s, 2H), 7.10-8.00 (m, 7H)

IR: 2955 (s), C-H asymmetric stretch of  $\text{CH}_3$  group  
2922 (s), C-H asymmetric stretch of  $\text{CH}_2$  group  
2870 (s), C-H symmetric stretch of  $\text{CH}_3$  group  
2852 (s), C-H symmetric stretch of  $\text{CH}_2$  group  
1629 (m), 1596 (m), 1501 (m), C=C stretching  
850 (m), 815 (m), 744 (m), C-H out of plane deformation for 2-substituted naphthalene

MS:

$\text{M}^+$  432 ( $^{120}\text{Sn}$ )

291, 289, 287;  $\text{Sn}(n\text{-butyl})_3^+$  ( $^{120}\text{Sn}$ ,  $^{118}\text{Sn}$ ,  $^{116}\text{Sn}$  respectively)

235, 233, 231;  $\text{SnH}(n\text{-butyl})_2^+$  ( $^{120}\text{Sn}$ ,  $^{118}\text{Sn}$ ,  $^{116}\text{Sn}$  respectively)

179, 177, 175;  $\text{SnH}_2(n\text{-butyl})^+$  ( $^{120}\text{Sn}$ ,  $^{118}\text{Sn}$ ,  $^{116}\text{Sn}$  respectively)

141; (base peak)  $\text{NpCH}_2^+$

UV (EtOH):  $\lambda_{\text{max}} = 333\text{nm}$  ( $\epsilon=1200$ )

CHN: Calculated for  $\text{C}_{23}\text{H}_{36}\text{Sn}$

Required C 64.06 H 8.42

Found C 65.04 H 9.09

### 16. Trimethyl(2-naphthalenylmethyl)stannane

This compound was prepared by the method described in experiment 3, using 2-bromomethylnaphthalene (6.60g;0.030mol), chlorotrimethylstannane (5.00g;0.025mol), magnesium turnings (0.78g;0.033mol), and 1,2-dibromoethane (0.5ml) with irradiation of ultrasound for 2h. The resultant solid was recrystallised from ethanol to give 3.5g (46%) yield with mp 60°C (lit mp 59-60°C; Bullpit et al, 1976).

### Analysis

<sup>1</sup>H NMR: relative to SnMe<sub>3</sub>; 0.00 (s, 9H), 2.40 (s, 2H), 7.2-7.6 (m, 7H)

IR: 3048 (m), aromatic C-H stretch  
2981 (m), 2917 (m), aliphatic C-H stretching  
1626 (m), 1595 (s), C=C stretching  
860 (m), 825 (s), 719 (m), 2-substituted naphthalene

MS:

M<sup>+</sup> 306, 304, 302 (<sup>120</sup>Sn, <sup>118</sup>Sn, <sup>116</sup>Sn respectively)  
165,163,161; Sn(CH<sub>3</sub>)<sub>3</sub><sup>+</sup> (<sup>120</sup>Sn, <sup>118</sup>Sn, <sup>116</sup>Sn respectively)  
141, NpCH<sub>2</sub><sup>+</sup>

UV (MeOH): λ<sub>max</sub> = 335nm (ε=1000), 318nm (ε=1000)

CHN:	Calculated for C <sub>14</sub> H <sub>18</sub> Sn		
	Required	C 55.13	H 5.95
	Found	C 55.48	H 5.90

### 17. Trimethyl(1-pyrenylmethyl)silane

A.

Trichlorosilane (17.7g;0.130mol) was added dropwise with stirring to a mixture of 1-pyrenecarboxaldehyde (10.0g;0.043mol) and tri-*n*-propylamine (6.2g;0.043mol) in anhydrous THF (50ml). On complete addition the mixture was refluxed for 2h, cooled, and excess pentane was added. The precipitated amine hydrochloride was filtered off and the filtrate was transferred rapidly and distilled, firstly at atmospheric pressure to remove undesired pentane/THF/trichlorosilane and then under vacuum to obtain the desired product. This was collected in a flask immersed in liquid nitrogen to give 6.0g (40%) yield of trichloro(1-methylpyrene)silane with bp 220°C/3mm.

B.

MeMgBr (20ml;3M solution in ether;0.06mol) was added dropwise with stirring under argon to trichloro(1-methylpyrene)silane (6.0g;0.017mol) in anhydrous ether (50ml). The mixture was stirred overnight and then refluxed for 3h. The reaction mixture was cooled and then quenched

with saturated aqueous  $\text{NH}_4\text{Cl}$  solution, extracted with ether, dried (magnesium sulphate), and concentrated to give a pale yellow solid. The crude product was recrystallised (EtOH) to give 1.8g (37%) of pale yellow crystals with mp 69-70°C.

### Analysis

$^1\text{H}$  NMR: relative to  $\text{SiMe}_3$ ; 0.00 (s, 9H), 2.70 (s, 2H), 7.40-8.10 (m, 9H)

IR: 3039 (m), aromatic C-H stretch  
2953 (m), aliphatic C-H stretch  
1602 (m), C=C stretch  
1247 (s), Si-C stretch of  $\text{SiMe}_3$  group

MS:  $\text{M}^+$  288, 215 ( $\text{pyreneCH}_2^+$ ), 73 ( $\text{SiMe}_3^+$ ; base peak)

UV (MeOH):  $\lambda_{\text{max}}$  = 379nm ( $\epsilon=2400$ ), 358nm ( $\epsilon=6200$ ), 347nm ( $\epsilon=17800$ ), 331nm ( $\epsilon=17600$ )

CHN: Calculated for  $\text{C}_{20}\text{H}_{20}\text{Si}$   
Required C 83.28 H 6.99  
Found C 83.52 H 7.54

### 18. Trimethyl-2-propenylsilane

Magnesium turnings (2.60g;0.11mol) and anhydrous ether

(30ml) were placed under argon. A solution of allyl bromide (8.60ml;0.10mol) in anhydrous ether (30ml) was added dropwise with stirring and on complete addition the mixture was refluxed for 1.5h. On cooling chlorotrimethylsilane (10.90g;0.10mol) was added dropwise with stirring and after complete addition the mixture was refluxed for a further 1.5h. The reaction mixture was then cooled and quenched with cold saturated ammonium chloride solution. The solution was extracted with ether, dried (magnesium sulphate), and concentrated. Distillation of the crude product gave 4.8g (42%) yield with bp 86°C (lit bp 86-87°C; Koizumi et al, 1989).

#### Analysis

<sup>1</sup>H NMR: Relative to SiMe<sub>3</sub>; 0.00 (s,9H), 1.50 (d,2H), 4.80 (d,2H), 5.75 (m,1H)

IR: 3079 (m), C-H stretch of =CH<sub>2</sub> group  
2957 (s), 2900 (m), aliphatic C-H stretching  
1630 (s), C=C stretch  
1251 (s), Si-C stretch of SiMe<sub>3</sub> group  
894 (s), =CH<sub>2</sub> out of plane bending

MS: M<sup>+</sup> 114, 73 (SiMe<sub>3</sub><sup>+</sup>; base peak), 41 (C<sub>3</sub>H<sub>5</sub><sup>+</sup>)

UV (MeOH):  $\lambda_{\max}$  = 271nm ( $\epsilon$ =100), 213nm ( $\epsilon$ =1150)

## 19. Triphenyl-2-propenylsilane

Triphenylchlorosilane (13.25g;0.045mol) dissolved in anhydrous THF (30ml) was added dropwise with stirring under argon to allylmagnesium bromide (50ml;1M solution in Et<sub>2</sub>O;0.050mol). After stirring at room temperature overnight the reaction mixture was quenched by pouring into cold ammonium chloride solution. The separated organic layer was dried (sodium sulphate) and the solvent was evaporated to give 10g (74%) of triphenyl-2-propenylsilane which was recrystallised from ethanol with mp 81-82°C (lit mp 84-84°C; Henry and Noltes, 1960).

### Analysis

<sup>1</sup>H NMR:            2.40 (d,2H), 4.90 (d,2H), 5.90 (m,1H), 7.10-  
                         7.70 (m,15H)

IR:                    1626 (m), C=C stretch  
                         1426 (s), 1112 (s), Ph-Si stretching  
                         893 (s), =CH<sub>2</sub> out of plane bending  
                         733 (s), 699 (s), monosubstituted benzene

UV (EtOH):         $\lambda_{max} = 270\text{nm}$  ( $\epsilon=650$ )

MS:                    M<sup>+</sup> 300

CHN:                    Calculated for C<sub>21</sub>H<sub>20</sub>Si

Required	C 83.94	H 6.71
Found	C 83.87	H 6.75

## 20. Tri-*n*-butyl-2-propenylstannane

Magnesium turnings (3.6g;0.14mol) and anhydrous ether (50ml) were placed under argon. A solution of allyl bromide (8ml;0.09mol) in anhydrous ether (15ml) was placed in the dropping funnel. A 1-2ml portion of the allyl bromide solution was added into the reaction flask. A temperature rise and cloudiness indicated that the reaction had commenced. The remainder of the allylbromide solution was added dropwise with continued stirring at such a rate as to maintain a gentle reflux. After complete addition which required approximately 1.5h, the mixture was refluxed for a further 1.5h. During reflux the dropping funnel was charged with bis(tri-*n*-butyltin)oxide (18g;0.03mol) in anhydrous ether (30ml). After reflux, heating was stopped and the bis(tri-*n*-butyltin)oxide solution was added at such a rate as to maintain the temperature between 36-38°C. The reaction mixture was refluxed for 1.5h and then stirred at room temperature overnight. The reaction mixture was cooled in an ice bath and quenched with saturated ammonium chloride solution. The supernatant solution was decanted through glass wool on to 20g of ice in a separating funnel. The residual solids were washed with three portions of hexane and the washes were decanted into the separating funnel.

After the phases were separated the aqueous phase was washed with an additional portion of hexane. The combined organic extracts were washed with saturated ammonium chloride solution (50ml) and then with brine (50ml). The organic layer was dried (magnesium sulphate) filtered, and concentrated. Bulb to bulb distillation gave 11.0g (56%) yield with bp 50°C/0.02mm (lit bp 89°C/0.3mm; Schwartz and Post, 1964).

### Analysis

<sup>1</sup>H NMR: 0.50-1.70 (m, 29H), 5.00-5.60 (m, 3H)

IR: 3076 (w), C-H stretch of =CH<sub>2</sub> group  
2956 (s), C-H asymmetric stretch of CH<sub>3</sub> group  
2924 (s), C-H asymmetric stretch of CH<sub>2</sub> group  
2871 (s), C-H symmetric stretch of CH<sub>3</sub> group  
2854 (s), C-H symmetric stretch of CH<sub>2</sub> group  
1620 (m), C=C stretch  
877 (m), =CH<sub>2</sub> out of plane bending

UV (EtOH):  $\lambda_{\text{max}} = 240\text{nm}$  ( $\epsilon=5000$ )

MS:

M<sup>+</sup> 332, 330, 328 (<sup>120</sup>Sn, <sup>118</sup>Sn, <sup>116</sup>Sn respectively)  
291, 289, 287; Sn(*n*-butyl)<sub>3</sub><sup>+</sup> (<sup>120</sup>Sn, <sup>118</sup>Sn, <sup>116</sup>Sn respectively)  
235, 233, 231; SnH(*n*-butyl)<sub>2</sub><sup>+</sup> (<sup>120</sup>Sn, <sup>118</sup>Sn, <sup>116</sup>Sn respectively)  
177, 175, 173; Sn(*n*-butyl)<sup>+</sup> (<sup>120</sup>Sn, <sup>118</sup>Sn, <sup>116</sup>Sn respectively)

121, 119, 117; SnH<sup>+</sup> (<sup>120</sup>Sn, <sup>118</sup>Sn, <sup>116</sup>Sn respectively)

41; C<sub>3</sub>H<sub>5</sub><sup>+</sup>

<sup>13</sup>C NMR:

3	2	1	Sn	a	b	c	d
109.1	138.2	16.2		9.1	29.1	27.4	13.7

### 21. 2-butenyltri-*n*-butylstannane

This compound was prepared by the method described in experiment 3, using crotylchloride (4.34g; 4.70ml; 0.048mol), chlorotri-*n*-butylstannane (13.0g; 10.8ml; 0.040mol), magnesium turnings (1.25g; 0.052mol), and 1,2-dibromoethane (0.5ml) with irradiation of ultrasound for 2h. Bulb to bulb distillation gave 9.5g (69%) yield of the trans isomer with bp 90°C/0.05mm.

#### Analysis

<sup>1</sup>H NMR: 0.40-2.10 (m, 32H), 4.90-5.70 (m, 2H)

IR: 2959 (s), C-H asymmetric stretch of CH<sub>3</sub> group  
2923 (s), C-H asymmetric stretch of CH<sub>2</sub> group  
2871 (s), C-H symmetric stretch of CH<sub>3</sub> group  
2854 (s), C-H symmetric stretch of CH<sub>2</sub> group  
1594 (m), C=C stretching  
1462 (m), 1376 (m), C-H deformation

UV (EtOH):  $\lambda_{\text{max}} = 264\text{nm}$  ( $\epsilon=70$ )

MS:  $M^+$  346 ( $^{120}\text{Sn}$ )

291, 289, 287;  $\text{Sn}(n\text{-butyl})_3^+$  ( $^{120}\text{Sn}$ ,  $^{118}\text{Sn}$ ,  $^{116}\text{Sn}$  respectively)

235, 233, 231;  $\text{SnH}(n\text{-butyl})_2^+$  ( $^{120}\text{Sn}$ ,  $^{118}\text{Sn}$ ,  $^{116}\text{Sn}$  respectively)

177, 175, 173;  $\text{Sn}(n\text{-butyl})^+$  ( $^{120}\text{Sn}$ ,  $^{118}\text{Sn}$ ,  $^{116}\text{Sn}$  respectively)

121, 119, 117;  $\text{SnH}^+$  ( $^{120}\text{Sn}$ ,  $^{118}\text{Sn}$ ,  $^{116}\text{Sn}$  respectively)

55;  $\text{C}_4\text{H}_7^+$

## 22. Tri-*n*-butyl (2-methyl-2-propenyl) stannane

This compound was prepared by the method described in experiment 3, using 3-chloro-2-methylpropene (4.34g; 4.70ml; 0.048mol), chlorotri-*n*-butylstannane (13.0g; 10.8ml; 0.040mol), magnesium turnings (1.25g; 0.052mol), and 1,2-dibromoethane (0.5ml) with irradiation of ultrasound for 2h. Bulb to bulb distillation gave 8.5g (62%) yield with bp 89°C/0.10mm (lit bp 121-122°C/4mm; Naruta, 1980).

### Analysis

$^1\text{H}$  NMR: 0.50-2.10 (m, 35H), 5.20 (t, 1H)

IR: 3072 (m), C-H stretch of =CH<sub>2</sub> group  
2955 (s), C-H asymmetric stretch of CH<sub>3</sub> group  
2921 (s), C-H asymmetric stretch of CH<sub>2</sub> group  
2871 (s), C-H symmetric stretch of CH<sub>3</sub> group

2853 (s), C-H symmetric stretch of CH<sub>2</sub> group  
 1627 (m), C=C stretching  
 1461 (m), 1375 (m), C-H deformation  
 860 (m), CH<sub>2</sub> out of plane deformation

UV (EtOH):  $\lambda_{\max} = 245\text{nm}$  ( $\epsilon=6000$ )

MS:

M<sup>+</sup> 346 (<sup>120</sup>Sn)  
 291, 289, 287; Sn(*n*-butyl)<sub>3</sub><sup>+</sup> (<sup>120</sup>Sn, <sup>118</sup>Sn, <sup>116</sup>Sn respectively)  
 235, 233, 231; SnH(*n*-butyl)<sub>2</sub><sup>+</sup> (<sup>120</sup>Sn, <sup>118</sup>Sn, <sup>116</sup>Sn respectively)  
 179, 177, 175; SnH<sub>2</sub>(*n*-butyl)<sup>+</sup> (<sup>120</sup>Sn, <sup>118</sup>Sn, <sup>116</sup>Sn respectively)  
 121, 119, 117; SnH<sup>+</sup> (<sup>120</sup>Sn, <sup>118</sup>Sn, <sup>116</sup>Sn respectively)  
 55; CH<sub>2</sub>=C(CH<sub>3</sub>)CH<sub>2</sub><sup>+</sup>

<sup>13</sup>C NMR:

4	3	2	1	Sn	a	b	c	d
25.0	105.6	146.3	20.6		9.4	29.1	27.4	13.7

### 23. Tri-*n*-butyl(3-methyl-2-butenyl) stannane

This compound was prepared by the method described in experiment 3, using 1-chloro-3-methyl-2-butene (5.0g; 0.048mol), chlorotri-*n*-butylstannane (13.0g; 10.8ml; 0.040mol), magnesium turnings (1.25g; 0.052mol), and 1,2-dibromoethane (0.5ml) with irradiation of ultrasound for 2h. Bulb to bulb distillation

gave 11.0g (77%) yield with bp 93°C/0.01mm (lit bp 114-116°C/1mm; Naruta, 1980).

### Analysis

<sup>1</sup>H NMR: 0.70-1.70 (m, 35H), 5.30 (m, 1H)

IR: 2957 (s), C-H asymmetric stretch of CH<sub>3</sub> group  
2921 (s), C-H asymmetric stretch of CH<sub>2</sub> group  
2871 (s), C-H symmetric stretch of CH<sub>3</sub> group  
2852 (s), C-H symmetric stretch of CH<sub>2</sub> group  
1659 (w), C=C stretching  
1462 (m), 1375 (m), C-H deformation

MS:

M<sup>+</sup> 360, 358, 356 (<sup>120</sup>Sn, <sup>118</sup>Sn, <sup>116</sup>Sn respectively)  
291, 289, 287; Sn(*n*-butyl)<sub>3</sub><sup>+</sup> (<sup>120</sup>Sn, <sup>118</sup>Sn, <sup>116</sup>Sn respectively)  
235, 233, 231; SnH(*n*-butyl)<sub>2</sub><sup>+</sup> (<sup>120</sup>Sn, <sup>118</sup>Sn, <sup>116</sup>Sn respectively)  
179, 177, 175; SnH<sub>2</sub>(*n*-butyl)<sup>+</sup> (<sup>120</sup>Sn, <sup>118</sup>Sn, <sup>116</sup>Sn respectively)  
121, 119, 117; SnH<sup>+</sup> (<sup>120</sup>Sn, <sup>118</sup>Sn, <sup>116</sup>Sn respectively)  
69; C<sub>5</sub>H<sub>9</sub><sup>+</sup>

UV (EtOH): λ<sub>max</sub> = 263nm (ε=160)

<sup>13</sup>C NMR:

5 4 3 2 1 Sn a b c d

10.7 26.0 125.3 123.0 17.4 9.5 29.3 27.4 13.7

#### 24. Tri-*n*-butyl(3-phenyl-2-propenyl)stannane

Cinnamyl chloride (7.3g;0.048mol) in anhydrous THF (15ml) was added dropwise under argon with external irradiation of ultrasound to a mixture of chlorotri-*n*-butylstannane (13g;10.8ml;0.040mol), magnesium turnings (0.25g;0.052mol), and 1,2-dibromoethane (0.5ml) in anhydrous THF (20ml). After 2h irradiation the reaction was quenched with saturated aqueous ammonium chloride solution. The resultant solution was washed with ether and the combined organic extracts were dried (magnesium sulphate) and evaporated. Bulb to bulb distillation gave 7.3g (44%) yield of the trans isomer with bp 162°C/0.5mm (lit bp 163-166/0.4mm; Naruta, 1980).

#### Analysis

<sup>1</sup>H NMR: 0.70-2.10 (m,29H), 4.20 (d,2H), 7.30 (s,5H)

IR: 2957 (s), C-H asymmetric stretch of CH<sub>3</sub> group  
2921 (s), C-H asymmetric stretch of CH<sub>2</sub> group  
2871 (s), C-H symmetric stretch of CH<sub>3</sub> group  
2852 (s), C-H symmetric stretch of CH<sub>2</sub> group  
1640 (m), C=C stretching of allyl group  
1600 (m), 1496 (m), C=C stretching (aromatic)  
957 (s), *trans* CH=CH

UV (MeOH):  $\lambda_{\max} = 268\text{nm}$

MS:  $M^+ = 408$  ( $^{120}\text{Sn}$ )

291, 289, 287;  $\text{Sn}(n\text{-butyl})_3^+$  ( $^{120}\text{Sn}$ ,  $^{118}\text{Sn}$ ,  $^{116}\text{Sn}$  respectively)

235, 233, 231;  $\text{SnH}(n\text{-butyl})_2^+$  ( $^{120}\text{Sn}$ ,  $^{118}\text{Sn}$ ,  $^{116}\text{Sn}$  respectively)

179, 177, 175;  $\text{SnH}_2(n\text{-butyl})^+$  ( $^{120}\text{Sn}$ ,  $^{118}\text{Sn}$ ,  $^{116}\text{Sn}$  respectively)

121, 119, 117;  $\text{SnH}^+$  ( $^{120}\text{Sn}$ ,  $^{118}\text{Sn}$ ,  $^{116}\text{Sn}$  respectively)

## 25. [(4-ethenylphenyl)methyl]trimethylsilane

Lithium diisopropylamide (10.7g; 0.1 mol) was obtained as a solid and transferred to a reaction vessel under nitrogen in an Atmosbag (Aldrich). THF (80ml) was added under nitrogen and the mixture was stirred for a few minutes. Then 4-methylstyrene (11.8g; 0.1 mol) was added dropwise, when the mixture turned yellow. After complete addition chlorotrimethylsilane (10.9g; 0.1 mol) in anhydrous THF (60ml) was dropped slowly into the stirred mixture for 3h at room temperature. On complete addition the mixture was stirred for a further 1h. The THF was evaporated and the residue was distilled to give 6.7g (35%) yield with bp  $55^\circ\text{C}/0.3\text{mm}$  (lit bp  $48^\circ\text{C}/0.15\text{mm}$ ; Reynolds et al, 1977).

### Analysis

$^1\text{H}$  NMR: relative to  $\text{SiMe}_3$ ; 0.00 (s, 9H), 2.20 (s, 2H),

5.00-5.70 (m, 2H), 6.40-6.70 (m, 1H), 7.00-7.30  
(m, 4H)

IR: 3088 (w), C-H stretching of =CH<sub>2</sub> group  
3050 (w), C-H stretching of =CH- group  
2956 (s), C-H asymmetric stretch of CH<sub>3</sub> group  
  
2899 (m), C-H symmetric stretch of CH<sub>3</sub> group  
1629 (m), 1608 (m), C=C stretching (lit 1633  
and 1608; Reynolds et al, 1977)  
1252 (vs), Si-C stretch of SiMe<sub>3</sub> group

MS: M<sup>+</sup> 190, 117 (CH<sub>2</sub>=CH-C<sub>6</sub>H<sub>4</sub>CH<sub>2</sub><sup>+</sup>), 73 (SiMe<sub>3</sub><sup>+</sup>; base  
peak)

## 26. Hexamethyldisilane

To a suspension of lithium in oil (58.14g; 30% dispersion containing 1% sodium; 2.50mol) was added anhydrous THF (98ml). The resulting mixture was degassed with nitrogen through a gas dispersion tube for 15min. The condenser was charged with dry ice/acetone. A slow stream of nitrogen was passed through the reaction mixture and chlorotrimethylsilane (161.2ml; 1.25mol) was added in one portion via a funnel. The reaction mixture was stirred at room temperature for 15min and then refluxed for 8h. Diatomaceous earth was added to the cooled reaction mixture and the resultant mixture was filtered through the

additional diatomaceous earth. The filter cake was washed well with ether (unreacted lithium was destroyed by cautious addition of methanol prior to discarding the filter cake.) The combined filtrate and ether washings were washed with water, dried with magnesium sulphate, and decanted into a flask fitted with a receiver cooled in a bath of dry ice/acetone. The mixture was distilled at 160°C (bath temperature) and atmospheric pressure until the mineral oil residue was shown to be free of product by glc analysis.

### Analysis

<sup>1</sup>H NMR:            0.05 (s)

IR:                    2952 (vs), C-H asymmetric stretch  
                         2894 (s), C-H symmetric stretch  
                         1246 (vs), Si-C stretch of SiMe<sub>3</sub> group  
                         834 (s), Si-C stretch of SiMe<sub>3</sub> group

UV (MeOH):         $\lambda_{\max}$  = 270nm ( $\epsilon=50$ ), 209nm ( $\epsilon=500$ )

### 27. Trimethyl[(2-naphthalenyloxy)methyl]silane

Dimethylsulphoxide (100ml; anhydrous) was added to NaH (4.0g; 60% in oil; 0.1mol; obtained by washing with anhydrous ether [3 times 50ml] under argon). To this suspension was added 2-naphthol (14.4g; 0.1mol) in anhydrous DMSO (100ml)

and the mixture was stirred at room temperature overnight. Then chloromethyltrimethylsilane (13.9ml; 0.1mol) was added and stirring was continued for 8h. After hydrolysis with water and extraction with ether, the ether layer was washed several times with water, dried ( $\text{MgSO}_4$ ), and concentrated. Recrystallisation of the residue from ethanol gave 14.0g (61%) yield with mp  $35^\circ\text{C}$ .

### Analysis

$^1\text{H}$  NMR: relative to  $\text{SiMe}_3$ ; 0.00 (s, 9H), 3.40 (s, 2H), 6.95-7.40 (m, 7H)

IR: 3059 (s), aromatic C-H stretch  
2957 (s), 2895 (s), 2820 (m), aliphatic C-H stretching  
1250 (s), Si-C stretch of  $\text{SiMe}_3$  group  
1118 (s), C-O stretch

MS:  $\text{M}^+$  230, 141 (base peak;  $\text{C}_{11}\text{H}_9^+$ ), 73 ( $\text{SiMe}_3^+$ )

UV (EtOH):  $\lambda_{\text{max}} = 325\text{nm}$  ( $\epsilon=1600$ )

### 28. Diphenyliodonium hexafluorophosphate

(Crivello and Lam, 1978; Crivello and Lam, 1979)

A mixture of  $\text{KIO}_3$  (100g; 0.46 mol), acetic anhydride (200

ml), and benzene (90 ml; 1.0 mol), was placed into a flask equipped with a mechanical stirrer and a condenser and cooled to  $-5^{\circ}\text{C}$  (dry ice/acetone). Then conc.  $\text{H}_2\text{SO}_4$  (70 ml) was added dropwise with stirring over a period of 3h during which time the temperature was maintained at  $-5^{\circ}\text{C}$ . When the addition was complete the mixture was stirred for a further 2.5h at  $-5^{\circ}$  to  $0^{\circ}\text{C}$  and then allowed to reach room temperature and left standing overnight. Distilled water (400 ml) was slowly added to hydrolyse the remaining acetic anhydride. Then a slight excess of  $\text{KPF}_6$  in water (200 ml) was added and the mixture was stirred for 1h to complete the double decomposition. The organic layer was separated and the aqueous layer was washed with benzene (2 x 100ml). The organic layers were combined and the product was precipitated by the addition of ether, filtered off, and recrystallised twice from IPA to give 49.0g (25%) yield with mp  $191-192^{\circ}\text{C}$ .

### Analysis

$^1\text{H}$  NMR: 7.60-8.40 (m)

IR: 3095 (m), 3058 (m), aromatic C-H stretching  
1580 (m), 1564 (s), C=C stretching  
741 (s), 700 (w), monosubstituted benzene

UV (EtOH):  $\lambda_{\text{max}} = 266\text{nm}$  ( $\epsilon=2400$ )

MS: 204 (PhI<sup>+</sup>), 127 (I<sup>+</sup>), 77 (C<sub>6</sub>H<sub>5</sub><sup>+</sup>)

CHN: Calculated for C<sub>12</sub>H<sub>10</sub>F<sub>6</sub>IP

Required C 33.83 H 2.37

Found C 33.59 H 2.38

## 29. Triphenylsulphonium hexafluorophosphate

(Crivello and Lam, 1978)

A mixture of diphenyliodonium hexafluorophosphate (10.15g; 0.025 mol), diphenylsulphide (4.66g; 0.025 mol), and copper (II) benzoate (0.2g; 0.0006 mol) was heated with stirring under argon for 3h (oil bath temperature 120°C). On cooling the crystalline material was collected by filtration and washed several times with ether to remove iodobenzene and then air-dried. The fawn coloured crystals were recrystallised from 95% ethanol/water to give 6.1g (60%) yield of colourless needles with mp 193-194°C.

### Analysis

<sup>1</sup>H NMR: 7.85 (s)

IR: 3099 (w), aromatic C-H stretch

1585 (w), C=C stretch

752 (s), 704 (w), monosubstituted benzene

UV (EtOH):  $\lambda_{\max}$  = 275nm ( $\epsilon=2900$ ), 268nm ( $\epsilon=3900$ )

MS: 186 ( $\text{Ph}_2\text{S}^+$ ), 77 ( $\text{C}_6\text{H}_5^+$ ), 32 ( $\text{S}^+$ )

CHN: Calculated for  $\text{C}_{18}\text{H}_{15}\text{F}_6\text{PS}$

Required	C	52.94	H	3.70
----------	---	-------	---	------

Found	C	53.17	H	3.84
-------	---	-------	---	------

## 2.8 References

- Bach, R.D., and Scherr, P.A., (1973). *Tet.Lett.*, 1099
- Benkesser, R.A., and Smith, W.E., (1969). *J.Am.Chem.Soc.*,  
91, 1556
- Benkeser, R.A., Gaul, J.M., and Smith, W.E., (1969).  
*J.Am.Chem.Soc.*, 91, 3666
- Bey, A.E., and Weyenberg, D.R., (1966). *J.Org.Chem.*, 31,  
2036
- Bock, H., and Alt, H., (1969). *Chem.Ber.*, 102, 1534
- Bock, H., Mollère, P., Becker, G., and Fritz, G., (1972).  
*J.Organomet.Chem.*, 46, 89
- Borg, R.M., and Mariano, P.S., (1986). *Tet.Lett.*, 27, 2821
- Boschi, R., Lappert, M.F., Pedley, J.B., Schmidt, W., and  
Wilkins, B.T., (1973). *J.Organomet.Chem*, 50, 69
- Bowser, R., & Davidson, R.S., (1992) 'Current Trends in  
*Sonochemistry*', Royal Society of Chemistry, Ed. G.J. PRice,  
50-58
- Bullpitt, M., Kitching, W., Adcock, W., and Doddrell, D.,  
(1976). *J.Organomet.Chem.*, 116, 187

Butcher, E., Rhodes, C.J., Standing, M., Davidson, R.S., and Bowser, R., (1992). *J.Chem.Soc., Perkin II*, 1469

Bygden, A., (1912). *Berichte*, **45**, 707

Calas, R., and Dunogués, J., (1976). *J.Organomet.Chem.Rev.*, **2**, 277

Chan, T.H., and Fleming, I., (1979). *Synthesis*, 761

Chen, S., Ullrich, J.W., and Mariano, P.S., (1983). *J.Am.Chem.Soc.*, **105**, 6160

Cohen, S.G., Parola, A.H., and Parsons, G.H., (1973). *Chem.Rev.*, **73**, 141

Colvin, E., (1981). "Silicon in Organic Synthesis", Butterworths, London

Crivello, J.V., and Lam, J.H.W., (1978). *J.Org.Chem.*, **43**, 3055

Crivello, J.V., and Lam, J.H.W., (1979). *J.Polym.Sci., Polym.Chem.Edn.*, **17**, 977

Davidson, R.S., (1975). "Molecular Association", (ed) Foster, R., Academic Press, London, **1**, 216

Davidson, R.S., and Trethewey, K.R., (1975). *Chem.Commun.*,

Davidson, R.S., (1983). "Advances in Physical Organic Chemistry", (eds.) Bethel, D., and Gold, V., Academic Press, London, 19, 1

Davies, A.G., Roberts, B.P., and Smith, J.M., (1970). *Chem. Commun.*, 557

Davies, A.G., Roberts, B.P., and Smith, J.M., (1972). *J.Chem.Soc., Perkin II*, 2221

Davies, A.G., (1977). *Proceedings A.M.P.E.R.E. Colloq. CNRS, Organic Free Radicals, Aix-en-Provence*

Dinnocenzo, J.P., Farid, S., Goodman, J.L., Gould, I.R., Todd, W.P., and Mattes, S.L., (1989). *J.Am.Chem.Soc.*, 111, 8973

Eaborn, C., and Parker, S.H., (1955). *J.Chem.Soc.*, 126

Eaborn, C., and Shaw, R.A., (1955). *J.Chem.Soc.*, 1420

Eaborn, C., (1956). *J.Chem.Soc.*, 4858

Eaton, D.F., (1979). *Photog.Sci.Eng.*, 23, 150

Eaton, D.F., (1980a). *J.Am.Chem.Soc.*, 102, 3278

- Eaton, D.F., (1980b). *J.Am.Chem.Soc.*, **102**, 3280
- Eaton, D.F., (1981). *J.Am.Chem.Soc.*, **103**, 7235
- Egorov, Yu.P., Leites, L.A., Tolstikova, N.G., and Tschernyshev, E.A., (1961). *Izv.Akad.Nauk USSR, Ser.Khim.*, 445
- Evans, S., Green, J.C., Joachim, P.J., Orchard, A.F., Turner, D.W., and Maier, J.P., (1979). *J.Chem.Soc., Faraday Trans.2*, **68**, 905
- Gatechair, L.R., and Pappas, S.P., (1983). *ACS Symposium Series*, **212**, 173
- George, M.V., Peterson, D.J., and Gilman, H., (1960). *J.Am.Chem.Soc.*, **82**, 403
- Hageman, H.J., (1985). *Progress in Organic Coatings*, **13**, 123
- Hanstein, W., Berwin, H.J., and Traylor, T.G., (1970a). *J.Amer.Chem.Soc.*, **92**, 829
- Hanstein, W., Berwin, H.J., and Traylor, T.G., (1970b). *J.Amer.Chem.Soc.*, **92**, 7476
- Hauser, C.R., and Hance, C.R., (1951). *J.Am.Chem.Soc.*, **73**, 5846

Hayashi, T., Katsuro, Y., Okamoto, Y., and Kumada, M., (1981). *Tet.Lett.*, **22**, 4449

Henry, M.C., and Noltes, J.G., (1960). *J.Am.Chem.Soc.*, **82**, 555

Hilinski, E.F., Huppert, D., Kelley, D.F., Milton, S.V., and Rentzepis, P.M., (1984). *J.Amer.Chem.Soc.*, **106**, 1951

Hosomi, A., and Traylor, T.G., (1975). *J.Amer.Chem.Soc.*, **97**, 3682

Hudrilik, P.F., Waugh, M.A., & Hudrilik, A.M., (1984) *J. Organomet. Chem.*, **271**, 69

Johnston, L.J., and Scaiano, J.C., (1985). *J.Amer.Chem.Soc.*, **107**, 6368

Ketley, A.D., and Tsao, J-H, (1979). *J.Rad.Curing*, **22**

Kira, M., Yoshida, H., and Sakurai, H., (1985). *J.Amer.Chem.Soc.*, **107**, 7767

Koizumi, T., Fuchigami, T., and Nonaka, T., (1989). *Bull.Chem.Soc.Jpn.*, **62**, 219

Kyushin, S., Nakadaira, Y., & Ohashi, M., (1990) *Chem.Letts.*, 2191

Lan, A.J.Y., Quillen, S.L., Heuckeroth, R.O., and Mariano, P.S., (1987). *J.Am.Chem.Soc.*, **106**, 6439

Lan, A.J.Y., Heuckeroth, R.O., and Mariano, P.S., (1984). *J.Am.Chem.Soc.*, **109**, 2738

Leites, L.A., (1963). *Izv.Akad.Nauk USSR, Ser.Khim.*, 1525

Lyons, A.R., and Symons, M.C.R., (1971). *Chem.Commun.*, 1068

Maruyama, K., Imahori, H., Osuka, A., Takuwa, A., and Tagawa, H., (1986). *Chem.Lett.*, 1719

Maruyama, K., and Imahori, H., (1989). *Bull.Chem.Soc.Jpn.*, **62**, 816

Mizuno, K., Ikeda, M., and Otsuji, Y., (1985a). *Tet.Lett.*, **26**, 461

Mizuno, K., Terasaka, K., Ikeda, M., and Otsuji, Y., (1985b). *Tet.Lett.*, **26**, 5819

Mizuno, K., Toda, S., and Otsuji, Y., (1987). *Chem.Lett.*, 203

Mizuno, K., Terasaka, K., Yasueda, M., and Otsuji, Y., (1988a). *Chem.Lett.*, 145

Mizuno, K., Ikeda, M., and Otsuji, Y., (1988b). *Chem.Lett.*,

- Mizuno, K., Nakanishi, K., and Otsuji, Y., (1988c).  
*Chem.Lett.*, 1833
- Moore, C.J., and Kitching, W., (1973). *J.Organomet.Chem.*,  
59, 225
- Naruta, Y., (1980). *J.Am.Chem.Soc.*, 102, 3774
- Naruta, Y., Nishigaichi, Y, and Maruyama, K., (1986).  
*Chem.Lett.*, 1857
- Nesmeyanov, A.N., and Kritskaya, I.I., (1958).  
*Dokl.Akad.Nauk SSSR*, 121, 447
- Neumann, W.P., Niermann, H., and Sommer, R., (1961).  
*Angew.Chem.*, 73, 768
- Ohga, K., and Mariano, P.S., (1982). *J.Am.Chem.Soc.*, 104,  
617
- Petrov, A.D., Egorov, Yu.P., Mironov V.F., Nikishkin, G.I.,  
and Bulgakova, A.A., (1956). *Izv.Akad.Nauk USSR, Ser.Khim.*,  
50
- Pitt, C.G., (1970). *J.Organomet.Chem.*, 23, C35
- Pitt, C., and Bock, H., (1972). *J.Chem.Soc., Chem.Commun.*,

Reynolds, W.F., Hamer, G.K., and Bassindale, A.R., (1977).  
*J.Chem.Soc., Perkin II*, 971

Roberts, R.M.G., and Kaissi, F.El, (1968).  
*J.Organomet.Chem.*, 12, 79

Sankararaman, S., & Kochi, J.K., (1989). *J.Chem.Soc., Chem. Commun.* , 1800

Sarkar, T.K., (1990a). *Synthesis*, 969

Sarkar, T.K., (1990b). *Synthesis*, 1101

Schwartz, W.T., and Post, H.W., (1964). *J.Organomet.Chem.*,  
2, 357

Schweig, A., Weidner, U., and Manuel, G., (1973a).  
*J.Organomet.Chem.*, 67, C4

Schweig, A., Weidner, U., and Manuel, G., (1973b).  
*J.Organomet.Chem.*, 54, 145

Seyferth, D., and Weiner, M.A., (1961). *J.Org.Chem.*, 26,  
4797

Sirimanne, S.R., Li, Z., Vander Veer, D.R., and Talbot,  
L.M., (1991). *J.Am.Chem.Soc*, 113, 1766

- Slocum, G.H., Kaufmann, K., and Schuster, G.B., (1981).  
*J.Amer.Chem.Soc.*, **103**, 4625
- Soundararajan, N., and Platz, M.S., (1987). *Tet.Letts.*, **28**,  
2813
- Still, W.C., (1976). *J.Org.Chem.*, **41**, 3063
- Sulpizio, A., Albini, A., Alessandro, N.D., Fasani, E., and  
Pietra, S., (1989). *J.Am.Chem.Soc.*, **111**, 5773
- Takuwa, A., Tagawa, H., Iwamoto, H., Soga, O., and Maruyama,  
K., (1987). *Chem.Lett.*, 1091
- Takuwa, A., Fujii, N., Tagawa, H., and Iwamoto, H., (1989).  
*Bull.Chem.Soc.Jpn.*, **62**, 336
- Takuwa, A., Nishigaichi, Y., Yamashita, K., and Iwamoto,  
H., (1990). *Chem.Lett.*, 639
- Takuwa, A., Nishigaichi, Y., and Iwamoto, H., (1991).  
*Chem.Lett.*, 1013
- Tamborski, C., Ford, F.E., and Soloski, E.J., (1963).  
*J.Org.Chem.*, **28**, 237
- Traylor, T.G., and Ware, J.C., (1967). *J.Amer.Chem.Soc.*,  
**89**, 2304

Tu, C.L., and Mariano, P.S., (1987). *J.Am.Chem.Soc.*, 109, 5287

Turro, N.J., (1978). "Modern Molecular Photochemistry", Benamin Cummings, Menlo Park, California

Valkovich, P.B., Ito, T.J., and Weber, W.P., (1974). *J.Org.Chem.*, 39, 3543

Vedeneyev, V.I., Gurvich, L.V., Kondrat'yev, V.N., Medvedev, V.A., and Frankevich, Ye.L., (1966). "Bond Energies, Ionisation Potentials and Electron Affinities", Arnold, London

Weidner, U., and Schweig, A., (1972a). *J.Organomet.Chem.*, 39, 261

Weidner, U., and Schweig, (1972b). *Angew.Chem.,Internat.Edit.Engl.*, 11, 146

Wilkinson, G., Stone, F.G.A., and Abel, E.W. (eds) (1982). "Comprehensive Organometallic Chemistry", Pergamon Press

## **Chapter 3.**

# **PHOTOINITIATION OF FREE RADICAL POLYMERISATION USING ORGANOMETALLIC AMINES OF SILICON AND TIN**

### 3.1 Introduction

A number of organometallic amines of the general formula:



(where  $R' = \text{Me, Et}$ ;  $M = \text{Si, Sn}$ ;  $R = \text{Me, n-Bu, Ph}$ ;  $n = 1, 2, 3$ )

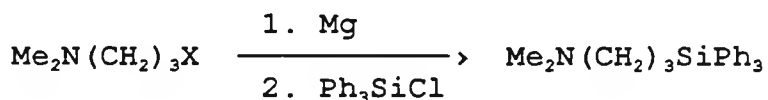
have been synthesised and tested for use as photoinitiators in free radical polymerisation reactions. It was of interest to determine how these electron donors behaved both on their own and in conjunction with sensitisers, such as electron acceptors, in free radical photopolymerisations. The rates of polymerisation have been determined using the technique of RTIR spectroscopy which has been described earlier (see section 1.7.2). From a mechanistic point of view both the formation and the subsequent fragmentation of the radical cations, formed in charge transfer schemes, were of interest and were probed using EPR spectroscopy (see section 1.7.4).

### 3.2 Previous synthetic routes

A number of routes exist for the synthesis of these compounds, but most of them require a multi-step procedure (Sato et al, 1976; Suggs and Lee, 1986). The most direct route for synthesising the stannylalkylamines involves the lithiation of tri-*n*-butyltin chloride at 0°C, followed by

reaction with an  $\alpha$ -dimethylamino- $\omega$ -haloalkane (Sato *et al*, 1976). Using this method 3-(N,N-dimethylamino)propyltri-*n*-butyltin was obtained in 18% yield.

It was decided to search for a more convenient synthetic route for a number of these compounds to obviate the necessity for the multi-step preparations which often involved the preparation of air and moisture sensitive intermediates. It was noted that a synthesis of  $\text{Ph}_3\text{Si}(\text{CH}_2)_3\text{NMe}_2$  using a Grignard reagent had been reported (US 3,853,994).

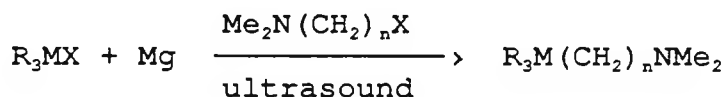


A similar procedure involving a Grignard reagent has also been reported for the synthesis of the analogous stannane  $\text{Me}_2\text{N}(\text{CH}_2)_3\text{SnPh}_3$  (Meganem, 1980). In a separate finding it had been reported that ultrasound could be used to effect the Barbier reaction (a modified Grignard procedure) for the preparation of allylstannanes (Naruta *et al*, 1986).

### 3.2.1 Synthetic routes used

This reaction was extended to prepare a number of allylic, benzylic, and naphthyllic silanes and stannanes, reported herein, and similar methodology was applied in the synthesis of aminoalkylsilanes and stannanes to illustrate further possibilities of ultrasound in synthetic organic chemistry (Bowser and Davidson, 1992). Using this procedure it has

been found that  $\alpha$ -dimethylamino- $\omega$ -chloroalkanes react with chlorotrimethylsilane and chlorotri-*n*-butylstannane to give reasonable yields of dimethylaminoalkyl-silanes and stannanes respectively in the presence of magnesium and with the application of ultrasound at room temperature.



R = Me, Bu, Ph; M = Si, Sn ; X = halogen ; n = 2, 3

This route has been employed to synthesise a number of silylalkylamines and stannylalkylamines using a 'one-pot' procedure with relatively short reaction times and reasonable yields as outlined below in table 3.1.

Table 3.1 The reaction times and yields of the synthesis of a number of dimethylaminoalkylsilanes and stannanes using ultrasound

COMPOUND	REACTION TIME <sup>a</sup> / hours	YIELD/ %
Me <sub>2</sub> N(CH <sub>2</sub> ) <sub>3</sub> SiMe <sub>3</sub>	4	37
Me <sub>2</sub> N(CH <sub>2</sub> ) <sub>3</sub> SnBu <sub>3</sub>	2	35
Me <sub>2</sub> N(CH <sub>2</sub> ) <sub>2</sub> SiPh <sub>3</sub>	4	40
Me <sub>2</sub> N(CH <sub>2</sub> ) <sub>2</sub> SnPh <sub>3</sub>	4	35
Me <sub>2</sub> N(CH <sub>2</sub> ) <sub>3</sub> SiPh <sub>3</sub>	4	30
Me <sub>2</sub> N(CH <sub>2</sub> ) <sub>2</sub> SnMe <sub>3</sub>	2	45

<sup>a</sup>= all reactions carried out at 25°C with THF as solvent.

What is immediately apparent from table 1 is that although the reaction yields are moderate the reaction times are significantly reduced when compared to the multi-step procedures mentioned earlier. The mechanism of the reaction is of interest since using the Barbier ultrasound route there is no prior formation of the alkyl metal halide unlike traditional Grignard procedures. In this case the haloalkylamine is added slowly to a solution of the trisubstituted metal halide and magnesium turnings. The haloalkylamine is added at such a rate as to form an *in-situ* Grignard reagent with the magnesium which immediately reacts with the excess trisubstituted metal halide to complete the reaction. In practice one cannot be sure if the sequence of events begins with the metallation of the silyl/stannyl chloride or whether the alkyl metal halide is formed and then reacts rapidly with the silyl/stannyl chloride. There is no doubt, however, that the success of the synthetic strategy depends upon the activation of magnesium by ultrasound.

### 3.3 Applications of alkylaminosilanes and stannanes

One area that these compounds have been investigated is in the base promoted reactions of quaternary ammonium salts, which include the Stevens rearrangement, the Sommelet-Hauser rearrangement, and the Hoffmann elimination (Pine, 1970). An early report on this type of reaction involved the



Later work has shown an improved Sommelet-Hauser rearrangement in non-basic media with the minimum formation of the Stevens rearrangement products (Nakano and Sato, 1985; Nakano and Sato, 1987). A number of these compounds, including  $\text{Bu}_3\text{Sn}(\text{CH}_2)_3\text{NMe}_2$ , have been found to exhibit fungicidal and bacteriological properties (Ger Offen 2,801,700). A similar claim was made of aminoalkylsilane derivatives which can be used as hypotensive agents (US 3,853,994). The aminoalkylsilanes and both their acid addition and quaternary ammonium salts have been shown to be useful since they possess pharmacological activity. In particular these compounds, such as  $\text{Ph}_3\text{Si}(\text{CH}_2)_3\text{NMe}_2$ , can act as mild tranquillisers when applied in a capsule or tablet form.

Another interesting application of these compounds that was investigated involved their use as antiknock additives in the combustion of engine fuels (Cullis et al, 1985).

### 3.4 Electron paramagnetic resonance (EPR) spectroscopy results

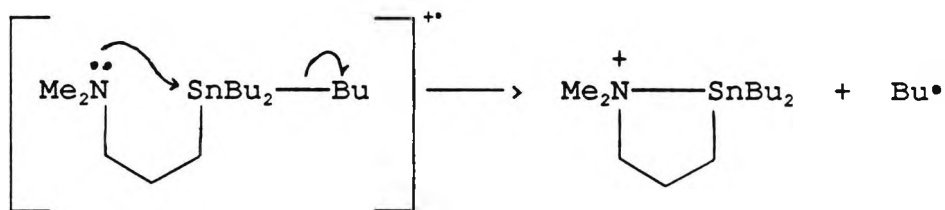
It is known that *t*-amines will form charge transfer complexes with suitable acceptors. This readiness to form such complexes can be attributed, in part, to the low oxidation potentials of *t*-amines. Similarly the organometallic amines synthesised are expected to be effective in charge transfer schemes due to the low oxidation potentials of these *t*-amines. Thus the oxidation

potential for  $\text{Me}_2\text{NCH}_2\text{SiMe}_3$ , has been calculated to be 8.20 eV (Bock et al, 1979) which renders this organometallic amine potentially useful in charge transfer schemes. It is expected that with a suitable acceptor charge transfer from the amine to the acceptor gives rise to the amine radical cations. It is of particular interest from a mechanistic point of view on determining the fragmentation pathways available to the radical cations so produced. This information can then be applied in the design of new photoactive compounds. One method that has been used to assess the role of the radical cations produced is epr spectroscopy. Epr spectroscopy was used in order to detect the formation and monitor the subsequent fragmentation of the radical cations of  $\text{Me}_2\text{N}(\text{CH}_2)_3\text{SnBu}_3$  and  $\text{Me}_2\text{N}(\text{CH}_2)_3\text{SiMe}_3$ . These compounds, in a solid fluorotrichloromethane matrix (77K), were exposed to  $\gamma$ -irradiation (1Mrad) using a  $^{60}\text{Co}$  source. Following the recording of the spectra at 77K the temperature of the matrix was gradually increased to the melting point of the matrix (160K) and spectra were recorded, wherever possible, of the breakdown products (Butcher et al, 1992a; Butcher et al, 1992b).

The epr spectra recorded at 77K for  $[\text{Me}_2\text{N}(\text{CH}_2)_3\text{SnBu}_3]^{\bullet+}$  can be assigned to *n*-butyl radicals as the sole paramagnetic product. This is a rather interesting contrast to the behaviour of the radical cation derived from tetra-*n*-butylstannane which under similar conditions, gave a stable radical cation and only a minor yield of *n*-butyl radicals. The functional change on going from the tetra-*n*-

butylstannane to  $\text{Me}_2\text{N}(\text{CH}_2)_3\text{SnBu}_3$ , is formally remote with respect to the metal centre and yet the radical cation of the latter must be highly unstable to give fragmentation at 77K. This radical cation is probably not an energy minimum inferring that reorganisation of the molecular geometry occurs after ionisation and prior to the dissociation pathway. Consideration of the ionisation potential data (Vedeneyev *et al*, 1966) for  $\text{R}_3\text{N}$  and  $\text{R}_4\text{Sn}$  ( $\text{R} = \text{alkyl}$ ) compounds favours the electron loss as being from the tin unit and so the structure of the primary radical cation would be expected to be similar to that of  $[(n\text{-Bu})_4\text{Sn}^{\bullet+}]$ . It is proposed, therefore, that scheme 3.1 accounts for the behaviour and observed C-Sn bond cleavage of the radical cation giving rise to *n*-butyl radicals.

Scheme 3.1 The proposed fragmentation of  $[\text{Me}_2\text{N}(\text{CH}_2)_3\text{SnBu}_3]^{\bullet+}$  at 77K from epr spectroscopic evidence



Results for  $[\text{Me}_2\text{N}(\text{CH}_2)_3\text{SiMe}_3]^{\bullet+}$  indicate that the radical cation is observed as a normal nitrogen centred  $\pi$ -radical (Eastland *et al*, 1984) and is entirely stable up to the melting point of the matrix (160K). This result is in agreement with the ionisation potential data for  $\text{R}_3\text{N}$  and  $\text{R}_4\text{Si}$  compounds (Eastland *et al*, 1984) and with previous

mechanistic conjecture from the photochemical studies of compounds of this type (Hasegawa et al, 1988b).

### 3.5 UV curing results

#### 3.5.1 UV curing results of Et<sub>2</sub>NCH<sub>2</sub>SiMe<sub>3</sub>

Initially Et<sub>2</sub>NCH<sub>2</sub>SiMe<sub>3</sub> was synthesised and evaluated for potential use as an initiator of free radical polymerisation. The free radical initiating properties of this amine were tested by incorporation into a suitable monomer, TMPTA, both on its own and in conjunction with sensitisers. The results are presented below in table 3.2.

Table 3.2 UV curing results of the polymerisation of TMPTA using Et<sub>2</sub>NCH<sub>2</sub>SiMe<sub>3</sub> in the presence and absence of sensitisers

E X P T	INITIATING SYSTEM	% w/w  in TMPTA	NUMBER OF PASSES
			In Air
1	Et <sub>2</sub> NCH <sub>2</sub> SiMe <sub>3</sub>	1.7	* <sup>a</sup>
2	Et <sub>2</sub> NCH <sub>2</sub> SiMe <sub>3</sub> + ITX	1.7 1.8	8 <sup>a</sup>
3	ITX	1.8	8 <sup>a</sup>
4	Et <sub>2</sub> NCH <sub>2</sub> SiMe <sub>3</sub> + DMC	1.9 0.8	35 <sup>b</sup>
5	DMC	0.8	55 <sup>b</sup>

ITX = mixture of 1-(and 2-)isopropylthioxanthone

DMC = 3-benzoyl-5,7-dimethoxycoumarin

a Belt speed = 10 ft/min

b Belt speed = 230 ft/min

When used on its own (EXPT 1) the amine did not effect polymerisation of TMPTA when tested in air in the UV Colordry apparatus. The incorporation of a sensitiser such as ITX did not give an enhanced cure rate (EXPT 2) when compared to the curing using ITX on its own (EXPT 3). When DMC was used as a sensitiser there was a small synergistic effect (EXPT 4) when compared to the result of DMC on its own (EXPT 5). This evidence is substantiated by an earlier claim that the photoaddition of  $\text{Et}_2\text{NCH}_2\text{SiMe}_3$  to 9,10-dicyanoanthracene (DCA) is inefficient (Hasegawa et al, 1988a). It was demonstrated that the photoaddition gave a variety of different products in low yields. It was proposed that the low efficiency of adduct formation might be due to a low rate of coupling of the  $\alpha$ -amino radical,  $\text{Et}_2\text{NCH}_2^\bullet$ , to a DCA-derived radical based on steric and electronic effects.

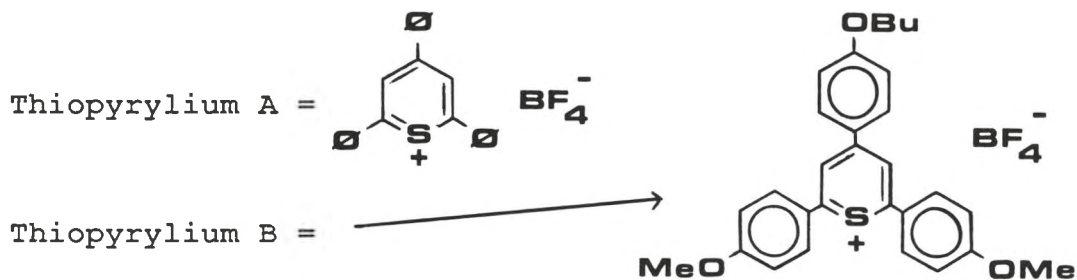
### 3.5.2 UV curing results of dimethylaminoalkylsilanes

In an attempt to reduce the steric bulk around the nitrogen two further amines,  $\text{Me}_2\text{NCH}_2\text{SiPh}_3$  and  $\text{Me}_2\text{N}(\text{CH}_2)_3\text{SiMe}_3$  were subsequently synthesised. Testing of the above compounds both with and without sensitisers showed that they could be effective in free radical polymerisation as seen from the

results in table 3.3.

**Table 3.3** UV curing results of dimethylaminoalkylsilanes in the presence and absence of sensitizers

E X P T	INITIATOR	NUMBER OF PASSES			
		Touching Quartz	Touching Glass	In Air	Glass Filter
1	Me <sub>2</sub> NCH <sub>2</sub> SiPh <sub>3</sub>	1	2	*	*
2	Me <sub>2</sub> N(CH <sub>2</sub> ) <sub>3</sub> SiMe <sub>3</sub>	1	11	*	*
3	Me <sub>2</sub> N(CH <sub>2</sub> ) <sub>3</sub> SiMe <sub>3</sub> + thiopyrylium A	1	5	*	*
4	thiopyrylium A	7	23	*	*
5	Me <sub>2</sub> N(CH <sub>2</sub> ) <sub>3</sub> SiMe <sub>3</sub> + thiopyrylium B	1	3	*	*
6	thiopyrylium B	3	6	*	*
7	Me <sub>2</sub> N(CH <sub>2</sub> ) <sub>3</sub> SiMe <sub>3</sub> + DCA	4	15	*	*
8	DCA	6	15	*	*

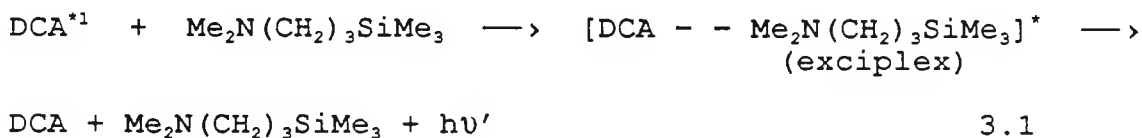


DCA = 9,10-dicyanoanthracene

Belt speed = 10 ft/min for all experiments

The results indicate that these compounds could be effective in radical polymerisations as evidenced by the sensitised polymerisation using the thiopyrylium salts (EXPT's 3 & 5).

When the amine  $\text{Me}_2\text{N}(\text{CH}_2)_3\text{SiMe}_3$  was used with DCA (EXPT 7) a decrease in the rate of polymerisation was noticed when compared to the amine in the absence of any sensitiser (EXPT 2). This can be explained by the collapse of the exciplex formed during irradiation with regeneration of the starting materials as depicted in equation 3.1.



Thus the amine quenches the fluorescence of DCA without formation of any reactive intermediates. This explanation would also support the fact that Mariano and co-workers observed a low yield of photoaddition products in the reaction of  $\text{Et}_2\text{NCH}_2\text{SiMe}_3$  with DCA (Hasegawa et al, 1988a).

### 3.5.3 UV curing results of dimethylaminoalkylsilanes and stannanes

An investigation into the initiating properties of the amines used on their own in a free radical polymerisable monomer, TMPTA, was investigated using the UV Colordry apparatus described earlier. The results are presented below in table 3.4.

Table 3.4 UV curing results for a number of dimethylaminoalkyl- silanes and stannanes (1% w/w) in TMPTA

E X P T	INITIATOR	NUMBER OF PASSES			
		Touching Quartz	Touching Glass	In Air	Glass Filter
1	Me <sub>2</sub> NCH <sub>2</sub> SiPh <sub>3</sub>	1	2	*	*
2	Me <sub>2</sub> N(CH <sub>2</sub> ) <sub>3</sub> SiMe <sub>3</sub>	1	2	*	*
3	"	2 <sup>a</sup>	8 <sup>a</sup>	-	-
4	Me <sub>2</sub> N(CH <sub>2</sub> ) <sub>3</sub> SiPh <sub>3</sub>	4	12	*	*
5	Me <sub>2</sub> N(CH <sub>2</sub> ) <sub>3</sub> SnBu <sub>3</sub>	1	3	*	*
6	"	7 <sup>a</sup>	24 <sup>a</sup>	-	-
7	Me <sub>2</sub> N(CH <sub>2</sub> ) <sub>2</sub> SnMe <sub>3</sub>	1	1	*	*
8	"	6 <sup>a</sup>	15 <sup>a</sup>	-	-
9	TMPTA	6	40	*	*

\* = no polymerisation detected after 30 passes

- = experiment not performed

a = belt speed = 160 ft/min

Belt speed = 10 ft/min for all other experiments

When air is excluded the amines have initiating properties during the photopolymerisation process. This occurs for all the compounds tested when a cover slide of either quartz or

glass is used. The amines may form a charge transfer complex with the monomer which would result in the production of some  $\alpha$ -aminoalkyl radicals, which could then initiate polymerisation. The amines do not show evidence of polymerisation when air is present during photolysis.

#### 3.5.4 Sensitisation of polymerisation using benzanthrone

It is well established that carbonyl/amine initiating systems are of value in free radical photopolymerisation. The photoreduction of aromatic ketones with amines has been shown to occur via the formation of an excited complex (exciplex) (Sander et al, 1972). It is the excited triplet of the carbonyl group which forms an exciplex with the amine. The exciplex is stabilised to a certain extent by the formation of a weak charge transfer complex due to the low ionisation potential of the amine. Thus the formation of the exciplex will depend on both the ionisation potential of the amine and the reduction potential of the carbonyl compound. The exciplex can collapse by a number of different routes including:

1. Efficient quenching of the excited triplet of the carbonyl group resulting in regeneration of the starting materials.
2. Electron transfer from the amine to the ketone in which radical ions are produced.
3. Hydrogen-abstraction from the amine by the ketone in which ketyl and amine radicals are produced.

Generally *t*-amines are favoured since the relative reactivity is related to the ease with which the amine is oxidised which is tertiary > secondary > primary. Also *t*-amines are good hydrogen donors since they have a hydrogen atoms which are situated in an  $\alpha$ -position to the nitrogen and are activated. This is important when considering the hydrogen abstraction mechanism which is strongly dependent on the C-H bond strength and will be related to the activation energy for the process.

The photoreduction of the ketone depends on the nature of the excited state (Hutchinson and Ledwith, 1973). Aromatic ketones have two different types of chromophore which can produce the excited triplet state. These are derived from:

1. The aromatic nucleus:  $\pi, \pi^*$  transition
2. The carbonyl group:  $n, \pi^*$  transition

Both types of excited state have been photoreduced by *t*-amines. As a result of the photoreduction free radicals are produced which are efficient photoinitiators of free radical polymerisation. The rates of polymerisation of various ketone/*t*-amine hybrid systems have previously been determined (Ledwith and Purbrick, 1973; Davidson and Goodin, 1982). It has been shown that it is the  $\alpha$ -aminoalkyl radical that is efficient at initiating polymerisation (Block et al, 1971; Hutchinson et al, 1973). Another added bonus is that the  $\alpha$ -aminoalkyl radical so produced is

effective at reducing oxygen inhibition of free radical polymerisation (see section 1.4.5).

### 3.5.5 UV curing results of dimethylaminoalkylsilanes and stannanes with benzanthrone

From the results presented previously it was proposed to test a number of the dimethylaminoalkyl- silanes and stannanes with an aromatic ketone, benzanthrone, in order to test the free radical initiating properties of these hybrid systems. The UV curing results of the combinations tested in the monomer TMPTA are presented in table 3.5.

Table 3.5 Sensitisation of polymerisation of TMPTA using dimethylaminoalkyl- silanes and stannanes (1% w/w) with benzanthrone (1% w/w)

E X P T	INITIATING SYSTEM	NUMBER OF PASSES			
		Touching Quartz	Touching Glass	In Air	Glass Filter
1	Me <sub>2</sub> N(CH <sub>2</sub> ) <sub>2</sub> SnMe <sub>3</sub> + benzanthrone	1 (1)	1 (1)	5 (*)	15 (*)
2	"	1 (6)	1 (15)	12 (-)	* (-)
3	Me <sub>2</sub> N(CH <sub>2</sub> ) <sub>3</sub> SiMe <sub>3</sub> + benzanthrone	1 (1)	1 (2)	16 (*)	* (*)
4	"	1 (3)	2 (8)	- (-)	- (-)
5	Me <sub>2</sub> N(CH <sub>2</sub> ) <sub>3</sub> SiPh <sub>3</sub> + benzanthrone	3 (4)	6 (12)	27 (*)	* (*)
6	benzanthrone	5	12	26	*

( ) = UV curing results for dimethylaminoalkylsilane/stannane in the absence of sensitiser

\* = no polymerisation detected after 30 passes

- = experiment not performed

Belt speed = 160 ft/min in EXPT's 2 & 4

Belt speed = 10 ft/min in all other experiments

The results in table 3.5 give evidence of sensitisation of the amines  $\text{Me}_2\text{N}(\text{CH}_2)_2\text{SnMe}_3$  (EXPT's 1 and 2) and  $\text{Me}_2\text{N}(\text{CH}_2)_3\text{SiMe}_3$  (EXPT's 3 and 4) when used in conjunction with benzanthrone in the polymerisation of TMPTA. For  $\text{Me}_2\text{N}(\text{CH}_2)_2\text{SnMe}_3$  (EXPT's 1 and 2) sensitisation occurs for all four experimental conditions of polymerisation tested. Thus an increase in the rate of polymerisation as evidenced in the reduced number of passes when compared to the amine on its own [EXPT's 1 and 2: figures in brackets ( )] and benzanthrone on its own (EXPT 6) was realised. The results in EXPT 1 show that there is polymerisation observed when air is present (both in air and with a glass cover slide).

### 3.6 Real-time infrared (RTIR) spectroscopy results

#### 3.6.1 RTIR results of dimethylaminoalkylsilanes and stannanes

The RTIR spectra of the photopolymerisation of TMPTA using the organometallic amines were recorded in order to give an indication of the role of homolytic cleavage in the

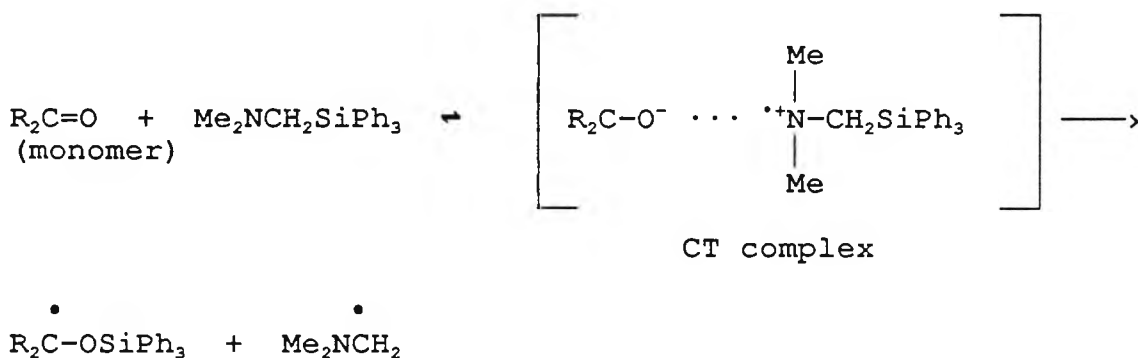
polymerisation mechanism. The situation is complicated by the fact that TMPTA absorbs in the UV region ( $\lambda$  (sh) = 240nm [ $\epsilon=300$ ]). Thus it cannot be ruled out that a charge transfer (CT) complex may be formed between the amine and the monomer resulting in a different mechanism of initiation to that of homolytic cleavage of the amine. The results are shown below in table 3.6.

Table 3.6 RTIR spectroscopy results for the photopolymerisation of TMPTA using organometallic amines

EXPT	INITIATOR	UV/ $\lambda_{max}$ ( $\epsilon$ )	% mol in TMPTA	$R_p$ (max) / mol/l/s	% Conv/ at 1 min
1	$Me_2NCH_2SiPh_3$	271 (1100)	0.9	0.167	14.8
2	$Me_2N(CH_2)_2SiPh_3$	265 (1400)	0.9	0.053	5.0
3	$Me_2N(CH_2)_3SiPh_3$	270 (1350)	0.9	0.075	5.8
4	$Me_2N(CH_2)_3SiMe_3$	273 (100)	1.9	0.095	6.4
5	$Me_2N(CH_2)_3SnBu_3$	270 (100)	0.8	0.065	6.9
6	$Me_2N(CH_2)_2SnMe_3$	269 (100)	1.2	0.342	18.0
7	$Me_2N(CH_2)_2SnPh_3$	257 (1800)	0.7	0.077	13.3

For the series  $Me_2N(CH_2)_nSiPh_3$  (where  $n = 1, 2, 3$ ) it is shown that when  $n = 1$  (EXPT 1) there is a relatively high degree of conversion and  $R_p$ (max) value obtained when compared to the other amines in this series (where  $n = 2$  &  $3$ : EXPT's 2 and

3 respectively). This is thought to be related to the expected hyperconjugative effect which operates between the Si and the  $\beta$ -N via the alkyl link ( $n = 1$ ). When the alkyl link is increased to  $-(\text{CH}_2)_2-$  or  $-(\text{CH}_2)_3-$  (EXPT's 2 and 3 respectively) in this series the hyperconjugative effect is minimised resulting in the reduced degree of conversion and  $R_{p(\text{max})}$  values obtained. It is expected that this  $\beta$ -effect will stabilise the formation of a radical cation formed via a CT complex with the monomer resulting in reactive  $\alpha$ -aminoalkyl radicals shown below.



A similar mechanism can be proposed to account for the relatively high values of the degree of conversion and  $R_{p(\text{max})}$  for the stannanes,  $\text{Me}_2\text{N}(\text{CH}_2)_2\text{SnR}_3$  (where  $\text{R} = \text{Me}, \text{Ph}$  in EXPT's 6 & 7 respectively). The CT complex formation is likely to be linked to the oxidation potentials of the amine donors which could explain why the silane in this series  $\text{Me}_2\text{N}(\text{CH}_2)_2\text{SiPh}_3$  (EXPT 2) does not exhibit a similar reactivity to the above stannanes.

It is apparent that in the series  $\text{Me}_2\text{N}(\text{CH}_2)_3\text{MR}_3$  (EXPT's 3, 4, & 5) there is a reduced activity towards polymerisation when

compared to the other amines. This could be due to structural features that have been noted earlier which involve the coordination of the nitrogen lone pair into the available d orbitals of the metal as shown below.



This would stop these compounds forming exciplexes to any great extent and could explain the reduction in the degree of conversion and  $R_{p(max)}$  values. It is anticipated that this type of structure is more important for tin compounds than silicon compounds due to the greater ability of tin to extend coordination through the use of d-orbitals in bonding.

### 3.6.2 RTIR results of dimethylaminoalkylsilanes and stannanes with benzanthrone

RTIR spectroscopy was used to substantiate the earlier work carried out using the UV Colordry apparatus for the sensitisation of polymerisation of TMPTA using benzanthrone with the organometallic amines. The results are presented below in table 3.7.

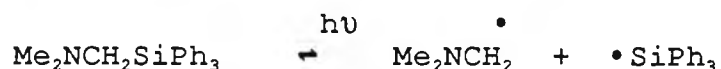
Table 3.7 RTIR spectroscopy results for the photopolymerisation of TMPTA using organometallic amines sensitised using benzanthrone

E X P T	INITIATING SYSTEM	UV/ $\lambda_{\text{max}}$ ( $\epsilon$ )	% mol in TMPTA	R <sub>p</sub> (max) / mol/l/s	% Conv/ at 1 min
1	Benzanthrone + Me <sub>2</sub> NCH <sub>2</sub> SiPh <sub>3</sub>	see expt 6 271 (1100)	1.3 0.9	0.679	32.2
2	Benzanthrone + Me <sub>2</sub> N(CH <sub>2</sub> ) <sub>3</sub> SiMe <sub>3</sub>	see expt 6 273 (100)	1.3 1.9	1.395	40.2
3	Benzanthrone + Me <sub>2</sub> N(CH <sub>2</sub> ) <sub>3</sub> SnBu <sub>3</sub>	see expt 6 270 (100)	1.3 0.8	0.435	30.9
4	Benzanthrone + Me <sub>2</sub> N(CH <sub>2</sub> ) <sub>2</sub> SnMe <sub>3</sub>	see expt 6 269 (100)	1.3 1.2	1.366	35.3
5	Benzanthrone + Me <sub>2</sub> N(CH <sub>2</sub> ) <sub>2</sub> SnPh <sub>3</sub>	see expt 6 257 (1800)	1.3 0.7	0.581	45.8
6	Benzanthrone	395 (10000) 305 (8000)	1.3	0.052	22.7

The results show that the sensitisation of polymerisation of TMPTA using benzanthrone with the organometallic amines is very efficient. The mechanism of sensitisation is likely to involve the formation of an exciplex between the sensitiser and the amine which subsequently collapses to give an  $\alpha$ -aminoalkyl radical which can initiate polymerisation.

One interesting feature is observed when comparing the values of the degree of conversion and  $R_{p(max)}$  for  $Me_2N(CH_2)_3SiMe_3$  (EXPT 2) and  $Me_2N(CH_2)_3SnBu_3$  (EXPT 3). The silane shows a greater increase in the values of the degree of conversion and  $R_{p(max)}$  when compared to the stannane. This could be explained by the earlier observation that the N is coordinated to the Sn in the stannane which effectively reduces the possibility of forming an exciplex with the sensitiser and thus reduces the effect of sensitisation as demonstrated. The silicon compound does not undergo this coordination to any great extent and thus the N is free to form an exciplex with the sensitiser resulting in sensitisation of polymerisation.

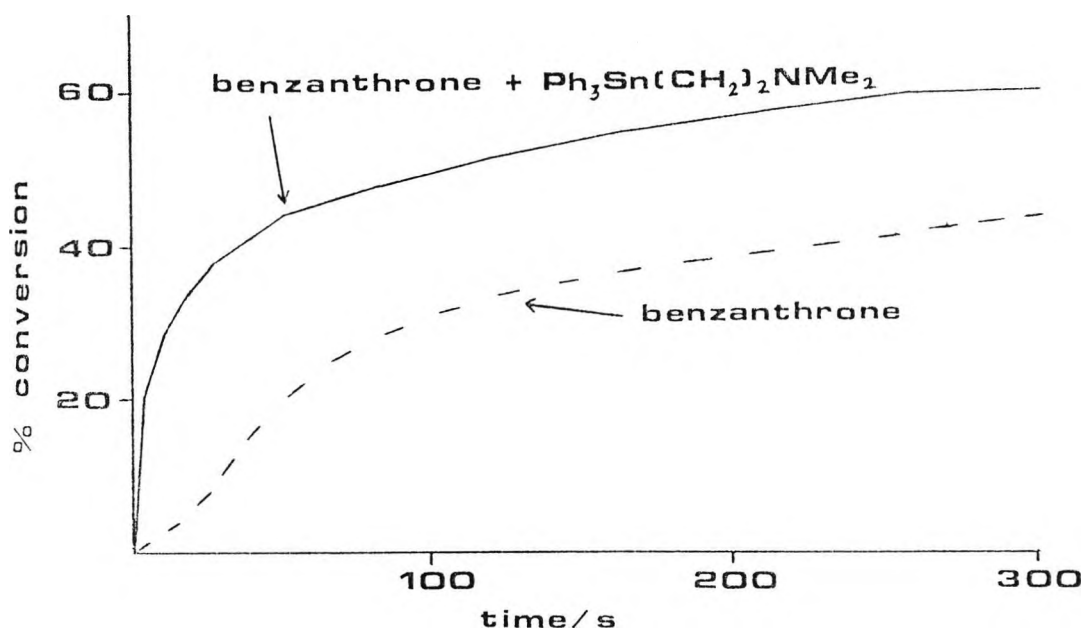
The effect of sensitisation in the case of  $Me_2NCH_2SiPh_3$  (EXPT 1) is not as evident as for the other amines since there may be some homolytic cleavage of this compound, which competes with the sensitisation process.



Another interesting feature is seen when comparing the kinetic curves of the RTIR spectra of benzanthrone (EXPT 6) with the situation of benzanthrone + amine (EXPT's 1 to 5). In the former case excited state benzanthrone presumably abstracts a hydrogen from the resin to yield a monomer radical capable of initiating polymerisation. In the latter case polymerisation occurs via sensitisation with the production of  $\alpha$ -aminoalkyl radicals which are extremely

efficient at initiating polymerisation. The rates of polymerisation via the two different routes may be compared when viewing the RTIR kinetic traces shown below in figure 3.1.

Figure 3.1 A plot of the degree of conversion versus time obtained from the RTIR spectroscopy results of the curing of TMPTA for an organometallic amine in the presence and absence of a sensitiser (benzanthrone)



Other evidence for the formation of  $\alpha$ -aminoalkyl radicals being formed in the sensitised experiment is that under the conditions tested no observable induction period was noticed. It is well documented that  $\alpha$ -aminoalkyl radicals are good scavengers of oxygen which effectively reduces the

oxygen inhibition of polymerisation (see section 1.4.5). Thus in this case, RTIR spectroscopy has been used to calculate different rates of polymerisation for the situations with benzanthrone in the presence and in the absence of amines. From the results it can be inferred that a different mechanism of polymerisation occurs for the two situations described. This points to the value of RTIR spectroscopy as a diagnostic technique which, when used with other evidence, may be used to infer reaction mechanisms.

### 3.7 Experimental section

See section 2.7 for general experimental details. All  $^1\text{H}$  NMR were run in  $\text{CDCl}_3$  with TMS as the internal standard, where used. IR spectra were recorded using neat films or KBr discs. Methanol was used as the solvent for UV spectra.

### 30. Triphenyl(N,N-dimethylaminomethyl)silane

A.

Equipment was dried overnight at  $160^\circ\text{C}$ . Trimethylsilyl iodide was supplied in a 5g ampoule. Trimethylsilyl iodide (5g;0.025mol) in anhydrous ether (10ml) was added to the flask. At  $0^\circ\text{C}$  2-methyl-2-butene (0.15ml) was added followed by dropwise addition of N,N,N',N'-tetramethylenediamine (2.56g;0.025mol) in anhydrous ether (10ml). A white precipitate formed immediately and this mixture was allowed to stir for 20 min. The precipitate was collected by vacuum filtration and washed with anhydrous ether (3 x 20ml), air-dried, and rapidly transferred to a vacuum desiccator to give 3.35g (72%) of dimethyl(methylene)ammonium iodide (Bryson et al, 1980).

#### Analysis

$^1\text{H}$  NMR: 3.60 (s,6H), 8.20 (s,2H)

B.

Thiophenol (2g;18mmol) was added at room temperature to a

stirred suspension of NaH (0.8g;60%;20mmol) under nitrogen. After 0.5h dimethyl(methylene)ammonium iodide (3.35g;80mmol) was added as a solid and the resulting solution was stirred overnight. Following the addition of water (40ml) the resulting mixture was extracted with ether (3 x 40ml) and the combined organic extracts were washed successively with a saturated NaHCO<sub>3</sub> solution, water, and brine, dried over MgSO<sub>4</sub>, filtered, and concentrated in vacuo, leaving 2.4g (80%) of a yellow oil of dimethylaminomethylphenylsulphide (Bryson et al, 1980).

#### Analysis

<sup>1</sup>H NMR: 2.20 (s,6H), 4.40 (s,2H), 7.00-7.50 (m,5H)

C.

THF (25ml) was slowly added under nitrogen, with stirring to a mixture of chlorotriphenylsilane (2.95g;0.01mol) and Li (30% dispersion in mineral oil;0.92g;0.04mol). A few minutes after the addition of the solvent a white precipitate was noticed. Within 20 min the reaction mixture turned light yellow; the colour gradually turned orange-brown and finally black-brown, after 3h stirring at room temperature. This solution of triphenylsilyllithium was added under nitrogen to an ice-cold solution of dimethylaminophenyl sulphide (1.18g;7mmol) in anhydrous THF (10ml). After addition the mixture was stirred at room temperature for 3h and hydrolysed with saturated ammonium chloride solution. The THF layer was separated and the

aqueous layer was extracted with ether. The combined organic extracts were concentrated and the residue was extracted with 10% HCl solution. The acid extract was neutralised and extracted with ether, dried ( $\text{MgSO}_4$ ), and concentrated. The solid residue was recrystallised from pet ether to give 1.0g (35%) with mp 111-112°C (lit mp 111-113°C; Sato et al, 1976).

#### Analysis

$^1\text{H NMR}$ : 2.20 (s, 6H), 2.70 (s, 2H), 7.20-7.70 (m, 15H)

IR: 3064 (m), aromatic C-H stretch  
2926 (m), aliphatic C-H stretch  
2810 (s), C-H asymmetric stretch of  $\text{NCH}_3$  group  
2763 (s), C-H symmetric stretch of  $\text{NCH}_3$  group  
1426 (m), C-H bending  
1109 (m), Ph-Si stretch  
784 (m), 700 (m), monosubstituted benzene

UV:  $\lambda_{\text{max}} = 271\text{nm}$  ( $\epsilon=1100$ )

MS:  $\text{M}^+$  317, 259 ( $\text{Ph}_3\text{Si}^+$ ), 77 ( $\text{C}_6\text{H}_5^+$ ), 58 ( $\text{Me}_2\text{NCH}_2^+$ )

#### 31. N-(Trimethylsilylmethyl)-N,N'-diethylamine

A solution of diethylamine (58.5ml; 0.55mol) and iodomethyltrimethylsilane (12.0g; 0.05mol) in anhydrous

methanol (25ml) was stirred at reflux for 20h, cooled and diluted with pentane (250ml) and aqueous potassium carbonate (50ml;5%). The separated pentane layer was washed with distilled water, dried, and the pentane was evaporated. The residue was distilled to give 5.6g (64%) yield with bp 148-149°C (lit bp 146-148°C; Hasegawa et al, 1988a).

### Analysis

<sup>1</sup>H NMR: 0.20 (s,9H), 1.10 (t,6H), 2.00 (s,2H), 2.50 (q,4H)

IR: 2970 (s), 2791 (m), C-H stretching  
1452 (m), 1417 (m), C-H bending  
1248 (m), Si-C stretch

UV:  $\lambda_{\max}$  = 214nm ( $\epsilon$ =800)

### 32. 3-N,N'-Dimethylamino-1-triphenylsilylpropane

N,N-Dimethylaminopropylchloride (3.0g;0.025mol) in anhydrous THF (15ml) was added dropwise at room temperature under argon with external irradiation of ultrasound to a mixture of chlorotriphenylsilane (6.0g;0.020mol), magnesium turnings (0.65g;0.027mol), and 1,2-dibromoethane (0.5ml) in anhydrous THF. After 4h irradiation the reaction was quenched with saturated aqueous NH<sub>4</sub>Cl solution and then extracted with

ether. The combined organic extracts were dried (magnesium sulphate) and concentrated. The solid residue was purified initially by column chromatography ( $\text{CCl}_4/\text{alumina}$ ;  $R_f=0.80$ ) and then recrystallisation ( $\text{EtOH}$ ) to give 2.1g (30%) yield with mp  $75-76^\circ\text{C}$ .

### Analysis

$^1\text{H NMR}$ : 1.30-1.90 (m, 4H), 2.20-2.60 (m, 8H), 7.20-7.70 (m, 15H)

IR: 3050 (m), aromatic C-H stretch  
2930 (m), aliphatic C-H stretch  
2810 (m), C-H asymmetric stretch of  $\text{NCH}_3$  group  
2765 (m), C-H symmetric stretch of  $\text{NCH}_3$  group  
1425 (m), C-H bending  
1100 (m), Ph-Si stretch  
740 (s), 700 (s), monosubstituted benzene

UV:  $\lambda_{\text{max}} = 270\text{nm}$  ( $\epsilon = 1350$ )

MS:  $M^+$  345, 259 ( $\text{Ph}_3\text{Si}^+$ ), 77 ( $\text{C}_6\text{H}_5^+$ ), 58 ( $\text{Me}_2\text{NCH}_2^+$ )

### 33. 2-N,N'-Dimethylamino-1-triphenylsilylethane

This compound was prepared by the method described in

experiment 32, using 2-dimethylaminoethylchloride (2.2g;0.02mol), chlorotriphenylsilane (5.0g;0.017mol), magnesium turnings (0.53g;0.022mol), and 1,2-dibromoethane (0.5ml) with irradiation of ultrasound for 4h. The solid residue was purified initially by column chromatography (CCl<sub>4</sub>/alumina; R<sub>f</sub>=0.80) and then recrystallisation (EtOH) which gave 2.2g (40%) yield with mp 61°C (lit mp 66-72°C; Sato et al, 1976).

### Analysis

<sup>1</sup>H NMR: 1.25 (t,2H), 2.10 (s,6H), 2.60 (t,2H), 7.20-7.70 (m,15H)

IR: 3055 (m), aromatic C-H stretch  
2930 (m), aliphatic C-H stretch  
2810 (m), C-H asymmetric stretch of NCH<sub>3</sub> group  
2764 (m), C-H symmetric stretch of NCH<sub>3</sub> group  
1424 (s), C-H bending  
1105 (s), Ph-Si stretch  
750 (s), 700 (s), monosubstituted benzene

UV:  $\lambda_{\max}$  = 265nm ( $\epsilon$ =1400)

MS: 259 (Ph<sub>3</sub>Si<sup>+</sup>), 77 (C<sub>6</sub>H<sub>5</sub><sup>+</sup>), 58 (Me<sub>2</sub>NCH<sub>2</sub><sup>+</sup>)

#### 34. 2-N,N'-Dimethylamino-1-triphenylstannylethane

This compound was prepared by the method described in experiment 32, using 2-dimethylaminoethylchloride (2.2g;0.02mol), chlorotriphenylstannane (6.6g;0.017mol), magnesium turnings (0.53g;0.022mol), and 1,2-dibromoethane (0.5ml) with irradiation of ultrasound for 4h. The solid residue was purified initially by column chromatography (CCl<sub>4</sub>/silica; R<sub>f</sub>=0.50) and then recrystallisation (EtOH) which gave 2.5g (35%) yield with mp 80-81°C (lit mp 81-83°C; Sato and Ban, 1973).

#### Analysis

<sup>1</sup>H NMR: 1.70 (t,2H), 2.10 (s,6H), 2.60 (t,2H), 7.20-7.70 (m,15H)

IR: 3045 (m), aromatic C-H stretch  
2940 (m), aliphatic C-H stretch  
2810 (m), C-H asymmetric stretch of NCH<sub>3</sub> group  
2765 (m), C-H symmetric stretch of NCH<sub>3</sub> group  
1425 (s), C-H bending  
726(s), 695 (s), monosubstituted benzene

UV:  $\lambda_{\max}$  = 257nm ( $\epsilon$ =1800)

MS: 351 (Ph<sub>3</sub><sup>120</sup>Sn<sup>+</sup>), 120 (<sup>120</sup>Sn<sup>+</sup>), 58 (Me<sub>2</sub>NCH<sub>2</sub><sup>+</sup>)

### 35. 3-N,N'-Dimethylamino-1-trimethylsilylpropane

This compound was prepared by the method described in experiment 32, using 3-dimethylaminopropylchloride (5.0g;0.041mol), chlorotrimethylsilane (3.7g;0.034mol), magnesium turnings (1.07g;0.045mol), and 1,2-dibromoethane (0.5ml) with irradiation of ultrasound for 4h. The residue was purified by column chromatography (CHCl<sub>3</sub>/silica; R<sub>f</sub>=0.65) which gave 2.0g (37%) yield.

#### Analysis

<sup>1</sup>H NMR: Relative to SiMe<sub>3</sub>: 0.00 (s, 9H), 0.40-0.50 (m, 2H),  
1.30-1.50 (m, 2H), 2.20-2.60 (m, 8H)

IR: 2953 (s), 2896 (m), C-H stretching  
2815 (m), C-H asymmetric stretch of NCH<sub>3</sub> group  
2765 (m), C-H symmetric stretch of NCH<sub>3</sub> group  
1463 (m), C-H deformation  
1248 (s), Si-C stretch

MS: M<sup>+</sup> 159, 73 (SiMe<sub>3</sub><sup>+</sup>), 58 (Me<sub>2</sub>NCH<sub>2</sub><sup>+</sup>)

UV:  $\lambda_{\max}$  = 273nm ( $\epsilon$  = 100)

### 36. 3-N,N'-Dimethylamino-1-tri-n-butylstannylpropane

This compound was prepared by the method described in experiment 32, using 3-dimethylaminopropylchloride (3.0g;0.025mol), chlorotri-n-butylstannane (6.7g;0.021mol), magnesium turnings (0.65g;0.027mol), and 1,2-dibromoethane (0.5ml) with irradiation of ultrasound for 2h. Bulb to bulb distillation of the residue gave 2.8g (35%) yield with bp 95°/0.01mm (lit bp 120°C/0.1mm; Suggs and Lee, 1986)

#### Analysis

<sup>1</sup>H NMR: 0.70-1.70 (m, 31H), 2.20 (m, 8H)

IR: 2955 (s), C-H asymmetric stretch of CH<sub>3</sub> group  
2923 (s), C-H asymmetric stretch of CH<sub>2</sub> group  
2871 (s), C-H symmetric stretch of CH<sub>3</sub> group  
2854 (s), C-H symmetric stretch of CH<sub>2</sub> group  
2813 (m), C-H asymmetric stretch of NCH<sub>3</sub> group  
2764 (m), C-H symmetric stretch of NCH<sub>3</sub> group  
2720 (w), C-H asymmetric stretch of NCH<sub>2</sub> group  
1461 (m), 1375 (m), C-H bending

MS: M<sup>+</sup> 376, 374, 372 (<sup>120</sup>Sn, <sup>118</sup>Sn, <sup>116</sup>Sn respectively)  
291, 289, 287; Sn(*n*-butyl)<sub>3</sub><sup>+</sup> (<sup>120</sup>Sn, <sup>118</sup>Sn, <sup>116</sup>Sn respectively)  
235, 233, 231; SnH(*n*-butyl)<sub>2</sub><sup>+</sup> (<sup>120</sup>Sn, <sup>118</sup>Sn, <sup>116</sup>Sn respectively)  
177, 175, 173; Sn(*n*-butyl)<sup>+</sup> (<sup>120</sup>Sn, <sup>118</sup>Sn, <sup>116</sup>Sn respectively)  
121, 119, 117; SnH<sup>+</sup> (<sup>120</sup>Sn, <sup>118</sup>Sn, <sup>116</sup>Sn respectively)

58;  $\text{Me}_2\text{NCH}_2^+$

UV:  $\lambda_{\text{max}} = 270\text{nm}$  ( $\epsilon=100$ )

### 37. 2-Dimethylaminoethyltrimethylstannane

This compound was prepared by the method described in experiment 32, using 2-dimethylaminoethylchloride (1.3g;0.012mol), chlorotrimethylstannane (2.0g;0.010mol), magnesium turnings (0.31g;0.013mol), and 1,2-dibromoethane (0.5ml) with irradiation of ultrasound for 2h. Bulb to bulb distillation of the residue gave 1.1g (45%) yield with bp  $82^\circ\text{C}$ .

#### Analysis

$^1\text{H}$  NMR: relative to  $\text{SnMe}_3$ ; 0.00 (s,9H), 0.70 (t,2H), 2.10 (m,8H)

IR: 2974 (s), 2937 (s), 2856 (s), C-H stretching  
2814 (s), C-H asymmetric stretch of  $\text{NCH}_3$  group  
2766 (s), C-H symmetric stretch of  $\text{NCH}_3$  group  
2721 (m), C-H asymmetric stretch of  $\text{NCH}_2$  group  
1460 (m), 1371 (m), C-H bending  
766 (s), Sn-C stretching of  $\text{SnMe}_3$

MS:

$M^+$  236, 234, 232 ( $^{120}\text{Sn}$ ,  $^{118}\text{Sn}$ ,  $^{116}\text{Sn}$  respectively)  
 165, 163, 161;  $\text{Sn}(\text{Me})_3^+$  ( $^{120}\text{Sn}$ ,  $^{118}\text{Sn}$ ,  $^{116}\text{Sn}$  respectively)  
 150, 148, 146;  $\text{Sn}(\text{Me})_2^+$  ( $^{120}\text{Sn}$ ,  $^{118}\text{Sn}$ ,  $^{116}\text{Sn}$  respectively)  
 135, 133, 131;  $\text{Sn}(\text{Me})^+$  ( $^{120}\text{Sn}$ ,  $^{118}\text{Sn}$ ,  $^{116}\text{Sn}$  respectively)  
 120;  $\text{Sn}$  ( $^{120}\text{Sn}$ )  
 58;  $\text{Me}_2\text{NCH}_2^+$

UV:  $\lambda_{\text{max}} = 269\text{nm}$  ( $\epsilon=100$ )

### 3.8 References

- Block, H., Ledwith, A., and Taylor, A.R., (1971). *Polymer*, **12**, 271
- Bock, H., Kaim, W., Kira, M., Osawa, H., and Sakurai, H., (1979). *J.Organomet.Chem.*, **164**, 295
- Bowser, R., and Davidson, R.S., (1992). "The use of Ultrasound in Organic Synthesis", Price, G.J. (Ed.), Royal Society of Chemistry, 50-58
- Bryson, T.A., Bonitz, G.H., Reichel, C.J., and Dardis, R.E., (1980). *J.Org.Chem.*, **45**, 524
- Butcher, E., Rhodes, C.J., Standing, M., Bowser, R., and Davidson, R.S., (1992a). *J.Chem.Soc., Perkin Trans. 2*, 1469
- Butcher, E., Rhodes, C.J., Bowser, R., and Davidson, R.S., (1992b). *J.Organomet.Chem.*, **436**, C5
- Cullis, C.F., Herron, D., and Hirschler, M.M., (1985). *Combustion and Flame*, **59**, 151
- Davidson, R.S., and Goodin, J.W., (1982). *Europ.Polym.J.*, **18**, 597
- Eastland, G.W., Rao, D.N.R., and Symons, M.C.R., (1984).

*J.Chem.Soc., Perkin Trans. II*, 1551

Hasegawa, E., Brumfield, M.A., Mariano, P.S., and Yoon, U.C., (1988a). *J.Org.Chem.*, **53**, 5435

Hasegawa, E., Xu, W., Mariano, P.S., Yoon, U.C., and Kim, K.U., (1988b). *J.Am.Chem.Soc.*, **110**, 8099

Hutchinson, J., Lambert, M.C., and Ledwith, A., (1973). *Polymer*, **14**, 250

Hutchinson, J., and Ledwith, A., (1973). *Polymer*, **14**, 405

Ledwith, A., and Purbrick, M.D., (1973). *Polymer*, **14**, 521

Meganem, F., (1980). *J.Soc.Chim.Tunis.*, (3), 13

Nakano, M., and Sato, Y., (1985). *J.Chem.Soc., Chem.Commun.*, 1684

Nakano, M., and Sato, Y., (1987). *J.Org.Chem.*, **52**, 1844

Naruta, Y., Nishigaichi, Y., and Maruyama, K., (1986). *Chem.Lett.*, 1857

Pine, S.H., (1970). "*Org.Reactions*", **18**, 403, Wiley, NY

Sander, M.R., Osborn, C.L., and Trecker, D.J., (1972).

*J. Polym. Sci, A1, 10, 3173*

Sato, Y., Ban, Y., (1973). *J. Org. Chem., 38, 4373.*

Sato, Y., Ban, Y., and Shirai, H., (1974). *J. Chem. Soc., Chem. Commun., 182*

Sato, Y., Toyooka, T., Aoyama, T., and Shirai, H., (1975).  
*J. Chem. Soc., Chem. Commun., 640*

Sato, Y., Ban, Y., and Shirai, H., (1976).  
*J. Organomet. Chem., 113, 115*

Sato, Y., and Sakakibara, H., (1979). *J. Organomet. Chem., 166, 303*

Suggs, J.W., and Lee, K.S., (1986). *J. Organomet. Chem., 299, 297*

Vedeneyev, V.I., Gurvich, L.V., Kondrat'yev, V.N., Medvedev, V.A., and Frankevich, Ye.L., (1966). "Bond Energies, Ionisation Potentials and Electron Affinities", Arnold, London

Wardell, J.L., (1978). *Inorg. Chim. Acta, 26, L18*

Ger. Offen. 2,801,700

US 3,853,994

## **Chapter 4.**

# **PHOTOINITIATION OF FREE RADICAL AND CATIONIC POLYMERISATION USING IRON-ARENE COMPLEXES**

#### 4.1 Introduction

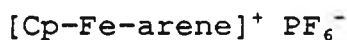
The first example of a transition metal sandwich complex that involved coordination of both a cyclopentadienyl and a benzenoid ring to the central metal atom was reported by Coffield *et al* in 1957 who prepared the iodide salt of  $\eta^6$ -mesitylene- $\eta^5$ -cyclopentadienyliron(II) (Coffield *et al*, 1957). The  $\eta^6$ -benzene analogue was prepared in 1960 by Green *et al* (Green *et al*, 1960). Extensive work by Nesmeyanov *et al* led to the development of a synthetic route of general applicability for a number of  $\eta^6$ -benzenoid- $\eta^5$ -cyclopentadienyl iron(II) complexes. The earliest example of this route reported in 1963 involved the reaction of ferrocene and benzene in the presence of aluminium chloride and aluminium powder as shown in equation 4.1 (Nesmeyanov *et al*, 1963).



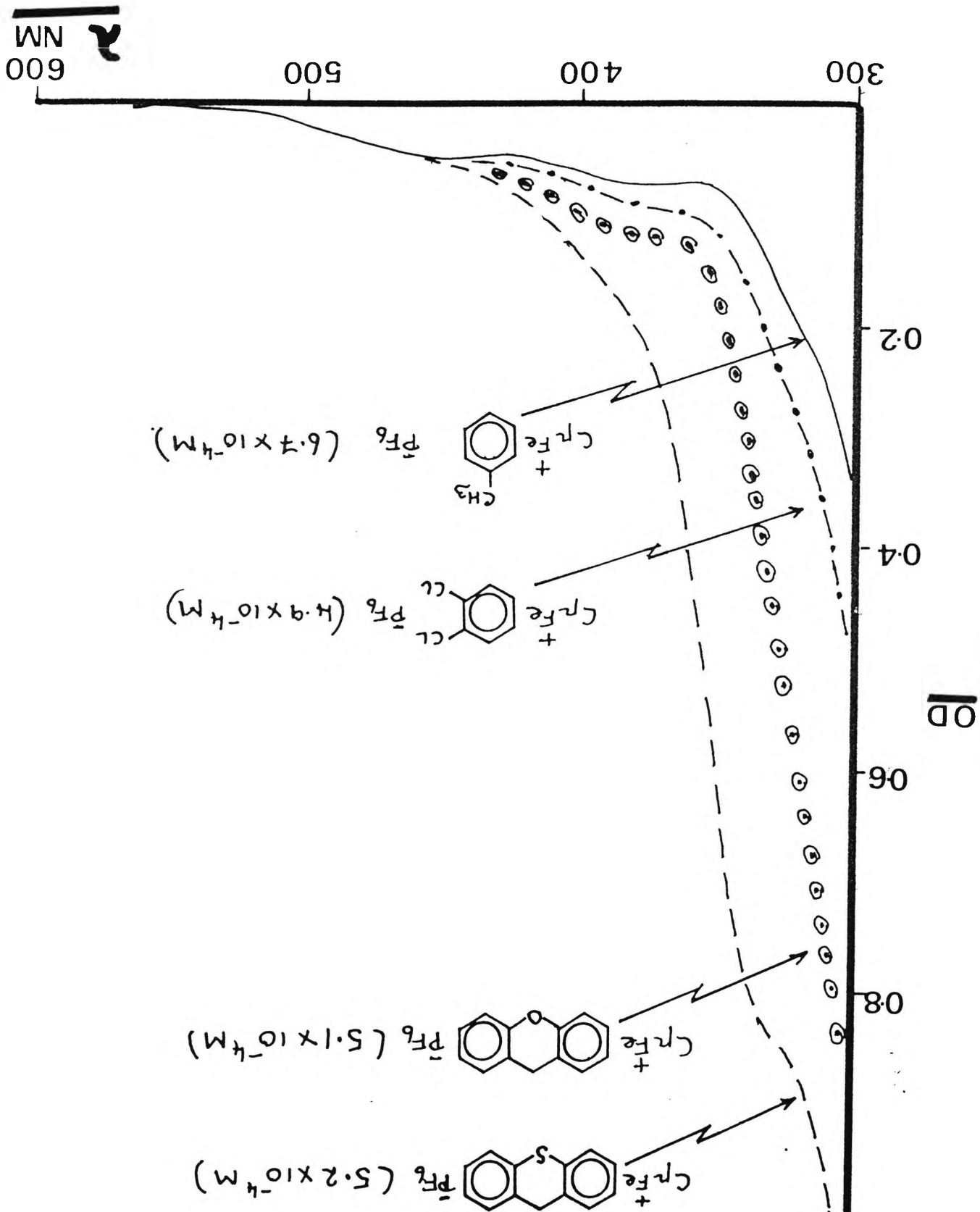
The iron-arene complexes are commonly isolated as either the hexafluorophosphate or the tetrafluoroborate salts. Various complexes were synthesised which contained electron-donating or electron-accepting substituents on either the arene or the cyclopentadienyl rings (Nesmeyanov *et al*, 1965; Nesmeyanov *et al*, 1966; Nesmeyanov *et al*, 1967). When polyaromatics such as biphenyl, naphthalene, and fluorene

were used in the ferrocene cyclopentadienyl ring replacement reaction Nesmeyanov et al discovered that only one of the rings took part in the ligand exchange with ferrocene (Nesmeyanov et al, 1966). It was also shown by Lee et al that the  $\pi$ -arene bis( $[\pi$ -cyclopentadienyl]iron) dications could be synthesised by reacting the corresponding monocations with excess ferrocene to substitute the remaining aromatic rings (Lee et al, 1972).

A number of iron arene salts were synthesised using the general procedure of Nesmeyanov outlined in equation 4.1. All the salts prepared were isolated as the hexafluorophosphate derivatives and may be represented by the general formulae:

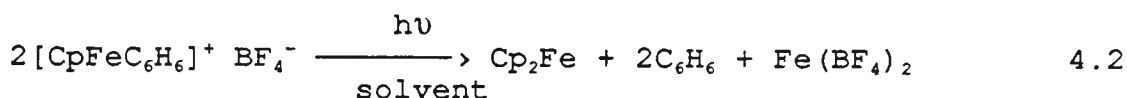


where the arene may be toluene, 4-chlorotoluene, 1,2-dichlorobenzene, fluorene, thioxanthene, or xanthene. In the case of the latter three derivatives only one of the available benzene rings is coordinated to iron which gives rise to the monocationic species. The compounds synthesised exhibit good absorption properties in the UV region which renders them useful for initiation of polymerisation. Examples of a number of the UV spectra of the iron-arene complexes are shown below.



## 4.2 Photochemistry of iron-arene complexes

In 1970 Nesmeyanov *et al* reported on the photolysis of benzene cyclopentadienyliron(II) tetrafluoroborate (Nesmeyanov *et al*, 1970). Irradiation in a variety of organic solvents gave ferrocene, the free arene, and the inorganic ion as outlined in equation 4.2.

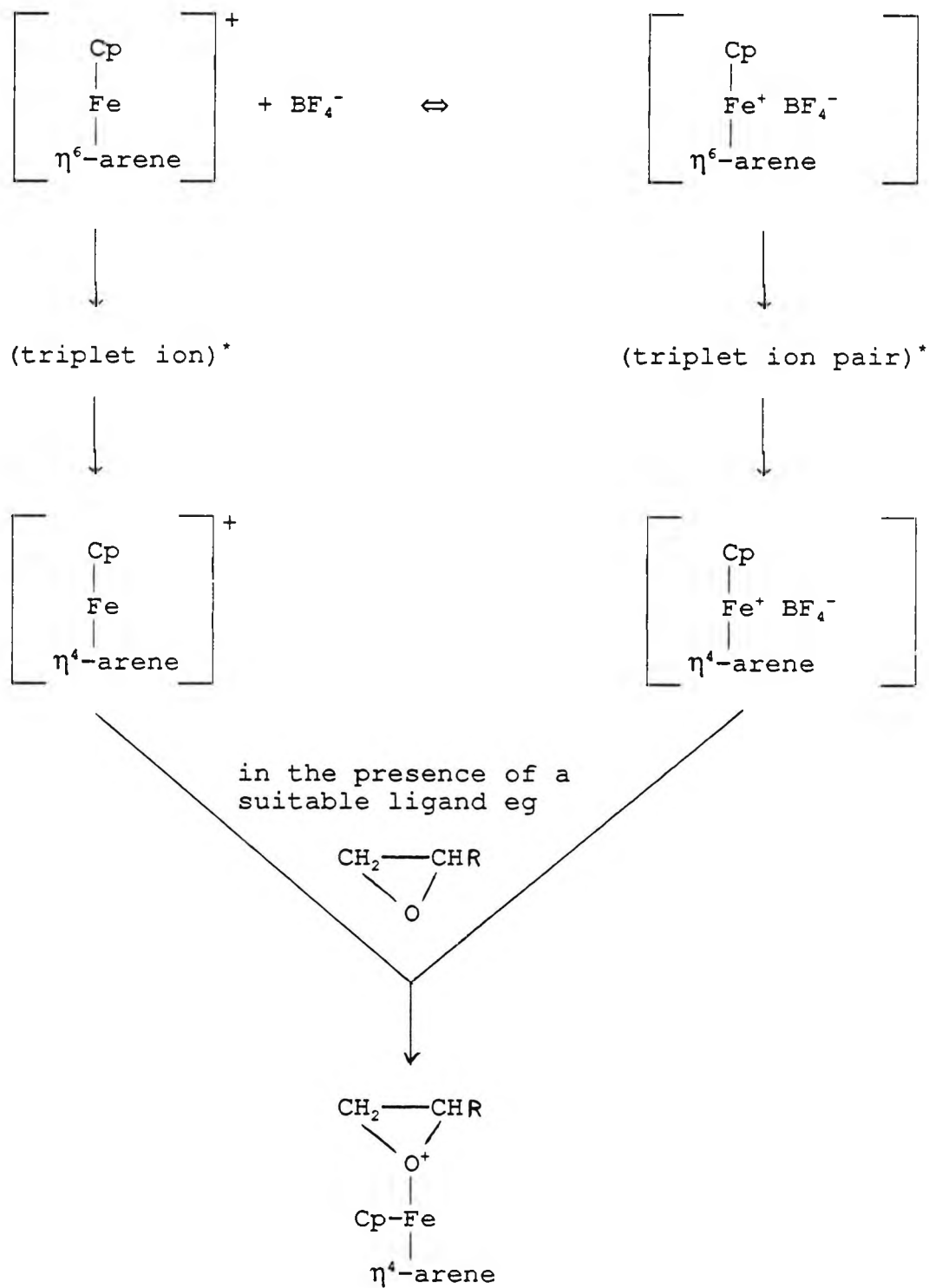


In the mid 1970's the electronic structure of  $[\text{CpFe-arene}]^+\text{X}^-$  complexes was investigated (Morrison *et al*, 1974; Morrison *et al*, 1975). This work showed by analogy to ferrocene that the low energy optical absorptions are spin allowed d-d transitions leading to  $a^1E_{1g}$ ,  $^1E_{2g}$ , and  $b^1E_{1g}$  states. Analysis of these states using molecular orbital theory leads to the prediction that excitation of the iron-arene complex will labilise the ligands (Albright, 1982; Zink, 1974). This prediction is supported by the experimental data. In 1980 Gill and Mann reported on the photochemically induced arene ligand replacement reactions of the cyclopentadienyl (p-xylene)iron(II) cation (Gill and Mann, 1980). Thus irradiation (436nm) of the ligand field bands of the cyclopentadienyl (p-xylene)iron(II) cation in dichloromethane gave a ligand field excited state which resulted, in the presence of suitable ligands such as CO, in products arising from metal-ligand bond scission including

cyclopentadienyliron(II)  $(\text{CO})_3^+$ . In 1983 the same workers extended the earlier work by Nesmeyanov *et al* (Nesmeyanov *et al*, 1970) when they reinvestigated the photolysis of an iron-arene complex in acetonitrile (Gill and Mann, 1983). They discovered that on photolysis of the cyclopentadienyl (*p*-xylene)iron(II) cation in acetonitrile a purple species characterised as the cyclopentadienyliron(II)  $(\text{CH}_3\text{CN})_3$  cation was isolated at  $-40^\circ\text{C}$ . This intermediate was then used to synthesise a number of iron(II)cyclopentadienyl complexes with a wide range of ligand substitution. In the same year Mann *et al* reported on the solvent and ion-pairing effects on the photochemical arene replacement reactions of the cyclopentadienyl (*p*-xylene)iron(II) cation (Schrenk *et al*, 1983). They suggested that the arene replacement reaction is consistent with nucleophilic attack of the medium on a ligand field excited state of iron. This can occur through pathways involving solvent assisted steps (in polar, nucleophilic solvents) or anion assisted steps (in non polar, weakly nucleophilic solvents). These experiments and others led Mann to propose that the photoactive species in these reactions is the  $a^3E_{1g}$  ligand field state with a triplet energy of 42kcal/mol and a short triplet lifetime of  $< 1.5\text{ns}$  (McNair *et al*, 1984). More recently further advances have been made on the mechanism of photolysis of the iron-arene complexes (Chrisope *et al*, 1989). The mechanism of photolysis was shown to proceed via a multistep process in which the replacement of the arene is controlled by the identity of the counterion and the concentration of the

attacking ligands. A summary of the mechanism is given below in scheme 4.1.

Scheme 4.1 Photochemistry of iron-arene complexes

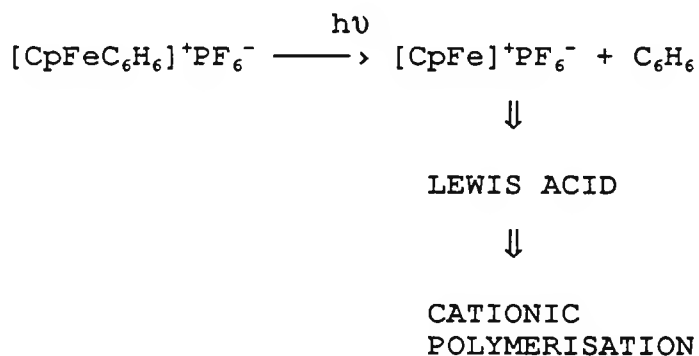


It is this reaction with epoxides that has received much attention in the field of photoimaging discussed in the next section.

#### 4.3 Photoimaging using iron-arene complexes

On photolysis of the iron-arene complexes the uncharged ligand is removed resulting in an unsaturated cation, a Lewis acid, which is capable of initiating cationic polymerisation (EP 0094915, 1984; EP 0126712; Zweifel and Meier, 1985) as shown in scheme 4.2.

Scheme 4.2 Mechanism of cationic polymerisation of epoxides using iron-arene salts



The photolysis of the iron-arene complexes was sensitised with the use of anthracene derivatives (Meier and Zweifel, 1985).

The spectral response of the iron-arene initiators was

altered by varying the arene ligand and in some cases the initiators were suitable for laser applications (Meier and Zweifel, 1986). Photolysis in the presence of ethylene oxide yielded white crystalline iron crown ether complexes whose structure was determined by X-ray analysis (Meier and Rhis, 1985), indicating that iron-arene complexes form Lewis acids on irradiation. The initial UV absorption of these initiators changes on irradiation with a gradual reduction in UV absorbance as irradiation proceeds. This leads to a bleachable system so that light penetration is possible throughout the film thickness. It was found that heat treatment was required to complete the polymerisation to a fully crosslinked resin. It was noted that the oxidation state of the iron in these photoinitiators is +2, before and after irradiation. Oxidation of the iron to the +3 state was only possible after irradiation. If the irradiation was carried out in the presence of an oxidant, such as cumene hydroperoxide, the iron +3 species, a stronger Lewis acid, was obtained with increased reactivity in epoxide polymerisation. As a result of electron exchange interactions in the iron complex/oxidant system, radical species were formed (in addition to Lewis acid) and mixed radical/cationic polymerisations are possible.

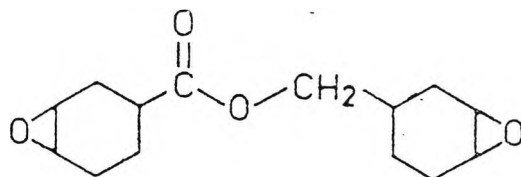
From DSC experiments it was shown that the iron-arene photoinitiators are less reactive than Brønsted acids obtained from triarylsulphonium salts. A heat treatment (around 100°C) was required to complete polymerisation. The

DSC trace showed a narrow enthalpy peak which has been interpreted mechanistically as a uniform reaction pathway (Lohse and Zweifel, 1986). DSC evidence was also presented to show that in the presence of oxidant an iron +3 species was more reactive (heat treatment 50°C) than the iron +2 species in the absence of any oxidant. The photoinitiating properties of several iron arene complexes used in the polymerisation of epoxides have been reviewed in a number of articles (Curtis et al, 1986; Roloff et al, 1986; Klingert et al, 1988).

#### 4.4 UV curing results for iron-arene complexes in cationic polymerisation

A number of the iron-arene salts prepared have been investigated for their use as photoinitiators in the presence of a typical cycloaliphatic difunctional epoxide, 3,4-epoxycyclohexylmethyl-3',4'-epoxycyclohexane carboxylate (Degacure K126 from Degussa) shown below.

Structural Formula



The photoinitiators were incorporated at 1% w/w in the above monomer and tested on the UV Colordry moving belt system described earlier (see section 1.7.1). Since the monomer molecule contains two epoxy groups, chain propagation will

develop in three dimensions to yield ultimately a highly crosslinked polymer network. The results are presented below in table 4.1.

Table 4.1 UV curing results for the cationic polymerisation of 3,4-epoxycyclohexylmethyl-3',4'-epoxycyclohexane carboxylate using iron-arene photoinitiators

E X P T	INITIATOR	NUMBER OF PASSES			
		Touching Quartz #	Touching Glass #	In Air	Glass Filter
1	[CpFe-fluorene] <sup>+</sup>	14	18	3	7
2	[CpFe-xanthene] <sup>+</sup>	19	19	4	10
3	[CpFe-toluene] <sup>+</sup>	11	11	2	4
4	[CpFe-thioxanthene] <sup>+</sup>	*	*	*	*

All above iron complexes isolated as their PF<sub>6</sub><sup>-</sup> salts

(Moving belt speed = 10ft/min, Coating thickness = 25μ)

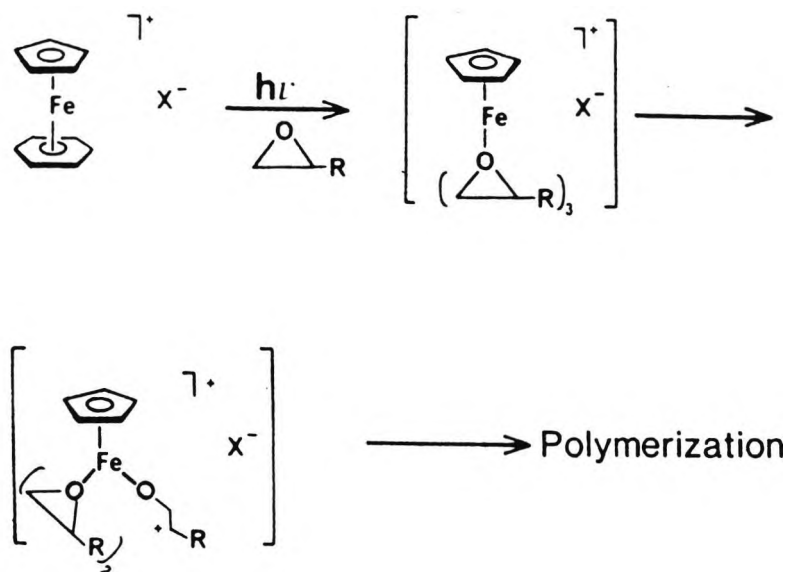
\* curing observed, but not to tack-free state after 30 passes

# curing observed at edges first

The first general point to note is that the rate of cure in air and under glass filter is greater than the corresponding touching quartz or touching glass experiment. Thus the polymerisation proceeds at a greater rate for cationic polymerisation using these initiators when air is present. This is in marked contrast to free radical polymerisation

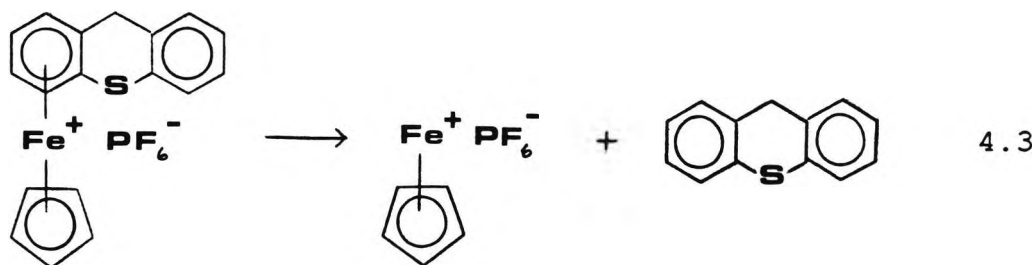
where the reverse is normally true due to the oxygen inhibition effect. It is proposed that oxygen actually enhances the cure rate for these compounds in cationic polymerisation. The oxidation state of the iron in these complexes is +2. The proposed role of oxygen is to oxidise the compounds with iron in the +2 oxidation state to the +3 oxidation state. Iron in the +3 oxidation state is a better Lewis acid than the +2 oxidation state. This effectively means that the better Lewis acid (+3 oxidation state) will be more reactive towards an epoxide, a Lewis base, and hence require a lower number of passes, indicating a greater rate of polymerisation, to achieve a tack-free cure. This process is outlined in scheme 4.3.

Scheme 4.3 A general mechanism for the polymerisation of epoxides using iron-arene salts



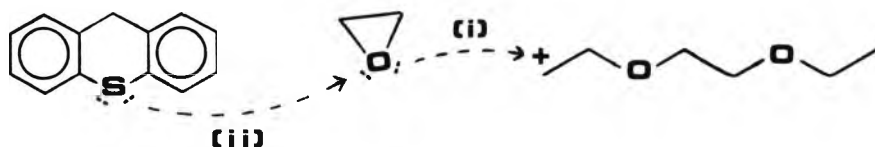
This also explains why the results with touching quartz and touching glass cure is always noticed at the edges first since oxygen is present here and the above scheme may operate.

The second point to note is that the thioxanthene derivative (EXPT 4, Table 4.1) was observed to cure well initially but does not reach a tack free cure after 30 passes. This could be due to the nucleophilic character of sulphur and its ability to increase its coordination. On photolysis a Lewis acid is released, which can initiate polymerisation, along with the thioxanthene group as shown in equation 4.3.



As polymerisation proceeds the sulphur atom of the thioxanthene group can act as a nucleophile to attack the growing polymer chain terminating polymerisation as shown in scheme 4.4.

Scheme 4.4 The nucleophilic character of sulphur in the cationic polymerisation of an epoxide



This would result in a large number of low molecular weight polymers which could explain the observed phenomenon.

Attempts were made to increase the rate of cationic polymerisation using the iron-arene compounds in conjunction with co-initiators. The approach used was to incorporate electron acceptors into the formulation in order that the oxidation of the iron-arene complexes from the +2 oxidation state to the +3 oxidation state would be accelerated giving rise to a greater rate of polymerisation. The iron-arene complexes (1% w/w) were used in conjunction with;

(1)  $\text{Ph}_2\text{I}^+\text{PF}_6^-$  (1% w/w)

(2)  $\text{Ph}_3\text{S}^+\text{PF}_6^-$  (1% w/w)

which were incorporated into the above monomer. The results indicated no beneficial effect of adding either of the above compounds. Previous studies indicated that the reactivity of the iron-arene complexes in cationic polymerisation can be enhanced

in the presence of the oxidant cumene hydroperoxide (Meier and Zweifel, 1986). This suggests that the role of oxygen is crucial in the electron exchange on going from the iron (II) to the iron (III) species.

#### 4.5 UV curing results for iron-arene complexes in free radical polymerisation

Although there have been several reports on the initiation of cationic polymerisation using the iron-arene salts relatively little attention has been given to the free radical initiating properties of these complexes. One recent report gave details of the related ferrocene sensitised photopolymerisations of vinyl monomers by means of kinetic and spectroscopic analyses (Tsubakiyama *et al*, 1991).

It was decided to investigate the possible free radical initiating properties of the iron-arene complexes.

The iron-arene complexes (1% w/w) were tested in both tripropyleneglycol diacrylate (TPGDA) and trimethylolpropane triacrylate (TMPTA) using the UV Colordry apparatus described earlier (see section 1.7.1). The results using the difunctional monomer, TPGDA, are presented in table 4.2, and the results using the trifunctional monomer, TMPTA, are given in table 4.3.

Table 4.2 UV curing results for the free radical polymerisation of TPGDA initiated by iron-arene complexes

E X P T	INITIATOR	NUMBER OF PASSES			
		Touching Quartz	Touching Glass	In Air	Glass Filter
1	[CpFe-thioxanthene] <sup>+</sup>	9	20	28	*
2	[CpFe-xanthene] <sup>+</sup>	12	*	*	*
3	[CpFe-1,2-dichlorobenzene] <sup>+</sup>	6	25	*	*
4	[CpFe-toluene] <sup>+</sup>	10	19	*	*
5	[CpFe-fluorene] <sup>+</sup>	11	25	*	*
6	[CpFe-4-chlorotoluene] <sup>+</sup>	9	(*)	*	*
7	TPGDA	*	*	*	*

All above iron complexes isolated as their PF<sub>6</sub><sup>-</sup> salts

(Moving belt speed = 10ft/min, Coating thickness = 25μ)

\* curing not observed after 30 passes

(\*) curing observed but not tack-free after 30 passes

Table 4.3 UV curing results for the free radical polymerisation of TMPTA initiated by iron-arene complexes

E X P T	INITIATOR	NUMBER OF PASSES			
		Touching Quartz	Touching Glass	In Air	Glass Filter
1	[CpFe-4-chloro- toluene] <sup>+</sup>	5	10	*	*
2	[CpFe-1,2-dichl- orobenzene] <sup>+</sup>	4	7	*	*
3	[CpFe-thioxanth- ene] <sup>+</sup>	4	9	*	*
4	[CpFe-fluorene] <sup>+</sup>	4	8	*	*
5	[CpFe-xanthene] <sup>+</sup>	6	13	*	*
6	[CpFe-toluene] <sup>+</sup>	3	6	*	*
7	TMPTA	6	*	*	*

All above iron complexes isolated as their PF<sub>6</sub><sup>-</sup> salts

Moving belt speed = 10ft/min, \* = curing not observed after 30 passes

The results in tables 4.2 and 4.3 indicate that the iron-arene complexes will initiate the polymerisation of acrylate monomers, presumably via a free radical pathway. The results also show that the rate of polymerisation is greater for the triacrylate (TMPTA) than for the diacrylate (TPGDA) as evidenced by the reduced number of passes for the complexes in table 4.3 when compared to table 4.2.

One interesting result in TPGDA is that the thioxanthene derivative (EXPT 1, Table 4.2) cures when touching glass (20 passes) and also in air (28 passes). It is proposed that this is due to the special nature of the thioxanthene group in reducing the inhibitive effect of oxygen on the polymerisation rate (see section 2.5.1).

#### 4.5.1 UV curing results for iron-arene complexes with N-methyldiethanolamine in free radical polymerisation

An attempt was made to reduce the oxygen inhibition effect for the free radical polymerisation of TPGDA using the iron-arene complexes. Thus N-methyldiethanolamine (5% w/w), which has been shown to act as an efficient oxygen scavenger (see section 1.4.5), was incorporated into the formulation along with the corresponding iron-arene initiator (1% w/w). The UV curing results are presented below in table 4.4.

Table 4.4 UV curing results for the free radical polymerisation of TPGDA initiated by iron-arene complexes (1% w/w) in the presence of N-methyldiethanolamine (5 %w/w)

E X P T	INITIATING SYSTEM	NUMBER OF PASSES			
		Touching Quartz	Touching Glass	In Air	Glass Filter
1	[CpFe-thioxanthene] <sup>+</sup> + Am	4 (9)	7 (20)	24 (28)	* (*)
2	[CpFe-xanthene] <sup>+</sup> + Am	9 (12)	* (*)	* (*)	* (*)
3	[CpFe-1,2-dichlorobenzene] <sup>+</sup> + Am	10 (6)	* (25)	* (*)	* (*)
4	[CpFe-toluene] <sup>+</sup> + Am	3 (10)	16 (19)	* (*)	* (*)
5	[CpFe-fluorene] <sup>+</sup> + Am	14 (11)	* (25)	* (*)	* (*)
6	[CpFe-4-chlorotoluene] <sup>+</sup> + Am	25 (9)	* (*)	* (*)	* (*)
7	Am	1	3	30	*

All above iron complexes isolated as their PF<sub>6</sub><sup>-</sup> salts

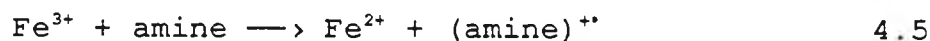
Am = N-methyldiethanolamine incorporated at 5% w/w TPGDA

(Moving belt speed = 10ft/min, Coating thickness = 25μ)

\* curing not observed after 30 passes

The amine used, N-methyldiethanolamine, will initiate polymerisation when it is used on its own (EXPT 7, table 4.4). The mechanism of this polymerisation is probably one of H-abstraction by the monomer from the amine to give α-aminoalkyl radicals which are capable of both (i) initiating polymerisation and (ii) reducing the effect of oxygen

inhibition. In comparison to this result all the other experiments in table 4.4 show a decrease in the rate of polymerisation. A possible explanation for this phenomenon is that the amine is being consumed in other reactions which reduce its effectiveness in its dual role. It is proposed that the amine reacts with the iron (III) species (produced in a photocatalysed oxidative process from the iron (II) species) which reduces the effectiveness of both the iron (III) species and the amine in initiating polymerisation as outlined in equations 4.4 and 4.5 below.



When the original photoactive iron (II) species in equation 4.4 has been consumed, producing the photoinactive iron (II) species in equation 4.5, then the amine can go on to initiate polymerisation via the  $\alpha$ -aminoalkyl radicals. Due to competitive absorption with the iron species and arene fragments the efficiency of this process is somewhat reduced in all cases when compared to the case where the amine is used on its own. It would appear that it is not beneficial to use electron donors as co-initiators in radical polymerisation in conjunction with iron-arene complexes.

## 4.6 Real-Time Infrared (RTIR) Spectroscopy results for iron-arene complexes

### 4.6.1 Introduction

The iron-arene compounds have been tested utilising the technique of RTIR Spectroscopy which has been described earlier (see section 1.7.2). The compounds have been irradiated using a medium pressure mercury lamp for a period of five minutes during which time the polymerisation kinetic curve was recorded. It is possible to calculate both the degree of conversion and the rate of polymerisation,  $R_p$ , at any time during the experiment.

### 4.6.2 RTIR results of iron-arene complexes in free radical polymerisation

A summary of the results is given below in table 4.5.

Table 4.5 RTIR spectroscopy results of the free radical polymerisation of TMPTA initiated by iron-arene complexes

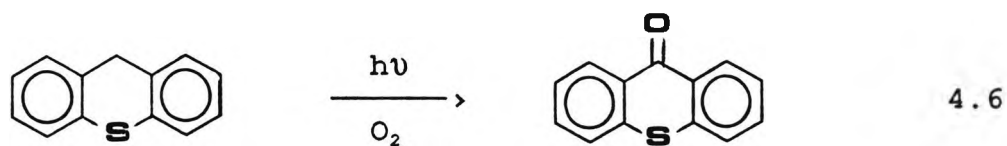
EXPT	INITIATOR	Induction Period/seconds	R <sub>p</sub> (max) / 10 <sup>-2</sup> mol/l/s	Degree of Conversion (5 minutes) / %
1	[CpFe-toluene] <sup>+</sup>	36	0.9	16
2	[CpFe-4-chloro-toluene] <sup>+</sup>	18	0.9	18
3	[CpFe-1,2-dichlorobenzene] <sup>+</sup>	15	1.3	20
4	[CpFe-thioxanthene] <sup>+</sup>	1	1.9	34
5	[CpFe-fluorene] <sup>+</sup>	18	1.3	25
6	[CpFe-xanthene] <sup>+</sup>	6	1.5	24

All above complexes isolated as their PF<sub>6</sub><sup>-</sup> salts and formulated at 0.5% w/w in TMPTA

The first point to make is that the iron-arene compounds are capable of initiating the free radical polymerisation of an acrylate monomer. This is evidenced by the reduction in the 810cm<sup>-1</sup> absorption in the IR spectrum corresponding to the disappearance of the C=C stretching vibration for all the compounds tested. A general trend that appears from table 4.5 is that the R<sub>p</sub>(max) value is related to the degree of conversion which in turn is related to the induction period observed.

Thus the toluene derivative (EXPT 1, Table 4.5) shows the longest induction period (36s), has the lowest degree of conversion (16%), and the lowest rate of polymerisation ( $0.9 \times 10^{-2}$  mol/l/s). In contrast to this the thioxanthene derivative (EXPT 4, Table 4.5) has the shortest induction period (1s), with the highest degree of polymerisation (34%), and the highest rate of polymerisation ( $1.9 \times 10^{-2}$  mol/l/s).

A further point of interest is the particularly short induction period of 1 second shown for the thioxanthene derivative. This is thought to be due to the role of the thioxanthene moiety in the polymerisation mechanism. The induction period is primarily due to the effect of oxygen inhibition of polymerisation. It is believed that the thioxanthene group has an effect on reducing the effect of oxygen inhibition on the polymerisation process. The thioxanthene group can react with oxygen present to yield thioxanthone thus reducing oxygen inhibition of polymerisation as shown below in equation 4.6.



#### 4.6.3 UV curing results for cationic polymerisation using an iron-arene salt sensitised with a diphenyliodonium salt

It is known that thioxanthone sensitises diphenyliodonium

salts in cationic polymerisation (Gatechair and Pappas, 1982). This sensitisation was proposed to be via an electron transfer mechanism and model calculations showed that the free energy for this process,  $\Delta G = -22\text{Kcal/mol}$ , which is in accordance with a diffusion controlled reaction (Rehm and Weller, 1969; Arnold and Maroulis, 1976). Therefore, it was decided to test  $\eta^6$ -thioxanthene- $\eta^5$ -cyclopentadienyliron hexafluorophosphate (1% w/w) in the presence of diphenyliodonium hexafluorophosphate (1% w/w) and the cycloaliphatic diepoxide monomer, 3,4-epoxycyclohexylmethyl-3',4'-epoxycyclohexane carboxylate, to see if any sensitisation of polymerisation occurred. The formulation was tested using the UV Colordry moving belt system (see section 1.7.1) the results are given in table 4.6.

Table 4.6 Cationic polymerisation of an epoxide using diphenyliodonium hexafluorophosphate sensitised with an iron arene salt

E X P T	INITIATOR	NUMBER OF PASSES			
		Touching Quartz	Touching Glass	In Air	Glass Filter
1	[CpFe-thioxanthene] <sup>+</sup>	(*)	(*)	(*)	(*)
2	Ph <sub>2</sub> I <sup>+</sup> PF <sub>6</sub> <sup>-</sup>	4	*	4	*
3	[CpFe-thioxanthene] <sup>+</sup> + Ph <sub>2</sub> I <sup>+</sup> PF <sub>6</sub> <sup>-</sup>	2	13	1	9
4	"	-	-	3	-

[CpFe-thioxanthene]<sup>+</sup> isolated as the PF<sub>6</sub><sup>-</sup> salt.

(Coating thickness = 25μ for all experiments, moving belt speed = 10ft/min for all experiments except EXPT 4 = 80ft/min)

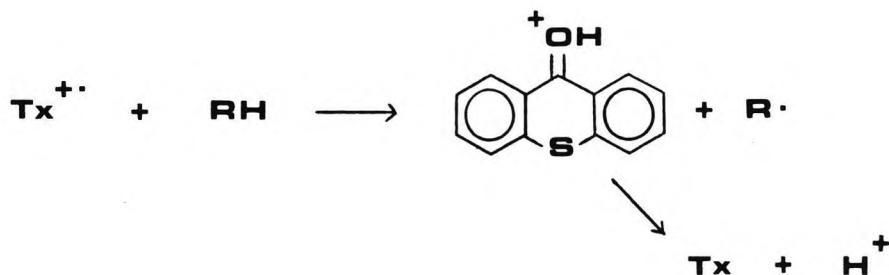
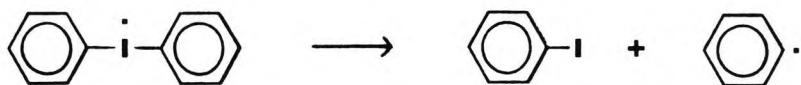
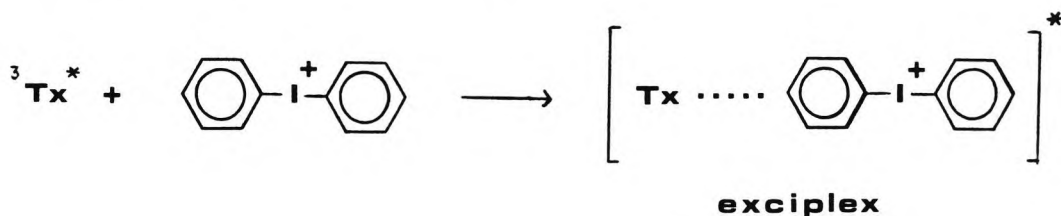
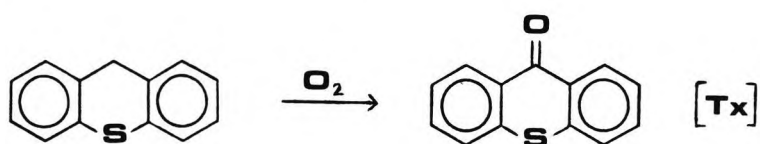
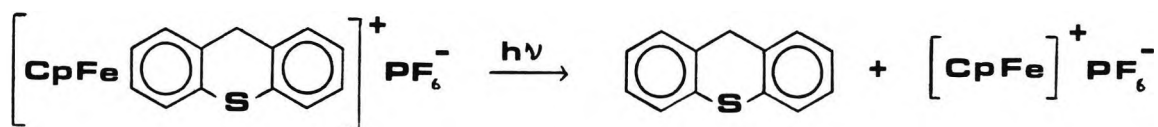
(\*) = curing observed but not to tack-free state

\* = curing not observed after 30 passes

- = experiment not performed

The results indicate a definite sensitisation for all four experimental conditions. What can be seen from table 4.6 is that the polymerisation proceeds at a greater rate when atmospheric oxygen is present than when it is excluded by the use of a touching slide (EXPT 3, Table 4.6). This can be seen when comparing the results of touching quartz (2 passes) versus in air (1 pass, or 3 passes at faster belt speed) where both experiments receive the full output of the lamp. This effect can also be seen when comparing the results of touching glass (13 passes) versus glass filter (9 passes) where both experiments receive the same amount of filtered light. This indicates that the presence of oxygen is important in the mechanism of polymerisation and the following sequence in scheme 4.5 is proposed to account for the above observations.

Scheme 4.5 The role of oxygen in the sensitisation of diphenyliodonium hexafluorophosphate in cationic polymerisation using  $\eta^6$ -thioxanthene- $\eta^5$ -cyclopentadienyliron hexafluorophosphate

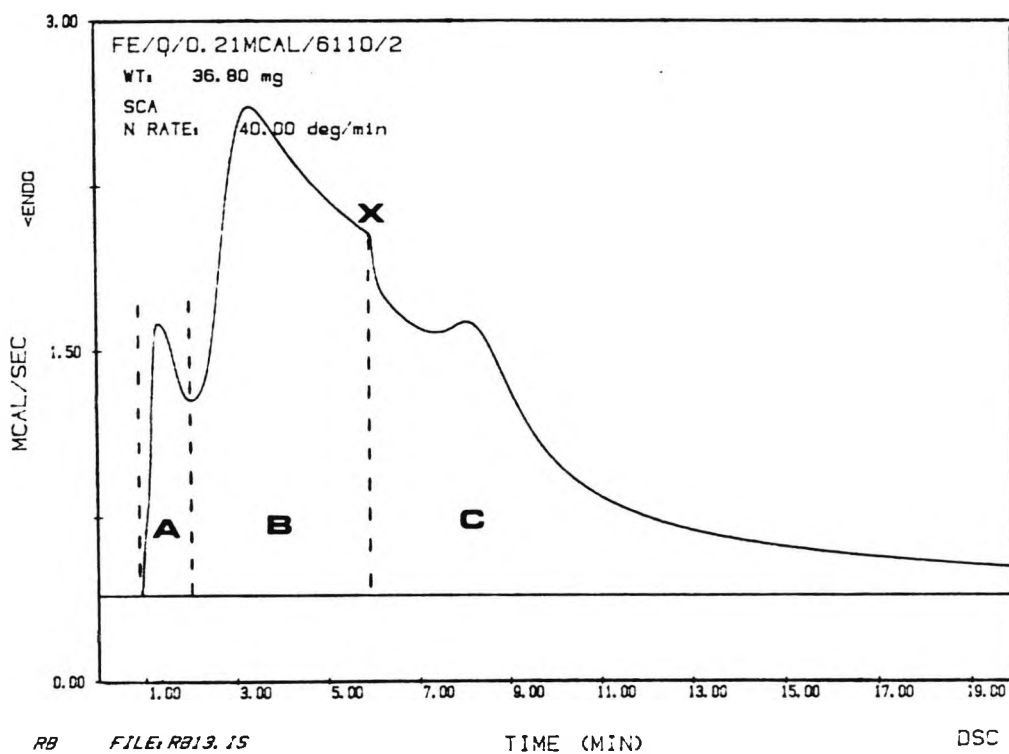


4.7 Photo-differential scanning calorimetry (Photo-DSC)  
results of iron-arene complexes

An iron arene complex has been tested using the technique of Photo-DSC described earlier (see section 1.7.3).

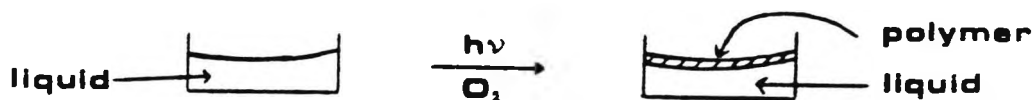
4.7.1 Photo-DSC results of iron-arene complexes in  
cationic polymerisation

Figure 4.1 The Photo-DSC results for the cationic polymerisation of an epoxide initiated by an iron-arene complex



A sample of  $\eta^6$ -fluorene- $\eta^5$ -cyclopentadienyliron hexafluorophosphate (1% w/w) in 3,4-epoxycyclohexylmethyl-3',4'-epoxycyclohexane carboxylate was irradiated in the presence of air to give the polymerisation trace in figure 4.1. The trace may be visualised in three different sections represented by;

A. The liquid sample initially forms a solid polymeric meniscus in the DSC sample pan as the initiator reacts with oxygen present at the air/liquid interface to effect polymerisation. This is represented below.



This gives rise to the sharp exothermic peak shown in A.

B. The remainder of the bulk in the DSC sample pan is polymerised in part B. The rate reaches a maximum and then slowly decreases.

C. At point X the light source was turned off as the rate of polymerisation is declining. The rate continues to decline and then proceeds to reach another maximum. This is thought to be due to the Tromsdorff Effect in which autoacceleration of polymerisation takes place. After the maximum the polymerisation rate gradually declines. It is noticeable that this decline is much more gradual than for a trace of a free radical polymerisation. This emphasises

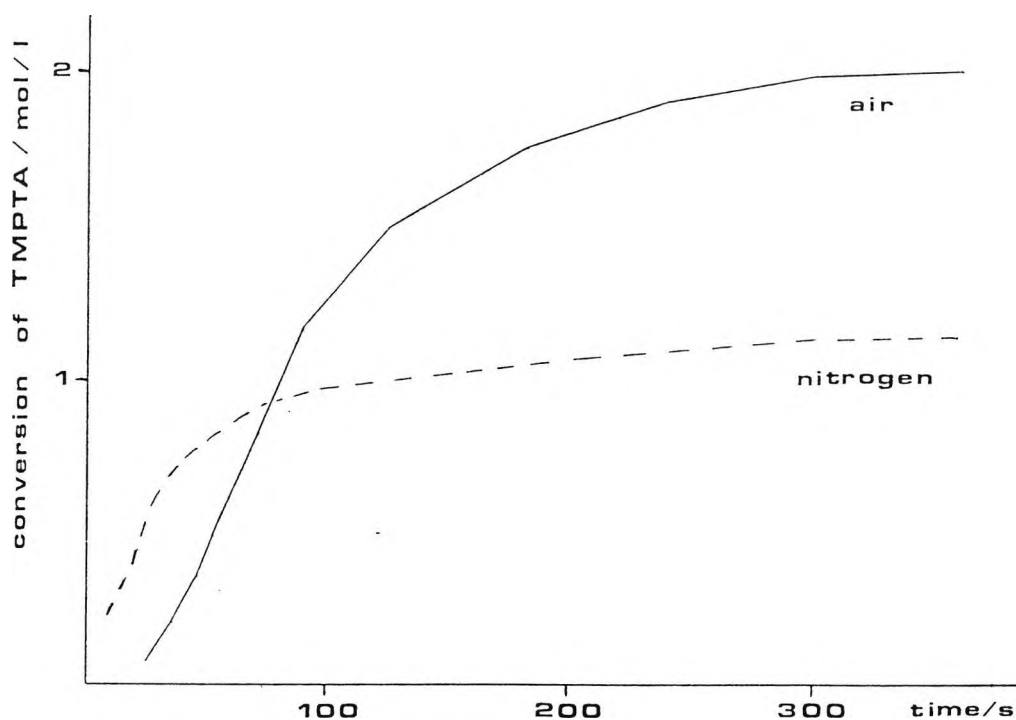
the 'living polymer' nature so often exhibited by cationic polymerisations.

A similar experiment was performed but this time the sample was irradiated in the presence of nitrogen instead of in air. During the same time period of irradiation no polymerisation was detected and the sample remained liquid in the DSC sample pan. This same sample was then irradiated in the presence of air (oxygen) and again no polymerisation was detected and the sample remained liquid after the same time period of irradiation. A possible explanation for this observation is that in the presence of nitrogen the initiator was photolysed giving rise to only iron II species which are not reactive at this light intensity and wavelength under isothermal conditions to initiate polymerisation. When air is readmitted into the DSC chamber the photoinitiator concentration has been depleted to a much lower level so that there is virtually no original photoinitiator present. This in effect means that no iron III species can be formed and explains why no polymerisation was observed. Therefore, to be of use this initiator must be photolysed in the presence of an oxidant (in this case oxygen) so that a beneficial effect on the rate of polymerisation may be seen.

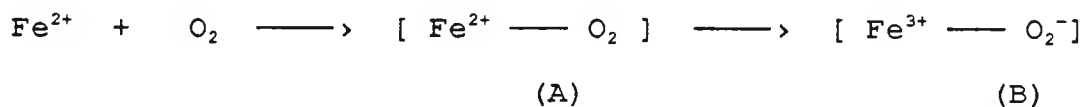
4.7.2 Photo-DSC results of iron-arene complexes in free radical polymerisation

Photo-DSC has been used to look at the free radical polymerisation of  $\eta^6$ -fluorene- $\eta^5$ -cyclopentadienyliron hexafluorophosphate (1% w/w) in the presence of TMPTA. Figure 4.2 shows the effect of irradiation of the complex in the presence of air and under nitrogen.

Figure 4.2 The Photo-DSC results for the free radical polymerisation of TMPTA, in air and under nitrogen, initiated by an iron-arene complex



As for cationic polymerisation it is proposed that the iron II species reacts with oxygen to produce an iron III species. The precise mechanism of this reaction is in some doubt but an initial step is likely to be:



The electronic possibilities of A include one-electron acceptance by  $\text{O}_2$  so that there is effectively a coordinated superoxide ion (and  $\text{Fe}^{3+}$ ) as shown in (B). This gives rise to a possibility of a radical species which could go on to initiate polymerisation.

In a nitrogen atmosphere there is virtually no induction period observed and polymerisation ensues. When air is present the polymerisation curve shows a noticeable induction period which is gradually overcome as the rate of polymerisation increases. This is presumably due to the reaction above occurring and giving rise to more free radical species. In the presence of air the degree of conversion is much greater than when nitrogen is present. This indicates that a certain amount of air is beneficial to the radical polymerisation using this initiator, though presumably there will be a balance between the beneficial effect, as it is used to oxidise the initiator, and the detrimental effect of oxygen inhibition of polymerisation.

A further experiment involved the use of an electron donor, benzyltri-*n*-butylstannane, with the fluorene derivative. Independent experiments were performed in air (oxygen) to give DSC results of;

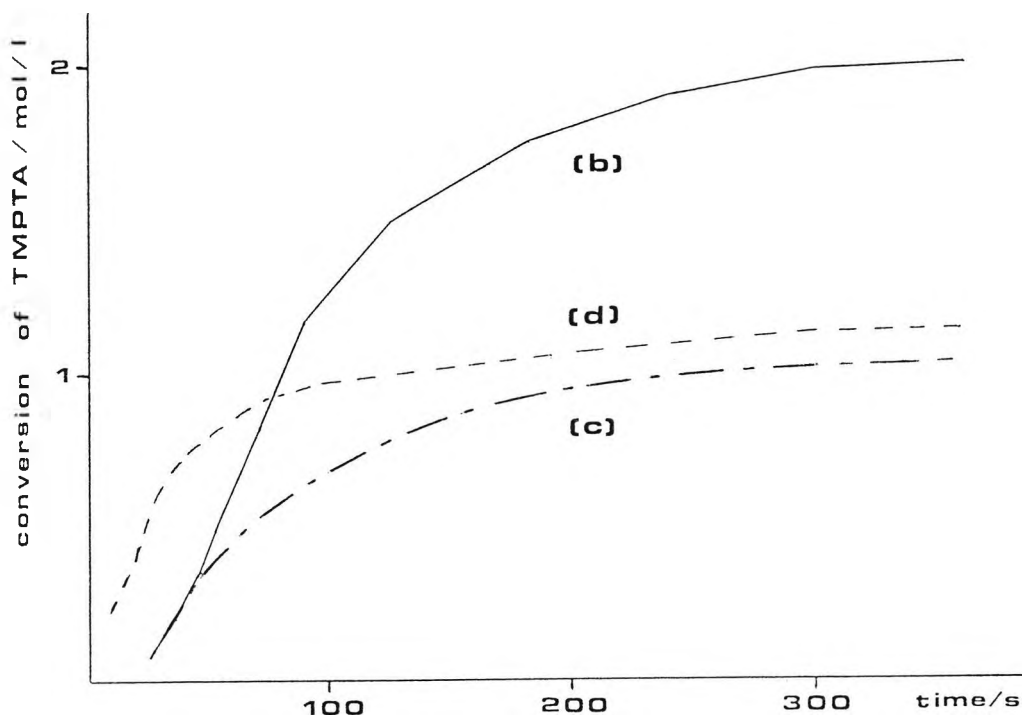
- (a) Benzyltri-*n*-butylstannane (1% w/w) in TMPTA
- (b) Fluorene derivative (1%w/w) in TMPTA
- (c) Fluorene derivative (1%w/w) + benzyltri-*n*-butylstannane (1% w/w) in TMPTA

It was found that;

- (a) did not polymerise in air
- (b) & (c) showed polymerisation in air

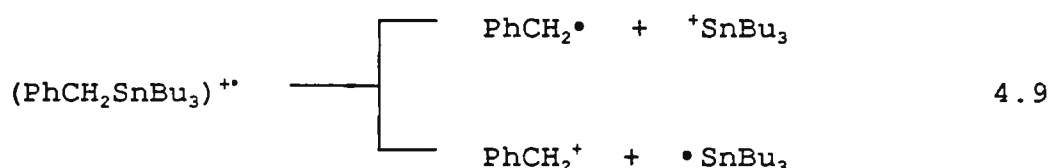
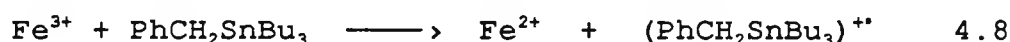
The resultant DSC traces for experiments (b) and (c) are shown in figure 4.3 below along with trace (d) which represents the polymerisation of the fluorene derivative (1% w/w) in TMPTA under a nitrogen atmosphere.

Figure 4.3 The Photo-DSC results for the free radical polymerisation of TMPTA initiated by an iron-arene complex (on it's own in air [b] and nitrogen [d], and in the presence of  $\text{PhCH}_2\text{SnBu}_3$  in air [c])



The results show that the overall degree of conversion is lower when the two compounds are tested together, ie. curve (c), than when the fluorene derivative is tested on its own, ie. curve (b). This could be due to a combination of electron transfer reactions and the depletion of oxygen by any tin radicals produced as outlined in scheme 4.6 below.

Scheme 4.6 Proposed reaction scheme for the photopolymerisation of TMPTA in air using  $\eta^6$ -fluorene- $\eta^5$ -cyclopentadienyliron hexafluorophosphate (1% w/w) with benzyltri-*n*-butylstannane (1% w/w)



Consider curve (c) which represents the formulation of the stannane + fluorene derivative. Initially the predominant reaction is that shown in equation 4.7. This gives rise to the production of iron (III) species which can then react with the stannane as shown in equation 4.8. The radical cation of the stannane, so formed, in equation 4.8 may then fragment as depicted in equation 4.9 to yield a tri-*n*-butyltin radical which is known to react with oxygen as shown in equation 4.10 (Bennett and Howard, 1972). This depletes the available oxygen level for the reaction with the original iron-arene, shown in equation 4.7, and thus reduces the reactivity towards polymerisation.

Another interesting feature is observed when comparing the DSC traces of the formulation of the stannane + fluorene

derivative in air (curve c) with the formulation of the fluorene derivative in nitrogen (curve d). The combination in air (curve c) exhibits a reactivity that is similar to the iron (II) species on its own in nitrogen (curve d). This is further evidence to support the reaction scheme 4.6 shown above. The two curves (c and d) show a remarkably similarity with the main difference being the oxygen inhibition of the mixture (c) giving an induction period and a slightly lower overall percentage conversion.

#### 4.8 Experimental Section

See section 2.7 for general experimental details. All  $^1\text{H}$  NMR were run in acetone- $\text{d}^6$  with TMS as the internal standard. All IR spectra were recorded using KBr discs. Methanol was used as the solvent for all UV spectra.

#### 38. $\eta^6$ -methylbenzene- $\eta^5$ -cyclopentadienyliron hexafluorophosphate

A mixture of ferrocene (15.0g; 81 mmol), powdered anhydrous  $\text{AlCl}_3$  (21.3g; 162 mmol), and Al powder (size  $20\mu$ ; 2.1g; 81 mg-atom), in toluene (300 ml) was refluxed overnight (bath temperature  $140^\circ\text{C}$ ). The colour of the solution changed from orange through light-green to red-brown. The mixture was cooled, and added to iced-water (400ml) carefully, and then stirred vigorously for a few minutes. The mixture was filtered prior to washing with ether. The aqueous layer was then treated with a slight excess of  $\text{KPF}_6$ . The pale-yellow precipitate was filtered off and purified by reprecipitation from acetone by addition of ether, followed by recrystallisation from ethanol to give 14.5g (50%) yield with mp  $164\text{--}165^\circ\text{C}$  (lit mp  $165^\circ\text{C}$ ; Astruc and Dabard, 1975).

#### Analysis

$^1\text{H}$  NMR: 6.40 (m, 5H), 5.15 (s, 5H), 2.50 (s, 3H)

IR: 3121 (m), aromatic C-H stretch

1464 (m), 1421 (m), C=C stretch

1114 (w), 1011 (w), Cp

UV:  $\lambda_{\text{max}} = 460\text{nm}$  ( $\epsilon=60$ ),  $360\text{nm}$  ( $\epsilon=100$ ),  $320\text{nm}$  ( $\epsilon=300$ )

MS: 213 (tolueneFeCp<sup>+</sup>), 186 (Cp<sub>2</sub>Fe<sup>+</sup>), 92 (toluene<sup>+</sup>), 65 (Cp<sup>+</sup>)

CHN: calculated for C<sub>12</sub>H<sub>13</sub>F<sub>6</sub>FeP

required C 40.25 H 3.66

found C 39.97 H 3.69

39.  $\eta^6$ -4-Chloro(methylbenzene)- $\eta^5$ -cyclopentadienyliron hexafluorophosphate

The title compound was synthesised by the same procedure used to obtain compound 38, using 4-chlorotoluene (100ml) as the refluxing solvent (bath temperature 190°C) with ferrocene (6.0g; 32mmol), AlCl<sub>3</sub> (8.0g; 60mmol), and Al powder (0.7g; 26mg-atom) to give 6.4g (45%) yield with mp 200°C (decomp.).

Analysis

<sup>1</sup>H NMR: 6.60 (m, 4H), 5.20 (s, 5H), 2.50 (s, 3H)

IR: 3122 (w), 3093 (w), aromatic C-H stretching  
2925 (w), aliphatic C-H stretch  
1456 (m), 1421 (m), C=C stretching

1096 (m), 1013 (w), Cp  
874 (s), 1,4-disubstituted benzene  
474 (s), Ph-Cl stretch

UV:  $\lambda_{\max} = 460\text{nm} (\epsilon=84), 380\text{nm} (\epsilon=184), 320\text{nm} (\epsilon=480)$

MS: 128, 127, 126, 125 (Cl-C<sub>6</sub>H<sub>4</sub>-Me<sup>+</sup>), 91 (C<sub>6</sub>H<sub>4</sub>-Me<sup>+</sup>)

CHN: Calculated for C<sub>12</sub>H<sub>12</sub>ClF<sub>6</sub>FeP  
required C 36.72 H 3.08  
found C 36.86 H 3.01

40.  $\eta^6$ -1,2-Dichlorobenzene- $\eta^5$ -cyclopentadienyliron  
hexafluorophosphate

The title compound was synthesised by the same procedure used to obtain compound 38, using 1,2-dichlorobenzene (100ml) as the refluxing solvent (bath temperature 190°C) with ferrocene (6.0g; 32mmol), AlCl<sub>3</sub> (8.0g; 60mmol), and Al powder (0.7g; 26mg-atom) to give 6.6g (50%) yield with mp 200°C (decomp).

Analysis

<sup>1</sup>H NMR: 6.90 (m, 4H), 5.41 (s, 5H)

IR: 3123 (s), 3092 (s), aromatic C-H stretch  
1426 (s), 1397 (s), C=C stretch  
1109 (m), 1012 (m), Cp

746 (s), 1,2-disubstituted benzene

UV:  $\lambda_{\text{max}}$  = 450nm ( $\epsilon=82$ ), 380nm ( $\epsilon=164$ ), 320nm ( $\epsilon=600$ )

MS: 186 ( $\text{Cp}_2\text{Fe}^+$ ), 146 (dichlorobenzene<sup>+</sup>), 65 ( $\text{Cp}^+$ ), 56 ( $\text{Fe}^+$ )

CHN: Calculated for  $\text{C}_{11}\text{H}_9\text{Cl}_2\text{F}_6\text{FeP}$   
required C 32.00 H 2.20  
found C 31.89 H 2.18

**41.  $\eta^6$ -Thioxanthene- $\eta^5$ -cyclopentadienyliron hexafluorophosphate**

A.

Thioxanthone (5.0g; 0.024 mol) was dissolved in anhydrous THF (300ml). Borane (48ml; 1M solution in THF; 0.048 mol) was added at room temperature with stirring under argon. The mixture was stirred for 1h and then refluxed for 3h. After cooling excess borane was decomposed by addition of ice-chips. The solution was diluted with an equal volume of water and the THF was removed. The resulting precipitate was filtered off in quantitative yield.

B.

A mixture of ferrocene (5.5g; 30 mmol),  $\text{AlCl}_3$  (16.0g; 120mmol), Al powder (0.81g; 30 mmol), and thioxanthene (4.7g; 24 mmol) was heated with mechanical stirring in decalin (75 ml) for 4h (bath temperature 190°C). After

cooling slightly the reaction mixture was poured onto iced-water (500 ml) with stirring. Any residual solid was washed out of the reaction flask with water and ether. After stirring for 10 min the solid material was filtered off. The aqueous layer was washed with ether and then treated with a slight excess of  $KPF_6$ . The precipitate was filtered off and purified by reprecipitation from acetone by addition of ether, followed by recrystallisation from ethanol to give 4.5g (40%) yield with mp 127-128°C.

#### Analysis

$^1H$  NMR: 7.60 (m, 4H), 6.60 (m, 4H), 4.70 (s, 5H), 4.1 (q, 2H)

IR: 3114 (w), aromatic C-H stretch  
1439 (m), 1418 (m), C=C stretching  
1104 (w), 1013 (w), Cp  
754 (m), 1,2-disubstituted benzene

UV:  $\lambda_{max}$  = 460nm ( $\epsilon=77$ ), 400nm ( $\epsilon=270$ ), 330nm ( $\epsilon=1600$ )

MS: 319 (thioxantheneFeCp<sup>+</sup>), 198 (thioxanthene<sup>+</sup>), 186 (Cp<sub>2</sub>Fe<sup>+</sup>), 121 (CpFe<sup>+</sup>), 56 (Fe<sup>+</sup>)

CHN: Calculated for C<sub>18</sub>H<sub>15</sub>F<sub>6</sub>FePS  
required C 46.60 H 3.26  
found C 46.47 H 3.20

#### 42. $\eta^6$ -Fluorene- $\eta^5$ -cyclopentadienyliron hexafluorophosphate

The title compound was synthesised by a similar procedure used to obtain compound 41, (part B) using fluorene (16.6g; 0.1mol), ferrocene (18.6g; 0.1mol), AlCl<sub>3</sub> (64.0g; 0.48mol), and Al powder (3.6g; 0.12mol) heated in decalin overnight (bath temperature 160°C) to give 23.0g (53%) yield with mp 161-162°C (decomp) (lit mp 163-165°C [decomp]; Helling and Hendrickson, 1977).

#### Analysis

<sup>1</sup>H NMR: 7.40-8.20 (m, 4H, ), 6.40-7.30 (m, 4H, ), 5.20 (s, 5H),  
4.5 (s, 1H), 4.20 (s, 1H)

IR: 3130 (w), aromatic C-H stretch  
1435 (m), 1421 (m), C=C stretching  
1108 (w), 1014 (w), Cp  
775 (s), 1,2-disubstituted benzene

UV:  $\lambda_{\text{max}}$  = 460nm ( $\epsilon=100$ ), 400nm ( $\epsilon=160$ ), 320nm ( $\epsilon=600$ )

MS: 287 (fluoreneFeCp<sup>+</sup>), 186 (Cp<sub>2</sub>Fe<sup>+</sup>), 166 (fluorene<sup>+</sup>)

CHN: calculated for C<sub>18</sub>H<sub>15</sub>F<sub>6</sub>FeP  
required C 50.03 H 3.50  
found C 50.02 H 3.43

#### 43. $\eta^6$ -Xanthene- $\eta^5$ -cyclopentadienyliron hexafluorophosphate

The title compound was synthesised by a similar procedure

used to obtain compound 41 (part B), using xanthene (10.0g; 55mmol), ferrocene (10.0g; 55mmol), AlCl<sub>3</sub> (29.3g; 220mmol), and Al powder (1.5g; 55mmol) heated in decalin for 5h (bath temperature 140°C) to give 11.0g (45%) yield with mp 114-115°C.

#### Analysis

<sup>1</sup>H NMR: 7.40 (m, 4H), 6.40 (m, 4H), 5.00 (s, 5H), 4.30 (s, 2H)

IR: 3125 (w), aromatic C-H stretch  
1457 (s), C=C stretch  
1263 (s), Ph-O stretch  
1110 (w), 1012 (w), Cp  
764 (s), 1,2-disubstituted benzene

UV:  $\lambda_{max}$  = 460nm ( $\epsilon$ =78), 390nm ( $\epsilon$ =196), 320nm ( $\epsilon$ =1176)

MS: 182 (xanthene<sup>+</sup>)

CHN: calculated for C<sub>18</sub>H<sub>15</sub>F<sub>6</sub>FeOP  
required C 48.24 H 3.37  
found C 48.13 H 3.25

#### 4.9 References

Albright, T.A., (1982). *Tetrahedron*, **38**, 1339

Arnold, D.R., and Maroulis, A.J., (1976). *J.Am.Chem.Soc.*,  
**98**, 5931

Astruc, D., and Dabard, R., (1975). *Bull.Soc.Chem.France*,  
2571

Bennett, J.E., and Howard, J.A., (1972). *J.Am.Chem.Soc.*,  
**94**, 8244

Chrisope, D.R., Kyung, M.P., and Schuster, G.B., (1989).  
*J.Am.Chem.Soc.*, **111**, 6195

Coffield, T.H., Sandel, V., and Closson, R.D., (1957).  
*J.Am.Chem.Soc.*, **79**, 5826

Curtis, H., Irving, E., and Johnson, B.F.G., (1986).  
*Chem.Brit.*, 327

Gatechair, L.R., and Pappas, S.P., (1982).  
*Org.Coat.Appl.Polym.Sci.Proc.*, **46**, 183 ACS Meeting, Las  
Vegas, March 25 - April 2

Gill, T.P., and Mann, K.R., (1980). *Inorg.Chem.*, **19**, 3007

- Gill, T.P., and Mann, K.R., (1983). *Inorg.Chem.*, **22**, 1986
- Green, M.L.H., Pratt, L., and Wilkinson, G., (1960).  
*J.Chem.Soc. A*, 989
- Helling, J.F., and Hendrickson, W.A., (1977).  
*J.Organomet.Chem.*, **141**, 99
- Klingert, B., Riediker, M., and Roloff, A., (1988).  
*Comments Inorg. Chem.*, **7**, 109
- Lee, C.C., Sutherland, R.G., and Thomson, B.J., (1972).  
*J.Chem.Soc.Chem.Comm.*, 907
- Lohse, F., and Zweifel, H., (1986). *Adv.Polym.Sci.*, **78**, 61
- McNair, A.N., Schrenk, J.L., and Mann, K.R., (1984).  
*Inorg.Chem.*, **23**, 2633
- Meier, K., and Rhis, G., (1985). *Angew.Chem.*, **97**, 879
- Meier, K., and Zweifel, H., (1985). *EP* 152 377
- Meier, K., and Zweifel, H., (1986). *J.Rad.Curing*, 26
- Morrison, W.H., Ho, E.Y., and Hendrickson, D.N., (1974).  
*J.Am.Chem.Soc.*, **96**, 3603

- Morrison, W.H., Ho, E.Y., and Hendrickson, D.N., (1975).  
*Inorg.Chem.*, 14, 500
- Nesmeyanov, A.N., Vol'kenau, N.A., and Bolesova, I.N.,  
(1963). *Tet.Lett.*, 1725
- Nesmeyanov, A.N., Vol'kenau, N.A., and Bolesova, I.N.,  
(1965). *Dokl.Akad.Nauk SSSR*, 160, 1327
- Nesmeyanov, A.N., Vol'kenau, N.A., and Bolesova, I.N.,  
(1966). *Dokl.Akad.Nauk SSSR*, 166, 607
- Nesmeyanov, A.N., Vol'kenau, N.A., Sirotkina, E.I., and  
Deryabin, V.V., (1967). *Dokl.Akad.Nauk SSSR*, 177, 1110
- Nesmeyanov, A.N., Vol'kenau, N.A., and Shilovtseva, L.S.,  
(1970). *Dokl.Akad.Nauk SSSR*, 190, 857
- Rehm, D., and Weller, A., (1969). *Ber.Bunsenges.*  
*Phys.Chem.*, 73, 834
- Roloff, A., Meier, K., and Riediker, M., (1986). *Pure &*  
*Appl. Chem.*, 58, 1267
- Schrenk, J.L., Palazzotto, M.C., Mann, K.R., (1983).  
*Inorg.Chem.*, 22, 4047
- Tsubakiyama, K., Fujisaki, S., Tabata, E., and Nakahara, S.,

(1991). *J.Macromol.Sci., Chem.A*, 28, 557

Zink, J.I., (1974). *J.Am.Chem.Soc.*, 96, 4464

Zweifel, H., and Meier, K., (1985). *Polym.Prepr.*, 26, 347

EP 094915 (1984) Ciba Geigy AG

EP 126712

# APPENDIX

## 5.1 Introduction

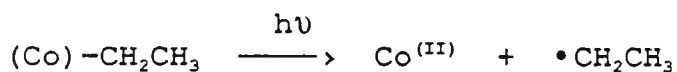
A preliminary investigation into some visible photoinitiators was carried out. Reports in the literature indicated that it could be of benefit to utilise cobaloximes and porphyrins as sources of alkyl radicals. It was proposed that the alkyl radicals, produced on irradiation of these complexes, could be used to initiate free radical polymerisation. The reaction mechanism in both the cobaloximes involves the cleavage of a metal-carbon bond which is in keeping with the theme of this work.

## 5.2 Cobaloximes

The photodealkylation of organocobalt derivatives of vitamin B<sub>12</sub> and of bisdimethylglyoximato-cobalt compounds ("cobaloximes") yields cobalt (II) derivatives of the parent chelates and alkyl radicals as the initial products (Shrauzer et al, 1968). The photolysis of alkylcobaloximes is initiated by excitation of the Co-C bond and proceeds by a mechanism related to charge-transfer (CT) induced photoreduction reactions of Co (III) complexes. The rate of Co-C bond photolysis depends essentially on the energy and intensity of the Co-C CT transition, both of which vary with the axial base attached to cobalt.

The photochemical reactions of alkylcobaloximes have been extensively studied (Dolphin, 1982). Golding et al (Golding et al, 1977) showed conclusively that for aqueous solutions

homolysis of the Co-C bond was the major primary process. Shrauzer *et al* (Shrauzer *et al*, 1968) drew similar conclusions. The methyl derivative gave both methane and ethane as photolysis products, the latter being formed by dimerisation. However, olefins were the major product for other alkylcobaloximes. An interesting mechanism has been proposed to explain this result (Shrauzer *et al*, 1968).



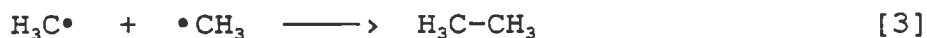
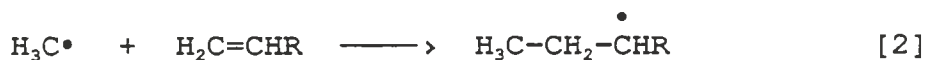
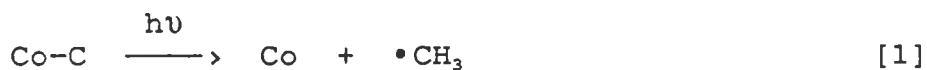
The aim of this work was to produce alkyl radicals in the presence of a free radical polymerisable monomer, TMPTA, to initiate polymerisation. What was not clear was the extent to which the alkyl radicals, produced on irradiation, would undergo initiation reactions in preference to other reactions such as recombination or disproportionation. In order to gain more information on the photoinitiating properties of these complexes the cobaloximes were incorporated into a polymerisable monomer, TMPTA, and tested using the UV Colordry apparatus described earlier (see section 1.7.1). The results are presented below.

E X P T	"COBALOXIME"	% w/w in TMPTA	NUMBER OF PASSES IN AIR
1	Me-Cobaloxime	1.0	19
2	Br(CH <sub>2</sub> ) <sub>4</sub> -Cobaloxime	1.0	*

2 lamps used for irradiation in both cases

\* = polymerisation not detected after 30 passes

The results indicate that the methyl-cobaloxime will initiate free radical polymerisation in air. This indicates that Co-C bond homolysis occurs on photolysis producing a methyl radical as shown below [1].



The methyl radical produced in [1] exists independently and must compete effectively with the dimerisation reaction [3] to initiate polymerisation [2].

In the case of the Br(CH<sub>2</sub>)<sub>4</sub> derivative it appears that either the extent of photolysis of the Co-C bond is low, or that on photolysis the recombination/disproportionation reactions

occur preferentially to the reaction initiating polymerisation.

These preliminary studies indicate some promise for further investigations of the methylcobaloxime derivative.

### 5.3 Porphyrins

The photochemistry of metalloporphyrins is of much interest in connection with the role of chlorophyll in photosynthesis. One report indicated that there was photoactivation of the metal-axial bond in aluminium porphyrins by visible light (Hirai et al, 1988). It has been known that photoactivation of a transition metal-axial ligand bond in metalloporphyrins brings about free radical dissociation, leading to the change in valence of the central metal (Imamura et al, 1985; Hendrickson et al, 1987).

In order to evaluate if this reaction could be used to produce free radicals capable of initiating polymerisation a porphyrin derivative was synthesised. First the free base porphyrin was synthesised using the procedure of Adler et al (Adler et al, 1970). This was reacted further with  $\text{CrCl}_2$  to yield the desired porphyrin  $\text{Cr}(\text{TPP})\text{Cl}$ , using the method described previously (Hoffmann and Basolo, 1977).

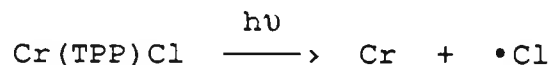
In order to determine the free radical-initiating properties of  $\text{Cr}(\text{TPP})\text{Cl}$  the porphyrin was incorporated (1% w/w) into

the free radically polymerisable monomer, TMPTA, and tested using the UV Colordry apparatus described earlier (see section 1.7.1). The result is presented below.

E X P T	"PORPHYRIN"	% w/w in TMPTA	NUMBER OF PASSES IN AIR
1	Cr(TPP)Cl	1.0	14

2 lamps used for irradiation

From the result it can be inferred that free radicals are produced from the photolysis of Cr(TPP)Cl, presumably via the following reaction:



The Cl• produced can then initiate free radical polymerisation. It may be of interest to replace the Cl with other ligands, eg. alkyl groups, to investigate this reaction further.

#### 5.4 Experimental section

##### (4-Bromo-n-butyl)bis[(2,3-butanedionedioximato)(1-)-N,N'](pyridine)cobalt

A suspension of cobalt (II) chloride ( 6.50g, 0.05 mol ) and dimethylglyoxime ( 11.6g, 0.10 mol) in methanol ( 190ml ) was stirred until all the cobalt chloride had dissolved. After adding sodium hydroxide ( 4g, 0.10 mol ) in water ( 12.5 ml ) the suspension was stirred under nitrogen for 10 min. Next 1,4-dibromobutane ( 7.50g ) was added, followed by sodium hydroxide ( 2.0g, 0.05 mol ). After 10 minutes the reaction mixture was filtered and diluted with water (500 ml). Excess dibromobutane was removed in an air stream. On adding pyridine (4.0g, 0.05 mol) a yellow precipitate formed which was washed , dried, and recrystallised (methanol). On cooling and standing crystals of 1,4-tetramethylenebis(pyridinatocobaloxime) formed. From the filtrate (methanol), on dilution with water (4-bromo-n-butyl)bis[(2,3-butanedionedioximato)(1-)-N,N'](pyridine)cobalt was obtained (2.1g, 17%) : mp 175-176°C

##### Analysis

$^1\text{H}$  NMR: 1.10 (m, 2H), 1.60 (m, 4H), 2.20 (s, 12H), 3.40 (m, 2H), 7.30 (m, 3H), 8.60 (m, 2H)

IR: 3438 (broad), O-H stretch  
3109 (w), 3041 (w), 3000 (w), aromatic C-H stretching  
2951 (m), 2911 (m), 2853 (w), aliphatic C-H stretching  
1602 (m), 1560 (m), C=C stretching

UV:  $\lambda_{(\max)}$  = 430nm (sh) [ $\epsilon=2500$ ], 380nm (sh) [ $\epsilon=2800$ ],  
266nm [ $\epsilon=11,000$ ]

CHN: Calculated for  $C_{17}H_{27}N_5O_4BrCo$

Theory	C	40.48	H	5.39	N	13.88
Found	C	40.47	H	5.40	N	13.59

(Methyl)bis[(2,3-butanedionedioximato)(1-)-N,N'](pyridine)cobalt

A suspension of dimethylglyoxime (13.8g; 0.12mol) and cobalt(II)chloride (7.12g; 0.06mol) in methanol (100ml) was stirred until all the cobalt chloride had dissolved. Then NaOH (4.8g; 50%; 0.12mol) and pyridine (5.0g; 0.06mol) were added. The stirred suspension was cooled ( $-10^{\circ}C$ ) and stirred for 15 min. after adding NaOH (2.4g; 50%; 0.06mol) and sodium borohydride (0.40g; 0.01mol). Next dimethylsulphate (8.1g; 0.06mol) was added and the solution was gradually warmed to room temperature under an air stream. The mixture was stirred with water (32ml) and pyridine (1.7g; 0.02mol). The orange crystals were

collected and dried to give 10.5g (46% yield) (Shrauzer & Windgassen, 1966)

### Analysis

IR: 3448 (broad), O-H stretch  
2896 (w), aliphatic C-H stretching  
1599 (m), 1556 (m), C=C stretching

UV:  $\lambda_{(\max)}$  = 440nm (sh) [ $\epsilon=2000$ ], 415nm (sh) [ $\epsilon=2500$ ],  
375nm (sh) [ $\epsilon=2800$ ], 266nm [ $\epsilon=11,000$ ]

CHN: Calculated for  $C_{14}H_{22}N_5O_4Co$

Theory	C	43.86	H	5.78	N	18.26
Found	C	42.95	H	5.66	N	17.89

### 5,10,15,20-Tetraphenyl-21H,23H-porphine

Pyrrole (28ml, 0.40 mol) and benzaldehyde (40ml, 0.40 mol) were added to refluxing propionic acid (400ml) and the mixture was refluxed for 30 min. The resulting mixture was filtered, washed (methanol and then water) and dried to give purple crystals (5.8g, 9%).

### Chloro(5,10,15,20-tetraphenyl-21H,23H-porphinato(2-)-N21,N23,N24)Chromium (Cr(TPP)Cl)

Tetraphenylporphyrin (2.5g) was dissolved in refluxing N,N'-

dimethylformamide (250ml). After complete solution had occurred chromous chloride (0.5g) was added. After a few minutes completion of reaction was checked using UV spectrophotometry. If the reaction was not complete another 0.25g of chromous chloride was added, the reaction allowed to proceed for another 10 minutes, and then rechecked for completion. This procedure was continued until completion of reaction. The reaction mixture was cooled and chilled, and distilled water (250ml) was added. The resultant precipitate was washed with water and dried in a vacuum oven for 1 hr at 100°C; yield of crude Cr(TPP)Cl, 1.5g.

#### Purification of Cr(TPP)Cl

Crude Cr(TPP)Cl (1.5g) was dissolved in chloroform (50ml) and applied to a dry alumina column (neutral Brockman Grade 1). Elution with chloroform gave a reddish band with the solvent front. This was followed by a light green band followed by a darker green band, (containing the Cr(TPP)Cl) After the Cr(TPP)Cl was eluted from the column (200ml) aqueous HCl (12M, 2ml) was added to the chloroform solution and left stirring overnight. The chloroform was removed and the solid was recrystallised from chloroform and dried in a vacuum desiccator to give Cr(TPP)Cl.

#### ANALYSIS

IR: 3053 (w), aromatic C-H stretch  
1641 (w), C=N stretch

1595 (m), C=C stretch

752 (s), 703 (s), monosubstituted benzene

UV:  $\lambda_{(max)}$  = 600nm, 560nm, 520nm, 448nm, 394nm

5.5 Table 5.1:      The oxidation and ionisation potentials  
for a number of silanes and stannanes

Allylic compounds	Oxidation potential/V	Ionisation potential/eV
$\text{CH}_2=\text{CHCH}_2\text{CMe}_3$		9.5 [1]
$\text{CH}_2=\text{CHCH}_2\text{SiMe}_3$	1.58 [2]	9.0 [1]
$\text{CH}_2=\text{C}(\text{Me})\text{CH}_2\text{SiMe}_3$	1.28 [2]	
$\text{Me}_2\text{C}=\text{CHCH}_2\text{SiMe}_3$	0.92 [2]	
$\text{CH}_2=\text{CHCH}_2\text{SnMe}_3$	1.06 [3]	
$\text{Me}_2\text{C}=\text{CHCH}_2\text{SnMe}_3$	0.68 [3]	
$\text{CH}_2=\text{CHCH}_2\text{SnBu}_3$		8.4 [4]
Benzylic compounds		
$\text{PhCH}_3$	1.98 [5]	
$\text{PhCH}_2\text{CMe}_3$		8.7 [1]
$\text{PhCH}_2\text{SiMe}_3$	1.38 [5]	8.4 [1]
4-Me-C <sub>6</sub> H <sub>4</sub> -Me	1.70 [5]	
4-Me-C <sub>6</sub> H <sub>4</sub> CH <sub>2</sub> SiMe <sub>3</sub>	1.17 [5]	
$\text{PhCH}_2\text{SnMe}_3$		8.1 [1]
$\text{PhCH}_2\text{SnBu}_3$	0.85 [6]	7.9 [1]

Table 5.1 continued overleaf

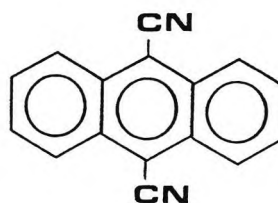
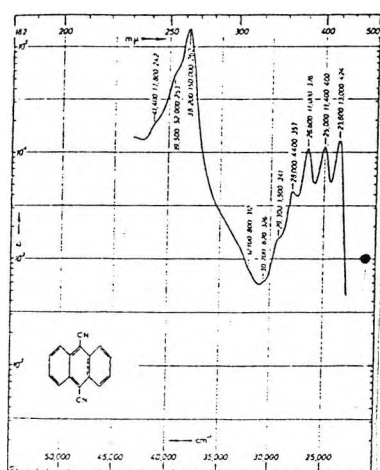
Table 5.1 continued

Naphthyllic compounds	Oxidation potential/V	Ionisation potential/eV
1-NpCH <sub>2</sub> SiMe <sub>3</sub>	0.96 [6]	7.8 [8]
2-NpCH <sub>2</sub> SiMe <sub>3</sub>	0.96 [6]	
2-NpCH <sub>2</sub> SnBu <sub>3</sub>	0.60 [6]	
Others		
Ph-CH=CHCH <sub>2</sub> SiMe <sub>3</sub>	0.91 [6]	
Me <sub>3</sub> Si-SiMe <sub>3</sub>	1.88 [7]	8.7 [7]

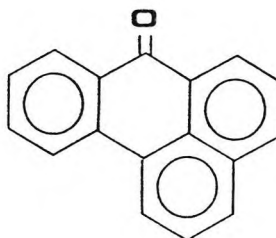
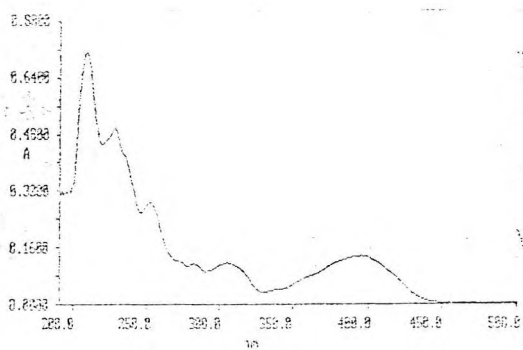
[1] = (Schweig et al, 1967), [2] = (Mizuno et al, 1985), [3] = (Takuwa et al, 1990), [4] = (Schweig et al, 1973), [5] = (Koizumi et al, 1989), [6] = (Mizuno et al, 1988), [7] = (Fukuzumi et al, 1990), [8] = (Pitt, 1973)

5.6

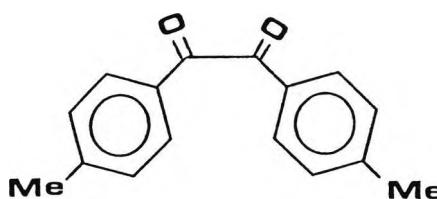
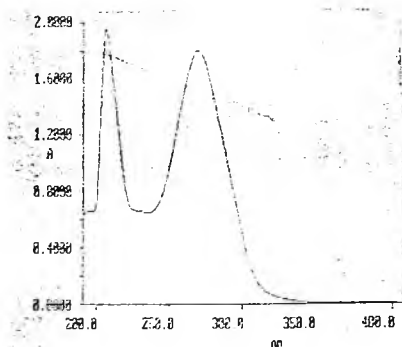
Figure 5.1 UV spectra



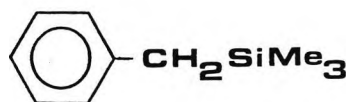
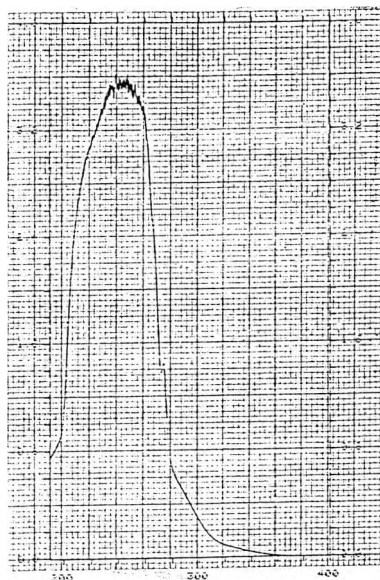
$$C = 1.1 \times 10^{-4} \text{ M}$$



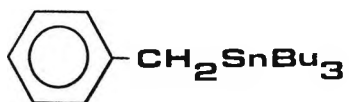
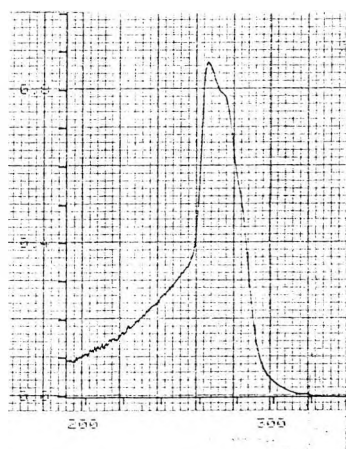
$$C = 7.2 \times 10^{-6} \text{ M}$$



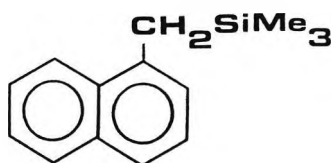
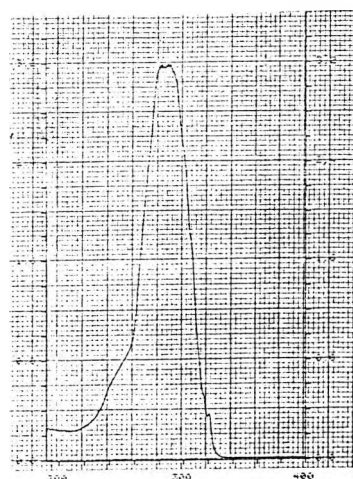
$$C = 6.2 \times 10^{-5} \text{ M}$$



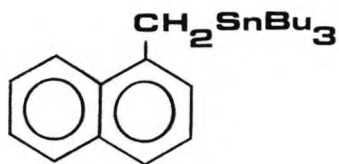
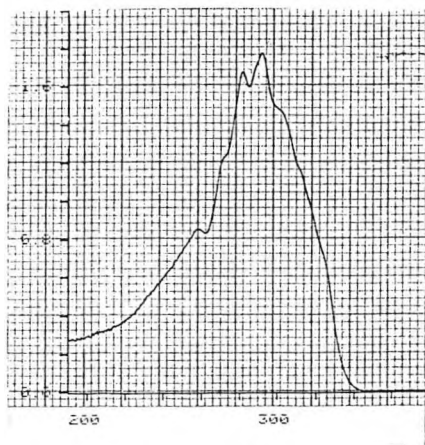
$$C = 1.9 \times 10^{-3} \text{ M}$$



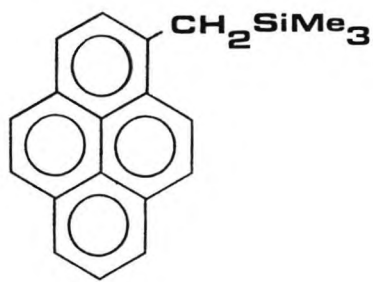
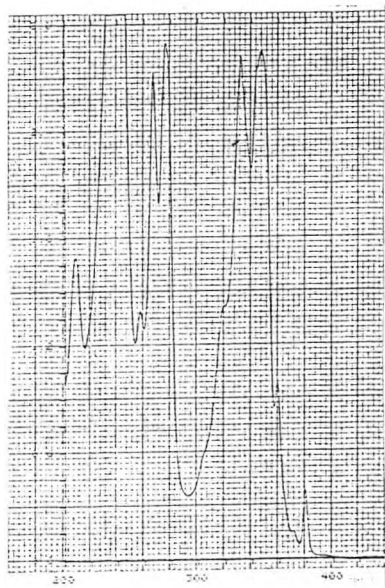
$$C = 1.0 \times 10^{-3} \text{ M}$$



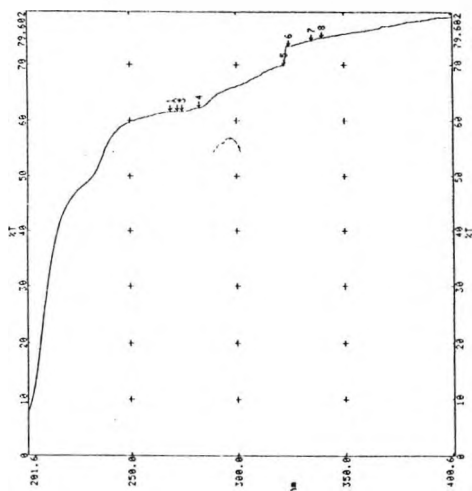
$$C = 5.3 \times 10^{-4} \text{ M}$$



$$C = 2.4 \times 10^{-4} \text{ M}$$



$$C = 1.6 \times 10^{-4} \text{ M}$$



polyethylene cover  
slip used in RTIR  
experiments

References

- Adler, A.D., Longo, F.R., Kampas, F., and Kim, J., (1970).  
*J.Inorg.Nucl.Chem.*, 32, 2443
- Dolphin, D, (ed.), (1982). "B12", Wiley, New York, Volume  
1
- Fukuzumi, S., Kitano, T., and Mochida, K., (1990).  
*Chem.Lett.*, 1741
- Golding, B.T., Kemp, T.J., Sellers, P.J., and Nocchi, E.,  
(1977). *J.Chem.Soc., Dalton Trans.*, 1266
- Hendrickson, D.N., Kinnaird, M.G., and Suslick, K.S.J.,  
(1987). *J.Am.Chem.Soc.*, 109, 1243
- Hirai, Y., Maruyama, H., Aida, T., and Inoue, S., (1988).  
*J.Am.Chem.Soc.*, 110, 7387
- Hoffmann and Basolo, (1977). *J.Am.Chem.Soc.*, 99, 8195
- Imamura, T., Jin, T., Suzuki, T., and Fujimoto, M., (1985).  
*Chem.Lett.*, 847
- Koizumi, T., Fuchigami, T., and Nonaka, T., (1989).  
*Bull.Soc.Chem.Jpn.* 62, 219

- Mizuno, K., Ikeda, M., and Otsuji, Y., (1985). *Tet.Lett.*  
26, 5819
- Mizuno, K., Yasueda, M., and Otsuji, Y., (1988).  
*Chem.Lett.*, 229
- Pitt, C.G., (1973). *J.Organomet.Chem.* 61, 49
- Shrauzer, G.N., and Windgassen, R.J., (1966).  
*J.Amer.Chem.Soc.*, 88, 3738
- Schweig, A., Weidner, U., and Manuel, G., (1967).  
*J.Organomet.Chem.* 67, C4
- Schweig, A., Weidner, U., and Manuel, G., (1973).  
*J.Organomet.Chem.* 54, 145
- Shrauzer, G.N., Sibert, J.W., and Windgassen, R.J., (1968).  
*J.Amer.Chem.Soc.*, 90, 6681
- Takuwa, A., Nishigaichi, Y., and Yamashita, K., (1990).  
*Chem.Lett.*, 639